Doctor's Thesis

Exact Analysis of Universal Critical Behavior and Ergodic Properties of Chaos

Guidance
Ken Umeno

Ken-ichi Okubo

Department of Applied Mathematics and Physics
Graduate School of Informatics
Kyoto University

2020

Contents

Chapter 1

Introduction

Historically, it was believed that the future state of a system could be exactly predicted if, like Laplace's demon, one possessed complete and exact information about the initial state[1, 2]; having at least approximate knowledge of the initial condition was thought to imply having approximate knowledge of the final state. However, in the late 19th century, H. Poincaré [3], studying the three-body problem in celestial mechanics, realized that a small difference in the initial condition can sometimes generate a large one in the final state, making prediction impossible. The accepted view came to be that, if a classical system is conservative, its orbits in phase space will converge to a fixed point, a cycle, or a quasi-periodic orbit.

In the 19th century, L. Boltzmann tried to show the existence of the arrow of time by proving that the H function monotonically decreases with time and can be constant only if the distribution function is Maxwellian (assuming the case of a dilute gas and the validity of the ergodic hypothesis)[4, 5, 6, 7]. Against Boltzmann's claim, Loschmidt argued from the time-reversal symmetry of classical mechanics that the time derivative of the H function can be positive,[7, 8] while Zermelo contended that, according to Poincaré's Recurrence Theorem, the H function after the recurrence time should be practically the same as it was initially[7, 9].

In 1963, the meteorologist Edward Lorenz [10] proposed his three-variable equation, the solutions of which showed that, even in deterministic systems, prediction may be impossible due to chaos: a small error in the initial state produces a large difference in the final state. At the same time as Lorenz, Y. Ueda [11], studying the solution of a certain nonlinear differential equation with an analog computer, discovered a chaotic attractor with a distinctive shape resembling a broken egg.

In the late 1970s, researchers began to study the origin of chaos. In 1978, M. Feigenbaum [1, 12, 13], studying the logistic map, proposed the scenario called the period-doubling route to chaos. Researchers have subsequently discovered various other routes to chaos, often arguing that there is an underlying universality among them. In 1980, Huberman and Rudnick [14] estimated by numerical simulation that the critical exponent of the Lyapunov exponent in the logistic map is $\frac{\log 2}{\log \delta} = 0.4498069...$, where $\delta = 4.6692016091029...$ is the Feigenbaum constant. In the same year, Pomeau and Manneville [15] estimated that the critical exponent of the Lyapunov exponent is $1/2$ in *Type* 1 and *Type* 3 intermittency. Aizawa, Murakami, and Kohyama reported that intermittent chaos can be observed in the modified Bernoulli map [16]. *Type* 1 and *Type* 3 intermittencies were also observed in physical experiments [17, 18].

In order to study statistical behavior in dynamical systems, ergodic theory has been developed. In 1931, the mathematician G. D. Birkhoff proved the ergodic theorem [19]. In the 1960s, S. Smale considered the idea of axiom-A systems, which are characterized by a hyperbolic structure [20, 21]. Axiom-A systems include both continuous-time and discrete-time systems. (In this thesis, only discrete-time dynamical systems are considered.) In the 1970s, the idea of the SRB measure was proposed by Sinai, Ruelle, and Bowen [22]. For axiom-A systems, it can be proved that the SRB measure is uniquely the physical measure $\rho = \lim_{n\to\infty} \frac{1}{n} \sum_{k=0}^{n-1} \delta_{f^k x}$, where δ, f and x represent the delta function, a map and a point, respectively[23]. Physical measure as the SRB measure is related to the foundations of statistical physics. G. Gallavotti [6] proposed the chaotic hypothesis, in which it is assumed that the system is an Anosov system, and therefore can be shown to have the SRB measure without assuming the ergodic hypothesis of Boltzmann. A number of systems, both continuous (e.g., Sinai billiards [24, 25], the Bunimovich stadium [26, 27], and the Lorentz gas [28]) and discrete (e.g., the Sawtooth map [29, 30], Arnold's cat map [31], and multi Baker's map [32]), are known to have SRB measure.

The attempt to obtain explicit formulae of invariant measures dates from the work of Ulam and von Neumann in the late 1940s. They obtained the exact formula of the invariant measure for the logistic map $x_{n+1} = bx_n(1 - x_n)$ at $b = 4$, $x_{n+1} = 4x_n(1 - x_n)$ (Ulam-von Neumann map) [33]. The ergodic invariant density function corresponding the Ulam-von Neumann map is $\rho(x) = \frac{1}{\pi\sqrt{x(1-x)}}$. In 1985, Katsura and Fukuda [34] generalized the Ulam-von Neumann map to $x_{n+1} = \dfrac{4x_n(1 - x_n)(1 - lx_n)}{(1 - lx_n^2)^2}$. Its ergodic invariant density is given by $\rho(x) = \frac{1}{2K(l)\sqrt{(1-x)(1-lx)}}$, where $K(l)$ represents the elliptic integral of the first kind [35]. In 1997, K. Umeno generalized the Katsura - Fukuda systems as

$$x_{n+1} = \frac{4x_n(1 - x_n)(1 - lx_n)(1 - mx_n)}{1 + -2(l + m + lm)x_n^2 + 8lmx_n^3 + ({}^2 + m^2 - 2lm - 2l^2m - 2lm^2 + l^2m^2)x_n^4},$$

the ergodic invariant density of which can be rewritten as $\rho(x) = \frac{1}{2K(l,m)\sqrt{x(1-x)(1-lx)(1-mx)}}$ where $K(l,m) \stackrel{\text{def}}{=} \int_0^1 \frac{du}{\sqrt{(1-u^2)(1-lu^2)(1-mu^2)}}$ [35]. In 1998, K. Umeno generalized a chaotic dynamics corresponding the double-angle formula of the cotangent function as $x_{n+1} = \left|\frac{1}{2}\left(|x_n|^\alpha - \frac{1}{|x_n|^\alpha}\right)\right|^{\frac{1}{\alpha}} \operatorname{sgn}\left\{x_n - \frac{1}{x_n}\right\}$; this system has ergodic invariant density $\rho(x) = \frac{\alpha}{\pi}\frac{|x|^{\alpha-1}}{1+|x|^{2\alpha}}$ [36]. These ergodic invariant measures are known to be physical measures [37]. In the above generalizations, even when we change the parameter, the systems remain strongly chaotic. However, we cannot modulate the degree of chaoticity (Lyapunov exponent). Thus, in these systems, we cannot observe the behavior at the edge of chaos by changing a parameter.

Chaotic Monte Carlo computation, proposed by K. Umeno [38], is an application of chaos in which the ergodic invariant measure can be obtained exactly.

To compute chaoticity, the Lyapunov exponent is usually evaluated: if it is positive, the corresponding orbit is chaotic. The Lyapunov time, which is the reciprocal of the largest Lyapunov exponent, is related to the calculation time about the Lyapunov exponent. Empirically, this calculation time tends to be long if the Lyapunov exponent is small and positive: in one reported case, it takes more than ten Lyapunov times [39].

Such weakly chaotic phenomena appear in celestial mechanics. For example, by calculating the motion of the solar system over 200 million years, J. Laskar numerically estimated that the largest Lyapunov exponent of the solar system is about $\frac{1}{5}(\text{Million years})^{-1}$ [40]. C. Froeschlé et. al. proposed the Fast Lyapunov Indicator (FLI) [39, 41] in the context of celestial mechanics. Since then, other indicators, such as the Orthogonal Fast Lyapunov Indicator (OFLI) [42] and Orthogonal Fast Lyapunov Indicator 2 (OFLI^2)[43], have been proposed.

1.1 Chaotic dynamics and Ergodic theorem

To study the properties of the evolution equation, we consider parameterized systems of the form $x_n = f_\alpha^n(x_0)$, where $x \in \mathbb{R}^m$, f, and α are a point, a map and a parameter, respectively. If we change the value of the parameter, the asymptotic behavior of the system may change, first bifurcating when the parameter reaches some threshold value, and then, after successive bifurcations, becoming complicated or chaotic [23].

To study the statistical properties of chaotic systems, we take the time averages of dynamical quantities using ergodic theory. We define the invariant measure by $\rho[f^{-n}(E)] = \rho(E), n > 0$ where E is a subset of the whole space [23]. If the system is ergodic, we can apply the following equation for every continuous function φ:

$$\lim_{n\to\infty} \frac{1}{n} \sum_{k=0}^{n-1} \varphi[f^n x_0] = \int \rho(dx)\varphi(x). \tag{1.1.1}$$

From this, we can obtain the time average by calculating the phase average with the invariant measure. Moreover, we can calculate the Lyapunov exponent, the indicator of chaos, as follows: According to [23], for the evolution equation $x_{n+1} = f(x_n)$, the difference of two initial points x_0 and x_0' after $n = N$ is

$$\begin{aligned} x_N - x_N' &= f^N(x_0) - f^N(x_0), \\ &\approx \tfrac{d}{dx}(f^N)(x_0)[x_0 - x_0']. \end{aligned} \tag{1.1.2}$$

By the chain rule of differentiation,

$$\frac{d}{dx}(f^N)(x_0) = D_x f(x_{N-1}) \cdot D_x f(x_{N-2}) \cdots D_x f(x_0). \tag{1.1.3}$$

Then, the average rate of exponential growth λ is defined as

$$\lambda \overset{\text{def}}{=} \lim_{N\to\infty} \frac{1}{N} \log \left| D_{x_0} f^N \delta x_0 \right| \tag{1.1.4}$$

According to Oseledec's ergodic theorem, if the system is ergodic, it has m Lyapunov exponents. Of these, λ is the largest; it does not depend on x_0. (In this thesis, only the largest Lyapunov exponent will be of importance hereafter, and the word largest will be dropped for simplicity.)

1.2 Universality at the edge of chaos

In 1978, M. J. Feigenbaum [12]discovered that there is a universal quantity at the edge of chaos in the logistic map $x_{n+1} = bx_n(1 - x_n)$. As the parameter b increases from zero, period-doubling bifurcation is observed. We define b_n as the parameter value at which n-fold bifurcation occurs. Let $\delta \overset{\text{def}}{=} \lim_{n\to\infty} \dfrac{b_{n+1} - b_n}{b_{n+2} - b_{n+1}}$. This limit exists and can be numerically evaluated; it is called the Feigenbaum constant $\delta = 4.6692016091029\ldots$. This behavior has been studied in various systems, including the driven anharmonic oscillator [44], plasma [45], and oscillatory flow [46].

The Lyapunov exponent λ is used to indicate chaoticity. It is calculated for each orbit; when its value is positive, the corresponding orbit is regarded as chaotic. The Lyapunov exponent reflects the universality of the behavior of dynamical systems making the transition from unstable to stable by changing parameters. In particular, near the critical parameter value α_c at which the Lyapunov exponent is zero, the Lyapunov exponent is approximately $\lambda \simeq C\,|\alpha - \alpha_c|^{\nu}$ where C is a constant and ν is a universal critical exponent for each route to chaos. In 1980, Huberman and Rudnick [14] estimated the critical exponent ν in the logistic map by numerical experiment as $\nu = \dfrac{\log 2}{\log \delta} = 0.4498069\ldots$. In the same year, Pomeau and Manneville [15] observed that *Type* 1 intermittency and *Type* 3 intermittency occur in the Lorentz equation and a map defined on a circle, respectively, and that their critical exponent is $\nu = \frac{1}{2}$. Another intermittent map, the modified Bernoulli map, is known [16] to have a Lyapunov exponent that can vary as $\lambda \sim \varepsilon^{1-\frac{2}{B}}$ where $\varepsilon \geq 0$ and $B \geq 2$. In each of these three cases, an exact expression for the invariant density function cannot be found analytically.

1.3 SRB measure

A dynamical system typically has uncountably many ergodic measures, not all of which can be observed physically [21]. It is therefore important to identify the physical measure through which the time average of a physical system can actually be calculated, for example by computer simulation. Sinai, Ruelle, and Bowen [22] have shown that in axiom-A systems (Anosov maps), there exists only one such physical measure: the SRB measure [21, 23]. According to Arnold and Avez [31], Anosov maps have mixing properties such that the ergodic relation (1.1.1) applies at almost every point x with respect to the Lebesgue measure[21]. This means that the initial density function weakly approaches the unique equilibrium distribution and the time averages approach equilibrium values [21]. Thus, the SRB measure connects dynamical systems to statistical physics. G. Gallavotti [6] assumed the chaotic hypothesis for multi-dimensional systems without assuming Boltzmann's ergodic hypothesis. With this assumption, the systems have the Anosov property and therefore a unique SRB measure. However, in this thesis, we do not assume the Anosov property; rather, we prove that certain systems have it when an appropriate condition is satisfied.

1.4 Mathematical Background

Let us begin with the definitions according to [47].

Definition 1.4.1 (σ-algebra [47])**.** *A collection $\mathscr{A}$ of subsets of a set X is a σ-algebra if:*

1. $A \in \mathscr{A} \implies X \backslash A \in \mathscr{A}$;

2. Given a finite or infinite sequence $\{A_k\}$ of subsets of X, $A_k \in \mathscr{A} \implies \cup_k A_k \in \mathscr{A}$; and

3. $X \in \mathscr{A}$

From 1. and 3. it holds that $\phi \in \mathscr{A}$. Then, for subsets $\{A_k\}$ such that $A_k \in \mathscr{A}$, $\cap_k A_k \in \mathscr{A}$ holds since $\cap_k A_k = X \backslash (\cup_k (X \backslash A_k))$. At last, for $A \in \mathscr{A}$ and $B \in \mathscr{A}$, it holds that $A \backslash B \in \mathscr{A}$ since $A \backslash B = A \backslash (X \cap B)$.

Definition 1.4.2 (measure [47]). *A real-valued function μ defined on a σ-algebra $\mathscr{A}$ is a measure if:*

1. $\mu(\phi) = 0$;

2. $\mu(A) \geq 0$ *for all* $A \in \mathscr{A}$; *and*

3. $\mu(\cup_k A_k) = \sum_k \mu(A_k)$ *if* $\{A_k\}$ *is a finite or infinite sequence of pairwise disjoint subsets of* $\mathscr{A}$, *that is,* $A_i \cap A_j = \phi$ *for* $i \neq j$.

Definition 1.4.3 (measure space [47]). *If $\mathscr{A}$ is a σ-algebra of subsets of X and if μ is a measure on $\mathscr{A}$, then the triple $(X, \mathscr{A}, \mu)$ is called measure space. The sets belonging to $\mathscr{A}$ are called measurable sets because for them, the measure is defined.*

Definition 1.4.4 (finite and normalized [47]). *A measure space $(X, \mathscr{A}, \mu)$ is called finite if $\mu(X) < \infty$. In particular, if $\mu(X) = 1$, then the measure space is said to be normalized or probabilistic.*

Definition 1.4.5 (measurable [47]). *Let $(X, \mathscr{A}, \mu)$ be a measure space. A real-valued function $f : X \to \mathbb{R}$ is measurable if $f^{-1}(\Delta) \in \mathscr{A}$ for every interval $\Delta \in \mathbb{R}$.*

Definition 1.4.6 (Cesaro convergence [47]). *A sequence of functions $\{f_n\}$, $f_n \in L^p$, $1 \leq p < \infty$ is (weakly) Cesaro convergent to $f \in L^p$ if*

$$\lim_{n \to \infty} \sum_{k=1}^{n} \frac{1}{n} \langle f_k , g \rangle = \langle f, g \rangle \tag{1.4.1}$$

for all $g \in L^{p'}$ where $\frac{1}{p} + \frac{1}{p'} = 1$.

Definition 1.4.7 (weakly convergence [47]). *A sequence of functions $\{f_n\}$, $f_n \in L^p$, $1 \leq p < \infty$ is weakly convergent to $f \in L^p$ if*

$$\lim_{n \to \infty} \langle f_n , g \rangle = \langle f, g \rangle \tag{1.4.2}$$

for all $g \in L^{p'}$ where $\frac{1}{p} + \frac{1}{p'} = 1$.

Definition 1.4.8 (strongly convergence [47]). *A sequence of functions* $\{f_n\}$, $f_n \in L^p$, $1 \leq p < \infty$ *is strongly convergent to* $f \in L^p$ *if*

$$\lim_{n\to\infty} \|f_n - f\|_{L^p} = 0. \tag{1.4.3}$$

Definition 1.4.9 (nonsingular [47]). *A measurable transformation* $S : X \to X$ *on a measure space* $(X, \mathscr{A}, \mu)$ *is nonsingular if* $\mu(S^{-1}(A)) = 0$ *for all* $A \in \mathscr{A}$ *such that* $\mu(A) = 0$.

Definition 1.4.10 (measure preserving [47]). *Let* $(X, \mathscr{A}, \mu)$ *be a measure space and* $S : X \to X$ *a measurable transformation. Then,* S *is said to be measure preserving if* $\mu(S^{-1}(A)) = \mu(A)$ *for all* $A \in \mathscr{A}$.

Definition 1.4.11 (ergodicity [47]). *Let* $(X, \mathscr{A}, \mu)$ *be a measure space.* $S : X \to X$ *is a measurable transformation on the measure space* $(X, \mathscr{A}, \mu)$. *The transformation* S *is called ergodic if every invariant set* $A \in \mathscr{A}$ *is such that either* $\mu(A) = 0$ *or* $\mu(X \backslash A) = 0$.

Definition 1.4.12 (mixing [47]). *Let* $(X, \mathscr{A}, \mu)$ *be a normalized measure space, and* $S : X \to X$ *a measure-preserving transformation.* S *is called mixing if*

$$\lim_{n\to\infty} \mu(A \cap S^{-n}(B)) = \mu(A)\mu(B), \ \textit{for all } A, B \in \mathscr{A}. \tag{1.4.4}$$

Definition 1.4.13 (exact [47]). *Let* $(X, \mathscr{A}, \mu)$ *be a normalized measure space, and* $S : X \to X$ *a measure-preserving transformation such that* $S(A) \in \mathscr{A}$ *for each* $A \in \mathscr{A}$. *If*

$$\lim_{n\to} \mu(S^n(A)) = 1, \ \textit{for every } A \in \mathscr{A}, \mu(A) > 0, \tag{1.4.5}$$

then S *is called exact.*

The definition of exactness is equivalent to the convergence to a stationary density f_*[48].

$$\lim_{n\to\infty} \|P^n f - f_*\| = 0 \tag{1.4.6}$$

where P is the associated Perron-Frobenius operator. The hierarchy of ergodicity is as follows. Exact $\subset$ Mixing $\subset$ Ergodic.

1.5 Outline of the thesis

In this thesis, we characterize chaotic systems by proving their ergodic properties. Using these properties, which lie at the core of chaos theory, we can obtain the critical exponent of the Lyapunov exponent or prove the uni-directionality of the time evolution of the density function.

In Chapter 1 we recall the history of chaos theory, and introduce the relation between chaos and the ergodic theorem.

In Chapter 2, we discuss the critical behavior of chaotic phenomena. The Lyapunov exponent is used to detect chaoticity. As the value of the Lyapunov exponent changes from non-positive in the non-chaotic state to positive in the chaotic state, it can characterize the instability of systems under adjustment of parameters. This behavior has attracted much interest physically and mathematically. At the critical point where the Lyapunov exponent is zero, we derive its critical exponent. More specifically, we treat generalized Boole (GB) transformations, which are maps extended from the Boole transformation with infinite ergodicity; the super generalized Boole transformations (SGB transformations), which are the generalized version of GB transformations, and extended super generalized Boole transformations (ESGB transformations), which are further extensions of SGB transformations. In this chapter, we show that there are three parameter regions in GB transformations [49]: a region in which the mixing property holds, a region in which infinite measure is preserved, and a region in which dissipation appears. We prove that the critical exponent is $1/2$ or unity at the critical point by rewriting the Lyapunov exponent explicitly with a parameter [49]. SGB transformations are countably infinite map sets, derived by adding one parameter to GB transformations [50]. We prove that SGB transformations preserve the Cauchy distribution, that they are exact in certain parameter ranges, and that the critical exponents are $1/2$ or unity for countably infinite maps [50]. This last result not only verifies the statement of Pomeau and Manneville that the critical exponent is $1/2$ for countably infinite maps, but also includes a new discovery: the critical exponent can be unity. Moreover, by proving exactness, we show that any initial density function converges to a unique equilibrium density function, proving unidirectionality. ESGB transformations are SGB transformations with an additional parameter by which we generalize the class of invariant density functions beyond the Cauchy distribution. We prove that ESGB transformations are exact in a certain parameter range with more generalized invariant density functions and that the critical exponents are $1/2$ in an exact region.

In Chapter 3, irreversibility is discussed for symplectic maps with time-reversal symmetry derived from a certain Hamiltonian. Time-reversal symmetry is not universal; there are unidirectional phenomena such as the increase in entropy. It is known that in Anosov maps, which are typical chaotic maps, any initial density function that is absolutely continuous to the Lebesgue measure converges to a unique equilibrium density function corresponding to the SRB measure by the mixing property. In Chapter 3, we generate discrete-time maps with time-reversal symmetry (Tan maps) from a certain Hamiltonian and, by proving that these maps are certainly Anosov maps, show that any initial density function (defined at all non-zero volume sets) converges to the uniform distribution [51]. Thus, it can be said that we succeed in generalizing the example for which unidirectionality of time was proven in Chapter 2, even though Tan maps have time-reversal symmetry. We also show that anomalous diffusion, which differs from normal diffusion such as Brownian motion, occurs when these maps have the Anosov property.

In Appendix A, we treat weakly chaotic systems, i.e., systems with a small positive Lyapunov exponent. In such systems, it is known that calculating the Lyapunov exponent is very time-consuming. The Lyapunov time, which is the reciprocal of the Lyapunov exponent, can be used as a rough estimate of calculation time. In some cases, it takes ten Lyapunov times to calculate the Lyapunov exponent [39]. In order to detect chaoticity more rapidly, Froeschlé et. al. [39, 41] devised the Fast Lyapunov Indicator(FLI). Subsequently, the Orthogonal Fast Lyapunov Indicator (OFLI) [42] and the Orthogonal Fast Lyapunov Indicator 2 (OFLI^2) [43] were developed; although more accurate than FLI, they are not faster. In Appendix A, we propose the Ultra Fast Lyapunov Indicator [52, 53], a faster chaos indicator than previous chaos indicators,.

In Appendix B, the scaling behavior of super-generalized Boole transformations for $K = 3, 4$ and 5 is shown.

Chapter 2

Universal Critical Behavior

This chapter is according to the [49] and [50].

2.1 Introduction

The route from stable states to chaotic (intermittent) states has attracted much attention from within the broader field of physics. This issue concerns the fundamental change of systems from a stable state to an unstable state and it is an essential theme to analyze the stability of physical systems. The route to chaos has also been studied theoretically and experimentally for systems such as Hamiltonian systems [54], map systems [14, 15, 55, 56, 57, 58], coupled oscillators [59], the Belousov-Zhabotinskii reaction [60], the Rayleigh-Benard convection [60], the Couette-Taylor flow [60], a noise-induced system [61], a thermoacoustic system [62], and optomechanics [63, 64, 65]. Theoretical classifications of routes to chaos such as the intermittency route, period-doubling route, and frequency locking route, have been proposed [60]. Frequently, these studies were motivated by attempts to discover the universality at the onset of chaos with respect to the critical exponent of the Lyapunov exponent , which has been extensively studied for characterizing chaotic systems and plays an important and essential role as a chaos indicator characterizing the degree of chaoticity quantitatively. The universality of the critical exponents in each route to chaos has been studied extensively by numerical simulations. In the case of the period-doubling route, Huberman and Rudnick [14] numerically estimated the critical exponent ν as $\nu = \frac{\log 2}{\log \delta}$, where δ represents the Feigenbaum constant. In terms of the intermittency route considered in this thesis, Pomeau and Manneville [15, 56] classified intermittency into three types and conjectured the universality of ν for each intermittent type. These authors [15] determined that *Type* 1 intermittency occurs when tangent bifurcation appears, and *Type 3* intermittency occurs when period-doubling bifurcation appears, a finding that was subsequently confirmed by others [66]. For example, *Type* 1 intermittency was observed in the Lorentz equation [15] and the logistic map [67]. Other researchers [68, 69] found that *Type* 1 intermittency occurs and superdiffusion is also observed in a climbing-sine map. Pomeau and Manneville [15] explained the reason why the critical exponent with the Lyapunov exponent is $\frac{1}{2}$ as follows. When *Type* 1 intermittency occurs, a "channel" exists between $x_{n+1} = S(x_n)$ where S represents a map and the bissectrix $x_{n+1} = x_n$. The function $S(x_n)$ is then expanded around a fixed point, such that this point can be assumed to be the original point, to obtain the following equation, $S(x_n) = x_n + x_n^2 + \varepsilon +$ (higher order terms). They estimated the number of iterative computations required to cross the channel to be of the order of $\varepsilon^{-\frac{1}{2}}$. Then they concluded that, in the vicinity of $\varepsilon = +0$, the Lyapunov exponent varies as $\varepsilon^{\frac{1}{2}}$ by using an elementary calculation and the numerical simulations. In the case of *Type* 3 intermittency, which was observed in NPN device [70], laser [71], hydrodynamical system [18] and a map system [72]. According to [15, 73], the reason why the critical exponent is $\frac{1}{2}$ in *Type* 3 intermittency is as follows. By approximation, the map $S(x_n)$ is locally expressed as $S(x_n) = -(1 + \varepsilon)x_n + ax_n^2 + \beta' x_n$ where α and β' are constant. Consider the map from x_n to x_{n+2}, truncate this map after third order of x, pick up to the first order of ε and we obtain the following equation. $x_n \mapsto x_{n+2} \simeq (1 + 2\varepsilon)x_n + \beta x_n^3$ where $\beta = -2(\beta' + \alpha^2)$. When β is positive, the bifurcation at $\varepsilon = 0$ is subcritical ant Type 3 intermittency occurs. Then, by elementary calculation, it is shown that Lyapunov exponent should grow like $\varepsilon^{\frac{1}{2}}$. Subsequent to the work by Pomeau and Manneville, the critical exponent was researched in various fields with relation to intermittency such as the Billiard system [74, 75], electronic circuits [76], plasma physics [77], and an intermittent map [72]. These studies, which were conducted by numerical simulations, suggest that their conjecture $\nu = \frac{1}{2}$ would be right. However, one can find it difficult to obtain analytically the value of critical exponent of Lyapunov exponents for given chaotic systems in general. There are few analytic formulas of ergodic invariant measures [35]. The analytic parametric density functions of ergodic invariant measure can be used for analytically estimating Lyapunov exponents for such specific systems. However, for most cases, that analytic result cannot be extended for the whole region of parameter space. Consequently, in previous studies, the critical exponent ν was either estimated numerically or an assumption about the ergodicity was necessary, without which the analytical formulae of the Lyapunov exponent λ could not be obtained.

2.2 Generalized Boole Transformations

2.2.1 Introduction-Generalized Boole transformations

In the case of the logistic map, Huberman and Rudnick [14] found a scaling behavior of Lyapunov exponent from zero to positive and Pomeau and Manneville [15] found a similar behavior of Lyapunov exponent. Both of them use numerical simulations.

Here, we consider the Boole transformation [78] given by

$$x_{n+1} = Tx_n = x_n - \frac{1}{x_n}, \tag{2.2.1}$$

which is known to preserves the Lebesgue measure dx as an invariant measure [79]. The Lebesgue measure dx is an infinite measure. Thus, we cannot normalize the invariant measure as a probability measure.

One can generalize the Boole transformation as two-parameter map family as Aaronson [80] treats the following generalized Boole transformations which are defined as

$$x_{n+1} = T_{\alpha,\beta}x_n = \alpha x_n - \frac{\beta}{x_n},\ \alpha > 0, \beta > 0, \tag{2.2.2}$$

preserving the Cauchy measure $\mu(dx)$ for $0 < \alpha < 1$ given by

$$\mu(dx) = \frac{\sqrt{\beta(1-\alpha)}}{\pi[x^2(1-\alpha)+\beta]}dx. \tag{2.2.3}$$

As a subset of the generalized Boole transformations, the map at $\alpha = \beta = 1/2$ corresponds to the exactly solvable chaos map [35] given by Ref. [36]

$$x_{n+1} = \frac{1}{2}\left(x_n - \frac{1}{x_n}\right). \tag{2.2.4}$$

K. Umeno showed that this map can be expressed by the double-angle formula of cot function having Lyapunov exponent $\lambda = \log 2$ and one can use Eq.(2.2.4) in order to generate general Lévy stable distributions via their superposition [36]. The generalized Boole transformations have the standard forms which do not depend on β. That is, by substituting x_n by $\sqrt{\frac{\beta}{\alpha}}y_n$, Eq. (2.2.2) is replaced by

$$\sqrt{\frac{\beta}{\alpha}}y_{n+1} = \alpha\sqrt{\frac{\beta}{\alpha}}y_n - \beta\sqrt{\frac{\alpha}{\beta}}\frac{1}{y_n},$$

which is nothing but

$$y_{n+1} = \alpha\left(y_n - \frac{1}{y_n}\right). \tag{2.2.5}$$

The transformation $P_{\alpha,\beta} : x_n \mapsto \sqrt{\frac{\beta}{\alpha}}y_n$ is a one-to-one diffeomorphism. Then the transformations of Eq. (2.2.5) have the same Lyapunov exponent for fixed α with this topological conjugacy relation. Consequently, the generalized Boole transformations have the same Lyapunov exponents which are independent of β.

2.2.2 Analytic Formula of Lyapunov exponents for the generalized Boole transformations

The ergodicity of similar kinds of this generalized Boole transformations was shown by Kempermann [81] and Letac [82]. We prove the theorem 1 concerning the mixing property of the generalized Boole transformations for $0 < \alpha < 1$ as follows.

Theorem 2.2.1. *The generalized Boole transformations in* $0 < \alpha < 1$ *have mixing property.*

Thus, we can prove the ergodicity with respect to the Cauchy measure in Eq. (2.2.3) for $0 < \alpha < 1$.

Proof. We obtain the relation of Eq. (2.2.5) by substituting x_n by $-\cot\pi\theta_n$ as,

$$\begin{aligned} \cot\pi\theta_{n+1} &= 2\alpha\cot 2\pi\theta_n, \\ \text{where} \qquad \theta_{n+1} &= \bar{T}_\alpha(\theta_n) = \frac{1}{\pi}\text{arccot}\left[2\alpha\cot 2\pi\theta_n\right]. \end{aligned} \tag{2.2.6}$$

The transformations

$$\bar{T}_\alpha : [0,1) \longrightarrow [0,1), \tag{2.2.7}$$

have the topological conjugacy relation with Eq. (2.2.5). Consider the following cylinder sets of $\bar{T}_\alpha^{-k}[0,1)$ on which $\bar{T}_\alpha^k$ is surjective to $[0,1)$, satisfying

$$I_{j,k} = [\nu_{j,k}, \nu_{j+1,k}),\ \nu_{j,k} < \nu_{j+1,k},\ \text{for } 0 \le j \le 2^k - 1, \tag{2.2.8}$$

$$\nu_{0,k} = 0 \text{ and } \nu_{2^k,k} = 1, \tag{2.2.9}$$

$$\bar{T}_\alpha^k I_{j,k} = [0,1), \tag{2.2.10}$$

$$\mu(I_{j,k}) = \frac{1}{2^k}. \tag{2.2.11}$$

For any measurable set A, and $\bar{T}_\alpha$-invariant measure μ, consider, for arbitrary $n(\geq k)$

$$\mu\left(\bar{T}_\alpha^{-n} A \cap B\right), \tag{2.2.12}$$

where it is enough to assume B is $\left[\nu_{j,k}, \nu_{j+1,k}\right)$ without loss of generality. Here, $\mu(B) = \frac{1}{2^k}$ and the number of the intervals of $\bar{T}_\alpha^{-n} A$ which are included by B is 2^{n-k}. Thus, the measure of $\bar{T}_\alpha^{-n} A$ on each interval $I_{j,k}$ whose measure $\mu(I_{j,k})$ is *equidistributed*, is $2^{-n}\mu(A)$. Then, for arbitrary $n(\geq k)$,

$$\mu\left(\bar{T}_\alpha^{-n} A \cap B\right) = 2^{n-k} \cdot (2^{-n}\mu(A)) = \mu(A) \cdot \mu(B) \tag{2.2.13}$$

Thus, the dynamical system $([0, 1), \bar{T}_\alpha, \mu)$ has mixing property according to the Ref. [31]. Therefore, the generalized Boole transformations for $0 < \alpha < 1$ have mixing property. □

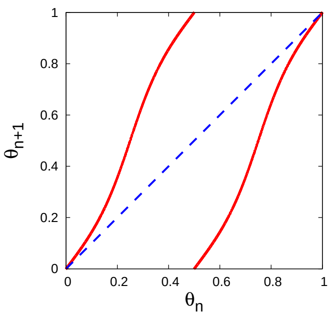

Figure 2.1: Solid lines correspond to the transformation $\bar{T}_{0.75}$ which is topologically conjugate with the generalized Boole transformation $T_{\alpha=0.75,\beta=0.75}$ and a dashed line corresponds to $\theta_{n+1} = \theta_n$. The transformations $\bar{T}_\alpha$ monotonically increase in the interval $[0, 0.5)$ or $[0.5, 1)$.

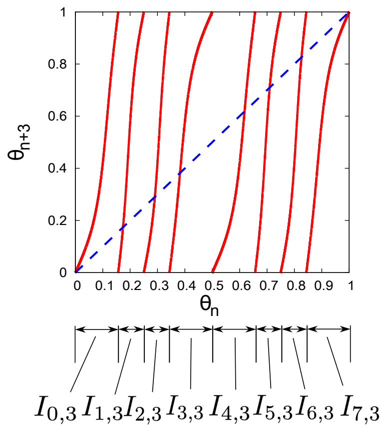

Figure 2.2: Solid lines correspond to the transformation $\bar{T}_{0.75}^3$ which is topologically conjugate with the generalized Boole transformation $T_{\alpha=0.75,\beta=0.75}^3$ and a dashed line corresponds to $\theta_{n+3} = \theta_n$. Here, the measure of each $I_{j,3}(0 \leq j \leq 7)$ is equidistributed.

Here, we prove the following theorem.

Theorem 2.2.2. *The generalized Boole transformations for* $0 < \alpha < 1$ *have the Lyapunov exponents given by*

$$\lambda(\alpha, \beta) = \log\left(1 + 2\sqrt{\alpha(1-\alpha)}\right).$$

Note that the Lyapunov exponents do not depend on the parameter β but purely depend on the parameter α.

Proof. By the ergodicity, we can calculate the Lyapunov exponents of the generalized Boole transformations as

$$\lambda(\alpha,\beta) = \int_{-\infty}^{\infty} \log\left|\alpha + \frac{\beta}{x^2}\right| \frac{\sqrt{\beta(1-\alpha)}}{\pi[x^2(1-\alpha)+\beta]}dx.$$

Here, we substitute $\sqrt{\alpha/\beta}x$ by y, then we obtain:

$$\begin{aligned}
\lambda(\alpha,\beta) &= \frac{1}{\pi}\sqrt{\frac{\alpha}{1-\alpha}}\int_{-\infty}^{\infty} \log\left|\alpha + \frac{\alpha}{y^2}\right| \frac{dy}{y^2 + \left(\sqrt{\frac{\alpha}{1-\alpha}}\right)^2}, \\
\log\left|\alpha + \frac{\alpha}{y^2}\right| &= \log\alpha + \log|1+iy| + \log|1-iy| - 2\log|y|.
\end{aligned}$$

Let us substitute p for $\sqrt{\frac{\alpha}{1-\alpha}}$ and put I_1, I_2, I_3 and I_4 as,

$$\begin{aligned}
\lambda(\alpha,\beta) &= I_1 + I_2 + I_3 + I_4, \\
I_1 &= \frac{p}{\pi}\int_{-\infty}^{\infty} \frac{\log\alpha}{y^2+p^2}dy, \\
I_2 &= \frac{p}{\pi}\int_{-\infty}^{\infty} \frac{\log|1+iy|}{y^2+p^2}dy, \\
I_3 &= \frac{p}{\pi}\int_{-\infty}^{\infty} \frac{\log|1-iy|}{y^2+p^2}dy, \\
I_4 &= -\frac{2p}{\pi}\int_{-\infty}^{\infty} \frac{\log|y|}{y^2+p^2}dy.
\end{aligned}$$

Evaluate I_1. We consider a function $f_1(z)$ defined by

$$f_1(z) = \frac{\log\alpha}{z+ip},$$

which is regular on upper half-plane. Thus we can integrate along the path C1 in Figure 2.3. Then we have the relations

$$I_1 = \log\alpha, \tag{2.2.14}$$

as $R \to \infty$.

Next, as for I_3, we consider a function $f_3(z)$ defined by

$$f_3(z) = \frac{\log|1-iz|}{z+ip},$$

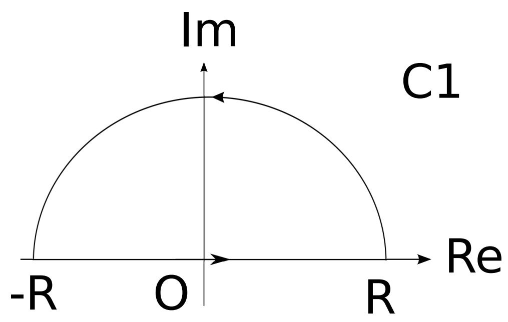

Figure 2.3: The integral path of I_1, I_2 and I_3

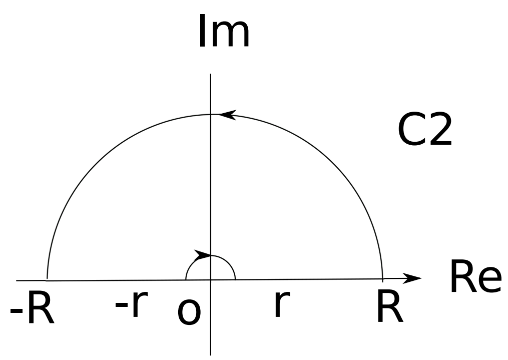

Figure 2.4: The integral path of I_4

which is regular on upper half-plane. Thus we can integrate $f_3(z)$ along the path C1 in Figure 2.3. We get:

$$I_3 = \log|1+p|, \tag{2.2.15}$$

as $R \to \infty$.

In terms of evaluating I_2, by applying a transformation as $y \to -y$ we have the relation $I_2 = I_3$.

As for I_4, we consider a function $f_4(z)$ defined by

$$f_4(z) = \frac{\log|z|}{z+ip} \tag{2.2.16}$$

which is regular along the path C2 in Figure 2.4 and on the inner part of C2. Then by integrating of $f_4(z)$ along C2, we obtain

$$I_4 = -2\log p, \tag{2.2.17}$$

as $r \to 0, R \to \infty$. As for $r \to 0$, we substitute z by $e^{i\theta}$ and we have the relation:

$$\left|\int_{\pi}^{0} \frac{\log r + 2\pi}{r^2 e^{2i\theta} - p^2} ire^{i\theta} d\theta\right| \leq \int_{0}^{\pi} \frac{|\log r + 2\pi|}{|r^2 e^{2i\theta} - p^2|} r d\theta.$$

Then we set $r < p/2$ and we obtain:

$$\frac{1}{\left|r^2 e^{2i\theta} + p^2\right|} < \frac{1}{|p|^2 - r^2} < \frac{4}{3}\frac{1}{|p|^2}.$$

Using these facts, we have

$$\begin{aligned} \int_0^{\pi} \frac{|\log r + 2\pi|}{\left|r^2 e^{2i\theta} - p^2\right|} r d\theta &< \int_0^{\pi} \frac{4}{3}\frac{|\log r + 2\pi|}{|p|^2} r d\theta, \\ &\leq \frac{4\pi}{3}\frac{r\,|\log r + 2\pi|}{|p|^2} \to 0 \text{ as } r \to 0. \end{aligned}$$

Therefore, we obtain analytic formula of the Lyapunov exponents for the generalized Boole transformations $\lambda(\alpha,\beta)$ as

$$\begin{aligned} \lambda(\alpha,\beta) &= \log\alpha + \log|1+p| + \log|1+p| - 2\log p, \\ &= \log\left(1 + 2\sqrt{\alpha(1-\alpha)}\right). \end{aligned} \tag{2.2.18}$$

□

The Lyapunov exponents do not depend on β, so that we can change the notation from $\lambda(\alpha,\beta)$ to $\lambda(\alpha)$. The invariant measure $\mu(dx)$ is Cauchy and smooth with respect to the Lebesgue measure. Thus, according to the Pesin identity [23, 108], we can calculate KS-entropy $h(\alpha)$ analytically as

$$h(\alpha) = \int_{-\infty}^{\infty} \lambda(\alpha)\mu(dx) = \lambda(\alpha). \tag{2.2.19}$$

Figure 2.5 shows the comparison results of our numerical estimate of the Lyapunov exponents for the generalized Boole transformations with
$\alpha = 0.1,\ 0.2,\ 0.3,\ 0.4,\ 0.5,\ 0.6,\ 0.7,\ 0.8$ and 0.9 using the long double precision and our analytic formula of the Lyapunov exponents. The initial condition of computation is $x_0 = 9.3$. The coincidence is remarkable as shown in Figure 2.5.

Equation (2.2.18) converges to zero in the limit of $\alpha \to 0$ and $\alpha \to 1$. However, different phenomena occur for $\alpha = 0$ and $\alpha = 1$ respectively. In the case of $\alpha = 0$, every orbits are periodic because

$$T^2_{\alpha,\beta}x = x.$$

On the other hand, at $\alpha = 1$, *subexponential chaos* [84, 85] occurs. Then, in calculation of finite Lyapunov exponents, the value does not converge to a constant but converges in distribution.

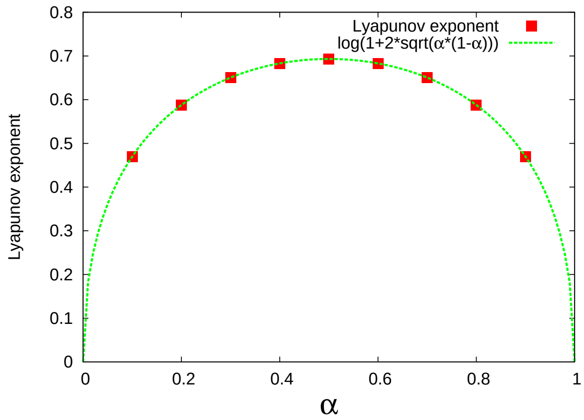

Figure 2.5: The numerical results of the finite Lyapunov exponents and analytic solution of the generalized Boole transformation.

2.2.3 Lyapunov exponents for $\alpha > 1$

Here, we prove another theorem.

Theorem 2.2.3. *The generalized Boole transformations for $\alpha > 1$ have the Lyapunov exponents given by*

$$\lambda(\alpha, \beta) = \log \alpha.$$

Proof. In the range of $\alpha > 1$, the generalized Boole transformations have two equilibrium points at $x_\pm = \pm\sqrt{\frac{\beta}{\alpha-1}}$. Two of them are unstable since the slope of the liner inclinations are both $\frac{dT_{\alpha,\beta}x}{dx}(x_\pm) = 2\alpha - 1 > 1$. Now by substituting x_n by $\frac{1}{z_n}$, we obtain another form of the generalized Boole transformations as

$$z_{n+1} = \frac{z_n}{\alpha - \beta z_n^2}. \tag{2.2.20}$$

The equilibrium points of Eq. (2.2.20) are $z = 0, \pm\sqrt{\frac{\alpha-1}{\beta}}$. Two points $z = \pm\sqrt{\frac{\alpha-1}{\beta}}$ are unstable. The equilibrium point at $z = 0$ are stable and attractive because

$$\left| \frac{d}{dz}\left(\frac{z}{\alpha - \beta z^2}\right)\bigg|_{z=0} \right| < 1. \tag{2.2.21}$$

Thus, for almost all initial points it is hold that

$$\lim_{n\to\infty} |x_n| = \infty. \tag{2.2.22}$$

Hence, the Lyapunov exponents of the generalized Boole transformations for $\alpha > 1$ are given by taking logarithmic function of inclination in the limit of $|x| \to \infty$ as

$$\lambda(\alpha, \beta) = \log \alpha. \tag{2.2.23}$$

$\square$

The complete behavior of Lyapunov exponent as a function of parameter α is shown in Figure 2.6.

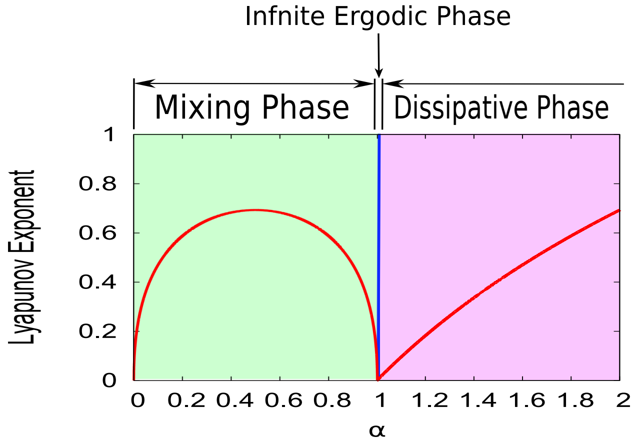

Figure 2.6: The classification of the phase of the generalized Boole transformation systems in the parameter space α via the analytic Lyapunov exponents.

According to Ref. [80], the generalized Boole transformations for $\alpha > 1$ are *dissipative* in the sense that, for almost all initial points, $|x_n| \to \infty$ as $n \to \infty$.

Table 2.1 summarizes a classification of the phase of systems by the nature of invariant measure. We can say the system is in *Mixing Phase* for $0 < \alpha < 1$, *Infinite Ergodic Phase* for $\alpha = 1$ and *Dissipative Phase* at $\alpha > 1$.

Table 2.1: The classification of phase of dynamical systems, invariant measure and Lyapunov exponents in terms of parameter α.

	$0 < \alpha < 1$	$\alpha = 1$	$\alpha > 1$
Phase	Mixing Phase	Infinite Ergodic Phase	Dissipative Phase
Invariant measure $\mu(dx)$	$\frac{\sqrt{\beta(1-\alpha)}}{\pi[x^2(1-\alpha)+\beta]}dx$	dx	
Lyapunov exponents	$\log\left(1 + 2\sqrt{\alpha(1-\alpha)}\right)$	0 (*subexponential chaos*)	$\log \alpha$

Table 2.2: The difference between types of Intermittency and critical exponents of the generalized Boole transformation.

	$\alpha \to 0+0$	$\alpha \to 1-0$	$\alpha \to 1+0$
Intermittency	*Type 3*	*Type 1*	
Critical Exponent	$\frac{1}{2}$	$\frac{1}{2}$	1

The standard Cauchy density function $\rho_\gamma(x)$ is defined by a scale parameter γ

$$\rho_\gamma(x) = \frac{\gamma}{\pi(x^2+\gamma^2)}. \tag{2.2.24}$$

According to the probability preservation relation [86], the density functions $\rho_\gamma(x)$ and $\rho_{\gamma'}(y)$ satisfy the relation

$$\rho_{\gamma'}(y)dy = \sum_{x=T_{\alpha,\beta}^{-1}y} \rho_\gamma(x)dx. \tag{2.2.25}$$

In the case of $\alpha = \beta = \frac{1}{2}$ [86], the scale parameter γ of Cauchy density function of invariant measure is updated in accordance with

$$\gamma' = \frac{1}{2}\left(\gamma + \frac{1}{\gamma}\right). \tag{2.2.26}$$

Then, γ converges to unity. Similarly, by the probability preservation relation, the scale parameter of the density function of the generalized Boole transformation is updated in accordance with

$$\gamma' = \alpha\gamma + \frac{\beta}{\gamma}, \tag{2.2.27}$$

and it converges to the fixed point $\gamma^* = \sqrt{\frac{\beta}{1-\alpha}}$.
As we make α close to unity from below, the scale parameter γ converges to infinity and the density function of invariant measure becomes the Lebesgue measure dx. For $\alpha > 1$, the fixed point of scale parameter γ^* must be an imaginary number. This fact shows for $\alpha > 1$, the density function of the invariant measure can *never* be a Cauchy distribution.

Compare with the AL map [85, 87] whose Lyapunov exponent diverges to infinity at the fixed point, the generalized Boole transformations for $\alpha > 1$ have the positive Lyapunov exponent $\log \alpha$ at the attractive fixed point $z = 0$.

2.2.4 Scaling behavior at $\alpha = 0, 1$

With parametric analytic formula of Lyapunov exponents, we can investigate a parametric dependency. The first derivative of the Lyapunov exponents with respect to α is given by

$$\frac{d\lambda}{d\alpha} = \begin{cases} \frac{1-2\alpha}{\sqrt{\alpha(1-\alpha)}\left(1+2\sqrt{\alpha(1-\alpha)}\right)}, & 0 < \alpha < 1, \\ \frac{1}{\alpha}, & \alpha > 1. \end{cases} \tag{2.2.28}$$

Remarkably, it diverges in the limit of $\alpha \to 0, \alpha \to 1-0$ as

$$\left| \lim_{t\to 0} \frac{d\lambda}{d\alpha}\bigg|_{\alpha=t} \right| = \infty, \quad \left| \lim_{t\to 1-0} \frac{d\lambda}{d\alpha}\bigg|_{\alpha=t} \right| = \infty. \tag{2.2.29}$$

This is similar to the well-known critical phenomena that the derivative of magnetization diverges at the critical temperature. This means that a *slight* modification of parameter α toward unity (the Boole transformations) from below causes a *large* effect on the value of Lyapunov exponent at the edge of $0 < \alpha < 1$. Furthermore, we can say that it is *extremely* difficult to numerically obtain the Lyapunov exponents near $\alpha = 1$ and $0 < \alpha < 1$ because for $\alpha = 1$ *subexponential chaos* [84, 85] occurs and we cannot determine a Lyapunov exponent for finite calculation.

According to Eq. (2.2.5), the generalized Boole transformation at the limit of $\alpha \to 1$ corresponds to the Boole transformation, such that a transition behavior between chaotic behavior and *subexponential* behavior [84] can be observed at $\alpha = 1$.

Consider the scaling behavior at $\alpha = 0, 1$. When $\alpha \simeq 0$ or "$\alpha \simeq 1$ and $0 < \alpha < 1$", the relation $0 < 2\sqrt{\alpha(1-\alpha)} \ll 1$ holds. Thus, we obtain a Taylor expansion of Eq. (2.2.18) as

$$\lambda(\alpha) = \sum_{n=1}^{\infty} \frac{(-1)^{n+1}}{n} \left(2\sqrt{\alpha(1-\alpha)}\right)^n. \tag{2.2.30}$$

Thus, the first approximation is given by the first term of the Taylor expansion

$$\lambda \simeq 2\sqrt{\alpha(1-\alpha)}, \tag{2.2.31}$$

$$\simeq \begin{cases} 2\sqrt{\alpha}, & \text{for} \quad \alpha \simeq 0, \\ 2\sqrt{1-\alpha}, & \text{for} \quad \alpha \simeq 1 \text{ and } 0 < \alpha < 1. \end{cases} \tag{2.2.32}$$

Then, the scaling behavior of Lyapunov exponents near $\alpha = 0, 1$ is shown as

$$\lambda \simeq \begin{cases} 2\alpha^{\frac{1}{2}}, & \text{for} \quad \alpha \simeq 0, \\ 2(1-\alpha)^{\frac{1}{2}}, & \text{for} \quad \alpha \simeq 1 \text{ and } 0 < \alpha < 1, \\ \alpha - 1, & \text{for} \quad \alpha \simeq 1 \text{ and } \alpha > 1. \end{cases} \tag{2.2.33}$$

In this section, we define a critical exponent as a power exponent of Lyapunov exponent. A critical exponent ν is defined by

$$\lambda \simeq C|\alpha - \alpha_c|^{\nu}, \tag{2.2.34}$$

where α_c is a critical point and C is a constant. Therefore, the both critical exponents ν at the egde of $0 < \alpha < 1$ of the scaling behavior of Lyapunov exponents are $\dfrac{1}{2}$. The Floquet multiplier for the fixed point for $\alpha = 0$ is -1 and for $\alpha = 1$ is 1. Thus, our analytic results agree with the prediction by Pomeau and Manneville [15] that critical exponents of Lyapunov exponents of *Type 1* (Floquet multiplier is unity) and *Type 3* (Floquet multiplier is -1) intermittency are $\frac{1}{2}$ respectively. The critical exponent in the limit of $\alpha \to 1 + 0$ is different from that of $\alpha \to 1 - 0$. This remarkable difference in critical exponents of Lyapunov exponents is caused by the difference between the mixing (ergodic) phase for $0 < \alpha \leq 1$ and the dissipative (non-ergodic) phase for $\alpha > 1$.

2.3 Super Generalized Boole Transformations

In above section, the authors [49] presented the analytical formula of the Lyapunov exponent λ as an explicit function in terms of the bifurcation parameter by showing the mixing property for the generalized Boole (GB) transformation. With respect to the GB transformation, we proved that both *Type 1* and *Type 3* intermittency occur and that the conjecture by Pomeau and Manneville is certainly correct.

In this section, we analytically prove that, for a countably infinite number of maps, it holds that

$$\lambda \sim C\,|\alpha - \alpha_c|^{\nu}\,,\ \nu = \frac{1}{2} \text{ or } 1, C > 0, \tag{2.3.1}$$

where α and α_c represent a bifurcation parameter and the critical point, respectively. In order to prove this, we propose additional generalized maps, the super generalized Boole (SGB) transformations, and show that there are parameter ranges in which the SGB transformations are *exact* (a stronger condition than ergodicity). This means that a countably infinite number of exact (ergodic) maps is obtained. Using this result, one can explicitly determine the analytical formulae of the Lyapunov exponents and critical exponents. The SGB transformations have advantages in their proven mathematical results, compared with the maps that were previously obtained [15]. Let us start with several definitions. We consider a set $Sing_S \in \mathbb{R}$ as consisting of the singular points for a map S when $S(x), x \in Sing_S$ cannot be defined.

Let us begin with definitions. The definitions of F_K and $S_{K,\alpha}$ are written as follows.

Definition 2.3.1. *Let $F_K : \mathbb{R}\backslash A \to \mathbb{R}\backslash A$ be a map denoted as [86]*

$$F_K(\cot\theta) \stackrel{\text{def}}{=} \cot K\theta, \tag{2.3.2}$$

where $K \in \mathbb{N}\backslash\{1\}$ and $A \stackrel{\text{def}}{=} \{x \in \mathbb{R} | {}^{\exists}n \in \mathbb{Z}; F_K^n(x) \in Sing_{F_K}\}$.

Using the function $F_K(x)$, we define two-parameterized one-dimensional maps, the super feneralized Boole Transformations (SGB) $S_{K,\alpha} : \mathbb{R}\backslash B \to \mathbb{R}\backslash B$ as follows.

Definition 2.3.2 (Super Generalized Boole Transformation)**.** *The map $S_{K,\alpha}$: $\mathbb{R}\backslash B \to \mathbb{R}\backslash B$ denoted as*

$$x_{n+1} = S_{K,\alpha}(x_n) \stackrel{\text{def}}{=} \alpha K F_K(x_n), \tag{2.3.3}$$

is referred to as the super generalized Boole Transformation, where $|\alpha| > 0$, $K \in \mathbb{N}\backslash\{1\}$ and $B \stackrel{\text{def}}{=} \{x \in \mathbb{R} | {}^{\exists}n \in \mathbb{Z}; S_{K,\alpha}^n(x) \in Sing_{S_{K,\alpha}}\}$.

For example, $S_{3,\alpha}$, $S_{4,\alpha}$, and $S_{5,\alpha}$ are as follows.

$$\begin{aligned} S_{3,\alpha}(x_n) &= 3\alpha\frac{x_n^3 - 3x_n}{3x_n^2 - 1}, && (2.3.4)\\ S_{4,\alpha}(x_n) &= 4\alpha\frac{x_n^4 - 6x_n^2 + 1}{4x_n^3 - 4x_n}, && (2.3.5)\\ S_{5,\alpha}(x_n) &= 5\alpha\frac{x_n^5 - 10x_n^3 + 5x_n}{5x_n^4 - 10x_n^2 + 1}. && (2.3.6) \end{aligned}$$

The derivative of $S_{K,\alpha}$ with respect to x is denoted as

$$\begin{aligned} S'_{2N,\alpha}(x) &= (2N)^2\alpha\frac{(1+x^2)^{2N-1}}{\left[\displaystyle\sum_{r=0}^{N-1}(-1)^r {}_{2N}\mathrm{C}_{2r+1}x^{2N-2r-1}\right]^2} \\ &\Rightarrow\ S'_{2N,\alpha}(x)\begin{cases} > 0, & \alpha > 0 \\ < 0, & \alpha < 0, \end{cases} \\ S'_{2N+1,\alpha}(x) &= (2N+1)^2\alpha\frac{(1+x^2)^{2N}}{\left[\displaystyle\sum_{r=0}^{N}(-1)^r {}_{2N+1}\mathrm{C}_{2r+1}x^{2(N-r)}\right]^2} \\ &\Rightarrow\ S'_{2N+1,\alpha}(x)\begin{cases} > 0, & \alpha > 0 \\ < 0, & \alpha < 0. \end{cases} \end{aligned}$$

The GB transformation $T_{\alpha,\alpha}$ in [49] corresponds to the map $S_{2,\alpha}$. Figure 2.7 shows the return maps of $S_{3,\frac{1}{3}}$, $S_{4,\frac{1}{4}}$, and $S_{5,\frac{1}{5}}$.

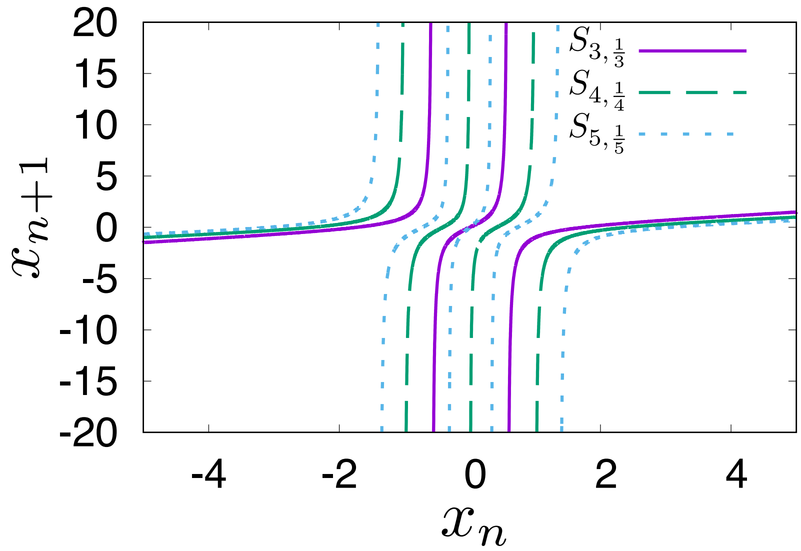

Figure 2.7: Return maps of $S_{3,\frac{1}{3}}, S_{4,\frac{1}{4}}$, and $S_{5,\frac{1}{5}}$. The solid, broken, and dotted lines correspond to the form of $S_{3,\frac{1}{3}}, S_{4,\frac{1}{4}}$, and $S_{5,\frac{1}{5}}$, respectively. The explicit forms of these three maps are provided in Eqs. (2.3.4), (2.3.5) and (2.3.6), respectively.

2.3.1 Invariant density

In this section, it is proven that the SGB transformations preserve the Cauchy distribution for a certain condition. Solving the Perron-Frobenius equation, it is shown that the Cauchy distribution is an invariant distribution for certain parameter ranges. As a preparation, define a function G_K written as follows.

Definition 2.3.3. *Let $G_K : \mathbb{R} \to \mathbb{R}$ be a map denoted as [86]*

$$G_K(\coth\theta) \overset{\text{def}}{=} \coth K\theta, \tag{2.3.7}$$

where $K \in \mathbb{N}\backslash\{1\}$.

The map $G_K(x)$ is denoted as

$$G_{2N}(x) = \frac{\sum_{k=0}^{N} {}_{2N}C_{2k} x^{2(N-k)}}{\sum_{k=0}^{N-1} {}_{2N}C_{2k+1} x^{2(N-k)-1}}, \tag{2.3.8}$$

$$G_{2N+1}(x) = \frac{\sum_{k=0}^{N} {}_{2N+1}C_{2k} x^{2(N-k)+1}}{\sum_{k=0}^{N} {}_{2N+1}C_{2k+1} x^{2(N-k)}}. \tag{2.3.9}$$

If one changes the variable from x to $\coth y$, one has that

$$\begin{aligned} G_{2N}(x) &= \coth(2Ny), \\ G_{2N+1}(x) &= \coth\{(2N+1)y\}. \end{aligned} \tag{2.3.10}$$

If one changes the variable from x to $\tanh y$, one has that

$$\begin{aligned} G_{2N}(x) &= \frac{1}{\tanh(2Ny)}, \\ G_{2N+1}(x) &= \tanh\{(2N+1)y\}. \end{aligned} \tag{2.3.11}$$

In the following, let us discuss the invariant density of SGB transformation. First, assume that the variable x_n obeys the Cauchy distribution

$$f_n(x_n) = \frac{1}{\pi}\frac{\gamma}{x_n^2+\gamma^2} \tag{2.3.12}$$

of which the scale parameter is $\gamma > 0$. According to [36, 86], the map $S_{K,\alpha}$ is K to one map (a non-injective map) as follows.

$$\begin{aligned} x_{n+1} &= \alpha K \cot K\theta = \alpha K F_K(x_n(j)), \\ x_n(j) &= \cot\left(\theta + j\frac{\pi}{K}\right), j = 1, 2, \cdots, K. \end{aligned} \tag{2.3.13}$$

Then, according to [86] and solving the Perron-Frobenius equation, one has that

$$\begin{aligned} f_{n+1}(x_{n+1})|dx_{n+1}| &= f_n(x_n(1))|dx_n(1)| + f_n(x_n(2))|dx_n(2)| + \cdots + f_n(x_n(K))|dx_n(K)|, \\ \left|\frac{dx_{n+1}}{dx_n}\right|_{x_n=x_n(j)} &= \frac{|\alpha|K^2\left(1+\frac{y^2}{\alpha^2K^2}\right)}{1+x_n^2(j)}. \end{aligned}$$

Then, it is clear that the variable x_{n+1} obeys the density function

$$f_{n+1}(x_{n+1}) = \frac{1}{\pi}\frac{|\alpha|KG_K(\gamma)}{x_{n+1}^2 + \alpha^2K^2G_K^2(\gamma)}. \tag{2.3.14}$$

Thus, the density about x changes from $f_n(x) = \dfrac{1}{\pi}\dfrac{\gamma}{x^2+\gamma^2}$ to $f_{n+1}(x) = \dfrac{1}{\pi}\dfrac{|\alpha|KG_K(\gamma)}{x^2 + \alpha^2K^2G_K^2(\gamma)}$. The scale parameter $\gamma > 0$ is then transformed in one iterative step as

$$\gamma \longmapsto |\alpha|KG_K(\gamma). \tag{2.3.15}$$

Now, for each K, let us obtain the fixed point $0 < \gamma_{K,\alpha} < \infty$, which satisfies the relation

$$\gamma_{K,\alpha} = |\alpha|KG_K(\gamma_{K,\alpha}), \tag{2.3.16}$$

and clarify the condition of α that there exists a solution of (2.3.16). If there exists a fixed point, this means that the Cauchy distribution is the invariant density for the map $S_{K,\alpha}$. We approach this problem by defining the Range A as follows.

Definition 2.3.4. *When the parameters (K,α) satisfy a condition such as*

$$\begin{cases} 0 < |\alpha| < 1 & \textit{in the case of} \quad K = 2N, \\ \dfrac{1}{K^2} < |\alpha| < 1 & \textit{in the case of} \quad K = 2N+1, \end{cases} \tag{2.3.17}$$

where $N \in \mathbb{N}$, we say that the parameters (K,α) are in Range A.

Because at $\alpha = \pm\frac{1}{K}$, the SGB transformation $S_{K,\alpha}$ is equivalent to the K-angle formula of the cot function such that

$$\cot\theta_{n+1} = x_{n+1} = \pm\cot(K\theta_n) = \cot(\pm K\theta_n). \tag{2.3.18}$$

It is obvious that the fixed point of scaling parameter $\gamma_{K,\pm\frac{1}{K}}$ is unity by simple calculation. In the following, we discuss the case in which $\alpha \neq \pm\frac{1}{K}$. Such lemmas hold.

Lemma 2.3.1. *For $\frac{1}{K} < |\alpha| < 1$, fix α and there is only one solution that satisfies (2.3.16) in the range of $\gamma_{K,\alpha} > 1$, and for $0 < |\alpha| < \frac{1}{K}$ there is no solution in the range of $\gamma_{K,\alpha} > 1$.*

Proof. The goal is to identify the condition of (K,α) in which there exists a solution $\gamma_{K,\alpha}$ satisfying (2.3.16) for $\gamma_{K,\alpha} > 1$. In the beginning, for simplicity, change the form of (2.3.16) as follows. In (2.3.16), change the variable from $\gamma_{K,\alpha} > 1$ to $\coth y$ as (2.3.10). One has that

$$\coth y = |\alpha| K \coth(Ky). \tag{2.3.19}$$

In the following, one identifies the condition (K, α) in which there exists a solution $y^*_{K,\alpha} > 0$ ($\coth y^*_{K,\alpha} > 1$) satisfying $\coth y^*_{K,\alpha} = |\alpha| K \coth(K y^*_{K,\alpha})$. A function $g(y)$ is defined to be

$$g(y) = \coth y - |\alpha| K \coth(Ky). \tag{2.3.20}$$

In the range where $y > 0$, since the function $\coth y$ decreases monotonically, it holds that

$$\coth y > \coth(Ky). \tag{2.3.21}$$

Then, if the condition $\frac{1}{K} < |\alpha| < 1$ is satisfied, one has that

$$g'(y) = (1 - \coth^2 y) - |\alpha| K^2 \left\{1 - \coth^2(Ky)\right\} < 0. \tag{2.3.22}$$

Thus, the function $g(y)$ decreases monotonically. Let us discuss the value at $y = 0$. In the limit of $y \longrightarrow +0$, it holds that from (2.3.8), (2.3.9) and (2.3.10),

$$\lim_{y \to +0} \frac{\coth\{Ky\}}{\coth y} = \begin{cases} \lim\limits_{y \to +0} \dfrac{{}_{2N}C_0 \coth^{2N} y}{{}_{2N}C_1 \coth^{2N} y} & = \frac{1}{2N}, \text{ for } K = 2N, \\ \lim\limits_{y \to +0} \dfrac{{}_{2N+1}C_0 \coth^{2N} y}{{}_{2N+1}C_1 \coth^{2N} y} & = \frac{1}{2N+1}, \text{ for } K = 2N+1. \end{cases}$$

Thus, one has that

$$\lim_{y \to +0} g(y) = \begin{cases} \lim\limits_{y \to +0} \coth y \times \left(1 - |\alpha| \dfrac{K}{2N}\right) & = +\infty, \text{ for } K = 2N, \\ \lim\limits_{y \to +0} \coth y \times \left(1 - |\alpha| \dfrac{K}{2N+1}\right) & = +\infty, \text{ for } K = 2N+1. \end{cases} \tag{2.3.23}$$

One also has that

$$\lim_{y \to \infty} g(y) = 1 - |\alpha| K < 0. \tag{2.3.24}$$

Thus, from (2.3.22), (2.3.23), and (2.3.24), it is proven that there is only one solution that satisfies $g(y) = 0$. Therefore, for $\frac{1}{K} < |\alpha| < 1$, a solution exists that satisfies (2.3.16) in the range of $\gamma_{K,\alpha} > 1$.

In the case of $0 < |\alpha| < \frac{1}{K}$, it holds that for any $y > 0$

$$g(y) > 0. \tag{2.3.25}$$

Then, there is no solution that satisfies $\gamma_{K,\alpha} > 1$. □

Lemma 2.3.2. *In the case of* $K = 2N$ *for* $0 < |\alpha| < \frac{1}{K}$*, assign a constant value to* α*. There is only one solution that satisfies* (2.3.16) *in the range of* $0 < \gamma_{K,\alpha} < 1$*, and for* $\frac{1}{K} < |\alpha|$ *there is no solution in the range of* $0 < \gamma_{K,\alpha} < 1$.

Proof. The goal is to identify the condition of (K, α) for which there exists a solution $\gamma_{K,\alpha}$ satisfying (2.3.16) for $0 < \gamma_{K,\alpha} < 1$. In the beginning, for simplicity, change the form of (2.3.16) as follows. In (2.3.16), change the variable from $0 < \gamma_{K,\alpha} < 1$ to $\tanh y$ as (2.3.11). One has that

$$\tanh y = \frac{|\alpha|(2N)}{\tanh(2Ny)}. \tag{2.3.26}$$

In the following, one identifies the condition (K, α) for which there exists a solution $y^*_{K,\alpha} > 0$ $(0 < \tanh y^*_{K,\alpha} < 1)$ satisfying $\tanh y^*_{K,\alpha} = \dfrac{|\alpha|(2N)}{\tanh(2Ny^*_{K,\alpha})}$. A function $h_{2N}(y)$ is defined to be

$$h_{2N}(y) = \tanh y - \frac{|\alpha|(2N)}{\tanh(2Ny)}. \tag{2.3.27}$$

The derivative of $h_{2N}(y)$ is denoted as

$$h'_{2N}(y) = 1 - \tanh^2 y + |\alpha|(2N)^2\frac{1 - \tanh^2(2Ny)}{\tanh^2(2Ny)} > 0. \tag{2.3.28}$$

One has that

$$\begin{aligned} h_{2N}(0) &= -\infty < 0, \\ h_{2N}(\infty) &= 1 - |\alpha|K > 0, \text{ for } 0 < |\alpha| < \tfrac{1}{K}. \end{aligned} \tag{2.3.29}$$

From (2.3.28) and (2.3.29), it is clear that in the case of $K = 2N$ for constant α, which satisfied $0 < |\alpha| < \frac{1}{K}$, there is only one solution that satisfies (2.3.16) in the range of $0 < \gamma_{K,\alpha} < 1$.

In the case of $\frac{1}{2N} < |\alpha|$, it holds that for all $y > 0$

$$h_{2N}(y) < 0. \tag{2.3.30}$$

Therefore, there is no solution that satisfies $0 < \gamma_{K,\alpha} < 1$. □

Lemma 2.3.3. *In the case of* $K = 2N+1$ *for* $\frac{1}{K^2} < |\alpha| < \frac{1}{K}$*, assign a constant value to* α*. There is only one solution that satisfies* (2.3.16) *in the range of* $0 < \gamma_{K,\alpha} < 1$*, and for* $\frac{1}{K} < |\alpha|$*, there is no solution in the range of* $0 < \gamma_{K,\alpha} < 1$.

Proof. The goal is to identify the condition of (K, α) for which there exists a solution $\gamma_{K,\alpha}$ satisfying (2.3.16) for $0 < \gamma_{K,\alpha} < 1$. In the beginning, for simplicity, change the form of (2.3.16) as follows. In (2.3.16), change the variable from $0 < \gamma_{K,\alpha} < 1$ to $\tanh y$ as (2.3.11). One has that

$$\tanh y = |\alpha|(2N+1)\tanh\{(2N+1)y\}\,. \tag{2.3.31}$$

In the following, one identifies the condition (K, α) for which there exists a solution $y^*_{K,\alpha} > 0$ satisfying $\tanh y^*_{K,\alpha} = |\alpha|(2N+1)\tanh\left\{(2N+1)y^*_{K,\alpha}\right\}$. A function $h_{2N+1}(y)$ is defined to be

$$h_{2N+1}(y) = \tanh y - |\alpha|(2N+1)\tanh\{(2N+1)y\}\,. \tag{2.3.32}$$

It holds that

$$\begin{aligned} h_{2N+1}(0) &= 0, \\ h_{2N+1}(\infty) &= 1 - |\alpha|(2N+1) > 0, \text{ for } \frac{1}{(2N+1)^2} < |\alpha| < \frac{1}{(2N+1)}. \end{aligned} \tag{2.3.33}$$

The derivative of $h_{2N+1}(y)$ is

$$\begin{aligned} h'_{2N+1}(y) &= 1 - |\alpha|(2N+1)^2 + |\alpha|(2N+1)^2\tanh^2\{(2N+1)y\} - \tanh^2 y, \\ h'_{2N+1}(0) &= 1 - |\alpha|(2N+1)^2 < 0, \text{ for } \frac{1}{(2N+1)^2} < |\alpha| < \frac{1}{2N+1}. \end{aligned} \tag{2.3.34}$$

The derivative $h'_{2N+1}(y)$ is also expressed using cosh functions as follows

$$h'_{2N+1}(y) = \frac{\cosh^2\{(2N+1)y\}\left[1 - |\alpha|(2N+1)^2\frac{\cosh^2 y}{\cosh^2\{(2N+1)y\}}\right]}{\cosh^2 y\cosh^2\{(2N+1)y\}}. \tag{2.3.35}$$

The function $J(y) = \dfrac{\cosh y}{\cosh\{(2N+1)y\}} \geq 0$ decreases monotonically since the derivative is denoted as

$$J'(y) = \frac{-\sinh(2Ny) - 2N\cosh y\sinh\{(2N+1)y\}}{\cosh^2\{(2N+1)y\}} < 0. \tag{2.3.36}$$

Considering the fact that

$$\lim_{y\to\infty}\frac{\cosh(y)}{\cosh(2N+1)y} = 0, \tag{2.3.37}$$

a part of $h'_{2N+1}(y)$, $\left[1 - |\alpha|(2N+1)\dfrac{\cosh^2 y}{\cosh^2\{(2N+1)y\}}\right]$ increases monotonically and there is a unique point y_* at which the sign of $h'_{2N+1}(y)$ changes from minus to plus. Therefore, there is a unique point $0 < y_{**} < \infty$ at which it holds that $h_{2N+1}(y_{**}) = 0$.

The above discussion indicates that, in the case of $K = 2N+1$ and $\dfrac{1}{K^2} < |\alpha| < \dfrac{1}{K}$, there is only one solution that satisfies (2.3.16) in the range of $0 < \gamma_{K,\alpha} < 1$.

In the case of $\frac{1}{K} < |\alpha|$, since it holds that for all $y > 0$,

$$h_{2N+1}(y) < 0, \tag{2.3.38}$$

there is no solution in the range of $0 < \gamma_{K,\alpha} < 1$. □

From the Lemmas 2.3.1, 2.3.2 and 2.3.3, such lemmas hold.

Lemma 2.3.4. *Consider the case of $K = 2N$.*
For $\dfrac{1}{K} \leq |\alpha| < 1$, there is a unique solution of (2.3.16) and the solution $\gamma_{K,\alpha}$ is in the range of $\gamma_{K,\alpha} \geq 1$. For $0 < |\alpha| < \dfrac{1}{K}$, there is a unique solution of (2.3.16) and the solution $\gamma_{K,\alpha}$ is in the range of $0 < \gamma_{K,\alpha} < 1$.

Lemma 2.3.5. *Consider the case of $K = 2N + 1$.*
For $\dfrac{1}{K} \leq |\alpha| < 1$, there is a unique solution of (2.3.16) and the solution $\gamma_{K,\alpha}$ is in the range of $\gamma_{K,\alpha} \geq 1$. For $\dfrac{1}{K^2} < |\alpha| < \dfrac{1}{K}$, there is a unique solution of (2.3.16) and the solution $\gamma_{K,\alpha}$ is in the range of $0 < \gamma_{K,\alpha} < 1$.

From Lemmas 2.3.4 and 2.3.5, this theorem holds.

Theorem 2.3.1. *When the parameters (K, α) are in Range A, the SGB transformations $\{S_{K,\alpha}\}$ preserve the Cauchy distribution and the scale parameter can be chosen uniquely.*

Although it has been proven that the map $S_{K,\alpha}$ preserves the Cauchy distribution and its scale parameter $\gamma_{K,\alpha}$ can be determined uniquely when the parameters (K, α) are in Range A, it is not straightforward to obtain the explicit form of fixed point $\gamma_{K,\alpha}$ for arbitrary K, because we have to solve the Kth-degree equations. From Theorem 2.3.1, the condition that there exists only one solution of (2.3.16), which satisfied $0 < \gamma_{K,\alpha} < \infty$, is nothing but the Range A.

2.3.2 Exactness

According to [47, 88, 89], the Perron-Frobenius operator and the exactness are defined as follows.

Definition 2.3.5 (Perron-Frobenius operator)**.** *Let* $(\mathcal{X}, \mathcal{A}, \mu)$ *be a measure space and let* f *be a density function on* $\mathcal{X}$*. If a map* $T : \mathcal{X} \to \mathcal{X}$ *is a non-singular transformation, the unique operator* $\mathcal{P} : L^1 \to L^1$ *defined by*

$$\int_A \mathcal{P} f(x)\mu(dx) = \int_{T^{-1}(A)} f(x)\mu(dx), \text{ for } A \in \mathcal{A} \tag{2.3.39}$$

is termed the Perron-Frobenius operator corresponding to T*.*

Definition 2.3.6 (Exactness)**.** *A map* T *on a phase space* $\mathcal{X}$ *with the Perron-Frobenius operator* $\mathcal{P}_T$ *and unique stationary density* f_* *is considered to be exact if and only if*

$$\lim_{n\to\infty} \|\mathcal{P}_T^n f - f_*\|_{L^1} = 0 \tag{2.3.40}$$

for every initial density $f \in \mathcal{D}$ *where* $\mathcal{D}$ *denotes the set of all densities on* $\mathcal{X}$*. This definition is equivalent to the following,*

$$\lim_{n\to\infty} \mu_*(T^n A) = 1, \ {}^{\forall}A \in \mathcal{A},\ \mu_*(A) > 0, \tag{2.3.41}$$

where $\mathcal{A}$ *denotes the* σ*-algebra and* μ_* *denotes the invariant measure corresponding to the invariant density* f_**.*

In terms of exactness, we obtain the following theorem.

Theorem 2.3.2. *If the parameters* (K, α) *are in Range A, the SGB transformations* $\{S_{K,\alpha}\}$ *are exact.*

Proof. This proof is based on that in Ref. [49]. In this proof, it is also assumed that $\alpha > 0$. One can prove the Theorem 2.3.2 in the case of $\alpha < 0$ as well as of $\alpha > 0$. For the map $S_{K,\alpha}$ defined by (2.3.3), substituting $\cot(\pi\theta_n)$ into x_n, one has the map $\bar{S}_{K,\alpha} : [0, 1) \to [0, 1)$ such that

$$\begin{aligned} \cot(\pi\theta_{n+1}) &= \alpha K \cot(\pi K \theta_n), \\ \theta_{n+1} &= \bar{S}_{K,\alpha}(\theta_n) = \frac{1}{\pi} \cot^{-1} \{\alpha K \cot(\pi K \theta_n)\}. \end{aligned} \tag{2.3.42}$$

The derivative of $\bar{S}_{K,\alpha}$ with respect to θ is as follows.

$$\bar{S}'_{K,\alpha}(\theta) = \frac{\alpha K^2 \left\{1 + \cot^2(\pi K \theta)\right\}}{\alpha^2 K^2 \cot^2(\pi K \theta) + 1} > 0 \ \text{ for } \ 0 < \alpha < 1. \tag{2.3.43}$$

Then, $\bar{S}_{K,\alpha}$ increases monotonically (in the case of $\alpha < 0$, $\bar{S}_{K,\alpha}$ decreases monotonically). Because it holds that

$$\frac{1}{\pi} \cot^{-1} \{\alpha K \cot(\pi K \theta_n)\} = \frac{1}{\pi} \cot^{-1} \left[\alpha K \cot\left\{\pi K \left(\theta_n + \frac{j}{K}\right)\right\}\right], \ j = 1, 2 \cdots, K, \tag{2.3.44}$$

the form of $\bar{S}_{K,\alpha}$ has translational symmetry and it can be constructed by shifting the form on $\left[0, \dfrac{1}{K}\right)$. That is, the map $\bar{S}_{K,\alpha}$ is a K to one map, and on any interval $\left[j, \dfrac{j}{K}\right), j = 0, \cdots, K-1$, the form of the map $\bar{S}_{K,\alpha}$ is the same as that on the interval $\left[0, \dfrac{1}{K}\right)$. Then by operating $\bar{S}_{K,\alpha}^{-1}$, the measure on $[0,1)$ is divided into K equivalently. We obtain intervals $\{I_{j,n}\}$ defined below by operating $\bar{S}_{K,\alpha}^{-n}$ into $[0,1)$. The interval $I_{j,n} \subset [0,1)$ is defined to be

$$\begin{array}{rcl} I_{j,n} & \overset{\text{def}}{=} & \left[\eta_{j,n}, \eta_{j+1,n}\right), \ \eta_{j,n} < \eta_{j+1,n}, 0 \leq j \leq K^n - 1, \\ \eta_{0,n} & = & 0 \ \text{ and } \ \eta_{K^n,n} = 1, \\ \bar{S}_{K,\alpha}^n(I_{j,n}) & = & [0,1), \\ \mu(I_{j,n}) & = & \dfrac{1}{K^n}. \end{array} \tag{2.3.45}$$

For any non-zero measure subset $C \subset [0,1)$, the set C includes a union of intervals $\displaystyle\bigcup_{j',n'} I_{j',n'}$. Then for an invariant density f_* and associated measure μ_* [89], it holds that

$$1 \geq \lim_{n\to\infty} \mu_*(\bar{S}_{K,\alpha}^n(C)) \geq \lim_{n\to\infty} \mu_* \left(\bar{S}_{K,\alpha}^n \left\{ \bigcup_{j',n'} I_{j',n'} \right\} \right) = 1. \tag{2.3.46}$$

Therefore, the map $\bar{S}_{K,\alpha}$ on a phase space $[0,1)$, is exact. Owing to the topological conjugacy, the map $S_{K,\alpha}$ is also exact. □

From Theorems 2.3.1 and 2.3.2, when the parameters (K,α) are in Range A, the map $S_{K,\alpha}$ preserves a certain Cauchy distribution f_* and any initial density function f defined on $\mathbb{R}\backslash B$ converges to f_* as

$$\lim_{n\to\infty} \|\mathcal{P}_{S_{K,\alpha}}^n f - f_*\|_{L^1} = 0. \tag{2.3.47}$$

For example, $S_{3,\alpha}$, $S_{4,\alpha}$, and $S_{5,\alpha}$ are *exact* for $\frac{1}{9} < |\alpha| < 1$, $0 < |\alpha| < 1$, and $\frac{1}{25} < |\alpha| < 1$, respectively. According to [47], if the SGB transformations are exact, then the corresponding dynamical systems are mixing and ergodic. Therefore the following Corollary holds.

Corollary 2.3.1. *Suppose that the parameters (K,α) are in Range A. Then the dynamical system $(\mathbb{R}\backslash B, S_{K,\alpha}, \mu_*)$ has the mixing property and it is ergodic where μ_* is the invariant measure corresponding to the invariant density f_*.*

Using the property of exactness, one can obtain the *explicit* formula of the Lyapunov exponent such that

$$\lambda_{K,\alpha} = \frac{1}{\pi}\int_{-\infty}^{\infty} \log\left|\frac{dS_{K,\alpha}}{dx}\right| \frac{\gamma_{K,\alpha}}{x^2+\gamma_{K,\alpha}^2} dx. \tag{2.3.48}$$

Pesin's formula indicates that the Kolmogorov-Sinai entropy is equivalent to the Lyapunov exponent since the SGB transformations are one-dimensional maps with ergodic invariant measures which are absolutely continuous with respect to the Lebesgue measure.

By changing the variable from x to $\cot\theta$, one has that

$$\frac{dS_{K,\alpha}}{dx} = \alpha K^2 \frac{\sin^2\theta}{\sin^2(K\theta)}. \tag{2.3.49}$$

Using mathematical induction, one proves that for $K \geq 2$, the following relation is true.

$$K^2 \frac{\sin^2\theta}{\sin^2(K\theta)} \geq 1. \tag{2.3.50}$$

For $K = 2$, one sees that (2.3.50) is true by simple calculation as

$$K^2 \frac{\sin^2\theta}{\sin^2(K\theta)} = \frac{1}{\cos^2\theta} \geq 1. \tag{2.3.51}$$

Assume that for $K = n \geq 2$, (2.3.50) is true. Then, since it holds that

$$(n-1)^2 \leq n^2 + 2\frac{\sin(n\theta)}{\sin\theta}\cos(n\theta)\cos\theta + 1 \leq (n+1)^2, \tag{2.3.52}$$

one has that

$$\begin{aligned} (n+1)^2 \frac{\sin^2\theta}{\sin^2\{(n+1)\theta\}} &= \frac{(n+1)^2}{\frac{\sin^2(n\theta)}{\sin^2\theta}\cos^2\theta + 2\frac{\sin(n\theta)}{\sin\theta}\cos(n\theta)\cos\theta + \cos^2\theta}, \\ &\geq \frac{(n+1)^2}{n^2+1+2\frac{\sin(n\theta)}{\sin\theta}\cos(n\theta)\cos\theta}, \\ &\geq 1. \end{aligned} \tag{2.3.53}$$

Thus for $K \geq 2$, (2.3.50) holds. Therefore, for $|\alpha| > 1$ and $K \geq 2$, it holds that

$$\left|\frac{dS_{K,\alpha}}{dx}\right| > 1. \tag{2.3.54}$$

For $|\alpha| > 1$, changing the variable as $z_n = 1/x_n$ enables the map $\widetilde{S}_{K,\alpha}$ to be obtained and it is defined as

$$\begin{cases} \widetilde{S}_{2N,\alpha}(z) & \stackrel{\text{def}}{=} \dfrac{\displaystyle\sum_{i=0}^{N-1}(-1)^i{}_{2N}C_{2N-2i-1}z^{2N-2i-1}}{\alpha K\displaystyle\sum_{i=0}^{N}(-1)^i{}_{2N}C_{2N-2i}z^{2N-2i}}, \\ \widetilde{S}_{2N+1,\alpha}(z) & \stackrel{\text{def}}{=} \dfrac{\displaystyle\sum_{i=0}^{N}(-1)^i{}_{2N+1}C_{2N-2i+1}z^{2N-2i+1}}{\alpha K\displaystyle\sum_{i=0}^{N}(-1)^i{}_{2N+1}C_{2N-2i}z^{2N-2i}}. \end{cases} \tag{2.3.55}$$

Then one has that $\left|\dfrac{d\widetilde{S}_{K,\alpha}}{dz}(0)\right| = \dfrac{1}{|\alpha|} < 1$, so that for any K, the point $z = 0$ is an attracting point for $|\alpha| > 1$. Then since for $|\alpha| > 1$, (2.3.54) holds, almost all orbits approach infinity. Thus, the Lyapunov exponent $\lambda_{K,\alpha}$ for $|\alpha| > 1$ is derived from the inclination at the infinite point as

$$\lambda_{K,\alpha} = \log|\alpha|, \quad \text{for } {}^\forall K \in \mathbb{N}\backslash\{1\}. \tag{2.3.56}$$

2.3.3 Scaling behavior

In this section, consider the scaling behavior near the point $(K,\alpha) = (\bar{N},\pm 1)$, $(2N,0)$ and $\left(2N+1,\pm\dfrac{1}{(2N+1)^2}\right)$ for any $\bar{N} \in \mathbb{N}\backslash\{1\}$ and $N \in \mathbb{N}$. According the following lemmas 2.3.6, 2.3.7, 2.3.8 and 2.3.9, one has that at $(K,\alpha) = (\bar{N},\pm 1)$, $(2N,0)$ and $\left(2N+1,\pm\dfrac{1}{(2N+1)^2}\right)$ for any $\bar{N} \in \mathbb{N}\backslash\{1\}$ and $N \in \mathbb{N}$,

$$\begin{aligned} \gamma_{K,\alpha} &= \infty, \ \text{for} \quad \alpha = \pm 1, \quad K = \bar{N},\ \bar{N} \in \mathbb{N}\backslash\{1\}, \\ \gamma_{K,\alpha} &= 0, \begin{cases} \text{for} \quad \alpha = 0 & \text{in the case of} \quad K = 2N, \qquad N \in \mathbb{N}, \\ \text{for} \quad \alpha = \pm\frac{1}{K^2} & \text{in the case of} \quad K = 2N+1, \quad N \in \mathbb{N}. \end{cases} \end{aligned} \tag{2.3.57}$$

Then by considering the scaling behavior at such critical points, the Lyapunov exponent converges to zero at $(K,\alpha) = (\bar{N},\pm 1)$, $(2N,0)$ and $\left(2N+1,\pm\dfrac{1}{(2N+1)^2}\right)$. A discussion of the critical phenomena requires the critical points to be defined as $\alpha_{\pm c1} = \pm 1$, $\alpha_{\pm c2} = \pm\dfrac{1}{(2N+1)^2}$ and $\alpha_{c3} = 0$ and the critical exponents ν_1, ν_2, and ν_3 corresponding to $\alpha_{\pm ci}, i = 1,2,3$ are defined. In terms of the scaling behavior of the Lyapunov exponents $\lambda \sim C\left|\alpha-\alpha_{\pm ci}\right|^{\nu_i}, C>0, i=1,2,3$, the following theorem holds.

Theorem 2.3.3. *Suppose that the parameters (K, α) are in Range A.*

- *For any $K \in \mathbb{N} \backslash \{1\}$, it holds that $\nu_1=\frac{1}{2}$ as $|\alpha| \to 1-0$.*
- *For any $K \in \mathbb{N} \backslash \{1\}$, it holds that $\nu_1=1$ as $|\alpha| \to 1+0$.*
- *For $K=2N+1$, it holds that $\nu_2=\frac{1}{2}$ as $|\alpha| \to \dfrac{1}{K^2}+0$.*
- *For $K=2N$, it holds that $\nu_3=\frac{1}{2}$ as $|\alpha| \to 0$.*

In order to prove of Theorem 2.3.3, consider the following lemmas.

First, the case of $\dfrac{1}{K}<|\alpha|<1 (\gamma_{K,\alpha}>1)$ is discussed.

Lemma 2.3.6. *In the case of $K=2N$, $\gamma_{2N,\alpha}$ behaves as*

$$\frac{1}{\gamma_{2N,\alpha}} = O(\sqrt{1-|\alpha|}) \tag{2.3.58}$$

in the limit of $\gamma_{2N,\alpha} \to \infty$.

Proof. In the case of $K=2N$, according to (2.3.19), (2.3.16) is rewritten as

$$|\alpha| = \frac{\coth y}{2N \coth(2Ny)}. \tag{2.3.59}$$

Then, one has that

$$\begin{aligned} 1-|\alpha| &= \frac{1}{2N} \cdot \frac{2N \displaystyle\sum_{k=0}^{N} {}_{2N}C_{2k} \cdot \gamma_{2N,\alpha}^{-2k} - \sum_{k=0}^{N-1} {}_{2N}C_{2k+1} \cdot \gamma_{2N,\alpha}^{-2k}}{\displaystyle\sum_{k=0}^{N} {}_{2N}C_{2k} \cdot \gamma_{2N,\alpha}^{-2k}}, \\ &= \frac{1}{2N} \cdot \frac{2N \cdot \gamma_{2N,\alpha}^{-2N} + \displaystyle\sum_{k=1}^{N-1} \frac{2k(2N+1)}{2k+1} {}_{2N}C_{2k} \cdot \gamma_{2N,\alpha}^{-2k}}{\displaystyle\sum_{k=0}^{N} {}_{2N}C_{2k} \cdot \gamma_{2N,\alpha}^{-2k}}. \end{aligned} \tag{2.3.60}$$

In the limit of $\gamma_{2N,\alpha} \to \infty$, it holds that

$$\begin{aligned} 1-|\alpha| &\sim \frac{4N^2-1}{3} \cdot \gamma_{2N,\alpha}^{-2}, \\ \therefore \frac{1}{\gamma_{2N,\alpha}} &= O\left(\sqrt{1-|\alpha|}\right). \end{aligned} \tag{2.3.61}$$

□

Lemma 2.3.7. *In the case of $K = 2N+1$, $\gamma_{2N+1,\alpha}$ behaves as*

$$\frac{1}{\gamma_{2N+1,\alpha}} = O(\sqrt{1-|\alpha|}) \tag{2.3.62}$$

in the limit of $\gamma_{2N+1,\alpha} \to \infty$.

Proof. In the case of $K = 2N+1$, according to (2.3.19), (2.3.16) is rewritten as

$$|\alpha| = \frac{\coth y}{(2N+1)\coth\{(2N+1)y\}}. \tag{2.3.63}$$

Then one has that

$$1-|\alpha| = \frac{1}{2N+1}\cdot\frac{\displaystyle\sum_{k=1}^{N}\frac{4k(N+1)}{2k+1}{}_{2N+1}C_{2k}\cdot\gamma_{2N+1,\alpha}^{-2k}}{\displaystyle\sum_{k=0}^{N}{}_{2N+1}C_{2k}\cdot\gamma_{2N+1,\alpha}^{-2k}}. \tag{2.3.64}$$

In the limit of $\gamma_{2N+1,\alpha} \to \infty$, it holds that

$$\begin{aligned} 1-|\alpha| &\sim \frac{4N(N+1)}{3}\cdot\gamma_{2N+1,\alpha}^{-2}, \\ \therefore \frac{1}{\gamma_{2N+1,\alpha}} &= O(\sqrt{1-|\alpha|}). \end{aligned} \tag{2.3.65}$$

$\square$

Lemma 2.3.8. *In the case of $K = 2N$, $\gamma_{2N,\alpha}$ behaves as*

$$\gamma_{2N,\alpha} \sim \sqrt{|\alpha|}. \tag{2.3.66}$$

in the limit of $\gamma_{2N,\alpha} \to 0$.

Proof. Discuss the case of $K = 2N$ and $0 < \alpha < \frac{1}{K}$. According to (2.3.26), (2.3.16) is rewritten as

$$|\alpha| = \frac{1}{2N}\tanh y\cdot\tanh(2Ny). \tag{2.3.67}$$

Then one has that

$$|\alpha| = \frac{1}{2N}\cdot\frac{\displaystyle\sum_{k=0}^{N-1}{}_{2N}C_{2k+1}\gamma_{2N,\alpha}^{2k+2}}{\displaystyle\sum_{k=0}^{N}{}_{2N}C_{2k}\gamma_{2N,\alpha}^{2k}}. \tag{2.3.68}$$

In the limit of $\gamma_{2N,\alpha} \to 0$, it holds that

$$\begin{aligned} |\alpha| &\sim \frac{1}{2N} \cdot 2N \cdot \gamma_{2N,\alpha}^2 = \gamma_{2N,\alpha}^2, \\ \therefore \gamma_{2N,\alpha} &\sim \sqrt{|\alpha|}. \end{aligned} \tag{2.3.69}$$

□

Lemma 2.3.9. *In the case of $K = 2N+1$, $\gamma_{2N+1,\alpha}$ behaves as*

$$\gamma_{2N+1,\alpha} = O\left(\sqrt{|\alpha| - \frac{1}{(2N+1)^2}}\right). \tag{2.3.70}$$

in the limit of $\gamma_{2N+1,\alpha} \to 0$.

Proof. Discuss the case of $K = 2N+1$ and $\dfrac{1}{K^2} < |\alpha| < \dfrac{1}{K}$. According to (2.3.31), (2.3.16) is rewritten as

$$|\alpha| = \frac{\tanh y}{(2N+1)\tanh\{(2N+1)y\}}. \tag{2.3.71}$$

Then one has that,

$$|\alpha| - \frac{1}{(2N+1)^2} = \frac{\displaystyle\sum_{k=1}^{N} \frac{4k(N+1)}{4k+1} {}_{2N+1}C_{2k} \cdot \gamma_{2N+1,\alpha}^{2k}}{\displaystyle (2N+1)^2 \sum_{k=0}^{N} {}_{2N+1}C_{2k+1} \cdot \gamma_{2N+1,\alpha}^{2k}}. \tag{2.3.72}$$

In the limit of $\gamma_{2N+1,\alpha} \to 0$, it holds that

$$\begin{aligned} |\alpha| - \frac{1}{(2N+1)^2} &\sim \frac{4N(N+1)\gamma_{2N+1,\alpha}^2}{5(2N+1)^2}, \\ \therefore \gamma_{2N+1,\alpha} &= O\left(\sqrt{|\alpha| - \tfrac{1}{(2N+1)^2}}\right). \end{aligned} \tag{2.3.73}$$

□

From Lemmas 2.3.6, 2.3.7, 2.3.8, and 2.3.9, one knows that there are relations between the parameter α and the scaling parameter $\gamma_{K,\alpha}$. For all α in Range A, the Lyapunov exponent is denoted as

$$\lambda_{K,\alpha} = \frac{1}{\pi} \int_{\mathbb{R}\setminus A} \log\left|S'_{K,\alpha}(x)\right| \frac{\gamma_{K,\alpha}}{\gamma_{K,\alpha}^2 + x^2} dx = \frac{1}{\pi} \int_{-\infty}^{\infty} \log\left|S'_{K,\alpha}(x)\right| \frac{\gamma_{K,\alpha}}{\gamma_{K,\alpha}^2 + x^2} dx < \infty, \tag{2.3.74}$$

$$\lambda_{K,\alpha} = \begin{cases} \dfrac{\gamma_{K,\alpha}}{\pi} \displaystyle\int_{-\infty}^{\infty} \log \left| S'_{K,\alpha}(x) \right| \frac{1}{\gamma_{K,\alpha}^2 + x^2} dx, & \text{for} \quad 0 < \gamma_{K,\alpha} < 1, \\ \dfrac{1}{\gamma_{K,\alpha}\pi} \displaystyle\int_{-\infty}^{\infty} \log \left| S'_{K,\alpha}(x) \right| \frac{1}{1 + (x/\gamma_{K,\alpha})^2} dx, & \text{for} \quad 1 \leq \gamma_{K,\alpha}. \end{cases} \tag{2.3.75}$$

Define an invariant density $\widehat{f}_{K,\alpha}(x)$ on $[0,1)$ for $\bar{S}_{K,\alpha}$. From simple calculation, it is obvious that $\widehat{f}_{K,\pm\frac{1}{K}}(x)$ is the uniform distribution. According to [47], define the entropy denoted as $H_K(\alpha) = H[\widehat{f}_{K,\alpha}] = -\int_{[0,1)} \widehat{f}_{K,\alpha}(x) \log \widehat{f}_{K,\alpha}(x) \mu(dx)$ and from the Proposition 9.1.1 in [47], one has the maximal entropy for the constant density $\widehat{f}_{K,\pm\frac{1}{K}}$. Since the dynamical system is ergodic when the parameters (K,α) are in Range A, almost all orbits do not converge and one sees that $-\infty < \lambda_{K,\alpha}$. Thus it holds that for all α in Range A

$$-\infty < \lambda_{K,\alpha} \leq \lambda_{K,\pm\frac{1}{K}} = \log|K| < \infty. \tag{2.3.76}$$

Accordingly define functions $\phi_1(\theta, \gamma_{K,\alpha})$ and $\phi_2(\theta, 1/\gamma_{K,\alpha})$ to be

$$\begin{aligned} \phi_1(\theta, \gamma_{K,\alpha}) &= \log \left| \frac{\alpha K^2 \sin^2\theta}{\sin^2 K\theta} \right| \frac{\gamma_{K,\alpha}}{\gamma_{K,\alpha}^2 \sin^2\theta + \cos^2\theta}, \\ \phi_2(\theta, 1/\gamma_{K,\alpha}) &= \log \left| \frac{\alpha K^2 \sin^2\theta}{\sin^2 K\theta} \right| \frac{1/\gamma_{K,\alpha}}{\sin^2\theta + (\cos\theta/\gamma_{K,\alpha})^2}, \end{aligned} \tag{2.3.77}$$

and also define a set of points $\{a_n\}_{n=1}^{K-1}$ such that at $\theta = a_n \in (0,\pi]$, the function $\log\left|\frac{\alpha K^2 \sin^2\theta}{\sin^2 K\theta}\right|$ is not continuous.

By changing the variable from x to $\cot\theta$, the Lyapunov exponent $\lambda_{K,\alpha}$ is rewritten as

$$\lambda_{K,\alpha} = \frac{1}{\pi} \int_0^{\pi} \phi_1(\theta, \gamma_{K,\alpha}) d\theta. \tag{2.3.78}$$

Now, the proof of Theorem 2.3.3 is as follows.

Proof. The integrand in (2.3.78) is continuous in $(a_n, a_{n+1}]$ for $0 \leq n \leq K-1$, where $a_0 = 0$ and $a_K = \pi$. The derivative of $\phi_1(\theta, \gamma_{K,\alpha})$ with respect to $\gamma_{K,\alpha}$ is as follows.

$$\begin{aligned} \frac{\partial \phi_1}{\partial \gamma_{K,\alpha}} &= \frac{1}{|\alpha|} \frac{\partial|\alpha|}{\partial \gamma_{K,\alpha}} \frac{\gamma_{K,\alpha}}{\gamma_{K,\alpha}^2 \sin^2\theta + \cos^2\theta} + \log|\alpha| \frac{-\gamma_{K,\alpha}^2 \sin^2\theta + \cos^2\theta}{(\gamma_{K,\alpha}^2 \sin^2\theta + \cos^2\theta)^2} \\ &+ \log\left|\frac{K^2 \sin^2\theta}{\sin^2 K\theta}\right| \frac{-\gamma_{K,\alpha}^2 \sin^2\theta + \cos^2\theta}{(\gamma_{K,\alpha}^2 \sin^2\theta + \cos^2\theta)^2}. \end{aligned} \tag{2.3.79}$$

The derivative is continuous on each interval $(a_n, a_{n+1}]$.
(i) In the limit of $|\alpha| \to 1-0$ ($\gamma_{K,\alpha} \to \infty$) for any K, change the variable as $z = \frac{1}{\gamma_{K,\alpha}}$ and denote the function $\phi_2(\theta, z)$ as

$$\phi_2(\theta, z) = \log \left| \frac{\alpha K^2 \sin^2\theta}{\sin^2 K\theta} \right| \frac{z}{\sin^2\theta + z^2\cos^2\theta}. \tag{2.3.80}$$

It holds that

$$\begin{aligned} \left|\lambda_{K,\alpha}\right| &< \infty, \\ \lambda_{K,\alpha} &= \frac{1}{\pi}\int_0^\pi \phi_2(\theta, z)d\theta, \\ &= \frac{1}{\pi}\sum_{n=0}^{K-1}\int_{a_n}^{a_{n+1}} d\theta \left[\phi_2(\theta,0) + \frac{\partial\phi_2}{\partial z}(\theta,0)z + O(z^2)\right], \\ &= \frac{z}{\pi}\sum_{n=0}^{K-1}\int_{a_n}^{a_{n+1}} d\theta \left[\frac{\partial\phi_2}{\partial z}(\theta,0) + O(z)\right]. \end{aligned} \tag{2.3.81}$$

Since $\lambda_{K,\alpha}$ and z are finite, $\frac{1}{\pi}\sum_{n=0}^{K-1}\int_{a_n}^{a_{n+1}} d\theta \left[\frac{\partial\phi_2}{\partial z}(\theta,0) + O(z)\right]$ is also finite. In addition, $\frac{\partial\phi_2}{\partial z}(\theta,0)$ does not depend on z. Therefore, according the Lemmas 2.3.6 and 2.3.7 in the limit of $z \to +0$ ($\gamma_{K,\alpha} \to \infty, |\alpha| \to 1-0$), it holds that

$$\therefore\ \lambda_{K,\alpha} \quad = \quad O(z) = O\left(\sqrt{1-|\alpha|}\right). \tag{2.3.82}$$

(ii) In the case of $K = 2N$, according to (2.3.69), there is a relation $\gamma_{K,\alpha} \sim \sqrt{|\alpha|}$ in the limit of $\gamma_{K,\alpha} \to +0$ ($|\alpha| \to 0$). Then, it holds that

$$\begin{aligned} |\lambda_{K,\alpha}| &< \infty, \\ \lambda_{K,\alpha} &= \frac{1}{\pi}\int_0^\pi \phi_1(\theta, \gamma_{K,\alpha})d\theta, \\ &= \frac{1}{\pi}\sum_{n=0}^{K-1}\int_{a_n}^{a_{n+1}} d\theta \left[\phi_1(\theta,0) + \frac{\partial\phi_1}{\partial\gamma_{K,\alpha}}(\theta,0)\gamma_{K,\alpha} + O(\gamma_{K,\alpha}^2)\right], \\ &= \frac{1}{\pi}\sum_{n=0}^{K-1}\int_{a_n}^{a_{n+1}} d\theta \left[\frac{\partial\phi_1}{\partial\gamma_{K,\alpha}}(\theta,0)\gamma_{K,\alpha} + O(\gamma_{K,\alpha}^2)\right]. \end{aligned} \tag{2.3.83}$$

Now, one has that

$$\frac{\partial\phi_1}{\partial\gamma_{K,\alpha}}(\theta,0)\gamma_{K,\alpha} \quad = \quad \gamma_{K,\alpha}\log|\alpha|\frac{1}{\cos^2\theta} + \gamma_{K,\alpha}\log\left|\frac{K^2\sin^2\theta}{\sin^2 K\theta}\right|\frac{1}{\cos^2\theta}. \tag{2.3.84}$$

With respect to the first term of (2.3.84), it holds that

$$\begin{aligned}
\log|\alpha| &= \log(1-1+|\alpha|) \\
&= \log\{1-(1-|\alpha|)\} \\
&= -(1-|\alpha|)-\tfrac{1}{2}(1-|\alpha|)^2-\tfrac{1}{3}(1-|\alpha|)^3-\cdots \\
&= O(1-|\alpha|).
\end{aligned} \tag{2.3.85}$$

Then, in the limit of $|\alpha| \to 0$ according to (2.3.69), following relation holds.

$$\gamma_{K,\alpha}\log|\alpha|\frac{1}{\cos^2\theta} = O(\sqrt{|\alpha|}-\sqrt{|\alpha|}|\alpha|) = O(\sqrt{|\alpha|}) \tag{2.3.86}$$

With respect to the second term of (2.3.84), it holds that according to (2.3.69)

$$\gamma_{K,\alpha}\log\left|\frac{K^2\sin^2\theta}{\sin^2 K\theta}\right|\frac{1}{\cos^2\theta} = O(\sqrt{|\alpha|}). \tag{2.3.87}$$

Therefore, according the Lemma 2.3.8 in the limit of $\gamma_{K,\alpha} \to +0$ ($|\alpha| \to 0$), it holds that

$$\lambda_{K,\alpha} = \frac{1}{\pi}\sum_{n=0}^{K-1}\int_{a_n}^{a_{n+1}} d\theta O(\sqrt{|\alpha|}) = O(\sqrt{|\alpha|}). \tag{2.3.88}$$

(iii) In the case of $K = 2N+1$, according to (2.3.73), there is a relation $|\alpha| \sim \dfrac{4N(N+1)}{5(2N+1)^2}\gamma_{K,\alpha}^2 + \dfrac{1}{(2N+1)^2}$ in the limit of $\gamma_{K,\alpha} \to +0$ ($|\alpha| \to \frac{1}{K^2}+0$). Then it holds that

$$\begin{aligned}
\left|\lambda_{K,\alpha}\right| &< \infty, \\
\lambda_{K,\alpha} &= \frac{1}{\pi}\int_0^\pi \phi_1(\theta,\gamma_{K,\alpha})d\theta, \\
&= \frac{1}{\pi}\sum_{n=0}^{K-1}\int_{a_n}^{a_{n+1}} d\theta\left[\phi_1(\theta,0)+\frac{\partial\phi_1}{\partial\gamma_{K,\alpha}}(\theta,0)\gamma_{K,\alpha}+O(\gamma_{K,\alpha}^2)\right], \\
&= \frac{\gamma_{K,\alpha}}{\pi}\sum_{n=0}^{K-1}\int_{a_n}^{a_{n+1}} d\theta\left[\frac{\partial\phi_1}{\partial\gamma_{K,\alpha}}(\theta,0)+O(\gamma_{K,\alpha})\right].
\end{aligned} \tag{2.3.89}$$

Thus, it also holds that $\dfrac{1}{\pi}\displaystyle\sum_{n=0}^{K-1}\int_{a_n}^{a_{n+1}} d\theta\left[\frac{\partial\phi_1}{\partial\gamma_{K,\alpha}}(\theta,0)+O(\gamma_{K,\alpha})\right]$ is finite and $\frac{\partial\phi_1}{\partial\gamma_{K,\alpha}}(\theta,0)$ does not depend on $\gamma_{K,\alpha}$. Therefore, according to the Lemma 2.3.9 in the limit of $\gamma_{K,\alpha} \to +0$ ($|\alpha| \to \frac{1}{K^2}+0$), it holds that

$$\lambda_{K,\alpha} = O(\gamma_{K,\alpha}) = O\left(\sqrt{|\alpha|-\frac{1}{K^2}}\right). \tag{2.3.90}$$

(iv) In the limit of $|\alpha| \to 1+0$ for any K, the Lyapunov exponent is denoted for $|\alpha| > 1$,

$$\begin{aligned} \lambda_{K,\alpha} &= \log|\alpha| = \log\{1 + (|\alpha| - 1)\}, \\ &= (|\alpha| - 1) - \tfrac{1}{2}(|\alpha| - 1)^2 + \tfrac{1}{3}(|\alpha| - 1)^3 - \cdots . \end{aligned} \tag{2.3.91}$$

Therefore, it holds that

$$\lambda_{K,\alpha} = O(|\alpha| - 1). \tag{2.3.92}$$

From equations (2.3.82), (2.3.88), (2.3.90) and (2.3.92), it is clear that for any K, the critical exponent of the Lyapunov exponent ν_1 is $\frac{1}{2}$ in the limit of $|\alpha| \to 1-0$, that for $K = 2N+1$, $\nu_2 = \frac{1}{2}$ in the limit of $|\alpha| \to \frac{1}{K^2} + 0$, that for $K = 2N$, $\nu_3 = \frac{1}{2}$ in the limit of $|\alpha| \to 0$ and that for any K, $\nu_1 = 1$ in the limit of $|\alpha| \to 1+0$. $\square$

The above discussion proves that the derivatives of the Lyapunov exponent with respect to parameter α diverge at the critical points, which means that the parameter dependence of the Lyapunov exponent diverges at the critical points. This result implies the difficulty of calculating the Lyapunov exponent near the critical points.

Discuss the Floquet multipliers in the cases of $(K, \alpha) = (\bar{N}, \alpha_{\pm c1})$ and $(2N + 1, \alpha_{\pm c2})$ for $\bar{N} \in \mathbb{N}\backslash\{1\}, N \in \mathbb{N}$. By changing the variable as $x = \cot\theta$, the derivative of the map $S_{K,\alpha}$ is rewritten as $\frac{dS_{K,\alpha}}{dx} = \alpha K^2 \frac{\sin^2\theta}{\sin^2 K\theta}$.

(i) In the case of $(\bar{N}, \alpha_{+c1})$, the derivatives at the infinite point are denoted as

$$\lim_{x\to+\infty} \frac{dS_{\bar{N},+1}}{dx} = \lim_{\theta\to+0} \frac{(\bar{N}\theta)^2}{\sin^2\bar{N}\theta} \frac{\sin^2\theta}{\theta^2} = 1. \tag{2.4.93}$$

Thus, the Floquet multiplier χ for $(K, \alpha) = (\bar{N}, \alpha_{+c1}), \bar{N} \in \mathbb{N}\backslash\{1\}$ is unity.

(ii) In the case of $(\bar{N}, \alpha_{-c1})$, consider the map $\widetilde{S}_{K,\alpha}$. The point $z = 0$ is the fixed point of $\widetilde{S}_{K,\alpha}$. Then the derivatives at the fixed point are denoted as

$$\lim_{x\to\pm\infty} = \frac{dS_{K,-1}}{dx} = -\lim_{\theta\to\pm0} \frac{K^2\theta^2}{\sin^2(K\theta)} \frac{\sin^2\theta}{\theta^2} = -1. \tag{2.4.94}$$

Thus, at $(K, \alpha) = (\bar{N}, \alpha_{-c1}), \bar{N} \in \mathbb{N}\backslash\{1\}$, it holds that $\chi = -1$.

(iii) In the case of $(2N + 1, \alpha_{+c2})$, the original point is the fixed point. Then, the derivative at the original point is denoted as

$$\frac{dS_{K,+\frac{1}{K^2}}}{dx}(0) = \frac{\sin^2(\frac{\pi}{2})}{\sin^2\left\{(2N+1)\frac{\pi}{2}\right\}} = 1. \tag{2.4.95}$$

Thus, at $(K, \alpha) = (2N + 1, \alpha_{+c2})$, it holds that $\chi = 1$.

(iv) In the case of $(2N+1, \alpha_{-c2})$, the original point is the fixed point. Then, the derivative at the original point is denoted as

$$\frac{dS_{K,-\frac{1}{K^2}}}{dx}(0) = -\frac{\sin^2(\frac{\pi}{2})}{\sin^2\left\{(2N+1)\frac{\pi}{2}\right\}} = -1. \tag{2.4.96}$$

Thus, at $(K, \alpha) = (2N+1, \alpha_{-c2})$, it holds that $\chi = -1$.

By considering (i), (ii), (iii) and (iv), it is clear that in the case of $(K, \alpha) = (\bar{N}, \alpha_{+c1})$ and $(2N+1, \alpha_{+c2}), \bar{N} \in \mathbb{N}\backslash\{1\}, N \in \mathbb{N}$, *Type 1* intermittency occurs and that in the case of $(K, \alpha) = (\bar{N}, \alpha_{-c1})$ and $(2N+1, \alpha_{-c2}), \bar{N} \in \mathbb{N}\backslash\{1\}, N \in \mathbb{N}$, *Type 3* intermittency occurs. Therefore, according to the above results and the Theorem 2.3.3, it has been proven that for a countably infinite number of *exact* maps, the *universal* scaling behavior (2.3.1) holds where *Type 1* and *Type 3* intermittency occur. In the Appendix B, the Floquet multipliers corresponding to $K = 3, 4$ and 5 are illustrated.

2.4.4 In the case of $K = 3, 4$ and 5

This subsection provides examples corresponding to $K = 3, 4$, and 5. The solutions of (2.3.16), which satisfy $0 < \gamma_{K,\alpha} < \infty$, are uniquely determined as follows.

$$\begin{aligned}
\gamma_{3,\alpha} &= \sqrt{\frac{9\alpha - 1}{3 - 3\alpha}}, \\
\gamma_{4,\alpha} &= \sqrt{\frac{6\alpha - 1 + \sqrt{32\alpha^2 - 8\alpha + 1}}{2(1-\alpha)}}, \\
\gamma_{5,\alpha} &= \sqrt{\frac{-5(1-5\alpha) + \sqrt{20(25\alpha^2 - 6\alpha + 1)}}{5(1-\alpha)}}
\end{aligned} \tag{2.4.97}$$

for $\alpha > 0$. In the following discussion, it is assumed that $\alpha > 0$. If one consider the case of $\alpha < 0$, by replacing α for $-\alpha$, one obtains the corresponding solutions. The above discussion indicates that *Type 1* intermittency occurs in the case of $K = 3, 4$, and 5 for $\alpha > 0$ (for $\alpha < 0$, *Type 3* intermittency occurs) . The Lyapunov exponents in the case of $K = 3, 4$, and 5 are given as follows.

$$\begin{aligned}
\lambda_{3,\alpha} &= \log\left|\frac{1}{\alpha}\left(\frac{3(1-\alpha)}{8}\right)^2\left[1 + \sqrt{\frac{9\alpha - 1}{3 - 3\alpha}}\right]^4\right|, \\
\lambda_{4,\alpha} &= \log\left|\frac{\alpha(1+\gamma_{4,\alpha})^6}{\gamma_{4,\alpha}^2(1+\gamma_{4,\alpha}^2)^2}\right|, \\
\lambda_{5,\alpha} &= \log\left|\frac{25}{256\alpha}\frac{(1-\alpha)^4}{(\sqrt{125\alpha^2 - 30\alpha + 5} + 11\alpha - 1)^2}|1+\gamma_{5,\alpha}|^8\right|.
\end{aligned} \tag{2.4.98}$$

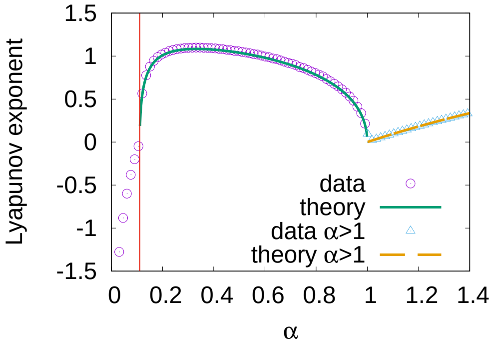

(a) $K = 3$

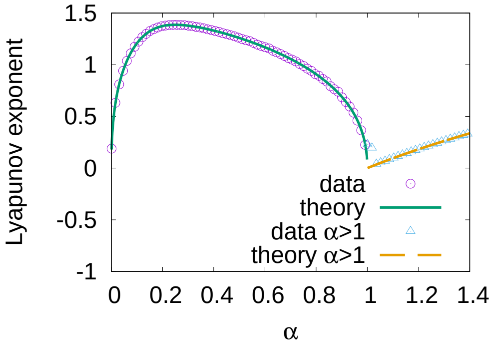

(b) $K = 4$

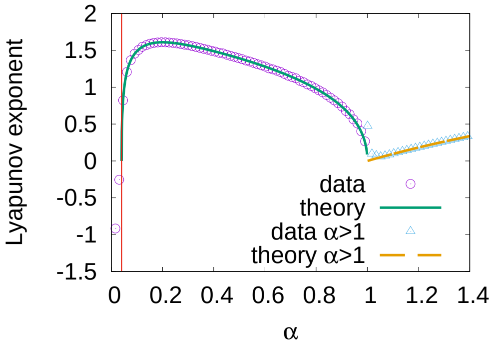

(c) $K = 5$

Figure 2.8: Relations between the Lyapunov exponents of the SGB transformations and α for $K = 3, 4$, and 5. Circles and triangles represent the numerical results for $\alpha < 1$ and $\alpha > 1$, respectively. Solid and broken lines represent the analytical results for $\alpha < 1$ and $\alpha > 1$, respectively. The initial point is $x_0 = 5\sqrt{7}$. The number of iterative steps is 1×10^5 for $\alpha < 1$ and 200 for $\alpha > 1$. The vertical line corresponds to $\alpha = \frac{1}{9}, \frac{1}{25}$, respectively.

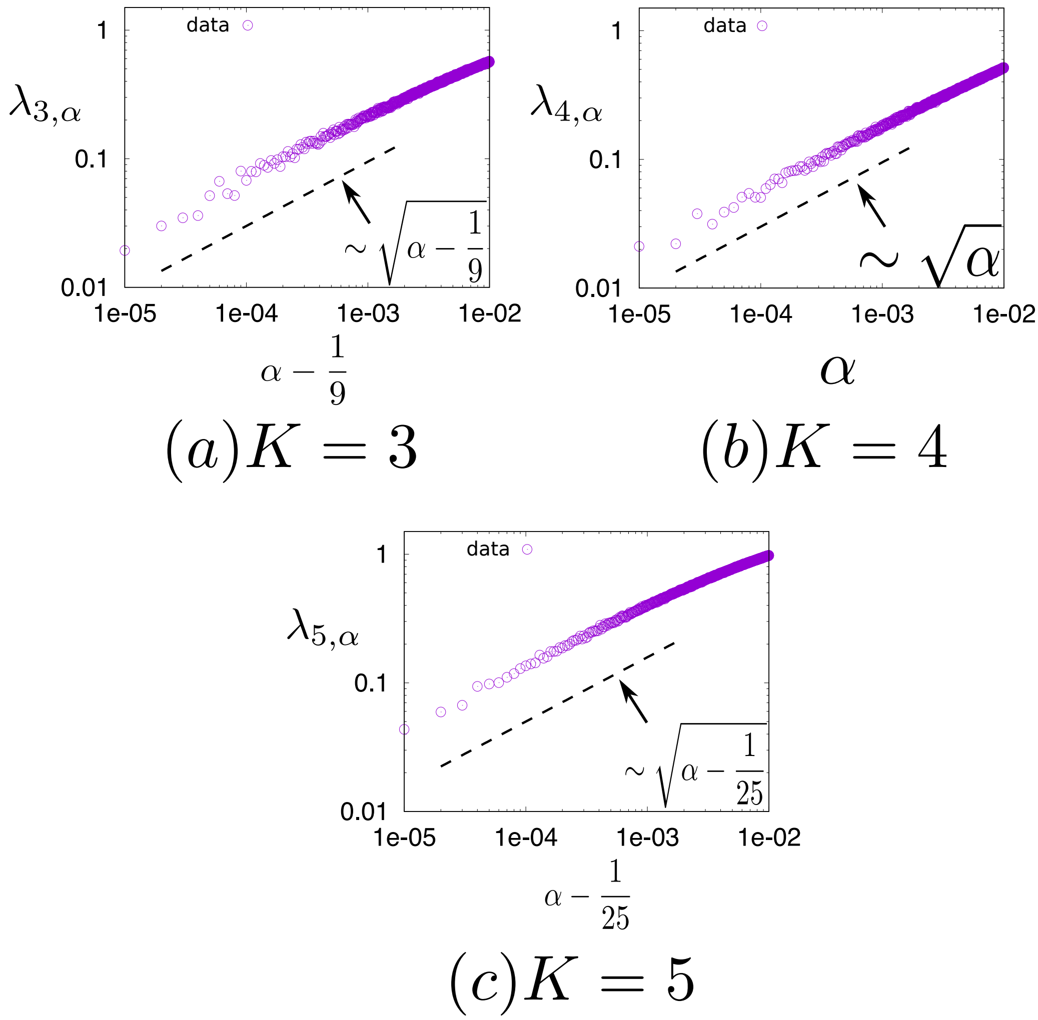

Figure 2.9: Scaling behavior of the Lyapunov exponents of the SGB transformation in the case of $K = 3, 4$, and 5. Circles represent the numerically simulated values and broken lines represent the order. The initial point is $x_0 = 5\sqrt{7}$. The number of iterative computations is 2×10^5.

Figures 2.8a, 2.8b, and 2.8c show the Lyapunov exponents against α in the case of $K = 3, 4$, and 5, respectively. The numerical simulations are seen to be exactly consistent with the obtained analytical formulae except for the vicinities of α_{+c_i} for $i = 1, 2, 3$. Because it holds that, at the critical points $\frac{\partial \lambda_{K,\alpha}}{\partial \alpha} = \pm\infty$, the parameter dependence of the Lyapunov exponent is observed to diverge at the critical points. This means that obtaining the true value of the Lyapunov exponent by numerical simulation would be computationally difficult. Figure 2.9 shows the scaling behavior of the Lyapunov exponent. These results show that $\nu_2 = \frac{1}{2}$ and

$\nu_3 = \dfrac{1}{2}$ in the case of $K = 3, 4$, and 5.

2.4.5 Infinite ergodicity for $\alpha = 1, -1$

Theorem 2.4.2. *The SGB transformations preserve the Lebesgue measure for* $\alpha = 1$ *or* -1.

Proof. The goal is to prove that

$$\left| S_{K,\pm 1}^{-1} I \right| = |I| \tag{2.4.99}$$

for any interval I according to [79] where $|\cdot|$ denotes the length of a interval. It is sufficient to verify this for intervals of $I = (0, \eta), \eta > 0$ and $I = (\eta, 0), \eta < 0$ according to [79].

(I) In the case of $\alpha = 1$

(In the following, (2.4.99) is proved for $\eta > 0$; the proof for $\eta < 0$ is similar.) The map $S_{K,1}$ increases monotonically. We have that

$$x_{n+1} = S_{K,1} x_n \tag{2.4.100}$$

and for $x_{n+1} = 0$, $x_n = \cot\theta_n, \theta_n \in [0, \pi]$ satisfies the following relation:

$$\begin{array}{rcl} K\theta_n & = & \dfrac{\pi}{2} + n\pi, n \in \mathbb{Z} \\ \theta_n & = & \dfrac{\pi}{2K} + \dfrac{n}{K}\pi, \\ 0 & \leq & \frac{\pi}{2K} + \frac{n}{K}\pi \leq \pi. \end{array} \tag{2.4.101}$$

The range of possible values for n is $n = 0, 1, 2, \cdots, K-1$. Then for x_n such that $x_{n+1} = 0$, it follows that

$$x_n = \cot\left(\frac{\pi}{2K} + \frac{n}{K}\pi\right), n = 0, 1, 2, \cdots, K-1. \tag{2.4.102}$$

For x_n such that $x_{n+1} = K\cot(K\theta_n) = \eta$, it follows that

$$\begin{array}{lcl} K\theta_n & = & \cot^{-1}\left(\frac{\eta}{K}\right) + m\pi \\ \theta_n & = & \frac{1}{K}\cot^{-1}\left(\frac{\eta}{K}\right) + \frac{m}{K}\pi, \\ 0 & \leq & \frac{1}{K}\cot^{-1}\left(\frac{\eta}{K}\right) + \frac{m}{K}\pi \leq \pi. \end{array} \tag{2.4.103}$$

Here, since

$$0 < \cot^{-1}\left(\frac{\eta}{K}\right) < \frac{\pi}{2}, \tag{2.4.104}$$

the range of possible values for m is given by

$$-\frac{1}{2} < -\frac{1}{\pi}\cot^{-1}\left(\frac{\eta}{K}\right) \leq m \leq K - \frac{1}{\pi}\cot^{-1}\left(\frac{\eta}{K}\right) < K, \tag{2.4.105}$$

that is $m = 0, 1, 2, \cdots, K-1$. Then θ_n is given by

$$\theta_n = \frac{1}{K}\cot^{-1}\left(\frac{\eta}{K}\right) + \frac{m}{K}\pi, m = 0, 1, 2, \cdots, K-1 \tag{2.4.106}$$

where $\eta = K\cot(K\theta_n)$. Because the cot function decreases monotonically for $\theta \in [0, \pi]$, the interval that is mapped from $(0, \eta)$ by $S_{K,1}^{-1}$ is

$$\bigcup_{m=0}^{K-1}\left(\cot\left(\frac{\pi}{2K} + \frac{m}{K}\pi\right), \cot\left\{\frac{1}{K}\cot^{-1}\left(\frac{\eta}{K}\right) + \frac{m}{K}\pi\right\}\right). \tag{2.4.107}$$

Then we have that

$$\left|S_{K,1}^{-1}(0, \eta)\right| = \sum_{m=0}^{K-1}\left[\cot\left\{\frac{1}{K}\cot^{-1}\left(\frac{\eta}{K}\right) + \frac{m}{K}\pi\right\} - \cot\left(\frac{\pi}{2K} + \frac{m}{K}\pi\right)\right]. \tag{2.4.108}$$

In the following discussion, we consider $\sum_{m=0}^{K-1}\cot\left(\frac{\pi}{2K} + \frac{m}{K}\pi\right)$.

(i) Case $K = 2N$ For $\sum_{m=0}^{K-1}\cot\left(\frac{\pi}{2K} + \frac{m}{K}\pi\right)$, Adding the terms corresponding to $m = 0$ and $m = K-1$, we obtain

$$\cot\left(\frac{\pi}{2K}\right) + \cot\left(\frac{\pi}{2K} + \frac{K-1}{K}\pi\right) = \cot\left(\frac{\pi}{2K}\right) + \cot\left(\pi - \frac{\pi}{2K}\right) = 0. \tag{2.4.109}$$

Adding the terms corresponding to $m = l$ and $m = K-1-l$, $l = 0, \cdots, \frac{K}{2} - 1$, we obtain

$$\cot\left(\frac{(2l+1)\pi}{2K}\right) + \cot\left(\pi - \frac{(2l+1)\pi}{2K}\right) = 0. \tag{2.4.110}$$

Thus, for $K = 2N$, the following relation holds:

$$\sum_{m=0}^{K-1}\cot\left(\frac{\pi}{2K} + \frac{m}{K}\pi\right) = 0. \tag{2.4.111}$$

(ii)Case $K = 2N+1$. We have

$$\begin{aligned}\sum_{m=0}^{K-1}\cot\left(\frac{\pi}{2K} + \frac{m}{K}\pi\right) &= \sum_{m=0}^{\frac{K-3}{2}}\cot\left(\frac{\pi}{2K} + \frac{m}{K}\pi\right) + \cot\left(\frac{K-1+1}{2K}\pi\right) + \sum_{m=\frac{K+1}{2}}^{K-1}\cot\left(\frac{\pi}{2K} + \frac{m}{K}\pi\right) \\ &= \sum_{m=0}^{\frac{K-3}{2}}\cot\left(\frac{\pi}{2K} + \frac{m}{K}\pi\right) + \sum_{m=\frac{K+1}{2}}^{K-1}\cot\left(\frac{\pi}{2K} + \frac{m}{K}\pi\right).\end{aligned} \tag{2.4.112}$$

Much as in (i), because the term corresponding to $m = l$ negates the term corresponding to $m = K - 1 - l$, $l = 0, \cdots, \frac{K-3}{2}$, it follows that

$$\sum_{m=0}^{K-1} \cot\left(\frac{\pi}{2K} + \frac{m}{K}\pi\right) = 0. \tag{2.4.113}$$

Thus, we have that

$$\left|S_{K,1}^{-1}(0,\eta)\right| = \sum_{m=0}^{K-1} \cot\left\{\frac{1}{K}\cot^{-1}\left(\frac{\eta}{K}\right) + \frac{m}{K}\pi\right\}. \tag{2.4.114}$$

In the following discussion, we calculate (2.4.114). Let the K roots x_n where $\eta = S_{K,1}x_n$ be denoted $\xi_i, i = 0, \cdots, K-1$. Because the map $S_{K,1}(x)$ corresponds to the K-angle formula of the cot function, η is given by

$$\eta = x_{n+1} = S_{K,1}(x_n) = K\frac{x_n^K + (K-2\text{th and following terms})}{Kx_n^{K-1} + (K-3\text{th and following terms})} \tag{2.4.115}$$

where $x_{n+1} = \eta$. Then it follows that

$$x_n^K - \eta x_n^{K-1} + (K-2\text{th and following terms}) = 0 \tag{2.4.116}$$

Because by definition ξ_i is a root of the above Kth-degree equation, it follows that $(x_n - \xi_0)(x_n - \xi_1)\cdots(x_n - \xi_{K-1}) = 0$. According to the relation between the roots and coefficients of a Kth-degree equation, we have that

$$\eta = \sum_{m=0}^{K-1} \xi_m = \sum_{m=0}^{K-1} \cot\left\{\frac{1}{K}\cot^{-1}\left(\frac{\eta}{K}\right) + \frac{m}{K}\pi\right\}. \tag{2.4.117}$$

Therefore, because

$$\left|S_{K,1}^{-1}(0,\eta)\right| = \eta, \tag{2.4.118}$$

(2.4.99) holds.

(II) In the case of $\alpha = -1$

Consider the case $\eta > 0$ as in (I). Because the map $S_{K,-1}$ decreases monotonically,

$$\begin{aligned} \left|S_{K,1}^{-1}(0,\eta)\right| &= \sum_{m=0}^{K-1}\left[\cot\left(\frac{\pi}{2K} + \frac{m}{K}\pi\right) - \cot\left\{\frac{1}{K}\cot^{-1}\left(\frac{-\eta}{K}\right) + \frac{m}{K}\pi\right\}\right] \\ &= -\sum_{m=0}^{K-1} \cot\left\{\frac{1}{K}\cot^{-1}\left(\frac{-\eta}{K}\right) + \frac{m}{K}\pi\right\}. \end{aligned} \tag{2.4.119}$$

For the map $S_{K,-1}$, the following relation holds:

$$\begin{aligned} \eta &= -K\frac{x_n^K+(K-2\text{th and following terms})}{Kx_n^{K-1}+(K-3\text{th and following terms})} \\ x_n^K &+ \eta x_n^{K-1} + (K-2\text{th and following terms}) = 0. \end{aligned} \tag{2.4.120}$$

According to the relation between the roots and coefficients of a Kth-degree equation,

$$\begin{aligned} -\eta &= \sum_{m=0}^{K-1} \xi_m = \sum_{m=0}^{K-1} \cot\left\{\frac{1}{K}\cot^{-1}\left(\frac{-\eta}{K}\right) + \frac{m}{K}\pi\right\} \\ \therefore -\sum_{m=0}^{K-1} \cot\left\{\frac{1}{K}\cot^{-1}\left(\frac{-\eta}{K}\right) + \frac{m}{K}\pi\right\} &= \eta \end{aligned} \tag{2.4.121}$$

Therefore, it follows that

$$\left|S_{K,1}^{-1}(0,\eta)\right| = -\sum_{m=0}^{K-1} \cot\left\{\frac{1}{K}\cot^{-1}\left(\frac{-\eta}{K}\right) + \frac{m}{K}\pi\right\} = \eta \tag{2.4.122}$$

and (2.4.99) holds. □

For $\alpha = \pm 1$, the SGB transformations preserve the Lebesgue measure, so the measure for the whole set cannot be normalized to unity. Then we define the ergodicity for the system with infinite measure as follows (according to Definition 1.4.11):

Definition 1.4.11 (ergodicity [47]). *Let $(X, \mathscr{A}, \mu)$ be a measure space. $S : X \to X$ is a measurable transformation on the measure space $(X, \mathscr{A}, \mu)$. The transformation S is called ergodic if every invariant set $A \in \mathscr{A}$ is such that either $\mu(A) = 0$ or $\mu(X \backslash A) = 0$.*

Theorem 2.3.3. *The SGB transformation is ergodic for $\alpha = 1$ or -1.*

Proof. For the map $S_{K,\pm 1}$ substituting $\cot(\pi\theta_n)$ into $x_n \in \mathbb{R}\backslash B$, one has the map $\bar{S}_{K,\pm 1} : X \overset{\text{def}}{=} \frac{1}{\pi}\text{arccot}(\mathbb{R}\backslash B) \to X$ such that

$$\theta_{n+1} = \bar{S}_{K,\pm 1}(\theta_n) = \frac{1}{\pi}\cot^{-1}\left\{\pm K\cot(\pi K\theta_n)\right\} \tag{2.3.123}$$

where $X \subset (0, 1)$. The map $\bar{S}_{K,\pm 1}$ is topologically conjugate to the map $S_{K,\pm 1}$, so that the ergodic properties of $\bar{S}_{K,\pm 1}$ are same as those of $S_{K,\pm 1}$. In terms of absolute value of the derivative of $\bar{S}_{K,\pm 1}$, it holds that

$$\left|\bar{S}'_{K,\pm 1}(\theta)\right| = \frac{K^2\left\{1 + \cot^2(\pi K\theta)\right\}}{K^2\cot^2(\pi K\theta) + 1} > 1, {}^{\forall}\theta \in X. \tag{2.3.124}$$

Take the contraposition for Definition 1.4.11 and we will show that

$$\text{for any } A \text{ s.t. } \mu(A) \neq 0, \text{ and } \mu(A^c) \neq 0 \Rightarrow \ A \text{ is not invariant.} \tag{2.3.125}$$

In a way similar to the proof of the exactness in SGB transformations, we define the intervals $\{I_{j,n}\}$ for which the following holds:

$$\begin{array}{rcl} I_{j,n} & \stackrel{\text{def}}{=} & (\eta_{j,n}, \eta_{j+1,n}), \ \eta_{j,n} < \eta_{j+1,n}, 0 \leq j \leq K^n - 1, \\ \eta_{0,n} & = & 0 \ \text{ and } \ \eta_{K^n,n} = 1, \\ \bar{S}^n_{K,\alpha}(I_{j,n}) & = & X. \end{array} \tag{2.3.126}$$

Figure 2.10 illustrates the case of $\{I_{j,1}\}_{0 \leq j \leq 4}$ when $(K, \alpha) = (5, 1)$.

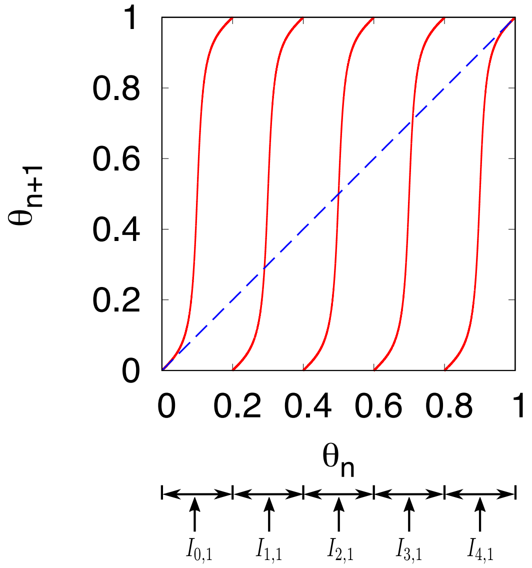

Figure 2.10: Solid lines correspond to the transformation $\bar{S}_{5,1}$ which is topologically conjugate to the super-generalized Boole transformation $S_{5,1}$. Dashed line corresponds to $\theta_{n+1} = \theta_n$.

Since the absolute value of the derivative $\bar{S}'_{K,\pm 1}$ is larger than unity, the length of the interval $I_{j,n}$ becomes infinitesimal as $n \to \infty$. Then, for any set A such that $\mu(A) \neq 0$, it follows that

$$^{\exists} p, q \text{ s.t.} I_{p,q} \subset A. \tag{2.3.127}$$

From the definition of $I_{p,q}$, it follows that

$$\begin{array}{rcl} \bar{S}^q_{K,\pm 1} I_{p,q} & = & X, \\ \therefore \bar{S}^q_{K,\pm 1} A & = & X. \end{array} \tag{2.3.128}$$

Next, for any set A such that $\mu(A^c) \neq 0$, it follows that

$$A \neq X. \tag{2.3.129}$$

Then, for any A such that $\mu(A) \neq 0$ and $\mu(A^c) \neq 0$, it follows that

$$^{\exists}q \in \mathbb{N} \text{ s.t. } \bar{S}^q_{K,\pm 1}A = X \text{ and } A \neq X. \tag{2.3.130}$$

This means that the set A is not invariant. Therefore, Theorem 2.3.3 holds. □

2.4 Further Extension of Super Generalized Boole transformations

Referring to [36], let us define a new map $U_{K,\alpha,\beta}$ which is extended from the super-generalized Boole transformations as follows:

$$x_{n+1} = U_{K,\alpha,\beta}(x_n) \stackrel{\text{def}}{=} \left|\alpha K F_K(|x|^\beta \mathrm{sgn}(x))\right|^{\frac{1}{\beta}} \mathrm{sgn}\left\{F_K(|x|^\beta \mathrm{sgn}(x))\right\} \tag{2.4.1}$$

First, let us show that the map $U_{K,\alpha,\beta}$ is a K-to-one map. Consider points $x_j, j = 1, \cdots, K$ on $\mathbb{R}$ as follows:

$$x_j = \left|\cot\left(\theta + j\frac{\pi}{K}\right)\right|^{\frac{1}{\beta}} \mathrm{sgn}\left(\cot\left(\theta + j\frac{\pi}{K}\right)\right), j = 1, \cdots, K. \tag{2.4.2}$$

Then, $|x_j|^\beta$ and $|x_j|^\beta \mathrm{sgn}(x)$ can be written as

$$\begin{aligned} |x_j|^\beta &= \begin{cases} \cot\left(\theta + j\frac{\pi}{K}\right), & \cot\left(\theta + j\frac{\pi}{K}\right) \geq 0, \\ -\cot\left(\theta + j\frac{\pi}{K}\right), & \cot\left(\theta + j\frac{\pi}{K}\right) < 0, \end{cases} \\ |x_j|^\beta \mathrm{sgn}(x_j) &= \cot\left(\theta + j\frac{\pi}{K}\right). \end{aligned} \tag{2.4.3}$$

By transfer x_j by $U_{K,\alpha,\beta}$, we obtain following equation.

$$U_{K,\alpha,\beta}(x_j) = |\alpha K \cot(K\theta)|^{\frac{1}{\beta}} \mathrm{sgn}\left\{\cot(K\theta)\right\}. \tag{2.4.4}$$

Then, define $y = |\alpha K \cot(K\theta)|^{\frac{1}{\beta}} \mathrm{sgn}\left\{\cot(K\theta)\right\}$ and we see that there exist K pieces $x_j, j = 1, \cdots, K$ which satisfy the relation $y = U_{K,\alpha,\beta}(x_j)$.

2.4.1 Invariant density of $U_{K,\alpha,\beta}$

First, assume that the variable x_n has the following density function:

$$\rho_n(x) = \frac{1}{\pi}\frac{\gamma|x|^{\beta-1}}{|x|^{2\beta} + \gamma^2}. \tag{2.4.5}$$

From the above discussion, we know that the map $U_{K,\alpha,\beta}$ is a K-to-one map. Then, solve the Perron-Frobenius equation that is equivalent to the probability preservation relation:

$$\rho_{n+1}(y)|dy| = \rho_n(x_1)|dx|_{x=x_1} + \cdots + \rho_n(x_K)|dx|_{x=x_K}. \tag{2.4.6}$$

Here,

$$\begin{aligned}\left|\frac{dy}{dx}\right|_{x=x_j} &= K|\alpha K|^{\frac{1}{\beta}} \frac{|\cot(K\theta)|^{\frac{1}{\beta}-1}\sin^2\left(\theta + j\frac{\pi}{K}\right)}{\left|\cot\left(\theta + j\frac{\pi}{K}\right)\right|^{\frac{1}{\beta}-1}\sin^2(K\theta)}, \\ &= K|\alpha K|^{\frac{1}{\beta}} \frac{|\cot(K\theta)|^{\frac{1}{\beta}-1}\left(1 + \frac{|y|^{2\beta}}{|\alpha K|^2}\right)}{\left|\cot\left(\theta + j\frac{\pi}{K}\right)\right|^{\frac{1}{\beta}-1}\left(1 + |x_j|^{2\beta}\right)}\end{aligned} \tag{2.4.7}$$

Then, $\rho_{n+1}(y)$ can be expressed as

$$\begin{aligned}\rho_{n+1}(y) &= \sum_{j=1}^{K} \rho_n(x_j)\left|\frac{dx}{dy}\right|_{x=x_j} \\ &= \frac{1}{K|\alpha K|^{\frac{1}{\beta}}|\cot(K\theta)|^{\frac{1}{\beta}-1}\left(1 + \frac{|y|^{2\beta}}{|\alpha K|^2}\right)} \sum_{j=1}^{K} \rho_n(x_j)\left|\cot\left(\theta + j\frac{\pi}{K}\right)\right|^{\frac{1-\beta}{\beta}}\left(1 + |x_j|^{2\beta}\right),\end{aligned} \tag{2.4.8}$$

Here, according to [86], $\sum_{j=1}^{K} \rho_n(x_j)\left|\cot\left(\theta + j\frac{\pi}{K}\right)\right|^{\frac{1-\beta}{\beta}}\left(1 + |x_j|^{2\beta}\right)$ can be rewritten as

$$\begin{aligned}\sum_{j=1}^{K} \rho_n(x_j)\left|\cot\left(\theta + j\frac{\pi}{K}\right)\right|^{\frac{1-\beta}{\beta}}\left(1 + |x_j|^{2\beta}\right) &= \frac{\beta}{\pi}\sum_{j=1}^{K}\frac{\gamma}{1 + (\gamma^2 - 1)\sin^2\left(\theta + j\frac{\pi}{K}\right)} \\ &= \frac{\beta}{\pi}\frac{KG_K(\gamma)\left(1 + \cot^2(K\theta)\right)}{G_K^2(\gamma) + \cot^2(K\theta)},\end{aligned} \tag{2.4.9}$$

where G_K is the K-angle formula of the coth function. Then, it holds that

$$\rho_{n+1}(y) = \frac{\beta}{\pi}\frac{|\alpha K|G_K(\gamma)|y|^{\beta-1}}{|\alpha K|^2 G_K^2(\gamma) + |y|^{2\beta}}. \tag{2.4.10}$$

Thus, by the Perron-Frobenius operator, the form of density function does not change but the parameter is changed to

$$\gamma \mapsto |\alpha|KG_K(\gamma). \tag{2.4.11}$$

Therefore, if the density function (2.4.5) is an invariant density, it is necessary that

$$\gamma = |\alpha|KG_K(\gamma). \tag{2.4.12}$$

Equation (2.4.12) does not depend on β so we can apply the same discussion given in Section 2.3.1. In conclusion, if (K, α) are in Range A, then the density (2.4.5) is an invariant density, and Eq. (2.4.12) has a unique solution.

2.4.2 Exactness for map $U_{K,\alpha,\beta}$

From the conclusion, regardless of β, we can apply the proof in [50]. First, put $x_n = |\cot(\pi\theta_n)|^{\frac{1}{\beta}} \operatorname{sgn}(\cot(\pi\theta_n))$. Then, it follows that

$$|\cot(\pi\theta_{n+1})|^{\frac{1}{\beta}} \operatorname{sgn}\{\cot(\pi\theta_{n+1})\} = |\alpha K \cot(\pi K\theta_n)|^{\frac{1}{\beta}} \operatorname{sgn}\{\cot(\pi K\theta_n)\} \quad (2.4.13)$$

Because the signs on both sides are the same, it follows that $\operatorname{sgn}\{\cot(\pi\theta_{n+1})\} = \operatorname{sgn}\{\cot(K\theta_n)\}$. Since $\alpha K > 0$, we have the following equation

$$\theta_{n+1} = \frac{1}{\pi}\cot^{-1}\{\alpha K \cot(K\theta_n)\}, \quad (2.4.14)$$

which is proven to be exact in Section 2.3.2 if (K, α) are in Range A. Therefore, we see that the map $U_{K,\alpha,\beta}$ is exact, if (K, α) are in Range A. Then, since $\rho(x) = O\left(\frac{1}{|x|^{1+\beta}}\right), |x| \to \infty$ when the (K, α) are in Range A, the initial density function converges to the stable distribution with characteristic exponent [90] $0 < \beta < 2$.

2.4.3 The relation betwenn γ and (K, α, β) in map $U_{K,\alpha,\beta}$

From above discussion, the behavior of γ as $\gamma \to \infty$ or $\gamma \to +0$ is the same as that in the SGB transformation. Then

- for any $K \in \mathbb{N}\backslash 1$, $\dfrac{1}{\gamma_{K,\alpha}} = O\left(\sqrt{1-|\alpha|}\right)$ in the limit of $|\alpha| \to 1-0$,
- in the case of $K = 2N$, $\gamma_{2N,\alpha} \sim \sqrt{|\alpha|}$ in the limit of $|\alpha| \to 0$ and
- in the case of $K = 2N+1$, $\gamma = O\left(\sqrt{|\alpha| - \frac{1}{(2N+1)^2}}\right)$ in the limit of $|\alpha| \to \frac{1}{(2N+1)^2} + 0$.

2.4.4 Critical exponent of Lyapunov exponent in map $U_{K,\alpha,\beta}$

In terms of the scaling behavior of the Lyapunov exponents $\lambda \sim C\,|\alpha - \alpha_{\pm ci}|^{\nu_i}, C > 0, i = 1, 2, 3$, for ESGB transformations, the following theorem holds.

Theorem 2.4.1. *Suppose that the parameters (K, α) are in Range A.*

- *For any $K \in \mathbb{N}\backslash\{1\}$, it holds that $\nu_1 = \frac{1}{2}$ as $|\alpha| \to 1-0$.*
- *For $K = 2N+1$, it holds that $\nu_2 = \frac{1}{2}$ as $|\alpha| \to \dfrac{1}{K^2} + 0$.*
- *For $K = 2N$, it holds that $\nu_3 = \frac{1}{2}$ as $|\alpha| \to 0$.*

Proof. Put $x = |\cot\theta|^{\frac{1}{\beta}} \mathrm{sgn}\{\cot\theta\}$ and it holds that

$$\begin{aligned}
\frac{dx}{d\theta} &= -\frac{|\cot\theta|^{\frac{1}{\beta}-1}}{\beta\sin^2\theta}, \\
\frac{dU}{d\theta} &= -\frac{K|\alpha K|^{\frac{1}{\beta}}}{\beta}\frac{|\cot(K\theta)|^{\frac{1}{\beta}-1}}{\sin^2(K\theta)}, \\
\therefore\ \frac{dU}{dx} &= \frac{dU}{d\theta}\frac{d\theta}{dx} \\
&= K|\alpha K|^{\frac{1}{\beta}}\frac{\sin^2\theta}{\sin^2(K\theta)}\left|\frac{\cot(K\theta)}{\cot\theta}\right|^{\frac{1}{\beta}-1}.
\end{aligned} \tag{2.4.15}$$

Then, the Lyapunov exponent is calculated as

$$\lambda = \frac{1}{\pi}\int_0^{\pi} d\theta \log\left|K|\alpha K|^{\frac{1}{\beta}}\frac{\sin^2\theta}{\sin^2(K\theta)}\left|\frac{\cot(K\theta)}{\cot\theta}\right|^{\frac{1}{\beta}-1}\right| \cdot \frac{\gamma|\cot\theta|^{\frac{\beta-1}{\beta}}}{\cot^2\theta+\gamma^2}. \tag{2.4.16}$$

When the invariant density is uniform, the Lyapunov exponent takes the maximum value and is finite. In the following discussion, put $A = K^{1+\frac{1}{\beta}}\frac{\sin^2\theta}{\sin^2(K\theta)}\left|\frac{\cot(K\theta)}{\cot\theta}\right|^{\frac{1}{\beta}-1}$ for simplicity (A does not depend on γ or α) and define ϕ_1 and ϕ_2 as follows:

$$\begin{aligned}
\phi_1(\theta,\gamma,\beta) &= \log||\alpha|^{\frac{1}{\beta}}A|\frac{\gamma|\cot\theta|^{\frac{\beta-1}{\beta}}}{\cot^2\theta+\gamma^2}, \\
\phi_2(\theta,z,\beta) &= \log\left||\alpha|^{\frac{1}{\beta}}A\right|\frac{\frac{1}{\gamma}|\cot\theta|^{\frac{\beta-1}{\beta}}}{\frac{1}{\gamma^2}\cot^2\theta+1} \\
&= \log\left||\alpha|^{\frac{1}{\beta}}A\right|\frac{z|\cot\theta|^{\frac{\beta-1}{\beta}}}{z^2\cot^2\theta+1}.
\end{aligned} \tag{2.4.17}$$

where $z \overset{\text{def}}{=} \frac{1}{\gamma}$.

(i) In the limit of $|\alpha| \to 1-0(\gamma_{K,\alpha} \to \infty)$, consider the partial derivative of ϕ_2 with respect to z (fixing θ and β, which do not depend γ, and considering the interval $(a_n, a_{n+1}]$ as in Section 2.3.3, in order not to make ϕ_2 diverge):

$$\frac{\partial\phi_2}{\partial z} = \frac{1}{|\alpha|\beta}\frac{z|\cot|^{\frac{\beta-1}{\beta}}}{z^2\cot^2\theta+1}\frac{\partial|\alpha|}{\partial z} + \log\left||\alpha|^{\frac{1}{\beta}}A\right|\frac{|\cot\theta|^{\frac{\beta-1}{\beta}}(1-z^2\cot^2\theta)}{(z^2\cot^2\theta+1)^2}. \tag{2.4.18}$$

Since, in the case of $K = 2N$, we have that $|\alpha| \sim 1 - \frac{4N^2-1}{3}z^2$, and in the case of $K = 2N+1$, we have that $|\alpha| \sim 1 - \frac{4N(N+1)}{3}z^2$, we see that in both cases $\frac{\partial\phi_2}{\partial z}$ does not diverge in the limit of $\alpha \to 1-0(\gamma \to +\infty)$. Then, in a way similar to Section 2.3.3, it follows that

$$\begin{aligned} |\lambda_{K,\alpha,\beta}| &< \infty, \\ \lambda_{K,\alpha,\beta} &= \frac{z}{\pi}\sum_{n=0}^{K-1}\int_{a_n}^{a_{n+1}} d\theta \left[\frac{\partial \phi_2}{\partial z}(\theta,0,\beta) + O(z)\right]. \end{aligned} \tag{2.4.19}$$

Since $\lambda_{K,\alpha,\beta}$ and z are finite, $\frac{1}{\pi}\sum_{n=0}^{K-1}\int_{a_n}^{a_{n+1}} d\theta \left[\frac{\partial \phi_2}{\partial z}(\theta,0,\beta) + O(z)\right]$ is also finite. Moreover, $\frac{\partial \phi_2}{\partial z}(\theta,0,\beta)$ does not depend on z. Therefore, in the limit of $z \to +0(\gamma_{K,\alpha} \to \infty, |\alpha| \to 1-0)$, it follows that

$$\lambda_{K,\alpha,\beta} = O(z) = O\left(\sqrt{1-|\alpha|}\right). \tag{2.4.20}$$

(ii) In the case of $K = 2N$ in the limit of $|\alpha| \to +0(\gamma_{2N,\alpha} \to \infty)$, we have that $\gamma_{2N,\alpha} \sim \sqrt{|\alpha|}$. Consider the partial derivative of ϕ_1 with respect to γ:

$$\frac{\partial \phi_1}{\partial \gamma} = \frac{1}{|\alpha|\beta}\frac{\gamma\,|\cot\theta|^{\frac{\beta-1}{\beta}}}{\cot^2\theta+\gamma^2}\frac{\partial|\alpha|}{\partial\gamma} + \log\left||\alpha|^{\frac{1}{\beta}}A\right|\frac{|\cot\theta|^{\frac{\beta-1}{\beta}}(\cot^2\theta-\gamma^2)}{(\cot^2\theta+\gamma^2)^2}. \tag{2.4.21}$$

Then, $\frac{\partial \phi_1}{\partial \gamma}$ does not diverge. It holds that

$$\begin{aligned} |\lambda_{2N,\alpha,\beta}| &< \infty, \\ \lambda_{2N,\alpha,\beta} &= \frac{1}{\pi}\sum_{n=0}^{K-1}\int_{a_n}^{a_{n+1}} d\theta \left[\frac{\partial \phi_1}{\partial \gamma_{2N,\alpha}}(\theta,0,\beta)\gamma_{2N,\alpha} + O(\gamma_{2N,\alpha}^2)\right]. \end{aligned} \tag{2.4.22}$$

Now, one has that

$$\frac{\partial \phi_1}{\partial \gamma_{2N,\alpha}}(\theta,0,\beta) = \frac{1}{\beta}\gamma_{2N,\alpha}\log|\alpha|\frac{|\cot\theta|^{\frac{\beta-1}{\beta}}}{\cot^2\theta} + \gamma_{2N,\alpha}\log|A|\frac{|\cot\theta|^{\frac{\beta-1}{\beta}}}{\cot^2\theta} \tag{2.4.23}$$

According to Section 2.3.3, the following relations hold in the limit of $|\alpha| \to +0$:

$$\begin{aligned} \gamma_{2N,\alpha}\log|\alpha|\frac{|\cot\theta|^{\frac{\beta-1}{\beta}}}{\cot^2\theta} &= O\left(\sqrt{|\alpha|}\right), \\ \gamma_{2N,\alpha}\log|A|\frac{|\cot\theta|^{\frac{\beta-1}{\beta}}}{\cot^2\theta} &= O\left(\sqrt{|\alpha|}\right). \end{aligned} \tag{2.4.24}$$

Therefore, in the limit of $|\alpha| \to +0$, it follows that

$$\lambda_{K,\alpha,\beta} = \frac{1}{\pi}\sum_{n=0}^{K-1}\int_{a_n}^{a_{n+1}} d\theta O\left(\sqrt{|\alpha|}\right) = O\left(\sqrt{|\alpha|}\right). \tag{2.4.25}$$

(iii) In the case of $K = 2N + 1$ in the limit of $|\alpha| \to +0 (\gamma_{2N,\alpha} \to \infty)$, we have that $\gamma_{2N+1,\alpha} = O\left(\sqrt{|\alpha| - \frac{1}{(2N+1)^2}}\right)$. Then, $\frac{\partial \phi_1}{\partial \gamma}$ does not diverge. Therefore, according to Section 2.3.3, it follows that

$$\begin{aligned} |\lambda_{2N+1,\alpha,\beta}| &< \infty, \\ \lambda_{2N+1,\alpha,\beta} &= \frac{\gamma_{2N+1,\alpha}}{\pi} \sum_{n=0}^{K-1} \int_{a_n}^{a_{n+1}} d\theta \left[\frac{\partial \phi_1}{\partial \gamma}(\theta, 0, \beta) + O(\gamma) \right]. \end{aligned} \tag{2.4.26}$$

Since $\lambda_{2N+1,\alpha,\beta}$ and $\gamma_{2N+1,\alpha}$ are finite, $\frac{1}{\pi} \sum_{n=0}^{K-1} \int_{a_n}^{a_{n+1}} d\theta \left[\frac{\partial \phi_1}{\partial \gamma}(\theta, 0, \beta) + O(\gamma) \right]$ is also finite. Moreover, $\frac{\partial \phi_1}{\partial \gamma}(\theta, 0, \beta)$ does not depend on $\gamma_{2N+1,\alpha}$. Therefore, in the limit of $\gamma_{2N+1,\alpha} \to +0$ ($|\alpha| \to \frac{1}{(2N+1)^2} + 0$) it follows that

$$\lambda_{2N+1,\alpha,\beta} = O(\gamma_{2N+1,\alpha}) = O\left(\sqrt{|\alpha| - \frac{1}{(2N+1)^2}}\right). \tag{2.4.27}$$

From equations (2.4.20), (2.4.25) and (2.4.27), we see that for the ESGB transformation

- the critical exponent of the Lyapunov exponent ν_1 is $\frac{1}{2}$ in the limit of $|\alpha| \to 1 - 0$ for any K,
- $\nu_2 = \frac{1}{2}$ in the limit of $|\alpha| \to \frac{1}{K^2} + 0$ for $K = 2N + 1$, and
- $\nu_3 = \frac{1}{2}$ in the limit of $|\alpha| \to +0$ for $K = 2N$.

□

2.5 Conclusion

In terms of generalized Boole transformation, we obtain the analytic formula of Lyapunov exponents for the generalized Boole transformations for the full range of parameters and prove the mixing of the map for $0 < \alpha < 1$. We also obtain the KS-entropy by using Pesin's formula. As a result, we can explicitly modulate Lyapunov exponent λ in the range of $\lambda \geq 0$ by changing parameter $\alpha > 0$. In addition, the absolute values of the derivative $d\lambda/d\alpha$ at $\alpha = 0$ to $\alpha = 1 - 0$ are proven to be *infinite*. Then, it is analytically shown to be extremely difficult to distinguish values of Lyapunov exponent near $\alpha = 0$ or $\alpha = 1$ because of such strong parameter dependency. The scaling behavior of our analytic Lyapunov exponents of the generalized Boole transformations is found to be consistent with Pomeau and Manneville's numerical results about intermittency of *Type 1* and *Type 3*. In addition, the critical exponent near $\alpha \to 1+0$ gives a new view of intermittency.

In terms of super generalized Boole transformations, this work is the first example in which the conjecture by Pomeau and Manneville expressed in (2.3.1) is analytically proven to be true for a countably infinite number of maps (the proposed super generalized Boole transformations). This research presented the theoretical picture of the stable-unstable transition for intermittent maps. In the course of providing the proof, we showed that the super generalized Boole (SGB) transformations preserve the unique Cauchy distribution, and also proved that SGB transformations are *exact* and that any initial density function converges to the invariant Cauchy distribution when the parameters (K, α) are in Range A. By applying the property of exactness, it becomes possible to obtain the *analytical* formulae of the Lyapunov exponents for the SGB transformations. In these transformations, the Lyapunov exponents $\lambda_{K,\alpha}$ are equivalent to the Kolmogorov-Sinai entropy as applied to Pesin's theorem. Using the analytical formulae of the Lyapunov exponents, we confirmed that for $K = 3, 4$, and 5, the derivative $\dfrac{\partial \lambda_{K,\alpha}}{\partial \alpha}$ diverges at the critical points and we obtained $\nu_1 = \nu_2 = \nu_3 = \dfrac{1}{2}$ for $K = 3, 4$, and 5. We also proved the critical exponents for a countably infinite number of maps. Thus, we proved the universality of the route to chaos for a large class of chaotic systems. Besides, we also proved that the SGB transformations preserve the Lebesgue measure at $\alpha = \pm 1$ for any K and that the SGB transformations are ergodic in the condition.

In terms of futher extension of super generalized Boole transformations (ESGB), we succeeded in extending the class of invariant density functions from the Cauchy distribution. In ESGB, we also proved that ESGB are exact when the parameter (K, α) are in Range A regardless of β. From exactness, we obtained the critical exponent of the Lyapunov exponent as $\nu_1 = \nu_2 = \nu_3 = \frac{1}{2}$, which demonstrate the estimation by Pomeau and Manneville for countably infinite maps whose invariant density belongs not only the Cauchy class but also more wider class. This means that the universality of the critical exponent $\delta = \frac{1}{2}$ can be applied to the wider class. This result broadened the horizons of study with route to chaos. As the future work, it is expected that the any power exponent for mean square displacement is obtained for ESGB.

In future, we plan to clarify the scaling relation between the critical exponent ν and the other critical exponents. Then, we expect that our analytic analysis can be useful for investigating physically chaotic systems further and this would enable us to obtain a new perspective of chaos in physics.

Chapter 3

The Arrow of Time

This chapter is according to [51].

3.1 Introduction

The problem of the arrow of time is known to be a controversial issue that a unidirectional time evolution occurs in a macroscopic scale although a microscopic system obeys an equation with time-reversal symmetry. In discussion about time irreversibility, it is important to specify time scales and which quantity evolves irreversibly. In the 19'th century, Boltzmann clarified irreversible behavior of an H-function by assuming the *molecular chaos hypothesis* [7, 91]. On Boltzmann's H-theorem, Loschmidt [8] claimed in a system with time-reversal symmetry, that the time derivative of the entropy would be negative in a backward motion. In addition, Zermelo [9] asserted that the value of the entropy would return to the initial value by quoting Poincaré's Recurrence Theorem. Kac showed how the irreversible behavior occurs in the Ehrenfest model when the initial condition is far from the equilibrium state using the mean recurrence time [92, 93]. In the Ehrenfest model, the state of the system evolves stochastically. In 1970's, for nonequilibrium systems in stationary and chaotic states, the idea of the SRB distribution was proposed by Sinai, Ruelle and Bowen using mixing Anosov diffeomorphisms, in which it was proved that there is a unique ergodic distribution [6, 22, 91]. If one proves that a dynamical system has a SRB measure, then it is guaranteed that initial density functions converge to the SRB density function (unique ergodic density function)[6, 94] in the sense of mixing. Using the property of the Anosov diffeomorphisms and SRB measure, one obtains the positive Kolmogorov-Sinai (KS) entropy h_{KS}. It is known that for Anosov systems, by coarse-graining, Boltzmann entropy can be denoted as a linear function in terms of time whose slope is represented by the Kolmogorov-Sinai entropy for certain time range by assuming appropriate conditions [29, 95, 96].

As an example of physical model having a SRB measure (a mixing invariant density function), Sinai [24, 27] proved the hyperbolicity, mixing property and ergodicity of dynamical systems with scatterers (Sinai billiards)[25]. Bunimovich [26, 27] also proved these properties in a stadium (Bunimovich stadium). As another example, the Lorentz gas is known where a periodic continuation of Sinai billiards' boundary is applied without any walls [28].

The Sinai billiards, Lorentz gas and Bunimovich stadium are known as famous chaotic and mixing dynamical models which have scatterers or walls. In these models, the properties of the dynamical systems such as mixing are caused by the existence of obstacles, scatterers, their shape and their position. Then, how about dynamical systems without obstacles, scatterers or walls? For symplectic maps, the Sawtooth map [29, 30], Arnold's cat map [31] and multi Baker's map [32] have been known as mixing symplectic maps without scatterers. However, their Jacobians are constant for any points and the maps are too ideal compared with the tangent map [97] and the standard map [29, 98, 99, 100].

In this thesis, a "macroscopic uni-direction" is defined by the convergence of initial density functions to an equilibrium distribution and the positivity of entropy rate in the time scale of relaxation. From the previous chapter, in the generalized Boole transformations, super generalized Boole transformations and extended super generalized Boole transformations where exactness is hold, it is proven that the initial density function converges to the equilibrium density function (the Cauchy distribution) so that one can observe the "macroscopic uni-direction". However, these three maps do not have time-reversal symmetry. In this chapter we propose a symplectic map with time-reversal symmetry derived from a Hamiltonian without scatterers or walls. In our model, we prove for certain parameter ranges that any initial density function defined except for a zero volume set relaxes uniquely to the uniform distribution, that the system is mixing using only information about the microscopic dynamical system [6] and that KS entropy is positive. In proving the above property, we show that the maps are Anosov diffeomorphisms. We also prove that *perfectly chaotic superdiffusion* occurs for the parameter ranges, which means that for almost all initial points superdiffusion occurs. This does not occur in the other maps discussed above. That is, in our model, we discover that there is a mathematical structure that connects an Anosov diffeomorphism (convergence of initial density functions to the uniform distribution and positivity of entropy rate) with *perfectly chaotic superdiffusion*.

3.2 Mechanics

Let us introduce our Hamiltonian

$$H(p_1,p_2,q_1,q_2) \overset{\text{def}}{=} \frac{p_1^2}{2}+\frac{p_2^2}{2}+V(q_1,q_2), \tag{3.2.1}$$

$$V(q_1,q_2) \overset{\text{def}}{=} -\frac{\varepsilon}{\pi}\log\left|\cos\{\pi(q_1-q_2)\}\right|. \tag{3.2.2}$$

where $\varepsilon \in \mathbb{R}$ is a perturbation parameter, $p_1,p_2 \in \mathbb{R}$ and $q_1,q_2 \in I_{\delta_{N,\Delta\tau}} \overset{\text{def}}{=} \left(-\frac{1}{2}+\frac{\delta_{N,\Delta\tau}}{\pi},\frac{1}{2}-\frac{\delta_{N,\Delta\tau}}{\pi}\right]$. On $I_{\delta_{N,\Delta\tau}}$, we identify $-\frac{1}{2}+\frac{\delta_{N,\Delta\tau}}{\pi}$ with $\frac{1}{2}-\frac{\delta_{N,\Delta\tau}}{\pi}$. We choose $\delta_{N,\Delta\tau}>0$ such as

$$\frac{\left|2\left(1-\frac{2\delta_{N,\Delta\tau}}{\pi}\right)-2\varepsilon(\Delta\tau)^2\left[\tan\left(\frac{\pi}{2}-\delta_{N,\Delta\tau}\right)-\tan\left(-\frac{\pi}{2}+\delta_{N,\Delta\tau}\right)\right]\right|}{\left(1-\frac{2\delta_{N,\Delta\tau}}{\pi}\right)} = N \in \mathbb{N}. \tag{3.2.3}$$

Figures 3.1 and 3.2 show the shape of the potential $V(q_1,q_2)$ when $\delta_{N,\Delta\tau}$ is small enough at $\varepsilon = 2.0, -2.0$, respectively. Then we consider the following map $T_{\varepsilon,\Delta\tau}$ that is obtained by the leap frog method (second order *time reversal symmetric* symplectic integrator) for the canonical equations of motion associated with (3.2.1).

$$T_{\varepsilon,\Delta\tau} : (\mathbb{R}^2\times I^2_{\delta_{N,\Delta\tau}})\backslash\Gamma \longrightarrow (\mathbb{R}^2\times I^2_{\delta_{N,\Delta\tau}})\backslash\Gamma, \tag{3.2.4}$$

$$\begin{pmatrix} p_1(n+1)\\ p_2(n+1)\\ q_1(n+1)\\ q_2(n+1)\end{pmatrix} = \begin{pmatrix} p_1(n)-\varepsilon\Delta\tau\tan\left[\pi\left\{q_1(n)+\frac{\Delta\tau}{2}p_1(n)-q_2(n)-\frac{\Delta\tau}{2}p_2(n)\right\}\right]\\ p_2(n)+\varepsilon\Delta\tau\tan\left[\pi\left\{q_1(n)+\frac{\Delta\tau}{2}p_1(n)-q_2(n)-\frac{\Delta\tau}{2}p_2(n)\right\}\right]\\ q_1(n)+p_1(n)\Delta\tau-\frac{\varepsilon(\Delta\tau)^2}{2}\tan\left[\pi\left\{q_1(n)+\frac{\Delta\tau}{2}p_1(n)-q_2(n)-\frac{\Delta\tau}{2}p_2(n)\right\}\right] \mod I_{\delta_{N,\Delta\tau}}\\ q_2(n)+p_2(n)\Delta\tau+\frac{\varepsilon(\Delta\tau)^2}{2}\tan\left[\pi\left\{q_1(n)+\frac{\Delta\tau}{2}p_1(n)-q_2(n)-\frac{\Delta\tau}{2}p_2(n)\right\}\right] \mod I_{\delta_{N,\Delta\tau}}\end{pmatrix}, \tag{3.2.5}$$

where $\Delta\tau$ represents a step size. The definition of Γ is a set $\{(p_1,p_2,q_1,q_2)\}$ such that there exists an integer n such that $T^n_{\varepsilon,\Delta\tau}(p_1,p_2,q_1,q_2) = (p_1',p_2',q_1',q_2')$, where $q_1'+(\Delta\tau/2)p_1'-q_2'-(\Delta\tau/2)p_2' = (2m+1)/2, m\in\mathbb{Z}$. It then turns out that the Lebesgue measure of Γ is zero. The definition of " mod $I_{\delta_{N,\Delta\tau}}$" is as follows.

Definition 3.2.1 (mod $I_{\delta_{N,\Delta\tau}}$)**.** *Define an operation* mod $I_{\delta_{N,\Delta\tau}} : \mathbb{R}\longrightarrow I_{\delta_{N,\Delta\tau}}$ *to be*

$$x \mod I_{\delta_{N,\Delta\tau}} \overset{\text{def}}{=} x-n\left(1-\frac{2}{\pi}\delta_{N,\Delta\tau}\right), \tag{3.2.6}$$

where $-\frac{1}{2}+\frac{\delta_{N,\Delta\tau}}{\pi}+n\left(1-\frac{2}{\pi}\delta_{N,\Delta\tau}\right) < x \le \frac{1}{2}-\frac{\delta_{N,\Delta\tau}}{\pi}+n\left(1-\frac{2}{\pi}\delta_{N,\Delta\tau}\right), n\in\mathbb{Z}.$

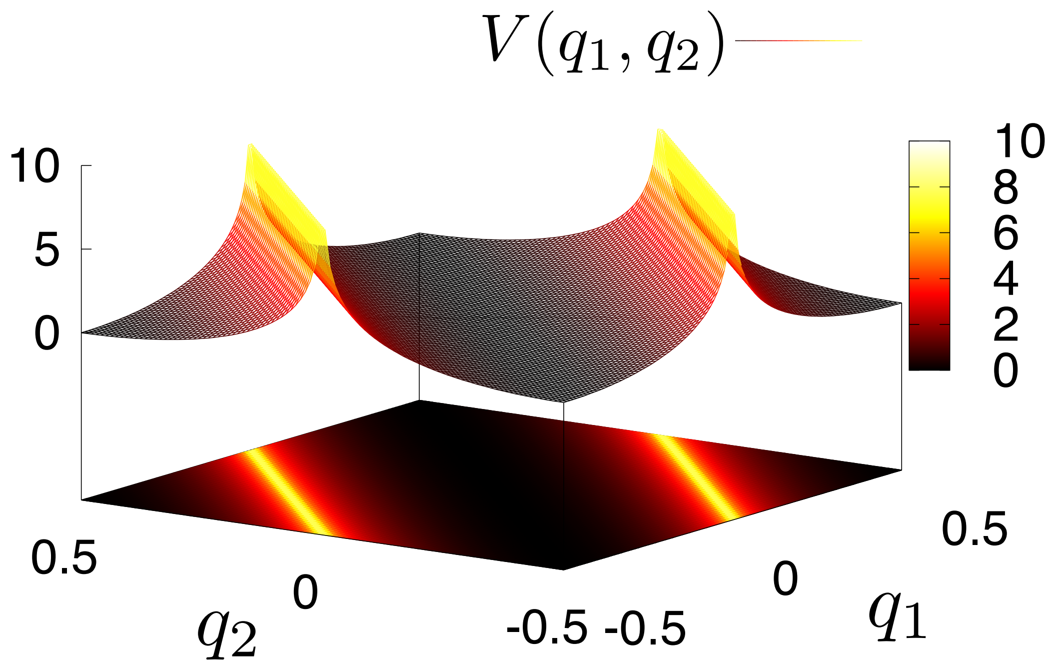

Figure 3.1: Shape of the periodic potential $V(q_1, q_2)$ for $\varepsilon = 2.0$ (repulsive force occurs) .

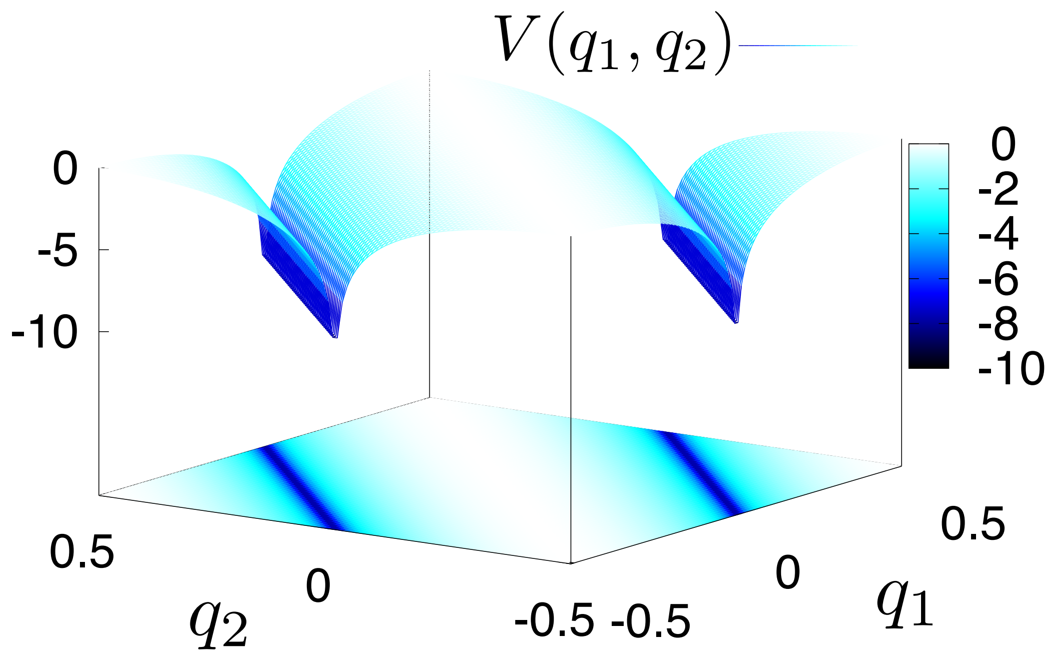

Figure 3.2: Shape of the periodic potential $V(q_1, q_2)$ for $\varepsilon = -2.0$ (attractive force occurs).

3.3 Transformation-Other symplectic maps

In this section, other maps $\widehat{T}_{\varepsilon,\Delta\tau}$ and $\widetilde{T}_{\varepsilon,\Delta\tau}$are derived from $T_{\varepsilon,\Delta\tau}$ in order to make the following proof simple. The flow is shown as follows.

$$T_{\varepsilon,\Delta\tau} \longrightarrow \widehat{T}_{\varepsilon,\Delta\tau} \longrightarrow \widetilde{T}_{\varepsilon,\Delta\tau}$$

First, the map $\widehat{T}_{\varepsilon,\Delta\tau}$ is introduced. In the map $T_{\varepsilon,\Delta\tau}$, one sees that there are two relations with regard to conservative quantities such that

$$\begin{aligned} p_1(n)+p_2(n) &= p_1(n-1)+p_2(n-1)=\cdots=p_1(0)+p_2(0) \overset{\text{def}}{=} C, \\ q_1(n)+q_2(n) &= q_0+nC, \end{aligned} \tag{3.3.1}$$

where $q_0 \overset{\text{def}}{=} q_1(0)+q_2(0)$. Then one can delete p_2 and q_2 from (3.2.5) by applying the above relations and can define the new map rewritten as following.

Definition 3.3.1 ($\widehat{T}_{\varepsilon,\Delta\tau}$). *Define a symplectic map* $\widehat{T}_{\varepsilon,\Delta\tau} : \left(\mathbb{R}\times I_{\delta_{N,\Delta\tau}}\right)\backslash\Gamma' \to \left(\mathbb{R}\times I_{\delta_{N,\Delta\tau}}\right)\backslash\Gamma'$ *to be*

$$\begin{pmatrix} p_1(n+1) \\ q_1(n+1) \end{pmatrix} = \begin{pmatrix} p_1(n)-\varepsilon(\Delta\tau)\tan\left[\pi\left\{2q_1(n)+\Delta\tau p_1(n)-q_0-C\Delta\tau\left(n+\frac{1}{2}\right)\right\}\right] \\ q_1(n)+p_1(n)\Delta\tau-\frac{\varepsilon(\Delta\tau)^2}{2}\tan\left[\pi\left\{2q_1(n)+\Delta\tau p_1(n)-q_0-C\Delta\tau\left(n+\frac{1}{2}\right)\right\}\right] \ mod\ I_{\delta_{N,\Delta\tau}} \end{pmatrix}. \tag{3.3.2}$$

where Γ' *represents a set* $\{(p_1(n),q_1(n))\}\subset(\mathbb{R}\times I_{\delta_{N,\Delta\tau}})$ *such that there exists an integer* k *which satisfies the condition that*

$$\begin{aligned} \widehat{T}^k_{\varepsilon,\Delta\tau}(p_1(n),q_1(n)) &= (p_1(n+k),q_1(n+k)), \\ \text{where } 2q_1(n+k)+\Delta\tau p_1(n+k)-q_0-C\Delta\tau\left(n+k+\frac{1}{2}\right) &= \frac{2m+1}{2},\ \ m\in\mathbb{Z}. \end{aligned} \tag{3.3.3}$$

One can reconstruct the map $T_{\varepsilon,\Delta\tau}$ using $\widehat{T}_{\varepsilon,\Delta\tau}$ and the relations (3.3.1). By introducing another symplectic map $\widehat{T}_{\varepsilon,\Delta\tau}$, one can decrease the number of freedom from four to two.

In the following, manifolds M and M' represent $I^2_{\delta_{N,\Delta\tau}}$ and $\left(\mathbb{R}\times I_{\delta_{N,\Delta\tau}}\right)\backslash\Gamma'$, respectively.

Second, the map $\widetilde{T}_{\varepsilon,\Delta\tau}$ is introduced from $\widehat{T}_{\varepsilon,\Delta\tau}$.

Definition 3.3.2 ($\widetilde{T}_{\varepsilon,\Delta\tau}$). *Define a symplectic map* $\widetilde{T}_{\varepsilon,\Delta\tau} : M \to M$ *to be*

$$\begin{pmatrix} s_{n+1}, \\ t_{n+1} \end{pmatrix} = \begin{pmatrix} g(t_n) \\ h(s_n,t_n) \end{pmatrix} = \begin{pmatrix} t_n \\ 2t_n - s_n + 2\varepsilon(\Delta\tau)^2\tan(\pi t_n) \quad \text{mod } I_{\delta_{N,\Delta\tau}} \end{pmatrix}. \tag{3.3.4}$$

The symplectic map $\widetilde{T}_{\varepsilon,\Delta\tau}$ is topologically semi-conjugate with $\widehat{T}_{\varepsilon,\Delta\tau}$ using a homeomorphism H defined by

$$\begin{pmatrix} s_n \\ t_n \end{pmatrix} = H \begin{pmatrix} p_1(n) \\ q_1(n) \end{pmatrix} = \begin{pmatrix} \Delta\tau p_1(n) + 2q_1(n) - q_0 - C\Delta\tau\,(n+1/2) & \mod I_{\delta_{N,\Delta\tau}} \\ J(p_1(n), q_1(n)) - q_0 - C\Delta\tau\,(n+3/2) & \mod I_{\delta_{N,\Delta\tau}} \end{pmatrix} \tag{3.3.5}$$

where $J(p_1(n), q_1(n)) \overset{\text{def}}{=} \Delta\tau p_1(n+1) + 2q_1(n+1)$.
For the symplectic maps $T_{\varepsilon,\Delta\tau}$, $\widehat{T}_{\varepsilon,\Delta\tau}$ and $\widetilde{T}_{\varepsilon,\Delta\tau}$ the following diagram commutes:

$$\begin{array}{ccc} \left(\mathbb{R}^2 \times I^2_{\delta_{N,\Delta\tau}}\right) \backslash \Gamma & \xrightarrow{T_{\varepsilon,\Delta\tau}} & \left(\mathbb{R}^2 \times I^2_{\delta_{N,\Delta\tau}}\right) \backslash \Gamma \\ & & \\ \left(\mathbb{R} \times I_{\delta_{N,\Delta\tau}}\right) \backslash \Gamma' & \xrightarrow{\widehat{T}_{\varepsilon,\Delta\tau}} & \left(\mathbb{R} \times I_{\delta_{N,\Delta\tau}}\right) \backslash \Gamma' \\ H \big\downarrow & & \big\uparrow H^{-1} \\ I^2_{\delta_{N,\Delta\tau}} & \xrightarrow{\widetilde{T}_{\varepsilon,\Delta\tau}} & I^2_{\delta_{N,\Delta\tau}} \end{array}$$

3.4 Time-reversal symmetry

In this section, it is shown that the symplectic maps $T_{\varepsilon,\Delta\tau}$ and $\widehat{T}_{\varepsilon,\Delta\tau}$ have time-reversal symmetry.

Definition 3.4.1. *Let $\mathcal{M}$ be either $\mathbb{R}^2 \times I^2_{\delta_{N,\Delta\tau}}$ or M' and $f : \mathcal{M} \to \mathcal{M}$ be a map. It is said that the map f has time-reversal symmetry when there exists an operator R_1 such that*

$$R_1 \circ f = f^{-1} \circ R_1, \tag{3.4.1}$$

where R_1 satisfies $R_1(\boldsymbol{p}, \boldsymbol{q}) = (-\boldsymbol{p}, \boldsymbol{q})$ [101].

When there is the operator R_1, the form of $f^{-1} \circ R_1$ is equivalent to that of $R_1 \circ f$, so that any orbit obtained by $\{f^{-n}\}_{n\in\mathbb{Z}}$ is also one obtained by $\{R_1 \circ f^n \circ R_1^{-1}\}_{n\in\mathbb{Z}}$. For any point $(\boldsymbol{p}(n), \boldsymbol{q}(n))$, it holds that

$$R_1 \circ T_{\varepsilon,\Delta\tau} \begin{pmatrix} p_1(n) \\ p_2(n) \\ q_1(n) \\ q_2(n) \end{pmatrix} = \begin{pmatrix} -p_1(n) + \varepsilon\Delta\tau \tan\left[\pi\left\{q_1(n) - \frac{\Delta\tau}{2}p_1(n) - q_2(n) + \frac{\Delta\tau}{2}p_2(n)\right\}\right] \\ -p_2(n) - \varepsilon\Delta\tau \tan\left[\pi\left\{q_1(n) - \frac{\Delta\tau}{2}p_1(n) - q_2(n) + \frac{\Delta\tau}{2}p_2(n)\right\}\right] \\ q_1(n) + p_1(n)\Delta\tau - \frac{\varepsilon(\Delta\tau)^2}{2}\tan\left[\pi\left\{q_1(n) - \frac{\Delta\tau}{2}p_1(n) - q_2(n) + \frac{\Delta\tau}{2}p_2(n)\right\}\right] \mod I_{\delta_{N,\Delta\tau}} \\ q_2(n) + p_2(n)\Delta\tau + \frac{\varepsilon(\Delta\tau)^2}{2}\tan\left[\pi\left\{q_1(n) - \frac{\Delta\tau}{2}p_1(n) - q_2(n) + \frac{\Delta\tau}{2}p_2(n)\right\}\right] \mod I_{\delta_{N,\Delta\tau}} \end{pmatrix}. \tag{3.4.2}$$

One can also have

$$T^{-1}_{\varepsilon,\Delta\tau} \circ R_1 \begin{pmatrix} p_1(n) \\ p_2(n) \\ q_1(n) \\ q_2(n) \end{pmatrix} = \begin{pmatrix} -p_1(n) + \varepsilon\Delta\tau \tan\left[\pi\left\{q_1(n) - \frac{\Delta\tau}{2}p_1(n) - q_2(n) + \frac{\Delta\tau}{2}p_2(n)\right\}\right] \\ -p_2(n) - \varepsilon\Delta\tau \tan\left[\pi\left\{q_1(n) - \frac{\Delta\tau}{2}p_1(n) - q_2(n) + \frac{\Delta\tau}{2}p_2(n)\right\}\right] \\ q_1(n) + p_1(n)\Delta\tau - \frac{\varepsilon(\Delta\tau)^2}{2}\tan\left[\pi\left\{q_1(n) - \frac{\Delta\tau}{2}p_1(n) - q_2(n) + \frac{\Delta\tau}{2}p_2(n)\right\}\right] \mod I_{\delta_{N,\Delta\tau}} \\ q_2(n) + p_2(n)\Delta\tau + \frac{\varepsilon(\Delta\tau)^2}{2}\tan\left[\pi\left\{q_1(n) - \frac{\Delta\tau}{2}p_1(n) - q_2(n) + \frac{\Delta\tau}{2}p_2(n)\right\}\right] \mod I_{\delta_{N,\Delta\tau}} \end{pmatrix}. \tag{3.4.3}$$

Therefore, it holds from Definition 3.4.1, (3.4.2) and (3.4.3), that the map $T_{\varepsilon,\Delta\tau}$ has time-reversal symmetry.
In the case of $\widehat{T}_{\varepsilon,\Delta\tau}$, the inverse $\widehat{T}^{-1}_{\varepsilon,\Delta\tau}$ is defined by

$$\widehat{T}^{-1}_{\varepsilon,\Delta\tau}\begin{pmatrix} p_1(n+1) \\ q_1(n+1) \end{pmatrix} = \begin{pmatrix} p_1(n+1)+\varepsilon\Delta\tau\tan\left[\pi\left\{2q_1(n+1)-\Delta\tau p_1(n+1)-q_0-C\Delta\tau\left(n+\frac{1}{2}\right)\right\}\right], \\ q_1(n+1)-p_1(n+1)\Delta\tau-\frac{\varepsilon(\Delta\tau)^2}{2}\tan\left[\pi\left\{2q_1(n+1)-\Delta\tau p_1(n+1)-q_0-C\Delta\tau\left(n+\frac{1}{2}\right)\right\}\right] \end{pmatrix}. \tag{3.4.4}$$

Then, it holds that

$$R_1\circ\widehat{T}_{\varepsilon,\Delta\tau}\begin{pmatrix} p_1(n) \\ q_1(n) \end{pmatrix} = \begin{pmatrix} -p_1(n)+\varepsilon(\Delta\tau)\tan\left[\pi\left\{2q_1(n)+\Delta\tau p_1(n)-q_0-C\Delta\tau\left(n+\frac{1}{2}\right)\right\}\right] \\ q_1(n)+p_1(n)\Delta\tau-\frac{\varepsilon(\Delta\tau)^2}{2}\tan\left[\pi\left\{2q_1(n)+\Delta\tau p_1(n)-q_0-C\Delta\tau\left(n+\frac{1}{2}\right)\right\}\right] \end{pmatrix}. \tag{3.4.5}$$

One can also have

$$\widehat{T}^{-1}_{\varepsilon,\Delta\tau}\circ R_1\begin{pmatrix} p_1(n) \\ q_1(n) \end{pmatrix} = \begin{pmatrix} -p_1(n)+\varepsilon(\Delta\tau)\tan\left[\pi\left\{2q_1(n)+\Delta\tau p_1(n)-q_0-C\Delta\tau\left(n+\frac{1}{2}\right)\right\}\right] \\ q_1(n)+p_1(n)\Delta\tau-\frac{\varepsilon(\Delta\tau)^2}{2}\tan\left[\pi\left\{2q_1(n)+\Delta\tau p_1(n)-q_0-C\Delta\tau\left(n+\frac{1}{2}\right)\right\}\right] \end{pmatrix}. \tag{3.4.6}$$

Therefore, it holds from Definition 3.4.1, (3.4.5) and (3.4.6), that the map $\widehat{T}_{\varepsilon,\Delta\tau}$ has time-reversal symmetry.

3.5 Exactness and Time-reversal symmetry

In this section, we will prove that the exactness is not compatible with time-reversal symmetry as follows. When a map S is exact, it holds that

$$\lim_{n\to\infty}\mu(S^A)=1, {}^\forall A\in\mathscr{A}, \mu(A)>0. \tag{3.5.1}$$

If we assume the map S has time-reversal symmetry in addition to exactness, for any set $A\in\mathscr{A}$ such that $0<\mu(A)<1$ it holds that

$$\lim_{n\to\infty}\mu(S^nA)=\lim_{n\to\infty}\mu(R^{-1}\circ S^{-n}\circ RA). \tag{3.5.2}$$

Since the value of measure is invariant if we apply the operator R or R^{-1}, we have that

$$\lim_{n\to\infty}\mu(S^nA)=\lim_{n\to\infty}\mu(S^{-n}A). \tag{3.5.3}$$

According to the property of measure preservation $\mu(S^{-1}A)=\mu(A)$, it holds that $\mu(S^{-n}A)=\mu(A), {}^\forall n\in\mathbb{N}$. Then it holds that

$$1=\lim_{n\to\infty}\mu(S^nA)=\lim_{n\to\infty}\mu(S^{-n}A)=\mu(A)<1. \tag{3.5.4}$$

This is a contradiction. Therefore, exactness is not compatible with time-reversal symmetry.

3.6 Compatition with other maps

From the above discussion, one sees that the symplectic maps $T_{\varepsilon,\Delta\tau}$ and $\widehat{T}_{\varepsilon,\Delta\tau}$ have time-reversal symmetry. That means if one chooses the one of two time direction as “forward direction" when entropy increases in that direction, then the entropy decreases in “inverse direction" . However, for systems with time-reversal symmetry, this time evolution in “inverse direction" occurs as time evolution in “forward direction" through the operator R_1. Since these two maps are symplectic, they conserve the Lebesgue measure. Table 3.1 shows whether systems satisfies the conditions of paradoxes by Loschmidt and Zermelo.

The condition of paradox by Loschmidt is that the system has time-reversal symmetry. In this thesis, a map T is called to have time-reversal symmetry when the form of $R_1 \circ T$ is same as that of $T^{-1} \circ R_1$ by changing the sign of momentum. Here, we distinguish “reversibility" and “time-reversal symmetry". As an example which does not have time-reversal symmetry although it is reversible, the following standard map [29, 98, 99, 100] can be illustrated as such an example.

$$T_{\text{standard}} \begin{pmatrix} p_n \\ x_n \end{pmatrix} = \begin{pmatrix} p_n - K \sin x_n \\ x_n + p_{n+1} \end{pmatrix}. \tag{3.6.1}$$

The inverse map is such that

$$T^{-1}_{\text{standard}} \begin{pmatrix} p_{n+1} \\ x_{n+1} \end{pmatrix} = \begin{pmatrix} p_{n+1} - K \sin(x_{n+1} - p_{n+1}) \\ x_{n+1} - p_{n+1} \end{pmatrix}. \tag{3.6.2}$$

Then, when one changes the variable such as $p \longrightarrow -p$, the form of $R_1 \circ T_{\text{standard}}$ is not consistent with $T^{-1}_{\text{standard}} \circ R_1$. Then, the standard map does not satisfy the condition of Loschmidt (time-reversal symmetry).

In the case of tangent map [97], the time evolution is denoted as

$$T_{\text{tangent}} \begin{pmatrix} p_n \\ x_n \end{pmatrix} = \begin{pmatrix} p_n + K x_n \\ x_n + c \tan\left\{\frac{1}{2}\left(p_n + K x_n\right)\right\} \end{pmatrix}. \tag{3.6.3}$$

The inverse map is such that

$$T^{-1}_{\text{tangent}} \begin{pmatrix} p_{n+1} \\ x_{n+1} \end{pmatrix} = \begin{pmatrix} -K x_{n+1} + p_{n+1} + K c \tan\left(\frac{p_{n+1}}{2}\right) \\ x_{n+1} - c \tan\left(\frac{p_{n+1}}{2}\right) \end{pmatrix}. \tag{3.6.4}$$

Then, the tangent map does not satisfy the condition of Loschmidt since $R_1 \circ T_{\text{tangent}}$ is not consistent with $T^{-1}_{\text{tangent}} \circ R_1$.

In the case of multi Baker's map [32],

$$B(n, x, y) = \begin{cases} \left(n - 1, 2x, \frac{y}{2}\right), & 0 \le x < \frac{1}{2}, \\ \left(n + 1, 2x - 1, \frac{y+1}{2}\right), & \frac{1}{2} < x < 1, \end{cases} \tag{3.6.5}$$

Table 3.1: Comparison among systems whether they satisfy the conditions of Loschmidt and Zermelo.

	$T_{\varepsilon,\Delta\tau}, \widehat{T}_{\varepsilon,\Delta\tau}$	Hamiltonian systems	standard map	tangent map	multi Baker's map
Reversibility	$\circ$	$\circ$	$\circ$	$\circ$	$\circ$
Loschmidt (time-reversal symmetry in the sense of $R_1 : (\boldsymbol{p}, \boldsymbol{q}) \mapsto (-\boldsymbol{p}, \boldsymbol{q})$)	$\circ$ (satisfied)	$\circ$	$\times$ (not satisfied)	$\times$	$\times$
Zermelo (measure preserving)	$\circ$	$\circ$	$\circ$	$\circ$	$\circ$

the inverse map is given by

$$B^{-1}(n,x,y) = \begin{cases} \left(n+1, \frac{x}{2}, 2y\right), & 0 \le y < \frac{1}{2}, \\ \left(n-1, \frac{x+1}{2}, 2y-1\right), & \frac{1}{2} < y < 1. \end{cases} \tag{3.6.6}$$

Note that there is an involution R' instead of R_1 such that

$$R'(n,x,y) \stackrel{\text{def}}{=} (n, 1-y, 1-x), \tag{3.6.7}$$

and it satisfies $R' \circ B = B^{-1} \circ R'$. However, in multi baker's map, one cannot determine which variable has momentum dimension between x and y. That means we cannot determine which represents moment among x and y. Then, we can say that multi Baker's map does not have a pair of momentum and position (p, q) and this map does not express the equation of motion directly. Thus, in this thesis, multi Baker's map is not considered to have time-reversal symmetry in the sense of Loschmidt (in the sense of changing the sign of the momentum $\boldsymbol{p} \to -\boldsymbol{p}$). Similarly, Arnold's cat map and the tangent map [97] do not have time-reversal symmetry although they are reversible. On the other hand, the map $T_{\varepsilon,\Delta\tau}$ and $\widehat{T}_{\varepsilon,\Delta\tau}$ have time-reversal symmetry in terms of $p_1 \to -p_1, p_2 \to -p_2$. In the case of generalized Boole transformation (GB transformation) or super generalized Boole transformation (SGB transformation), the map is not injective, so that they are not reversal.

The condition of paradox by Zermelo is that the system satisfies the condition of Poincaré's Recurrence Theorem. That is, the system needs to preserve measure [102, 103]. For example, our maps $T_{\varepsilon,\Delta\tau}$, $\widehat{T}_{\varepsilon,\Delta\tau}$ Hamiltonian systems, Arnold's cat map [31], multi Baker's map [31, 32], standard map [29, 98, 99, 100] and the tangent map [97] preserve the Lebesgue measure. Then, These systems satisfy the condition of Zeromelo's claim. Therefore, our maps $T_{\varepsilon,\Delta\tau}$ and $\widehat{T}_{\varepsilon,\Delta\tau}$ satisfy the conditions of paradoxes by both Loschmidt and Zermelo.

In above chapter, it is proven in GB transformations, SGB transformations or ESGB transformations, that an initial density function converges to the invariant Cauchy distribution and that the dynamical systems have positive KS entropy by showing the exactness for some parameter range. In this chapter to prove the convergence of the initial density functions to the uniform distribution and positivity of entropy rate, we have to show that the dynamical system is an Anosov system [6]. To this end, we construct other forms of the symplectic map denoted as $\widehat{T}_{\varepsilon,\Delta\tau}$ and $\widetilde{T}_{\varepsilon,\Delta\tau}$ derived from $T_{\varepsilon,\Delta\tau}$ to make the proof shorten. Then using the homeomorphism H defined by (3.3.5), the map $\widetilde{T}_{\varepsilon,\Delta\tau} : M \stackrel{\text{def}}{=} I^2_{\delta_{N,\Delta\tau}} \to M$ is obtained from $\widehat{T}_{\varepsilon,\Delta\tau}$ as

$$\begin{pmatrix} s_{n+1} \\ t_{n+1} \end{pmatrix} = \begin{pmatrix} t_n \\ 2t_n - 2\varepsilon(\Delta\tau)^2 \tan(\pi t_n) - s_n \mod I_{\delta_{N,\Delta\tau}} \end{pmatrix}, \tag{3.6.8}$$

where $x_n \stackrel{\text{def}}{=} (s_n, t_n) \in M$.
Notice that the Jacobian of the map $\widetilde{T}_{\varepsilon,\Delta\tau}$ is given by

$$J(x_n) = \begin{pmatrix} 0 & 1 \\ -1 & 2 - \frac{2\pi\varepsilon(\Delta\tau)^2}{\cos^2(\pi t_n)} \end{pmatrix}, \tag{3.6.9}$$

and it is not a constant matrix, and the case of constant matrices was studied by Franks [104]. The linear instability condition (for at least one eigenvalue of the Jacobian, its absolute value is larger than unity) for the map $\widetilde{T}_{\varepsilon,\Delta\tau}$ is straightforwardly obtained as

$$\varepsilon < 0 \quad \text{or} \quad \frac{2}{\pi(\Delta\tau)^2} < \varepsilon, \tag{3.6.10}$$

and this condition is related to the condition that the map is an Anosov diffeomorphism (Anosov system). In the case of $\widehat{T}_{\varepsilon,\Delta\tau}$, the local instability condition is the same as that of (3.6.10).

3.7 Compactness and Diffeomorphism

In this section, it is shown that

- the domain M is compact and $\widetilde{T}_{\varepsilon,\Delta\tau}$ is a diffeomorphism on M.

The domain $I_{\delta_{N,\Delta\tau}}$ is homeomorphic to the circle S since we identify $-\frac{1}{2} + \frac{\delta_{N,\Delta\tau}}{\pi}$ with $\frac{1}{2} - \frac{\delta_{N,\Delta\tau}}{\pi}$. Then the domain M is topologically conjugate with a torus $\mathbb{T}^2$ so that M is compact. Next, we show that the map $\widetilde{T}_{\varepsilon,\Delta\tau}$ is a diffeomorphism on M. To this end, one needs to show that the map $\widetilde{T}_{\varepsilon,\Delta\tau}$ is surjective, injective, and smooth and that its inverse is continuous.

(Proof of surjective): For any point $(s_{n+1}, t_{n+1}) \in M$, there is a point $(s_n, t_n) \in M$ such that

$$\begin{cases} s_n &= 2s_{n+1} + 2\varepsilon(\Delta\tau)^2 \tan(\pi s_{n+1}) - t_{n+1} \mod I_{\delta_{N,\Delta\tau}}, \\ t_n &= s_{n+1}. \end{cases} \tag{3.7.1}$$

Thus, the map $\widetilde{T}_{\varepsilon,\Delta\tau}$ is surjective.
(Proof of injective): We show that the map $\widetilde{T}_{\varepsilon,\Delta\tau}$ is injective by contradiction. Let (s_n, t_n) and (s'_n, t'_n) be two points which cannot be identified on M. If one assumes that the image (s_{n+1}, t_{n+1}) is identified with (s'_{n+1}, t'_{n+1}), then it holds that

$$\begin{aligned} s_{n+1} &= s'_{n+1}, \\ \text{Thus,}\quad t_n &= t'_n. \end{aligned} \tag{3.7.2}$$

Using $2t+2\varepsilon(\Delta\tau)^2 \tan(\pi t)$ is finite for $t \in I_{\delta_{N,\Delta\tau}}$ and (3.7.2), one obtains the relation $s_n = s'_n$. These results are in contradiction to the condition that $(s_n, t_n) \neq (s'_n, t'_n)$. Therefore, the map $\widetilde{T}_{\varepsilon,\Delta\tau}$ is injective.
(Proof of smoothness): It is obvious that $g, h, \frac{\partial g}{\partial t}, \frac{\partial h}{\partial s}$ and $\frac{\partial h}{\partial t}$ defined in (3.3.4) are continuous on M except for (s,t) where $s = \frac{1}{2} - \frac{\delta_{N,\Delta\tau}}{\pi}$ or $t = \frac{1}{2} - \frac{\delta_{N,\Delta\tau}}{\pi}$. Then let us discuss the smoothness at $\frac{1}{2} - \frac{\delta_{N,\Delta\tau}}{\pi}$. It is obvious that $g(t) = t$ and $\frac{\partial g}{\partial t}$ are continuous at $t = \frac{1}{2} - \frac{\delta_{N,\Delta\tau}}{\pi}$ and that $h(s,t) = 2t + 2\varepsilon(\Delta\tau)^2 \tan(\pi t) - s$ and $\frac{\partial h}{\partial s}$ are continuous at $s = \frac{1}{2} - \frac{\delta_{N,\Delta\tau}}{\pi}$ similarly.
Then, let us discuss the continuity of $h(s,t)$ and that of $\frac{\partial h}{\partial t}$ at $t = \frac{1}{2} - \frac{\delta_{N,\Delta\tau}}{\pi}$. From the definition of $\delta_{N,\Delta\tau}$, one obtains

$$\begin{aligned} \left| h\left(s, -\frac{1}{2} + \frac{\delta_{N,\Delta\tau}}{\pi}\right) - h\left(s, \frac{1}{2} - \frac{\delta_{N,\Delta\tau}}{\pi}\right) \right| &= N\left(1 - \frac{2\delta_{N,\Delta\tau}}{\pi}\right), \\ \text{Thus,}\ \left| h\left(s, -\frac{1}{2} + \frac{\delta_{N,\Delta\tau}}{\pi}\right) - h\left(s, \frac{1}{2} - \frac{\delta_{N,\Delta\tau}}{\pi}\right) \right| \mod I_{\delta_{N,\Delta\tau}} &= 0. \end{aligned}$$

Then, $h(s,t)$ is continuous at $t = \frac{1}{2} - \frac{\delta_{N,\Delta\tau}}{\pi}$ on torus M. Since $h(s,t)$ is an odd function with t, one obtains $\frac{\partial h}{\partial t}\left(s, -\frac{1}{2} + \frac{\delta_{N,\Delta\tau}}{\pi}\right) = \frac{\partial h}{\partial t}\left(s, \frac{1}{2} - \frac{\delta_{N,\Delta\tau}}{\pi}\right)$. Thus $\frac{\partial h}{\partial t}$ is continuous at $t = \frac{1}{2} - \frac{\delta_{N,\Delta\tau}}{\pi}$. The map $\widetilde{T}^{-1}_{\varepsilon,\Delta\tau}$ is also continuous on M. Therefore, the map $\widetilde{T}_{\varepsilon,\Delta\tau}$ is a diffeomorphism on M.

3.8 Proof of Anosov diffeomorphism for $\widetilde{T}_{\varepsilon,\Delta\tau}$

In this section, we prove that the map $\widetilde{T}_{\varepsilon,\Delta\tau}$ defined by (3.3.4) is an Anosov diffeomorphism for $\varepsilon < 0, \frac{2}{\pi(\Delta\tau)^2} < \varepsilon$. A point (s_n, t_n) of M is denoted as $x_n =$

(s_n, t_n). The Jacobian of the map $\widetilde{T}_{\varepsilon,\Delta\tau}$ is given by

$$J(x_n) = \begin{pmatrix} 0 & 1 \\ -1 & 2 - \frac{2\pi\varepsilon(\Delta\tau)^2}{\cos^2(\pi t_n)} \end{pmatrix}, \tag{3.8.1}$$

where components of the Jacobian $J(x_n)$ are on $\mathbb{R}$. According to [6, 31, 103, 104], an Anosov diffeomorphism is defined below.

Definition 3.8.1 (Anosov diffeomorphism)**.** *Let $\mathcal{M}^*$ be a compact manifold, $\|\cdot\|$ be a norm and $f : \mathcal{M}^* \to \mathcal{M}^*$ be a diffeomorphism. Consider the tangent space $T_x\mathcal{M}^*$ at each point $x \in \mathcal{M}^*$. If f satisfies the all of the following conditions*

(I) There exist the subspaces E_x^u and E_x^s, such that $T_x\mathcal{M}^* = E_x^u \oplus E_x^s$,

(II) $(D_x f)E_x^u = E_{f(x)}^u$, $(D_x f)E_x^s = E_{f(x)}^s$,

(III) There exist $K > 0$ and $0 < \lambda < 1$ determined by x and neither by $\boldsymbol{\xi}$ nor by n such that

$$\boldsymbol{\xi} \in E_x^u \Longrightarrow \|(Df^n)\boldsymbol{\xi}\| \geq K\left(\frac{1}{\lambda}\right)^n \|\boldsymbol{\xi}\|, \tag{3.8.2}$$

$$\boldsymbol{\xi} \in E_x^s \Longrightarrow \|(Df^{-n})\boldsymbol{\xi}\| \geq K\left(\frac{1}{\lambda}\right)^n \|\boldsymbol{\xi}\|, \tag{3.8.3}$$

then f is called an Anosov diffeomorphism.

The linear instability condition (for at least one eigenvalue of the matrix (3.8.1), its absolute value is larger than unity) for the map $\widetilde{T}_{\varepsilon,\Delta\tau}$ is

$$\varepsilon < 0, \quad \text{or} \quad \frac{2}{\pi(\Delta\tau)^2} < \varepsilon. \tag{3.6.10}$$

The linear instability condition is related to the condition that the map $\widetilde{T}_{\varepsilon,\Delta\tau}$ is an Anosov diffeomorphism for the map $\widetilde{T}_{\varepsilon,\Delta\tau}$.

We will prove that the map $\widetilde{T}_{\varepsilon,\Delta\tau}$ is an Anosov diffeomorphism for $\varepsilon < 0, \frac{2}{\pi(\Delta\tau)^2} < \varepsilon$. This proof is based on the idea used in [29]. To prove this, all the conditions *(I)*, *(II)* and *(III)* in Definition 3.8.1 should be satisfied. To do so, we first introduce definitions of cones L^+ and L^- and, then we have to show the following Lemmas.

Definition 3.8.2. *For any two dimensional non-zero vector on $T_{x_n}M, x_n \in M, n \in \mathbb{Z}$*

$$\boldsymbol{a}_n = (a_1(n), a_2(n)) \neq \boldsymbol{O},$$

define cones L^+ and L^- to be

$$\begin{aligned}
L^+(x_n) &= \{(a_1(n), a_2(n)); \|J(x_n)\boldsymbol{a}_n\| > \|\boldsymbol{a}_n\|\}, \\
L^-(x_n) &= \{(a_1(n), a_2(n)); \|J(\widetilde{T}^{-1}_{\varepsilon,\Delta\tau} x_n)^{-1}\boldsymbol{a}_n\| > \|\boldsymbol{a}_n\|\},
\end{aligned}$$

where $\|\cdot\|$ represents $\|\boldsymbol{a}(n)\| \equiv \sqrt{a_1^2(n) + a_2^2(n)}$.

Lemma 3.8.1. *When the condition $\varepsilon < 0$, $\frac{2}{\pi(\Delta\tau)^2} < \varepsilon$ is satisfied, it holds that*

$$J(x_n)\boldsymbol{a}_n \in L^+(\widetilde{T}_{\varepsilon,\Delta\tau} x_n), {}^\forall \boldsymbol{a}_n \in L^+(x_n), \tag{3.8.4}$$

This Lemma corresponds to the condition *(II)*.

Proof. It follows from a simple calculation that $\boldsymbol{a}_n \notin L^+(x_n)$ and $\boldsymbol{a}_n \notin L^-(x_n)$, when $a_2(n) = 0$ and $a_1(n) = 0$, respectively. Then consider the case where $a_2(n) \neq 0$ and $a_1(n) \neq 0$. The condition that $\boldsymbol{a}_n \in L^+(x_n)$ in (3.8.4) is expressed by

$$\boldsymbol{a}_n \in L^+(x_n) \Leftrightarrow \begin{cases} \frac{a_1(n)}{a_2(n)} > 1 - \frac{\pi\varepsilon(\Delta\tau)^2}{\cos^2(\pi t_n)}, & \varepsilon > \frac{2}{\pi(\Delta\tau)^2}, \\ \frac{a_1(n)}{a_2(n)} < 1 - \frac{\pi\varepsilon(\Delta\tau)^2}{\cos^2(\pi t_n)}, & \varepsilon < 0. \end{cases} \tag{3.8.5}$$

Choosing $\boldsymbol{a}_{n+1}$ as $J(x_n)\boldsymbol{a}_n = (a_1(n+1), a_2(n+1))$, one can rewrite the condition that $\boldsymbol{a}_{n+1} \in L^+(\widetilde{T}_{\varepsilon,\Delta\tau} x_n)$ in (3.8.4) is expressed as

$$\boldsymbol{a}_{n+1} \in L^+(\widetilde{T}_{\varepsilon,\Delta\tau} x_n) = L^+(x_{n+1}) \Leftrightarrow \begin{cases} \frac{a_1(n+1)}{a_2(n+1)} > 1 - \frac{\pi\varepsilon(\Delta\tau)^2}{\cos^2(\pi t_{n+1})}, & \varepsilon > \frac{2}{\pi(\Delta\tau)^2}, \\ \frac{a_1(n+1)}{a_2(n+1)} < 1 - \frac{\pi\varepsilon(\Delta\tau)^2}{\cos^2(\pi t_{n+1})}, & \varepsilon < 0. \end{cases} \tag{3.8.6}$$

To prove (3.8.4), we show below that (3.8.5) implies (3.8.6).

Substituting $a_1(n+1) = a_2(n)$ and $a_2(n+1) = -a_1(n) + 2\left(1 - \frac{\pi\varepsilon(\Delta\tau)^2}{\cos^2(\pi t_n)}\right) a_2(n)$, into (3.8.6), one has

$$\frac{a_1(n+1)}{a_2(n+1)} = \frac{a_2(n)}{-a_1(n) + 2\left(1 - \frac{\pi\varepsilon(\Delta\tau)^2}{\cos^2(\pi t_n)}\right) a_2(n)} = \frac{1}{-\frac{a_1(n)}{a_2(n)} + 2\left(1 - \frac{\pi\varepsilon(\Delta\tau)^2}{\cos^2(\pi t_n)}\right)}. \tag{3.8.7}$$

Then, when the condition (3.8.5) is satisfied, the condition (3.8.6) holds since it holds that inductively

$$\begin{cases} 1 - \frac{\pi\varepsilon(\Delta\tau)^2}{\cos^2(\pi t_k)} < \frac{a_1(k)}{a_2(k)} < 0, & {}^\forall k \geq n+1, \quad \varepsilon > \frac{2}{\pi(\Delta\tau)^2}, \\ 0 < \frac{a_1(k)}{a_2(k)} < 1 - \frac{\pi\varepsilon(\Delta\tau)^2}{\cos^2(\pi t_k)}, & {}^\forall k \geq n+1, \quad \varepsilon < 0. \end{cases}$$

Therefore the condition (3.8.4) holds. □

Lemma 3.8.2. *When the condition $\varepsilon < 0, \frac{2}{\pi(\Delta\tau)^2} < \varepsilon$ is satisfied, it holds that*

$$J(x_{n-1})^{-1}\boldsymbol{a}_n \in L^-(\widetilde{T}^{-1}_{\varepsilon,\Delta\tau}x_n), {}^\forall\boldsymbol{a}_n \in L^-(x_n). \tag{3.8.8}$$

Proof. The conditions $\boldsymbol{a}_n \in L^-(x_n)$ and $J(x_{n-1})^{-1}\boldsymbol{a}_n \in L^-(\widetilde{T}^{-1}_{\varepsilon,\Delta\tau}x_n)$ in (3.8.8) are expressed as

$$\boldsymbol{a}_n \in L^-(x_n) \Leftrightarrow \begin{cases} \frac{a_2(n)}{a_1(n)} > 1 - \frac{\pi\varepsilon(\Delta\tau)^2}{\cos^2(\pi t_{n-1})}, & \text{for } \varepsilon > \frac{2}{\pi(\Delta\tau)^2}, \\ \frac{a_2(n)}{a_1(n)} < 1 - \frac{\pi\varepsilon(\Delta\tau)^2}{\cos^2(\pi t_{n-1})}, & \text{for } \varepsilon < 0, \end{cases} \tag{3.8.9}$$

and

$$\begin{aligned} &\boldsymbol{a}_{n-1} \stackrel{\text{def}}{=} J(x_{n-1})^{-1}\boldsymbol{a}_n \in L^-(\widetilde{T}^{-1}_{\varepsilon,\Delta\tau}x_n) = L^-(x_{n-1}) \\ \Leftrightarrow &\begin{cases} \frac{a_2(n-1)}{a_1(n-1)} < 1 - \frac{\pi\varepsilon(\Delta\tau)^2}{\cos^2(\pi t_{n-2})}, & \text{for } \varepsilon > \frac{2}{\pi(\Delta\tau)^2}, \\ \frac{a_2(n-1)}{a_1(n-1)} > 1 - \frac{\pi\varepsilon(\Delta\tau)^2}{\cos^2(\pi t_{n-2})}, & \text{for } \varepsilon < 0. \end{cases} \end{aligned} \tag{3.8.10}$$

Substituting $a_1(n-1) = 2\left(1 - \frac{\pi\varepsilon(\Delta\tau)^2}{\cos^2(\pi t_{n-1})}\right) a_1(n) - a_2(n)$ and $a_2(n-1) = a_1(n)$ into (3.8.10), one can see the condition (3.8.10) holds when condition (3.8.9) holds. □

Definition 3.8.3. *Define a subset $LL_1^-(x_n)$ of $L^-(x_n)$ to be*

$$LL_1^-(x_n) \stackrel{\text{def}}{=} \begin{cases} \left\{(a_1(n), a_2(n)); -1 \le \frac{a_2(n)}{a_1(n)} < 0\right\} & \textit{for } \varepsilon > \frac{2}{\pi(\Delta\tau)^2}, \\ \left\{(a_1(n), a_2(n)); 0 < \frac{a_2(n)}{a_1(n)} \le 1\right\} & \textit{for } \varepsilon < 0. \end{cases} \tag{3.8.11}$$

From a simple calculation, it holds that

$$J(x_{n-1})^{-1}\boldsymbol{a}_n \in LL_1^-(x_{n-1}), {}^\forall\boldsymbol{a}_n \in LL_1^-(x_n). \tag{3.8.12}$$

Lemma 3.8.3. *For any point x_n and for any integer $k \in \mathbb{Z} \ge n$, there exists a deviation vector $\boldsymbol{a}_n$ such that*

$$\prod_{i=k}^{n} J(x_i)\boldsymbol{a}_n \in LL_1^-(x_{k+1}),\ \boldsymbol{a}_n \in LL_1^-(x_n). \tag{3.8.13}$$

Proof. We prove it by contradiction. We assume that

$${}^\exists y_n, {}^\exists k' \in \mathbb{Z} \ge n, {}^\forall\boldsymbol{a}_n \in LL_1^-(y_n) \text{ s.t. } \prod_{i=k'}^{n} J(y_i)\boldsymbol{a}_n \notin LL_1^-(y_{k'+1}). \tag{3.8.14}$$

One can obtain an orbit $\{y_m\}$ including y_n and $y_{n'}$ where $n' > k'+1 > n$. For all points, there exists the cone LL_1^-, so that there exists a vector $\boldsymbol{A}_{n'} \in LL_1^-(y_{n'})$. Then one chooses $\boldsymbol{A}_{k'+1}$ and $\boldsymbol{A}_n$ as

$$\boldsymbol{A}_{k'+1} \overset{\text{def}}{=} \prod_{i=k'+1}^{n'-1} J^{-1}(y_i)\boldsymbol{A}_{n'} \in LL_1^-(y_{k'+1}) \quad \because (3.8.8),$$

$$\boldsymbol{A}_n \overset{\text{def}}{=} \prod_{i=n}^{n'-1} J^{-1}(y_i)\boldsymbol{A}_{n'} \in LL_1^-(y_n),$$

$$\text{Thus,} \prod_{i=k'}^{n} J(y_i)\boldsymbol{A}_n \quad \in \quad LL_1^-(y_{k'+1}). \tag{3.8.15}$$

Equation (3.8.15) is contradictory to the (3.8.14). Therefore, Lemma 3.8.3 holds. □

From Lemmas 3.8.1, 3.8.2 and 3.8.3, define $LL^-(x_n)$ and $LL^+(x_n)$ as follows in order to prove that conditions *(I)*, *(II)* and *(III)* are satisfied.

Definition 3.8.4. *Define a subset $LL^-(x_n)$ of $LL_1^-(x_n)$ to be*

$$LL^-(x_n) \overset{\text{def}}{=} \left\{(a_1(n), a_2(n)); \boldsymbol{a}_n \in LL_1^-(x_n), \prod_{i=k}^{n} J(x_i)\boldsymbol{a}_n \in LL_1^-(x_{k+1}), {}^\forall k \geq n\right\}. \tag{3.8.16}$$

From Lemma 3.8.3 one can see that

$$J(x_n)\boldsymbol{a}_n \in LL^-(x_{n+1}), \ {}^\forall\boldsymbol{a}_n \in LL^-(x_n). \tag{3.8.17}$$

Definition 3.8.5. *Define a subset $LL^+(x_n)$ of $L^+(x_n)$ to be*

$$LL^+(x_n) \overset{\text{def}}{=} \begin{cases} \left\{(a_1(n), a_2(n)); -1 \leq \frac{a_1(n)}{a_2(n)} < 0\right\} & \text{for } \varepsilon > \frac{2}{\pi(\Delta\tau)^2}, \\ \left\{(a_1(n), a_2(n)); 0 < \frac{a_1(n)}{a_2(n)} \leq 1\right\} & \text{for } \varepsilon < 0. \end{cases} \tag{3.8.18}$$

From a simple calculation, it holds that

$$J(x_n)\boldsymbol{a}_n \in LL^+(x_{n+1}), {}^\forall\boldsymbol{a}_n \in LL^+(x_n). \tag{3.8.19}$$

Lemma 3.8.4. *When the condition $\varepsilon < 0, \frac{2}{\pi(\Delta\tau)^2} < \varepsilon$ is satisfied, the conditions (I) and (II) are satisfied.*

Proof. One can choose any eigenvector spaces E^u_x and E^s_x in $LL^+(x_n)$ and $LL^-(x_n)$, respectively so that combining (3.8.16) and (3.8.18):

$$E^u_{x_n} \subset LL^+(x_n), \;\; E^s_{x_n} \subset LL^-(x_n). \tag{3.8.20}$$

Combining (3.8.17), (3.8.19) and (3.8.20), one has that $J(x_n)E^u_{x_n} \subset LL^+(x_{n+1})$ and $J(x_n)E^s_{x_n} \subset LL^-(x_{n+1})$. Then, one can choose $E^u_{x_{n+1}}$, $E^s_{x_{n+1}}$ inductively by

$$E^u_{x_{n+1}} \stackrel{\text{def}}{=} J(x_n)E^u_{x_n}, \;\; E^s_{x_{n+1}} \stackrel{\text{def}}{=} J(x_n)E^s_{x_n}. \tag{3.8.21}$$

The subspaces $E^u_{x_n}$ and $E^s_{x_n}$ are linearly independent by definition, from which it holds that

$$T_{x_n}M = E^u_{x_n} \oplus E^s_{x_n}.$$

□

Lemma 3.8.5. *When the condition $\varepsilon < 0, \frac{2}{\pi(\Delta\tau)^2} < \varepsilon$ is satisfied, the condition (III) is satisfied.*

Proof. Let us define $\alpha_n \stackrel{\text{def}}{=} \left(1 - \frac{\pi\varepsilon(\Delta\tau)^2}{\cos^2(\pi t_n)}\right)$ and the stretching rate $\sigma(x_n, \boldsymbol{a}_n) \stackrel{\text{def}}{=} \frac{\|J(x_n)\boldsymbol{a}_n\|^2}{\|\boldsymbol{a}_n\|^2}$ which can be rewritten as

$$\begin{aligned}
\sigma(x_n, \boldsymbol{a}_n) &= \frac{a_1^2 + a_2^2 - 4\alpha_n a_1 a_2 + 4\alpha_n^2 a_2^2}{a_1^2 + a_2^2}, \\
&= 1 - 4\alpha_n \frac{a_1 a_2}{a_1^2 + a_2^2} + 4\alpha_n^2 \frac{a_2^2}{a_1^2 + a_2^2}, \\
&= 1 + 4\alpha_n \left(\alpha_n \sin^2\phi_n - \sin\phi_n \cos\phi_n\right),
\end{aligned}$$

where ϕ_n is defined such that $\sin^2\phi_n = \frac{a_2^2(n)}{a_1^2(n)+a_2^2(n)}$ and $\sin\phi_n\cos\phi_n = \frac{a_1(n)a_2(n)}{a_1^2(n)+a_2^2(n)}$, $-\pi < \phi \leq \pi$. Then, if $\boldsymbol{a}_n \in LL^+(x_n)$, then it holds that

$$F(\phi_n) \stackrel{\text{def}}{=} \alpha_n \sin^2\phi_n - \sin\phi_n\cos\phi_n \begin{cases} < 0, & \varepsilon > \frac{2}{\pi(\Delta\tau)^2}, \\ > 0, & \varepsilon < 0. \end{cases} \tag{3.8.22}$$

There are two cases for ε. The minimum value of σ for each case is calculated as follows.

(i) Case of $\varepsilon > \frac{2}{\pi(\Delta\tau)^2}$, From the condition that $\boldsymbol{a}_n \in LL^+(x_n) \Leftrightarrow -1 \leq \frac{a_1(n)}{a_2(n)} = \cot\phi_n < 0$, ϕ_n is defined in the range

$$-\frac{\pi}{2} < \phi_n \leq -\frac{\pi}{4}, \text{or } \frac{\pi}{2} < \phi_n \leq \frac{3}{4}\pi. \tag{3.8.23}$$

Since $F'(\phi) = \sin(2\phi)\,(\alpha_n - \cot(2\phi))$ is positive in this range, it follows that

$$\begin{aligned} F(\phi_n) &\leq F\left(-\frac{\pi}{4}\right) = F\left(\frac{3}{4}\pi\right) = \frac{1}{2}(\alpha_n + 1) < 0, \\ \therefore\ \sigma(x_n, \boldsymbol{a}_n) &\geq 1 + 2\alpha_n(\alpha_n + 1) \geq 1 + 2\left\{1 - \pi\varepsilon(\Delta\tau)^2\right\}\left\{2 - \pi\varepsilon(\Delta\tau)^2\right\}. \end{aligned}$$

Then by choosing $K = 1$, $\frac{1}{\lambda} = \sqrt{1 + 2\left\{1 - \pi\varepsilon(\Delta\tau)^2\right\}\left\{2 - \pi\varepsilon(\Delta\tau)^2\right\}} > 1$, one sees that condition (3.8.2) is satisfied.

(ii) Case of $\varepsilon < 0$,

For $0 < \cot\phi_n \leq 1$, the domain of ϕ_n is

$$-\frac{3}{4}\pi \leq \phi_n < -\frac{\pi}{2}, \text{or } \frac{\pi}{4} \leq \phi_n < \frac{\pi}{2}. \tag{3.8.24}$$

Since $F'(\phi)$ is positive in this range, one has that

$$\begin{aligned} F(\phi_n) &\geq F\left(-\frac{3}{4}\pi\right) = F\left(\frac{\pi}{4}\right) = \frac{1}{2}(\alpha_n - 1) > 0, \\ \therefore\ \sigma(x_n, \boldsymbol{a}_n) &\geq 1 + 2\alpha_n(\alpha_n - 1) \geq 1 - 2\pi\varepsilon(\Delta\tau)^2\left\{1 - \pi\varepsilon(\Delta\tau)^2\right\}. \end{aligned}$$

Then by choosing $K = 1$, $\frac{1}{\lambda} = \sqrt{1 - 2\pi\varepsilon(\Delta\tau)^2\left\{1 - \pi\varepsilon(\Delta\tau)^2\right\}} > 1$, one sees that condition (3.8.2) is satisfied. Besides, this relation about λ ($\lambda \to 1 - 0$ as $\varepsilon \to -0$) is equivalent to the fact that the Lyapunov exponent converges to zero value as $\varepsilon \to -0$.

Let us define the stretching rate $\sigma'(x_n, \boldsymbol{a}_n) \stackrel{\text{def}}{=} \frac{\|J^{-1}(\widetilde{T}^{-1}_{\varepsilon,\Delta\tau}x_n)\boldsymbol{a}_n\|^2}{\|\boldsymbol{a}_n\|^2} = \frac{\|J^{-1}(x_{n-1})\boldsymbol{a}_n\|^2}{\|\boldsymbol{a}_n\|^2}$ which can be rewritten as

$$\begin{aligned} \sigma'(x_n, \boldsymbol{a}_n) &= \frac{a_1^2 + a_2^2 - 4\alpha_{n-1}a_1a_2 + 4\alpha_{n-1}^2 a_1^2}{a_1^2 + a_2^2}, \\ &= 1 - 4\alpha_{n-1}\frac{a_1a_2}{a_1^2 + a_2^2} + 4\alpha_{n-1}^2\frac{a_1^2}{a_1^2 + a_2^2}, \\ &= 1 + 4\alpha_{n-1}\left(\alpha_{n-1}\sin^2\phi_n' - \sin\phi_n'\cos\phi_n'\right), \end{aligned}$$

where ϕ_n' is defined such that $\sin^2\phi_n' = \frac{a_1^2(n)}{a_1^2(n) + a_2^2(n)}$ and $\sin\phi_n'\cos\phi_n' = \frac{a_1(n)a_2(n)}{a_1^2(n) + a_2^2(n)}$, $-\pi < \phi' \leq \pi$. Then, if $\boldsymbol{a}_n \in LL^-(x_n)$, then it holds that

$$G(\phi_n') \stackrel{\text{def}}{=} \alpha_{n-1}\sin^2\phi_n' - \sin\phi_n'\cos\phi_n' \begin{cases} < 0, & \varepsilon > \frac{2}{\pi(\Delta\tau)^2}, \\ > 0, & \varepsilon < 0. \end{cases} \tag{3.8.25}$$

There are two cases for ε. The minimum value of σ' for each case is calculated as follows.
(i) Case of $\varepsilon > \frac{2}{\pi(\Delta\tau)^2}$,

From the condition that $\boldsymbol{a}_n \in LL^-(x_n) \Leftrightarrow -1 \leq \frac{a_2(n)}{a_1(n)} = \cot\phi'_n < 0$, ϕ'_n is defined in the range

$$-\frac{\pi}{2} < \phi'_n \leq -\frac{\pi}{4}, \text{or } \frac{\pi}{2} < \phi'_n \leq \frac{3}{4}\pi. \tag{3.8.26}$$

Then, in the same way as above discussion, it holds that

$$\begin{aligned} G(\phi'_n) &\leq \frac{1}{2}(\alpha_{n-1}+1) < 0, \\ \therefore \sigma'(x_n, \boldsymbol{a}_n) &\geq 1 + 2\alpha_{n-1}(\alpha_{n-1}+1) \geq 1 + 2\left\{1 - \pi\varepsilon(\Delta\tau)^2\right\}\left\{2 - \pi\varepsilon(\Delta\tau)^2\right\}. \end{aligned}$$

Then by choosing $K = 1$, $\frac{1}{\lambda} = \sqrt{1 + 2\left\{1 - \pi\varepsilon(\Delta\tau)^2\right\}\left\{2 - \pi\varepsilon(\Delta\tau)^2\right\}} > 1$, one sees that condition (3.8.3) is satisfied.
(ii) Case of $\varepsilon < 0$,

For $0 < \cot\phi'_n \leq 1$, the domain of ϕ'_n is

$$-\frac{3}{4}\pi \leq \phi'_n < -\frac{\pi}{2}, \text{or } \frac{\pi}{4} \leq \phi'_n < \frac{\pi}{2}. \tag{3.8.27}$$

Then, in the same way as above discussion, it holds that

$$\begin{aligned} G(\phi'_n) &\geq \frac{1}{2}(\alpha_{n-1}-1) > 0, \\ \therefore \sigma'(x_n, \boldsymbol{a}_n) &\geq 1 + 2\alpha_{n-1}(\alpha_{n-1}-1) \geq 1 - 2\pi\varepsilon(\Delta\tau)^2\left\{1 - \pi\varepsilon(\Delta\tau)^2\right\}. \end{aligned}$$

Then by choosing $K = 1$, $\frac{1}{\lambda} = \sqrt{1 - 2\pi\varepsilon(\Delta\tau)^2\left\{1 - \pi\varepsilon(\Delta\tau)^2\right\}} > 1$, one sees that condition (3.8.3) is satisfied. □

We now arrive at the position to state the first main theorem in this chapter.

Theorem 3.8.1. *Suppose that the condition $\varepsilon < 0$, $\frac{2}{\pi(\Delta\tau)^2} < \varepsilon$ is satisfied. The map $\widetilde{T}_{\varepsilon,\Delta\tau}$ on M is an Anosov diffeomorphism.*

Proof. From Lemma 3.8.4 and Lemma 3.8.5, the map $\widetilde{T}_{\varepsilon,\Delta\tau}$ on M is an Anosov diffeomorphism. □

According to [31], if maps are Anosov diffeomorphisms, then the corresponding dynamical systems are K-systems. Therefore Corollary below holds.

Corollary 3.8.1. *Suppose that the condition $\varepsilon < 0$, $\frac{2}{\pi(\Delta\tau)^2} < \varepsilon$ is satisfied. Then the dynamical system $(M, \widetilde{T}_{\varepsilon,\Delta\tau}, \mu)$ is a K-system with μ being the Lebesgue measure. In addition, $(M, \widetilde{T}_{\varepsilon,\Delta\tau}, \mu)$ has a mixing property.*

3.9 Proof of Anosov properties for $\widehat{T}_{\varepsilon,\Delta\tau}$

In this section, we prove that the map $\widehat{T}_{\varepsilon,\Delta\tau}$ defined by (3.3.2) has the same ergodic properties as an Anosov diffeomorphism for $\varepsilon < 0$ or $\frac{2}{\pi(\Delta\tau)^2} < \varepsilon$. At the beginning, we show that the map $\widehat{T}_{\varepsilon,\Delta\tau}$ satisfies the conditions *(I)*, *(II)* and *(III)* in Definition 3.8.1 where M' is not conpact. A point $(p_1(n), q_1(n))$ on M' is denoted as $X_n = (p_1(n), q_1(n))$. The Jacobian of the map $\widehat{T}_{\varepsilon,\Delta\tau}$ is then given by

$$J(X_n) = \begin{pmatrix} 1 - \frac{\pi\varepsilon(\Delta\tau)^2}{\cos^2\theta_n} & -\frac{2\pi\varepsilon(\Delta\tau)}{\cos^2\theta_n} \\ \Delta\tau - \frac{\pi\varepsilon(\Delta\tau)^3}{2\cos^2\theta_n} & 1 - \frac{\pi\varepsilon(\Delta\tau)^2}{\cos^2\theta_n} \end{pmatrix}, \tag{3.9.1}$$

where $\theta_n \overset{\text{def}}{=} \pi\left\{2q_1(n) + \Delta\tau p_1(n) - q_0 - C\Delta\tau\left(n + \frac{1}{2}\right)\right\}$. The linear instability condition for the map $\widehat{T}_{\varepsilon,\Delta\tau}$ is the same as that in (3.6.10).

Let us introduce a vector on $T_{X_n}M'$ as follows.

Definition 3.9.1. *For any two dimensional non-zero vector on $T_{X_n}M'$, $X_n \in M', n \in \mathbb{Z}$*

$$\boldsymbol{a}'_n = (a'_1(n), a'_2(n)) \neq \boldsymbol{O}, \tag{3.9.2}$$

define cones l^+ and l^- to be

$$\begin{aligned} l^+(X_n) &= \{(a'_1(n), a'_2(n)); \|J(X_n)\boldsymbol{a}'_n\| > \|\boldsymbol{a}'_n\|\}, \\ l^-(X_n) &= \{(a'_1(n), a'_2(n)); \|J(\widehat{T}^{-1}_{\varepsilon,\Delta\tau}X_n)^{-1}\boldsymbol{a}'_n\| > \|\boldsymbol{a}'_n\|\}, \end{aligned}$$

where $\|\cdot\|$ represents $\|\boldsymbol{a}'_n\| \equiv \sqrt{a'^2_1(n) + a'^2_2(n)}$.

To prove that the map $\widehat{T}_{\varepsilon,\Delta\tau}$ satisfies the conditions *(I)*, *(II)* and *(III)* in Definition 3.8.1, we have to show the following Lemmas.

Lemma 3.9.1. *When the condition $\varepsilon < 0, \frac{2}{\pi(\Delta\tau)^2} < \varepsilon$ is satisfied, there is a subset $ll^+(X_n)$ of $l^+(X_n)$ such that*

$$J(X_n)\boldsymbol{a}'_n \in ll^+(\widehat{T}_{\varepsilon,\Delta\tau}X_n), \ {}^\forall\boldsymbol{a}'_n \in ll^+(X_n) \tag{3.9.3}$$

Proof. Let us consider a vector $\boldsymbol{a}'_n$ such that $a'_2(n) \neq 0$. The condition that $\boldsymbol{a}'_n \in l^+(X_n)$ is expressed by

$$\boldsymbol{a}'_n \in l^+(X_n) \Leftrightarrow A_n\left(\frac{a'_1(n)}{a'_2(n)}\right)^2 + B_n\left(\frac{a'_1(n)}{a'_2(n)}\right) + C_n > 0, \tag{3.9.4}$$

where A_n, B_n and C_n are defined as

$$\begin{aligned} A_n &\stackrel{\text{def}}{=} \left(1 - \frac{\pi\varepsilon(\Delta\tau)^2}{\cos^2\theta_n}\right)^2 + (\Delta\tau)^2\left(1 - \frac{\pi\varepsilon(\Delta\tau)^2}{2\cos^2\theta_n}\right)^2 - 1, \\ B_n &\stackrel{\text{def}}{=} \left(1 - \frac{\pi\varepsilon(\Delta\tau)^2}{\cos^2\theta_n}\right)\left\{-\frac{4\pi\varepsilon(\Delta\tau)}{\cos^2\theta_n} + 2\Delta\tau\left(1 - \frac{\pi\varepsilon(\Delta\tau)^2}{2\cos^2\theta_n}\right)\right\}, \\ C_n &\stackrel{\text{def}}{=} \left\{\frac{\{2\pi\varepsilon(\Delta\tau)\}^2}{\cos^4\theta_n} + \left(1 - \frac{\pi\varepsilon(\Delta\tau)^2}{\cos^2\theta_n}\right)^2 - 1\right\}. \end{aligned} \tag{3.9.5}$$

For any $n \in \mathbb{Z}$ and $X_n \in M'$, if (3.6.10) is satisfied, then it holds that

$$A_n > 0, B_n > 0, C_n \quad > \quad 0, \tag{3.9.6}$$

$$B_n^2 - 4A_nC_n = \frac{\left[\left\{(\Delta\tau)^2 + 4\right\}\frac{\pi\varepsilon(\Delta\tau)^2}{\cos^2\theta} - 2(\Delta\tau)^2\right]^2}{(\Delta\tau)^2} \quad \geq \quad 0. \tag{3.9.7}$$

In this case, the condition (3.9.4) is rewritten as

$$\boldsymbol{a}'_n \in l^+(X_n) \Leftrightarrow \frac{a'_1(n)}{a'_2(n)} < \frac{-B_n - \sqrt{B_n^2 - 4A_nC_n}}{2A_n} \text{ or } \frac{-B_n + \sqrt{B_n^2 - 4A_nC_n}}{2A_n} < \frac{a'_1(n)}{a'_2(n)} \tag{3.9.8}$$

where $\frac{-B_n - \sqrt{B_n^2 - 4A_nC_n}}{2A_n} < \frac{-B_n + \sqrt{B_n^2 - 4A_nC_n}}{2A_n} < 0$.
Choosing $\boldsymbol{a}'_{n+1}$ as $J(X_n)\boldsymbol{a}'_{n+1} = (a_1(n+1), a_2(n+1))$, one sees that the condition that $\boldsymbol{a}'_{n+1} \in l^+(\widehat{T}_{\varepsilon,\Delta\tau}X_n)$ is expressed as

$$\begin{aligned} &\boldsymbol{a}'_{n+1} \in l^+(\widehat{T}_{\varepsilon,\Delta\tau}X_n) = l^+(X_{n+1}) \\ \Leftrightarrow\ &\frac{a'_1(n+1)}{a'_2(n+1)} < \frac{-B_{n+1} - \sqrt{B_{n+1}^2 - 4A_{n+1}C_{n+1}}}{2A_{n+1}} \text{ or } \frac{-B_{n+1} + \sqrt{B_{n+1}^2 - 4A_{n+1}C_{n+1}}}{2A_{n+1}} < \frac{a'_1(n+1)}{a'_2(n+1)} \end{aligned} \tag{3.9.9}$$

where $\frac{-B_{n+1} - \sqrt{B_{n+1}^2 - 4A_{n+1}C_{n+1}}}{2A_{n+1}} < \frac{-B_{n+1} + \sqrt{B_{n+1}^2 - 4A_{n+1}C_{n+1}}}{2A_{n+1}} < 0$.

Choosing a subset $ll^+(X_n)$ of $l^+(X_n)$ as

$$ll^+(X_n) = \left\{(a'_1(n), a'_2(n));\ \frac{a'_1(n)}{a'_2(n)} > 0\right\}, \tag{3.9.10}$$

and assuming that $a'_2(n+1) = 0$ and $\boldsymbol{a}'_n \in ll^+(X_n)$, one has that

$$\begin{aligned} a'_2(n+1) &= \Delta\tau\left(1 - \frac{\pi\varepsilon(\Delta\tau)^2}{2\cos^2\theta_n}\right)a'_1(n) + \left(1 - \frac{\pi\varepsilon(\Delta\tau)^2}{\cos^2\theta_n}\right)a'_2(n) = 0, \\ \frac{a'_1(n)}{a'_2(n)} &= -\frac{\left(1 - \frac{\pi\varepsilon(\Delta\tau)^2}{\cos^2\theta_n}\right)}{\left(1 - \frac{\pi\varepsilon(\Delta\tau)^2}{2\cos^2\theta_n}\right)} < 0. \end{aligned}$$

This is contradictory to $\frac{a_1'(n)}{a_2'(n)} > 0$. Then if $\boldsymbol{a}_n' \in ll^+(X_n)$, then $a_2'(n+1) \neq 0$. Substituting

$$\begin{aligned} a_1'(n+1) &= \left(1 - \frac{\pi\varepsilon(\Delta\tau)^2}{\cos^2\theta_n}\right) a_1'(n) - \frac{2\pi\varepsilon(\Delta\tau)}{\cos^2\theta_n} a_2'(n), && (3.9.11)\\ a_2'(n+1) &= \Delta\tau\left(1 - \frac{\pi\varepsilon(\Delta\tau)^2}{2\cos^2\theta_n}\right) a_1'(n) + \left(1 - \frac{\pi\varepsilon(\Delta\tau)^2}{\cos^2\theta_n}\right) a_2'(n) && (3.9.12)\end{aligned}$$

into $\frac{a_1'(n+1)}{a_2'(n+1)}$, one obtains

$$\begin{aligned} \frac{a_1'(n+1)}{a_2'(n+1)} &= \frac{\left(1 - \frac{\pi\varepsilon(\Delta\tau)^2}{\cos^2\theta_n}\right) a_1'(n) - \frac{2\pi\varepsilon(\Delta\tau)}{\cos^2\theta_n} a_2'(n)}{\Delta\tau\left(1 - \frac{\pi\varepsilon(\Delta\tau)^2}{2\cos^2\theta_n}\right) a_1'(n) + \left(1 - \frac{\pi\varepsilon(\Delta\tau)^2}{\cos^2\theta_n}\right) a_2'(n)},\\ &= \frac{\left(1 - \frac{\pi\varepsilon(\Delta\tau)^2}{\cos^2\theta_n}\right)\frac{a_1'(n)}{a_2'(n)} - \frac{2\pi\varepsilon(\Delta\tau)}{\cos^2\theta_n}}{\Delta\tau\left(1 - \frac{\pi\varepsilon(\Delta\tau)^2}{2\cos^2\theta_n}\right)\frac{a_1'(n)}{a_2'(n)} + \left(1 - \frac{\pi\varepsilon(\Delta\tau)^2}{\cos^2\theta_n}\right)} && (3.9.13)\end{aligned}$$

Here, if the condition that $\frac{a_1'(n)}{a_2'(n)} > 0 \Leftrightarrow \boldsymbol{a}_n' \in ll^+(X_n) \subset l^+(X_n)$ holds, then it holds that for $\varepsilon < 0$, $\frac{2}{\pi(\Delta\tau)^2} < \varepsilon$

$$\frac{a_1'(n+1)}{a_2'(n+1)} = \frac{\left(1 - \frac{\pi\varepsilon(\Delta\tau)^2}{\cos^2\theta_n}\right)\frac{a_1'(n)}{a_2'(n)} - \frac{2\pi\varepsilon(\Delta\tau)}{\cos^2\theta_n}}{\Delta\tau\left(1 - \frac{\pi\varepsilon(\Delta\tau)^2}{2\cos^2\theta_n}\right)\frac{a_1'(n)}{a_2'(n)} + \left(1 - \frac{\pi\varepsilon(\Delta\tau)^2}{\cos^2\theta_n}\right)} > 0 \Rightarrow \boldsymbol{a}_{n+1}' \in ll^+(X_{n+1}) \subset l^+(X_{n+1}).$$

Then, if $\boldsymbol{a}_n' \in ll^+(X_n) \subset l^+(X_n)$, then $\boldsymbol{a}_{n+1}' \in ll^+(X_{n+1}) \subset l^+(X_{n+1})$. □

Lemma 3.9.2. *When the condition $\varepsilon < 0$, $\frac{2}{\pi(\Delta\tau)^2} < \varepsilon$ is satisfied, there is a subset $ll_1^-(X_n)$ of $l^-(X_n)$ such that*

$$J(X_{n-1})^{-1}\boldsymbol{a}_n' \in ll_1^-(\widehat{T}_{\varepsilon,\Delta\tau}^{-1}X_n), {}^\forall\boldsymbol{a}_n' \in ll_1^-(X_n). \quad (3.9.14)$$

Proof. Let us consider a vector $\boldsymbol{a}_n'$ such that $a_2'(n) \neq 0$. The condition $\boldsymbol{a}_n' \in l^-(X_n)$ in (3.9.14) is expressed as

$$\begin{aligned} \boldsymbol{a}_n' \in l^-(X_n) &\Leftrightarrow \|\boldsymbol{a}_{n-1}'\|^2 - \|\boldsymbol{a}_n'\|^2 > 0,\\ &\Leftrightarrow A_{n-1}\left(\frac{a_1'(n)}{a_2'(n)}\right)^2 - B_{n-1}\left(\frac{a_1'(n)}{a_2'(n)}\right) + C_{n-1} > 0,\\ &\Leftrightarrow \frac{a_1'(n)}{a_2'(n)} < \frac{B_{n-1} - \sqrt{B_{n-1}^2 - 4A_{n-1}C_{n-1}}}{2A_{n-1}} \text{ or } \frac{B_{n-1} + \sqrt{B_{n-1}^2 - 4A_{n-1}C_{n-1}}}{2A_{n-1}} < \frac{a_1'(n)}{a_2'(n)} && (3.9.15)\end{aligned}$$

where $0 < \dfrac{B_{n-1} - \sqrt{B_{n-1}^2 - 4A_{n-1}C_{n-1}}}{2A_{n-1}} < \dfrac{B_{n-1} + \sqrt{B_{n-1}^2 - 4A_{n-1}C_{n-1}}}{2A_{n-1}}$.

The condition $J(X_{n-1})^{-1}\boldsymbol{a}'_n \in l^-(\widehat{T}^{-1}_{\varepsilon,\Delta\tau}X_n)$ in (3.9.14) is expressed as

$$\begin{aligned}
\boldsymbol{a}'_{n-1} &\overset{\text{def}}{=} J(X_{n-1})^{-1}\boldsymbol{a}'_n \in l^-(\widehat{T}^{-1}_{\varepsilon,\Delta\tau}X_n),\\
&\Leftrightarrow \|\boldsymbol{a}'_{n-2}\|^2 - \|\boldsymbol{a}'_{n-1}\|^2 > 0,\\
&\Leftrightarrow \frac{a'_1(n-1)}{a'_2(n-1)} < \frac{B_{n-2} - \sqrt{B_{n-2}^2 - 4A_{n-2}C_{n-2}}}{2A_{n-2}} \text{ or } \frac{B_{n-2} + \sqrt{B_{n-2}^2 - 4A_{n-2}C_{n-2}}}{2A_{n-2}} < \frac{a'_1(n-1)}{a'_2(n-1)},
\end{aligned} \tag{3.9.16}$$

where $0 < \frac{B_{n-2} - \sqrt{B_{n-2}^2 - 4A_{n-2}C_{n-2}}}{2A_{n-2}} < \frac{B_{n-2} + \sqrt{B_{n-2}^2 - 4A_{n-2}C_{n-2}}}{2A_{n-2}}$.

Choose a subset $ll_1^-(X_n)$ of $l^-(X_n)$ as

$$ll_1^-(X_n) = \left\{(a'_1(n), a'_2(n));\ \frac{a'_1(n)}{a'_2(n)} < 0\right\}. \tag{3.9.17}$$

It is obvious that for $\boldsymbol{a}'_n \in ll_1^-(X_n)$, it holds that $a'_2(n-1) \neq 0$ as follows. If $\boldsymbol{a}'_n \in ll_1^-(X_n)$, then substituting

$$a'_1(n-1) = \left(1 - \frac{\pi\varepsilon(\Delta\tau)^2}{\cos^2\theta_{n-1}}\right)a'_1(n) + \frac{2\pi\varepsilon(\Delta\tau)}{\cos^2\theta_{n-1}}a'_2(n), \tag{3.9.18}$$

$$a'_2(n-1) = -\Delta\tau\left(1 - \frac{\pi\varepsilon(\Delta\tau)^2}{2\cos^2\theta_{n-1}}\right)a'_1(n) + \left(1 - \frac{\pi\varepsilon(\Delta\tau)^2}{\cos^2\theta_{n-1}}\right)a'_2(n), \tag{3.9.19}$$

into $a'_1(n-1)$ and $a'_2(n-1)$, one obtains

$$\frac{a'_1(n-1)}{a'_2(n-1)} = \frac{\left(1 - \frac{\pi\varepsilon(\Delta\tau)^2}{\cos^2\theta_{n-1}}\right)\frac{a'_1(n)}{a'_2(n)} + \frac{2\pi\varepsilon(\Delta\tau)}{\cos^2\theta_{n-1}}}{-\Delta\tau\left(1 - \frac{\pi\varepsilon(\Delta\tau)^2}{2\cos^2\theta_{n-1}}\right)\frac{a'_1(n)}{a'_2(n)} + \left(1 - \frac{\pi\varepsilon(\Delta\tau)^2}{\cos^2\theta_{n-1}}\right)} < 0 \Rightarrow a'_2(n-1) \neq 0. \tag{3.9.20}$$

Therefore, it holds that $\boldsymbol{a}'_n \in ll_1^-(X_n) \subset l^-(X_n) \Rightarrow J(X_{n-1})^{-1}\boldsymbol{a}'_n = \boldsymbol{a}'_{n-1} \in ll_1^-(X_{n-1}) \subset l^-(X_{n-1})$. □

Lemma 3.9.3. *For any point X_n and for any integer $k \in \mathbb{Z} \geq n$, there exists a deviation vector $\boldsymbol{a}'_n$ such that*

$$\prod_{i=k}^{n} J(X_i)\boldsymbol{a}'_n \in ll_1^-(X_{k+1}),\ \boldsymbol{a}'_n \in ll_1^-(X_n). \tag{3.9.21}$$

Proof. We prove it by contradiction. We assume that

$$^{\exists}Y_n, {}^{\exists}k' \in \mathbb{Z} \geq n, {}^{\forall}\boldsymbol{a}'_n \in ll_1^-(Y_n) \text{ s.t. } \prod_{i=k'}^{n} J(Y_i)\boldsymbol{a}'_n \notin ll_1^-(Y_{k'+1}). \tag{3.9.22}$$

One can obtain an orbit $\{Y_m\}$ including Y_n and $Y_{n'}$ where $n' > k' + 1 > n$. For all points, there exists the cone ll_1^-, so that there exists a vector $\boldsymbol{A}'_{n'} \in ll_1^-(Y_{n'})$. Then one chooses $\boldsymbol{A}'_{k'+1}$ and $\boldsymbol{A}'_n$ as

$$\begin{aligned}
\boldsymbol{A}'_{k'+1} &\overset{\text{def}}{=} \prod_{i=k'+1}^{n'-1} J^{-1}(Y_i)\boldsymbol{A}'_{n'} \in ll_1^-(Y_{k'+1}) \quad \because (3.9.14),\\
\boldsymbol{A}'_n &\overset{\text{def}}{=} \prod_{i=n}^{n'-1} J^{-1}(Y_i)\boldsymbol{A}'_{n'} \in ll_1^-(Y_n).
\end{aligned}$$

Thus,

$$\prod_{i=k'}^{n} J(Y_i)\boldsymbol{A}'_n \in ll_1^-(Y_{k'+1}). \tag{3.9.23}$$

Equation (3.9.23) is contradictory to the (3.9.22). Therefore, Lemma 3.9.3 holds. □

From Lemmas 3.9.1, 3.9.2 and 3.9.3, define $ll^-(X_n)$ and $ll^+(X_n)$ as follows in order to prove that the conditions *(I)*, *(II)* and *(III)* are satisfied.

Definition 3.9.2. *Define a subset $ll^-(X_n)$ of $ll_1^-(X_n)$ to be*

$$ll^-(X_n) \overset{\text{def}}{=} \left\{(a'_1(n), a'_2(n)); \boldsymbol{a}'_n \in ll_1^-(X_n), \prod_{i=k}^{n} J(X_i)\boldsymbol{a}'_n \in ll_1^-(X_{k+1}), {}^{\forall}k \geq n\right\}. \tag{3.9.24}$$

From Lemma 3.9.3 one can see that

$$J(X_n)\boldsymbol{a}'_n \in ll^-(X_{n+1}), \ {}^{\forall}\boldsymbol{a}_n \in ll^-(X_n). \tag{3.9.25}$$

Definition 3.9.3. *Define a subset $ll^+(X_n)$ of $l^+(X_n)$ to be*

$$ll^+(X_n) \overset{\text{def}}{=} \left\{(a'_1(n), a'_2(n)); \frac{a'_1(n)}{a'_2(n)} > 0\right\}. \tag{3.9.26}$$

From a simple calculation, one sees that

$$J(X_n)\boldsymbol{a}'_n \in ll^+(X_{n+1}), \ {}^{\forall}\boldsymbol{a}'_n \in ll^+(X_n). \tag{3.9.27}$$

Lemma 3.9.4. *When the condition $\varepsilon < 0$, $\frac{2}{\pi(\Delta\tau)^2} < \varepsilon$ is satisfied, the conditions (I) and (II) are satisfied.*

Proof. One can choose any eigenvector spaces E^u_X and E^s_X in $ll^+(X_n)$ and $ll^-(X_n)$, respectively so that combining (3.9.24) and (3.9.26):

$$E^u_{X_n} \subset ll^+(X_n),\ \ E^s_{X_n} \subset ll^-(X_n). \tag{3.9.28}$$

Combining (3.9.25), (3.9.27) and (3.9.28), one has that $J(X_n)E^u_{X_n} \subset ll^+(X_{n+1})$ and $J(X_n)E^s_{X_n} \subset ll^-(X_{n+1})$. Then, one can choose $E^u_{X_{n+1}}$, $E^s_{X_{n+1}}$ inductively by

$$E^u_{X_{n+1}} \overset{\text{def}}{=} J(X_n)E^u_{X_n},\ \ E^s_{X_{n+1}} \overset{\text{def}}{=} J(X_n)E^s_{X_n}. \tag{3.9.29}$$

The subspaces $E^u_{X_n}$ and $E^s_{X_n}$ are linearly independent by definition, from which it holds that

$$T_{X_n}M = E^u_{X_n} \oplus E^s_{X_n}.$$

□

Lemma 3.9.5. *When the condition $\varepsilon < 0, \frac{2}{\pi(\Delta\tau)^2} < \varepsilon$ is satisfied, the condition (III) is satisfied.*

Proof. Let us define the stretching rate $\sigma(X_n, \boldsymbol{a}'_n) \overset{\text{def}}{=} \frac{\|J(X_n)\boldsymbol{a}'_n\|^2}{\|\boldsymbol{a}'_n\|^2}$ which can be rewritten as

$$\begin{aligned}
\sigma(X_n, \boldsymbol{a}'_n) &= \frac{(A_n+1)a_1'^2 + B_n a_1' a_2' + (C_n+1)a_2'^2}{a_1'^2 + a_2'^2} \\
&= 1 + A_n \frac{a_1'^2}{a_1'^2 + a_2'^2} + B_n \frac{a_1' a_2'}{a_1'^2 + a_2'^2} + C_n \frac{a_2'^2}{a_1'^2 + a_2'^2} \\
&= 1 + A_n \cos^2 \widetilde{\phi}_n + B_n \sin \widetilde{\phi}_n \cos \widetilde{\phi}_n + C_n \sin^2 \widetilde{\phi}_n
\end{aligned}$$

where $\widetilde{\phi}_n$ is defined such that $\cos^2 \widetilde{\phi}_n = \frac{a_1'^2(n)}{a_1'^2(n)+a_2'^2(n)}$, $\sin^2 \widetilde{\phi}_n = \frac{a_2'^2(n)}{a_1'^2(n)+a_2'^2(n)}$ and $\sin \widetilde{\phi}_n \cos \widetilde{\phi}_n = \frac{a_1'(n)a_2'(n)}{a_1'^2(n)+a_2'^2(n)}$, $-\pi < \widetilde{\phi} \le \pi$. Then, if $\boldsymbol{a}'_n \in ll^+(X_n)$, then

$$F(\widetilde{\phi}_n) \overset{\text{def}}{=} A_n \cos^2 \widetilde{\phi}_n + B_n \sin \widetilde{\phi}_n \cos \widetilde{\phi}_n + C_n \sin^2 \widetilde{\phi}_n > 0,\ \varepsilon < 0, \frac{2}{\pi(\Delta\tau)^2} < \varepsilon \tag{3.9.30}$$

and since $\frac{a_1'(n)}{a_2'(n)} > 0$, the variable $\widetilde{\phi}$ is defined on $(-\pi, -\frac{\pi}{2}) \cup (0, \frac{\pi}{2})$. There are two cases for X_n. The minimum value of σ for each case is calculated as follows.

The derivative of $F(\widetilde{\phi})$ is rewritten in

$$\begin{aligned}
F'(\widetilde{\phi}_n) &= (C_n - A_n)\sin 2\widetilde{\phi}_n + B_n \cos 2\widetilde{\phi}_n \\
&= \left[(C_n - A_n)^2 + B_n^2\right]\left[\frac{C_n - A_n}{(C_n - A_n)^2 + B_n^2}\sin 2\widetilde{\phi}_n + \frac{B_n}{(C_n - A_n)^2 + B_n^2}\cos 2\widetilde{\phi}_n\right] \\
&= \left[(C_n - A_n)^2 + B_n^2\right]\left[P_n \sin 2\widetilde{\phi}_n + Q_n \cos 2\widetilde{\phi}_n\right] \\
&= \left[(C_n - A_n)^2 + B_n^2\right]\left[\sin\left(2\widetilde{\phi}_n + \widetilde{\psi}_n\right)\right]
\end{aligned}$$

where P_n, Q_n and $\widetilde{\psi}$ are defined by

$$P_n \stackrel{\text{def}}{=} \frac{C_n - A_n}{(C_n - A_n)^2 + B_n^2}, \tag{3.9.31}$$

$$Q_n \stackrel{\text{def}}{=} \frac{B_n}{(C_n - A_n)^2 + B_n^2}, \tag{3.9.32}$$

$$\tan\widetilde{\psi}_n = \frac{Q_n}{P_n}, \widetilde{\psi}_n \in \left(-\frac{\pi}{2}, \frac{\pi}{2}\right). \tag{3.9.33}$$

(i) Case of $P_n \geq 0 \Leftrightarrow C_n \geq A_n$,
It holds that

$$\tan\widetilde{\psi}_n = \frac{Q_n}{P_n} > 0 \Rightarrow 0 < \widetilde{\psi}_n < \frac{\pi}{2}. \tag{3.9.34}$$

The variable $\widetilde{\psi}_n$ depends on X_n not on $\boldsymbol{a}'_n$. In this case, $F(\widetilde{\phi}_n)$ increases monotonously for $-\pi < \widetilde{\phi}_n < -\frac{\pi+\widetilde{\psi}_n}{2}$ and for $0 < \widetilde{\phi}_n < \frac{\pi-\widetilde{\psi}_n}{2}$ and decreases monotonously for $-\frac{\pi+\widetilde{\psi}_n}{2} < \widetilde{\phi}_n < -\frac{\pi}{2}$ and for $\frac{\pi-\widetilde{\psi}_n}{2} < \widetilde{\phi}_n < \frac{\pi}{2}$. Then the candidates for the minimal value of $F(\widetilde{\phi}_n)$ for $-\pi < \widetilde{\phi}_n < -\frac{\pi}{2}$ and $0 < \widetilde{\phi}_n < \frac{\pi}{2}$ are

$$F(-\pi) = F(0) = A_n, \tag{3.9.35}$$

$$F\left(-\frac{\pi}{2}\right) = F\left(\frac{\pi}{2}\right) = C_n. \tag{3.9.36}$$

In this case, $C_n \geq A_n > 0$. Then, the minimal value of $\sigma(X_n, \boldsymbol{a}'_n)$ by varying the vector $\boldsymbol{a}'_n$ is obtained as $1 + A_n$. With this minimal value and $A_n > 0$, one has

$$\begin{aligned}
\sigma(X_n, \boldsymbol{a}'_n) &\geq 1 + A_n \\
&\geq \left\{1 - \pi\varepsilon(\Delta\tau)^2\right\}^2 + (\Delta\tau)^2\left\{1 - \tfrac{\pi\varepsilon(\Delta\tau)^2}{2}\right\}^2 > 1.
\end{aligned} \tag{3.9.37}$$

(ii) Case of $P_n < 0 \Leftrightarrow C_n < A_n$,
It holds that

$$\tan\widetilde{\psi}_n = \frac{Q_n}{P_n} < 0 \Rightarrow -\frac{\pi}{2} < \widetilde{\psi}_n < 0. \tag{3.9.38}$$

In this case, $F(\widetilde{\phi}_n)$ decreases monotonously for $-\pi < \widetilde{\phi}_n < -\pi - \frac{\widetilde{\psi}_n}{2}$ and $0 < \widetilde{\phi}_n < -\frac{\widetilde{\psi}_n}{2}$ and increases monotonously for $-\pi - \frac{\widetilde{\psi}_n}{2} < \widetilde{\phi} < -\frac{\pi}{2}$ and $-\frac{\widetilde{\psi}_n}{2} < \widetilde{\phi}_n < \frac{\pi}{2}$. Then the candidates for the minimal value of $F(\widetilde{\phi}_n)$ for $-\pi < \widetilde{\phi}_n < -\frac{\pi}{2}$ and $0 < \widetilde{\phi}_n < \frac{\pi}{2}$ are

$$F\left(-\pi - \frac{\widetilde{\psi}_n}{2}\right) = F\left(-\frac{\widetilde{\psi}_n}{2}\right) = A_n \cos^2 \frac{\widetilde{\psi}_n}{2} - B_n \sin \frac{\widetilde{\psi}_n}{2} \cos \frac{\widetilde{\psi}_n}{2} + C_n \sin^2 \frac{\widetilde{\psi}_n}{2}.$$

From $A_n > C_n > 0$, it holds that

$$F\left(-\pi - \frac{\widetilde{\psi}_n}{2}\right) > C_n - B_n \sin \frac{\widetilde{\psi}_n}{2} \cos \frac{\widetilde{\psi}_n}{2} > C_n, \quad \because \sin \widetilde{\psi}_n < 0, B_n > 0. \qquad (3.9.39)$$

Then, the minimal value of $\sigma(X_n, \boldsymbol{a}'_n)$ by varying the vector $\boldsymbol{a}'_n$ is obtained as $1 + C_n$. With this minimal value and $C_n > 0$, one has

$$\begin{aligned} \sigma(X_n, \boldsymbol{a}'_n) &\geq 1 + C_n \\ &\geq \{2\pi\varepsilon(\Delta\tau)\}^2 + \left\{1 - \pi\varepsilon(\Delta\tau)^2\right\}^2 > 1. \end{aligned} \qquad (3.9.40)$$

Thus from (3.9.37) and (3.9.40), by choosing

$$\begin{aligned} K &= 1, \\ \frac{1}{\lambda} &= \min \left\{ \begin{array}{l} \sqrt{\left\{1 - \pi\varepsilon(\Delta\tau)^2\right\}^2 + (\Delta\tau)^2 \left\{1 - \frac{\pi\varepsilon(\Delta\tau)^2}{2}\right\}^2}, \\ \sqrt{\{2\pi\varepsilon(\Delta\tau)\}^2 + \left\{1 - \pi\varepsilon(\Delta\tau)^2\right\}^2} \end{array} \right\}, \end{aligned} \qquad (3.9.41)$$

one sees that condition (3.8.2) is satisfied. Besides, this relation about λ ($\lambda \to 1 - 0$ as $\varepsilon \to -0$) is equivalent to the fact that the Lyapunov exponent converges to zero value as $\varepsilon \to -0$.

Let us define the stretching rate $\sigma'(X_n, \boldsymbol{a}'_n) \stackrel{\text{def}}{=} \frac{\|J^{-1}(\widehat{T}^{-1}_{\varepsilon,\Delta\tau} X_n)\boldsymbol{a}'_n\|^2}{\|\boldsymbol{a}'_n\|^2} = \frac{\|J^{-1}(X_{n-1})\boldsymbol{a}'_n\|^2}{\|\boldsymbol{a}'_n\|^2}$ which can be rewritten as

$$\begin{aligned} \sigma'(X_n, \boldsymbol{a}'_n) &= \frac{(A_{n-1} + 1)a'^2_1 - B_{n-1}a'_1 a'_2 + (C_{n-1} + 1)a'^2_2}{a'^2_1 + a'^2_2} \\ &= 1 + A_{n-1}\frac{a'^2_1}{a'^2_1 + a'^2_2} - B_{n-1}\frac{a'_1 a'_2}{a'^2_1 + a'^2_2} + C_{n-1}\frac{a'^2_2}{a'^2_1 + a'^2_2} \\ &= 1 + A_{n-1} \cos^2 \widetilde{\phi}_n - B_{n-1} \sin \widetilde{\phi}_n \cos \widetilde{\phi}_n + C_{n-1} \sin^2 \widetilde{\phi}_n \end{aligned}$$

where $\widetilde{\phi}_n$ is defined such that $\cos^2\widetilde{\phi}_n = \frac{a_1'^2(n)}{a_1'^2(n)+a_2'^2(n)}$, $\sin^2\widetilde{\phi}_n = \frac{a_2'^2(n)}{a_1'^2(n)+a_2'^2(n)}$ and $\sin\widetilde{\phi}_n\cos\widetilde{\phi}_n = \frac{a_1'(n)a_2'(n)}{a_1'^2(n)+a_2'^2(n)}$, $-\pi < \widetilde{\phi} \le \pi$. Then, if $\boldsymbol{a}_n' \in ll^-(X_n)$, then

$$G(\widetilde{\phi}_n) \stackrel{\text{def}}{=} A_{n-1}\cos^2\widetilde{\phi}_n - B_{n-1}\sin\widetilde{\phi}_n\cos\widetilde{\phi}_n + C_{n-1}\sin^2\widetilde{\phi}_n > 0,\ \varepsilon < 0, \frac{2}{\pi(\Delta\tau)^2} < \varepsilon \tag{3.9.42}$$

and since $\frac{a_1'(n)}{a_2'(n)} < 0$, the variable $\widetilde{\phi}$ is defined on $(-\frac{\pi}{2}, 0) \cup (\frac{\pi}{2}, \pi)$. There are two cases for X_n. The minimum value of σ' for each case is calculated as follows.
The derivative of $G(\widetilde{\phi})$ is rewritten in

$$\begin{aligned} G'(\widetilde{\phi}_n) &= (C_{n-1} - A_{n-1})\sin 2\widetilde{\phi}_n - B_{n-1}\cos 2\widetilde{\phi}_n \\ &= \left[(C_{n-1} - A_{n-1})^2 + B_{n-1}^2\right]\left[P_{n-1}\sin 2\widetilde{\phi}_n - Q_{n-1}\cos 2\widetilde{\phi}_n\right] \\ &= \left[(C_{n-1} - A_{n-1})^2 + B_{n-1}^2\right]\left[\sin\left(2\widetilde{\phi}_n - \widetilde{\psi}_{n-1}\right)\right] \end{aligned}$$

where P_{n-1}, Q_{n-1} and $\widetilde{\psi}$ are defined by

$$P_{n-1} \stackrel{\text{def}}{=} \frac{C_{n-1} - A_{n-1}}{(C_{n-1} - A_{n-1})^2 + B_{n-1}^2}, \tag{3.9.43}$$

$$Q_{n-1} \stackrel{\text{def}}{=} \frac{B_{n-1}}{(C_{n-1} - A_{n-1})^2 + B_{n-1}^2}, \tag{3.9.44}$$

$$\tan\widetilde{\psi}_{n-1} = \frac{Q_{n-1}}{P_{n-1}}, \widetilde{\psi}_{n-1} \in \left(-\frac{\pi}{2}, \frac{\pi}{2}\right). \tag{3.9.45}$$

(i) Case of $P_{n-1} \ge 0 \Leftrightarrow C_{n-1} \ge A_{n-1}$,
It holds that

$$\tan\widetilde{\psi}_{n-1} = \frac{Q_{n-1}}{P_{n-1}} > 0 \Rightarrow 0 < \widetilde{\psi}_{n-1} < \frac{\pi}{2}. \tag{3.9.46}$$

The variable $\widetilde{\psi}_{n-1}$ depends on $\widehat{T}_{\varepsilon,\Delta\tau}^{-1}X_n = X_{n-1}$ not on $\boldsymbol{a}_n'$. In this case, $G(\widetilde{\phi}_n)$ increases monotonously for $-\frac{\pi}{2} < \widetilde{\phi}_n < -\frac{\pi}{2} + \frac{\widetilde{\psi}_{n-1}}{2}$ and for $\frac{\pi}{2} < \widetilde{\phi}_n < \frac{\pi}{2} + \frac{\widetilde{\psi}_{n-1}}{2}$ and decreases monotonously for $-\frac{\pi}{2} + \frac{\widetilde{\psi}_{n-1}}{2} < \widetilde{\phi}_n < 0$ and for $\frac{\pi}{2} + \frac{\widetilde{\psi}_{n-1}}{2} < \widetilde{\phi}_n < \pi$. Then the candidates for the minimal value of $G(\widetilde{\phi}_n)$ for $-\frac{\pi}{2} < \widetilde{\phi}_n < 0$ and $\frac{\pi}{2} < \widetilde{\phi}_n < \pi$ are

$$G(0) = G(\pi) = A_n, \tag{3.9.47}$$

$$G\left(-\frac{\pi}{2}\right) = G\left(\frac{\pi}{2}\right) = C_n. \tag{3.9.48}$$

In this case, $C_n \geq A_n > 0$. Then, the minimal value of $\sigma'(X_n, \boldsymbol{a}'_n)$ by varying the vector $\boldsymbol{a}'_n$ is obtained as $1 + A_n$. With this minimal value and $A_n > 0$, one has

$$\begin{aligned} \sigma'(X_n, \boldsymbol{a}'_n) &\geq 1 + A_n \\ &\geq \left\{1 - \pi\varepsilon(\Delta\tau)^2\right\}^2 + (\Delta\tau)^2 \left\{1 - \frac{\pi\varepsilon(\Delta\tau)^2}{2}\right\}^2 > 1. \end{aligned} \tag{3.9.49}$$

(ii) Case of $P_{n-1} < 0 \Leftrightarrow C_{n-1} < A_{n-1}$,
It holds that

$$\tan \widetilde{\psi}_{n-1} = \frac{Q_{n-1}}{P_{n-1}} < 0 \Rightarrow -\frac{\pi}{2} < \widetilde{\psi}_{n-1} < 0. \tag{3.9.50}$$

In this case, $G(\widetilde{\phi}_n)$ increases monotonously for $\frac{\widetilde{\psi}_{n-1}}{2} < \widetilde{\phi}_n < 0$ and $\pi + \frac{\widetilde{\psi}_{n-1}}{2} < \widetilde{\phi}_n < \pi$ and decreases monotonously for $-\frac{\pi}{2} < \widetilde{\phi}_n < \frac{\widetilde{\psi}_{n-1}}{2}$ and $\frac{\pi}{2} < \widetilde{\phi}_n < \pi + \frac{\widetilde{\psi}_{n-1}}{2}$. Then the candidates for the minimal value of $G(\widetilde{\phi}_n)$ for $-\frac{\pi}{2} < \widetilde{\phi}_n < 0$ and $\frac{\pi}{2} < \widetilde{\phi}_n < \pi$ are

$$G\left(\pi + \frac{\widetilde{\psi}_{n-1}}{2}\right) = F\left(\frac{\widetilde{\psi}_{n-1}}{2}\right) = A_{n-1}\cos^2\frac{\widetilde{\psi}_{n-1}}{2} - B_{n-1}\sin\frac{\widetilde{\psi}_{n-1}}{2}\cos\frac{\widetilde{\psi}_{n-1}}{2} + C_{n-1}\sin^2\frac{\widetilde{\psi}_{n-1}}{2}.$$

From $A_{n-1} > C_{n-1} > 0$, it holds that

$$G\left(\pi + \frac{\widetilde{\psi}_{n-1}}{2}\right) > C_{n-1} - B_{n-1}\sin\frac{\widetilde{\psi}_{n-1}}{2}\cos\frac{\widetilde{\psi}_{n-1}}{2} > C_{n-1}, \quad \because \sin\widetilde{\psi}_{n-1} < 0, B_{n-1} > 0. \tag{3.9.51}$$

Then, the minimal value of $\sigma'(X_n, \boldsymbol{a}'_n)$ by varying the vector $\boldsymbol{a}'_n$ is obtained as $1 + C_{n-1}$. With this minimal value and $C_{n-1} > 0$, one has

$$\begin{aligned} \sigma'(X_n, \boldsymbol{a}'_n) &\geq 1 + C_{n-1} \\ &\geq \{2\pi\varepsilon(\Delta\tau)\}^2 + \left\{1 - \pi\varepsilon(\Delta\tau)^2\right\}^2 > 1 \end{aligned} \tag{3.9.52}$$

Thus from (3.9.49) and (3.9.52), by choosing

$$\begin{aligned} K &= 1, \\ \frac{1}{\lambda} &= \min\left\{ \begin{array}{l} \sqrt{\left\{1 - \pi\varepsilon(\Delta\tau)^2\right\}^2 + (\Delta\tau)^2\left\{1 - \frac{\pi\varepsilon(\Delta\tau)^2}{2}\right\}^2}, \\ \sqrt{\{2\pi\varepsilon(\Delta\tau)\}^2 + \left\{1 - \pi\varepsilon(\Delta\tau)^2\right\}^2} \end{array} \right\}, \end{aligned} \tag{3.9.53}$$

one sees that condition (3.8.3) is satisfied. □

We now arrive at the position to state the second main theorem in this chapter.

Theorem 3.9.1. *Suppose that the condition $\varepsilon < 0, \frac{2}{\pi(\Delta\tau)^2} < \varepsilon$ is satisfied. The map $\widehat{T}_{\varepsilon,\Delta\tau}$ on M' has the same ergodic properties as an Anosov diffeomorphism.*

Proof. From Lemma 3.9.4 and Lemma 3.9.5, the map $\widehat{T}_{\varepsilon,\Delta\tau}$ satisfies the conditions *(I)*, *(II)* and *(III)* in Definition 3.8.1 where M' is not conpact. It is obvious that the map $\widehat{T}_{\varepsilon,\Delta\tau}$ is a diffeomorphism on M'. The domain of $\widehat{T}_{\varepsilon,\Delta\tau}$ is not compact. However, the map $\widetilde{T}_{\varepsilon,\Delta\tau}$ is topologically semi-conjugate with $\widehat{T}_{\varepsilon,\Delta\tau}$ through the transformation H. That is for any orbit $\{(p_1(n), q_1(n))\}$, there exists at least one corresponding orbit $\{(s_n, t_n)\}$. Therefore, the dynamical system $(M', \widehat{T}_{\varepsilon,\Delta\tau}, \mu)$ has the same ergodic properties as $(M, \widetilde{T}_{\varepsilon,\Delta\tau}, \mu)$. □

Similar to the case of $\widetilde{T}_{\varepsilon,\Delta\tau}$, Corollary below holds.

Corollary 3.9.1. *Suppose that the condition $\varepsilon < 0$, $\frac{2}{\pi(\Delta\tau)^2} < \varepsilon$ is satisfied. Then the dynamical system $(M', \widehat{T}_{\varepsilon,\Delta\tau}, \mu)$ is a K-system with the Lebesgue measure μ. In addition, $(M', \widehat{T}_{\varepsilon,\Delta\tau}, \mu)$ has a mixing property.*

A possible physical interpretation is as follows. The Lebesgue measure on $\mathbb{R}$ is an infinite measure and not a probability measure.

3.10 Convergence of initial density functions for Anosov diffeomorphisms

The following theorems give the proof of convergence of initial density functions to the uniform distribution and positivity of entropy rate for certain parameter ranges.

Theorem 3.7.1. *Suppose that the condition $\varepsilon < 0, \frac{2}{\pi(\Delta\tau)^2} < \varepsilon$ is satisfied. The map $\widetilde{T}_{\varepsilon,\Delta\tau}$ on M is an Anosov diffeomorphism.*

Theorem 3.8.1. *Suppose that the condition $\varepsilon < 0, \frac{2}{\pi(\Delta\tau)^2} < \varepsilon$ is satisfied. The map $\widehat{T}_{\varepsilon,\Delta\tau}$ on M' has the same ergodic properties as an Anosov diffeomorphism.*

Although Gallavotti assumed *chaotic hypothesis* [6, 91] in many-particle systems, we have *proven* directly for the systems with few degree of freedom that one of them is an Anosov system and that the other has the same ergodic properties as an Anosov system when the condition (3.6.10) is satisfied. According to Arnold and Avez [31], all Anosov diffeomorphisms are K-systems. Thus they have the mixing property. Therefore the dynamical systems defined as the triplet $(M, \widetilde{T}_{\varepsilon,\Delta\tau}, \mu)$ and $(M', \widehat{T}_{\varepsilon,\Delta\tau}, \mu)$ have the mixing property where μ corresponds to the Lebesgue measure. In general, the mixing property yields a relaxation process. Then we adapt this general scenario to our case.

According to Gallavotti [6, 91], an map $\widetilde{T}_{\varepsilon,\Delta\tau}$ or $\widehat{T}_{\varepsilon,\Delta\tau}$ has a unique probability distribution (SRB distribution) on phase space M or M', respectively. The Lebesgue measure μ is an invariant measure for $\widetilde{T}_{\varepsilon,\Delta\tau}$ on M and for $\widehat{T}_{\varepsilon,\Delta\tau}$ on M'. In addition, it is obvious that for every measurable partition ζ subordinate to unstable manifold, the conditional measures of the Lebesgue measure $\{\mu_x^{\zeta}\}$ is absolutely continuous with respect to the Lebesgue measure [23, 37]. Then the uniform distribution derived from the Lebesgue measure is the SRB distribution.

A convergence to the uniform distribution is proven for $(M, \widetilde{T}_{\varepsilon,\Delta\tau}, \mu)$ and $(M', \widehat{T}_{\varepsilon,\Delta\tau}, \mu)$ as described above for any initial density function defined except for a zero volume set [6] when the condition (3.6.10) is satisfied. In particular, the map $\widehat{T}_{\varepsilon,\Delta\tau}$ has time-reversal symmetry. Thus, for the map $\widehat{T}_{\varepsilon,\Delta\tau}$ which satisfies the condition of time reversibility and measure preserving, a convergence to the uniform distribution is proven.

In addition to this, correlation functions decay exponentially [6, 91, 94, 105, 106]. In other words in the regime, relaxation occurs, such that

$$\rho(s,t) \simeq \eta(s)\eta(t), \tag{3.9.1}$$

where ρ represents a density function on M and η represents the one dimensional uniform distribution defined on $I_{\delta_{N,\Delta\tau}}$.

For any orbit $\{(p_1(n), q_1(n))\}_{n\in\mathbb{Z}}$ of $\widehat{T}_{\varepsilon,\Delta\tau}$, there exists at least one corresponding orbit $\{(s_n, t_n)\}_{n\in\mathbb{Z}}$ of $\widetilde{T}_{\varepsilon,\Delta\tau}$ since the map $\widetilde{T}_{\varepsilon,\Delta\tau}$ is topologically semi-conjugate with $\widehat{T}_{\varepsilon,\Delta\tau}$. Then, for the corresponding orbit $\{(p_1(n), q_1(n))\}_{n\in\mathbb{Z}}$, time series $\{\varepsilon\Delta\tau\tan(\pi s_n)\}_{n\in\mathbb{Z}}$ obey the Cauchy distribution when $\{(s_n, t_n)\}_{n\in\mathbb{Z}}$ obey the uniform distribution as $N \to \infty$ and have mixing property. According to Ibragimov [107], if the stationary random process $\{x_k\}$ satisfies the strong mixing condition, then the sequence of distribution functions

$$F_n(z) = \mathbb{P}\left\{\frac{x_1 + x_2 + \cdots + x_n}{B_n} - A_n < z\right\} \tag{3.9.2}$$

where A_n and B_n are normalizing constants, can only converge to a stable law. Then in the dynamical system $(M', \widehat{T}_{\varepsilon,\Delta\tau}, \mu)$, any initial density function with p_1 defined except for a zero volume set converges to a stable law. In addition from Theorem 3.9.1, any initial density function relaxes to the uniform distribution defined on $\left(\mathbb{R} \times I_{\delta_{N,\Delta\tau}}\right) \setminus \Gamma'$.

3.10 Lyapunov exponent

Let us discuss the Lyapunov exponent of $\widetilde{T}_{\varepsilon,\Delta\tau}$. In the following, we consider the case in which N is large enough so that one can identify $I_{\delta_{N,\Delta\tau}}$ as $\left(-\frac{1}{2}, \frac{1}{2}\right]$ and the case in which the condition (3.6.10) is satisfied. Since the Lebesgue measure is the SRB measure one can obtain from the Pesin's identity [108] the Kolmogorov-Sinai (KS) entropy $h_{KS}(\widetilde{T}_{\varepsilon,\Delta\tau})$ (entropy per unit time) [109] for almost all initial points as

$$h_{KS}(\widetilde{T}_{\varepsilon,\Delta\tau}) = \iint_M \log\left|\det\left(D\widetilde{T}_{\varepsilon,\Delta\tau}|_{E^u}\right)\right| \mu(dx), \tag{3.10.1}$$

where $h_{KS}(\widetilde{T}_{\varepsilon,\Delta\tau})$ is positive since $\widetilde{T}_{\varepsilon,\Delta\tau}$ is an Anosov diffeomorphism.

According to Kac [93] and Chrikov [110], it cannot be said that the relaxation always occurs monotonically even though the system has mixing property. However, it is cosidered that the time average of entropy production rate is equivalent to the KS entropy and there are cases in which by assuming appropriate conditions, the KS entropy is consistent with the time derivative of the entropy [29, 95, 96].

In calculating $h_{KS}(\widetilde{T}_{\varepsilon,\Delta\tau})$, one needs the eigenvalue corresponding to the unstable direction expressed by $\gamma(t), t \in I_{\delta_{N,\Delta\tau}}$ with

$$\gamma(t) = \begin{cases} \gamma_-(t), & \text{when } \varepsilon > \frac{2}{\pi(\Delta\tau)^2}, \\ \gamma_+(t), & \text{when } \varepsilon < 0, \end{cases} \tag{3.10.2}$$

$$\gamma_\pm(t) = 1 - \frac{\pi\varepsilon(\Delta\tau)^2}{\cos^2(\pi t)} \pm \sqrt{\left(1 - \frac{\pi\varepsilon(\Delta\tau)^2}{\cos^2(\pi t)}\right)^2 - 1}, \tag{3.10.3}$$

where $h_{KS}(\widetilde{T}_{\varepsilon,\Delta\tau})$ is equivalent to the positive Lyapunov exponent $\lambda(\varepsilon,\Delta\tau)$ due to the Pesin's identity [108]. To obtain an explicit formula of the Lyapunov exponent, one substitutes (3.10.3) into $\det\left(D\widetilde{T}_{\varepsilon,\Delta\tau}|_{E^u}\right)$.

(i) in the case of $\varepsilon > \frac{2}{\pi(\Delta\tau)^2}$, the Lyapunov exponent is denoted as

$$
\begin{aligned}
\lambda(\varepsilon,\Delta\tau) &= \int_{-\frac{1}{2}}^{\frac{1}{2}} \log\left|1-\frac{\pi\varepsilon(\Delta\tau)^2}{\cos^2(\pi t)}-\sqrt{\left(1-\frac{\pi\varepsilon(\Delta\tau)^2}{\cos^2(\pi t)}\right)^2-1}\right| dt \\
&= \int_{-\frac{1}{2}}^{\frac{1}{2}} \log\left|\cos^2(\pi t)-\pi\varepsilon(\Delta\tau)^2-\sqrt{\left(\cos^2(\pi t)-\pi\varepsilon(\Delta\tau)^2\right)^2-\cos^4(\pi t)}\right| dt \\
&\quad - \int_{-\frac{1}{2}}^{\frac{1}{2}} \log\left|\cos^2(\pi t)\right| dt \\
&= \int_{-\frac{1}{2}}^{\frac{1}{2}} \log\left|\pi\varepsilon(\Delta\tau)^2-\cos^2(\pi t)+\sqrt{\left(\cos^2(\pi t)-\pi\varepsilon(\Delta\tau)^2\right)^2-\cos^4(\pi t)}\right| dt \\
&\quad - \int_{-\frac{1}{2}}^{\frac{1}{2}} \log\left|\cos^2(\pi t)\right| dt \\
&= \int_{-\frac{1}{2}}^{\frac{1}{2}} \log\left|\cos^2(\pi t)-\pi\varepsilon(\Delta\tau)^2\right| dt - \int_{-\frac{1}{2}}^{\frac{1}{2}} \log\left|\cos^2(\pi t)\right| dt \\
&\quad + \int_{-\frac{1}{2}}^{\frac{1}{2}} \log\left(1+\sqrt{1-\left(1-\frac{\pi\varepsilon(\Delta\tau)^2}{\cos^2(\pi t)}\right)^{-2}}\right) dt \\
&= \log\left[2\pi\varepsilon(\Delta\tau)^2-1+2\sqrt{\pi\varepsilon(\Delta\tau)^2\left\{\pi\varepsilon(\Delta\tau)^2-1\right\}}\right] \\
&\quad + \int_{-\frac{1}{2}}^{\frac{1}{2}} \log\left(1+\sqrt{1-\left(1-\frac{\pi\varepsilon(\Delta\tau)^2}{\cos^2(\pi t)}\right)^{-2}}\right) dt
\end{aligned}
\tag{3.10.4}
$$

(ii) in the case of $\varepsilon < 0$, the Lyapunov exponent is denoted as

$$\begin{aligned}
\lambda(\varepsilon, \Delta\tau) &= \int_{-\frac{1}{2}}^{\frac{1}{2}} \log \left| 1 - \frac{\pi\varepsilon(\Delta\tau)^2}{\cos^2(\pi t)} + \sqrt{\left(1 - \frac{\pi\varepsilon(\Delta\tau)^2}{\cos^2(\pi t)}\right)^2 - 1} \right| dt \\
&= \int_{-\frac{1}{2}}^{\frac{1}{2}} \log \left| \cos^2(\pi t) - \pi\varepsilon(\Delta\tau)^2 + \sqrt{\left(\cos^2(\pi t) - \pi\varepsilon(\Delta\tau)^2\right)^2 - \cos^4(\pi t)} \right| dt \\
&\quad - \int_{-\frac{1}{2}}^{\frac{1}{2}} \log \left| \cos^2(\pi t) \right| dt \\
&= \int_{-\frac{1}{2}}^{\frac{1}{2}} \log \left| \cos^2(\pi t) - \pi\varepsilon(\Delta\tau)^2 \right| dt - \int_{-\frac{1}{2}}^{\frac{1}{2}} \log \left| \cos^2(\pi t) \right| dt \\
&\quad + \int_{-\frac{1}{2}}^{\frac{1}{2}} \log \left(1 + \sqrt{1 - \left(1 - \frac{\pi\varepsilon(\Delta\tau)^2}{\cos^2(\pi t)}\right)^{-2}} \right) dt \\
&= \log \left[1 - 2\pi\varepsilon(\Delta\tau)^2 + 2\sqrt{\pi\varepsilon(\Delta\tau)^2 \left\{\pi\varepsilon(\Delta\tau)^2 - 1\right\}} \right] \\
&\quad + \int_{-\frac{1}{2}}^{\frac{1}{2}} \log \left(1 + \sqrt{1 - \left(1 - \frac{\pi\varepsilon(\Delta\tau)^2}{\cos^2(\pi t)}\right)^{-2}} \right) dt
\end{aligned} \tag{3.10.5}$$

From (3.10.5), in the condition such as $|\varepsilon| \ll 1$, it holds that

$$\begin{aligned}
&\log \left[1 - 2\pi\varepsilon(\Delta\tau)^2 + 2\sqrt{\pi\varepsilon(\Delta\tau)^2 \left\{\pi\varepsilon(\Delta\tau)^2 - 1\right\}} \right] \\
&= O\left(-2\pi\varepsilon(\Delta\tau)^2 + 2\sqrt{-\pi\varepsilon(\Delta\tau)^2 + \pi^2\varepsilon^2(\Delta\tau)^4} \right),
\end{aligned} \tag{3.10.6}$$

and that

$$-2\pi\varepsilon(\Delta\tau)^2 + 2\sqrt{-\pi\varepsilon(\Delta\tau)^2 + \pi^2\varepsilon^2(\Delta\tau)^4} = O(|\varepsilon|^{\frac{1}{2}}). \tag{3.10.7}$$

Then, it holds that in the condition such as $|\varepsilon| \ll 1$, we have

$$\log \left[1 - 2\pi\varepsilon(\Delta\tau)^2 + 2\sqrt{\pi\varepsilon(\Delta\tau)^2 \left\{\pi\varepsilon(\Delta\tau)^2 - 1\right\}} \right] = O(|\varepsilon|^{\frac{1}{2}}). \tag{3.10.8}$$

In terms of $\int_{-\frac{1}{2}}^{\frac{1}{2}} \log \left(1 + \sqrt{1 - \left(1 - \frac{\pi\varepsilon(\Delta\tau)^2}{\cos^2(\pi t)}\right)^{-2}} \right) dt$, it holds that

$$\log \left(1 + \sqrt{1 - \left(1 - \frac{\pi\varepsilon(\Delta\tau)^2}{\cos^2(\pi t)}\right)^{-2}} \right) = O\left(\sqrt{1 - \left(1 - \frac{\pi\varepsilon(\Delta\tau)^2}{\cos^2(\pi t)}\right)^{-2}} \right) = O\left(|\varepsilon|^{\frac{1}{2}} \right) \tag{3.10.9}$$

Thus, from Equations (3.10.8) and (3.10.9), when $0 < -\varepsilon \ll 1$, it holds that

$$\lambda(\varepsilon, \Delta\tau) = O(|\varepsilon|^{\frac{1}{2}}). \tag{3.10.10}$$

Therefore, the critical exponent of Lyapunov exponent ν is $\frac{1}{2}$ as $\varepsilon \to -0$. The value of the critical exponent is same as those of GB, SGB and ESGB transformations. Then, there is the possibility that we can apply intermittency route to chaos to our maps.

Since it is not necessarily that such an expression is simple enough, we assume the following so that an explicit expression is analytically obtained.
(Assumption): one can obtain the equivalent value of (3.10.1) if one substitutes $\langle \cos^2(\pi t)\rangle = 1/2$ into $\cos^2(\pi t)$ in Equations (3.10.4) and (3.10.5) .
Under this assumption, Equations (3.10.4) and (3.10.5) can be integrated as,

$$\lambda(\varepsilon, \Delta\tau) \simeq \begin{cases} \log\left[2\pi\varepsilon(\Delta\tau)^2 - 1 + 4\sqrt{\pi\varepsilon(\Delta\tau)^2\left\{\pi\varepsilon(\Delta\tau)^2 - 1\right\}} + \frac{4\pi\varepsilon(\Delta\tau)^2\left\{\pi\varepsilon(\Delta\tau)^2-1\right\}}{2\pi\varepsilon(\Delta\tau)^2-1}\right], & \varepsilon > \frac{2}{\pi(\Delta\tau)^2}, \\ \log\left[1 - 2\pi\varepsilon(\Delta\tau)^2 + 4\sqrt{\pi\varepsilon(\Delta\tau)^2\left\{\pi\varepsilon(\Delta\tau)^2 - 1\right\}} + \frac{4\pi\varepsilon(\Delta\tau)^2\left\{\pi\varepsilon(\Delta\tau)^2-1\right\}}{1-2\pi\varepsilon(\Delta\tau)^2}\right], & \varepsilon < 0. \end{cases} \tag{3.10.11}$$

Figure 3.3 shows the comparison between the numerical result and the analytical formula of the Lyapunov exponent. One sees that the numerical result is consistent with the analytical formula.

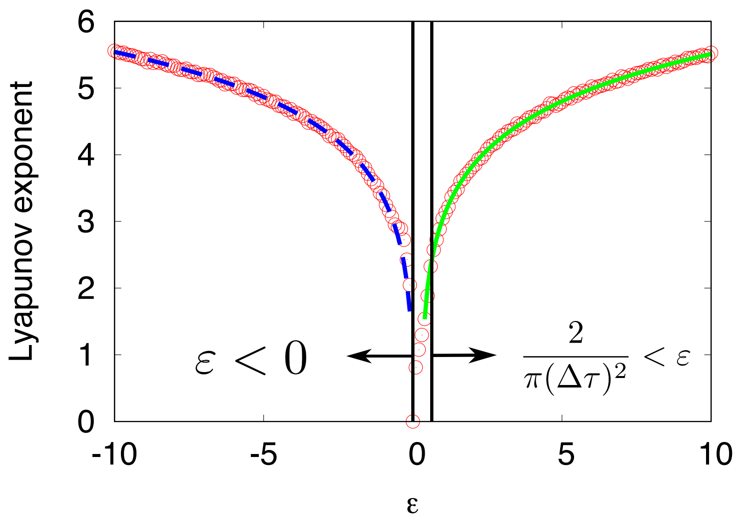

Figure 3.3: Numerical calculation of Lyapunov exponent (red circle) and analytical formula (lines) in the case of $\Delta\tau = 1$. A solid line corresponds to $\lambda(\varepsilon, \Delta\tau)$ for $\varepsilon < 0$ and a broken line corresponds to $\varepsilon > \frac{2}{\pi}$. The iteration number is 10^4. The initial deviation vector and point are as follows: $v_s = \frac{1}{\sqrt{2}}, v_t = \frac{1}{\sqrt{2}}$ and $(s, t) = (\frac{\sqrt{2}-1}{2}, \frac{\sqrt{3}-1}{2})$. A vertical line corresponds to $\varepsilon = \frac{2}{\pi}$.

3.11 Superdiffusion

Superdiffusion is a phenomenon in which the variance $\sigma^2(n)$ grow of order $n^\gamma, \gamma > 1$. That means that for a density function $P(x,n)$ [111] its variance

$$\sigma^2(n) \overset{\text{def}}{=} \int_{-\infty}^{\infty} (x - \langle x \rangle)^2 P(x,n)dx \tag{3.11.1}$$

diverges of order

$$\sigma^2(n) \propto n^\gamma, \gamma > 1. \tag{3.11.2}$$

For time series $\{p_n\}_{n=0}^{\infty}$, superdiffusion is also defined by using mean square displacement $\left\langle r^2(n) \right\rangle$ [112] defined by

$$\left\langle r^2(n) \right\rangle = \left\langle (p_n - p_0)^2 \right\rangle . \tag{3.11.3}$$

When mean square displacement $\left\langle r^2(n) \right\rangle$ obeys the following relation $\left\langle r^2(n) \right\rangle \propto n^\gamma, \gamma > 1$, we call superdiffusion occurs.

Here superdiffusion is a phenomenon which cannot be explained by the Central Limit Theorem and can be observed in various physical systems such as astrophysics [113], rotating flow [114], hydrogen in Vanadium [115], dense granular media [116] and ultracold atoms [117]. As the model of symplectic map in which superdiffusion occurs, standard map is known. The standard map is the most famous chaotic model associated with a classical Hamiltonian system in which one can observe the coexistence of the chaotic sea and KAM tori for a finite parameter range [98]. Then, the standard map is not ergodic for the whole domain [99]. It means that the measure of sets of points is less than unity in which chaos occurs. From the viewpoint of the time evolution, lots of works reported that superdiffusion occurs in the standard map due to the coexistence of chaotic regions and KAM tori [29, 98, 99, 100]. This phenomenon is referred to be, *not perfectly chaotic superdiffusion* [100].

From the viewpoint of the spacial structure, the standard map has a periodic potential and Hamiltonians with periodic potential appear in solid surfaces [118] and quantum chaos [119].

3.11.1 Distribution yielding superdiffusion

As a preparation for the following discussion, first we consider the such situation that the probability variable $\{x_n\}_{n=1}^{\infty}$ are independent and identically distributed in accordance with the Cauchy distribution whose scale parameter is γ and median is 0. According the the Generalized Central Limit Theorem [90], it holds that for the time series $\{x_n\}_{n=1}^{\infty}$,

$$\begin{aligned} \frac{\sum_{k=1}^{n} x_k - A_n}{n^{\frac{1}{\alpha}}} &\xrightarrow{\mathrm{d}} S(\alpha, \beta, \gamma, 0) \text{ as } n \to \infty, \\ A_n &= \begin{cases} 0 & 0 < \alpha < 1 \\ n^2 \Im \log \left(\varphi_x(\frac{1}{n})\right) & \alpha = 1 \\ n\mathbb{E}[x] & 1 < \alpha < 2 \end{cases} \end{aligned}, \tag{3.11.4}$$

(i) in the case of $0 < \alpha < 1$, the term $\frac{\sum_{k=1}^{n} x_k}{n^{\frac{1}{\alpha}}}$ neither converges to certain value nor diverges. Then the order of this term is denoted as

$$O\left(\sum_{k=1}^{n} x_k\right) = O\left(n^{\frac{1}{\alpha}}\right). \tag{3.11.5}$$

Thus, one has that

$$O\left(\left(\sum_{k=1}^{n} x_k\right)^2\right) = O\left(n^{\frac{2}{\alpha}}\right). \tag{3.11.6}$$

(ii) in the case of $\alpha = 1$, since the term $\Im \log \left(\varphi_x(\frac{1}{n})\right)$ corresponds to the imaginary part of characteristic function and the characteristic function of the Cauchy distribution is real number, then $A_n = 0$. Thus, the order of $\sum_{k=1}^{n} x_k$ is denoted similarly as

$$\begin{aligned} O\left(\sum_{k=1}^{n} x_k\right) &= O(n) \\ \therefore O\left(\left(\sum_{k=1}^{n} x_k\right)^2\right) &= O(n^2) \end{aligned}. \tag{3.11.7}$$

(iii) in the case of $1 < \alpha < 2$, one can always consider the case in which the mean value $\mathbb{E}[x]$ is removed. Then, one can apply the case (i). Thus it holds that

$$O\left(\left(\sum_{k=1}^{n} x_k\right)^2\right) = O\left(n^{\frac{2}{\alpha}}\right). \tag{3.11.8}$$

Therefore, from Eq. (3.11.7), the following relation holds.

$$\left\langle \left(\sum_{k=0}^{n-1} x_k\right)^2 \right\rangle \propto n^2. \tag{3.11.9}$$

Here, we consider a dynamics define by $p_{n+1} = p_n + x_n$ where $\{x_n\}$ are i.i.d and in accordance with the Cauchy distribution. At that time, from (3.11.9) the mean square displacement $\langle r^2(n)\rangle$ of p_n defined by (3.11.3) can be rewritten as

$$\begin{aligned}\langle r^2(n)\rangle &= \left\langle (p_n - p_0)^2 \right\rangle \\ &= \left\langle \left(\sum_{k=0}^{n-1} x_k\right)^2 \right\rangle \propto n^2.\end{aligned} \tag{3.11.10}$$

Therefore, it shows that superdiffusion occurs. In my dynamics, if the local instability condition is satisfied, variables $s_n = q_1(n) + \frac{\Delta\tau}{2}p_1(n) - q_2(n) - \frac{\Delta\tau}{2}p_2(n)$ obeys the uniform distribution. By considering the case that the number N is large enough in (3.2.3), we can consider that the variable s_n is uniformly distributed in $\left(-\frac{1}{2}, \frac{1}{2}\right]$. Then, by assuming that the variable $\{u_n = -\varepsilon\Delta\tau \tan(\pi s_n)\}_n$ are independent, it can be shown why superdiffusion occurs when local instability condition is satisfied.

According to the above description, we discuss the mathematical structure which connects an Anosov diffeomorphism with superdiffusion. In what follows, we focus on the map $T_{\varepsilon,\Delta\tau}$ or $\widehat{T}_{\varepsilon,\Delta\tau}$ and on the distribution of the momentum p_1. It will be shown that p_1 is represented by the sum of variables obeying the Cauchy distribution.

In detail, since the map $\widetilde{T}_{\varepsilon,\Delta\tau}$ is topologically semi-conjugate with $\widehat{T}_{\varepsilon,\Delta\tau}$, for any orbit $\{(p_1(n), q_1(n))\}_{n\in\mathbb{Z}}$, there is at least one corresponding orbit $\{(s_n, t_n)\}_{n\in\mathbb{Z}}$. In addition since points $\{s_n\}_{n\in\mathbb{Z}}$ obey the uniform distribution and have mixing property, points $\{u_k = -\varepsilon(\Delta\tau)\tan(\pi s_k)\}_{k\in\mathbb{Z}}$ obey the Cauchy distribution [49, 36]

$$f(u) = \frac{1}{\pi}\frac{|\varepsilon\Delta\tau|}{(\varepsilon\Delta\tau)^2 + u^2}, \tag{3.11.11}$$

and also have the mixing property. Similar to above discussion, Maryland transformation is known as the example in which the tangent function and the Cauchy distribution appear [120].

Figure 3.4 shows the distribution of $\{u_k\}_{k=1}^{n}$ for single orbit where $n = 10^6$ at $\varepsilon = 0.65$, $\Delta\tau = 1$ (where the local instability condition is satisfied) and N is large enough. The function $\rho(x)$ represents numerically obtained distribution and $\rho^*(x)$ shows the distribution defined in (3.11.11). Numerically obtained function $\rho(x)$ is consistent with the theoretical function $\rho^*(x)$. This numerical result ensures that the variables $\{u_k\}$ obey the Cauchy distribution defined by (3.11.11).

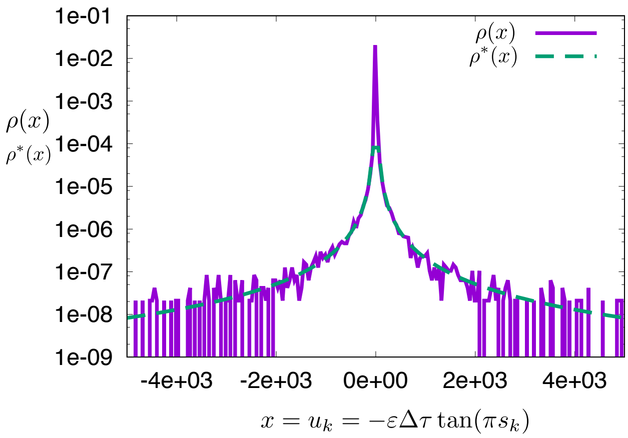

Figure 3.4: Distribution of $\{u_k\}$ at $\varepsilon = 0.65$ and $\Delta\tau = 1$. The function $\rho(x)$ represents the numerical result and $\rho^*(x)$ represent theoretical result defined by (3.11.11).

From (3.11.11), we can obtain a distribution of p_1 as follows. Since the momentum p_1 is expressed by $p_1(n) = p_1(0) + \sum_{k=1}^{n} u_k$, the density function of $\{p_1(n)\}$ uniquely converges to a stable law [107]. For a fixed n, if $\{u_k\}_{k=1}^{n}$ are independent when the number of ensemble m_e is infinity, then $\{p_1(n)\}_{\text{ensemble}} \overset{\text{def}}{=} \{p_1(n,i)\}_{i=1}^{m_e}$ obey the distribution

$$f(p_1(n)) = \frac{1}{\pi}\frac{|\alpha_n|}{\alpha_n^2 + p_1^2(n)}, \tag{3.11.12}$$

where i is an index of each initial point and α_n satisfies $\alpha_n = |n(\varepsilon\Delta\tau)|$. Consider the case that m_e is finite. With (3.11.12), one has that $\{y \overset{\text{def}}{=} p_1(n)/\sqrt{\sigma_{n,m_e}}\}_{\text{ensemble}}$ obey

$$g(y) = \frac{1}{\pi}\frac{|\alpha_n|\sqrt{\sigma_{n,m_e}}}{\alpha_n^2 + (\sqrt{\sigma_{n,m_e}}y)^2}, \tag{3.11.13}$$

where $\sqrt{\sigma_{n,m_e}}$ is a variance obtained from the finite number of ensemble data $\{p_1(n,i)\}_{i=1}^{m_e}$. Figures 3.5 and 3.6 show the density function $g(y)$ and the numerically obtained density function $G(y)$ at $\Delta\tau = 1, \varepsilon = 0.65 > \frac{2}{\pi}$ and $\varepsilon = -0.1 < 0$, respectively where y represents $\{y_i = p_1(100,i)/\sqrt{\sigma_{100,m_e}}\}_{i=1}^{m_e}$. The number of initial points is $m_e = 10^6$. In Figure 3.5, fitting $g(y)$ to the data using least square method, one obtains a fitted parameter $\widehat{\alpha}$ as $\widehat{\alpha} = 68.5 \simeq 0.65 \times 100$. In Figure 3.6, one obtains $|\widehat{\alpha}| = 12.8 \simeq 0.1 \times 100$. If $\{u_k\}$ are independent, then $\widehat{\alpha} = 65, 10$, respectively.

Therefore, for $\varepsilon < 0, \frac{2}{\pi(\Delta\tau)^2} < \varepsilon$ one can see that $\{p_1\}_{\text{ensemble}}$ nearly obeys the Cauchy distribution in the sense that $\{u_k\}$ are almost independent.

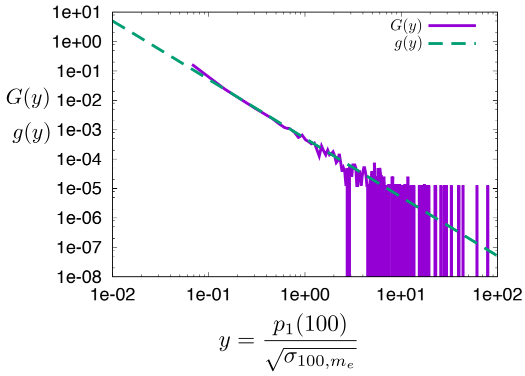

Figure 3.5: Density function $g(y)$ and $G(y)$ at $\varepsilon = 0.65$. Initial points $\{(p_1, p_2, q_1, q_2)\}$ are uniformly distributed on $\left(-\frac{1}{2}, \frac{1}{2}\right)^4$. The number of initial points is $m_e = 10^6$. The parameter $\widehat{\alpha}$ obtained by the least square method is $\widehat{\alpha} = 68.5 \simeq 100 \times 0.65$. The values of the variance for finite number of data $\{p_1(100, i)\}_{i=1}^{m_e}$ is $\sqrt{\sigma_{100,m_e}} = 4.24 \times 10^4$.

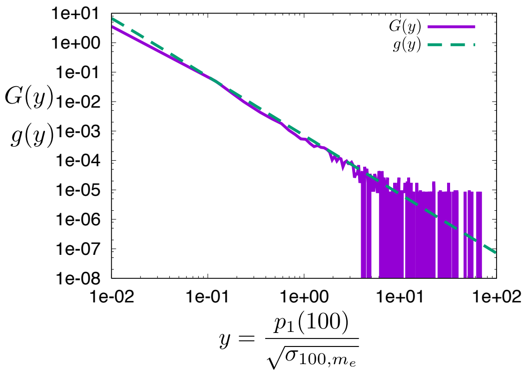

Figure 3.6: Density function $g(y)$ and $G(y)$ at $\varepsilon = -0.1$. Initial points $\{(p_1, p_2, q_1, q_2)\}$ are uniformly distributed on $\left(-\frac{1}{2}, \frac{1}{2}\right)^4$. The number of initial points is $m_e = 10^6$. The parameter $\widehat{\alpha}$ obtained by the least square method is $\widehat{\alpha} = 12.8 \simeq 100 \times 0.1$. The values of the variance for finite number of data $\{p_1(100, i)\}_{i=1}^{m_e}$ is $\sqrt{\sigma_{100,m_e}} = 5.77 \times 10^3$.

3.11.2 Superdiffusion in our system

Since $\{u_k = -\varepsilon(\Delta\tau)\tan(\pi s_k)\}_{k\in\mathbb{Z}}$ in accordance with the Cauchy distribution are nearly independent and $\{p_1(n)\}$ nearly obey the Cauchy distribution for finite time n (see the Figures 3.5 and 3.6), one can see that superdiffusion occurs. Figure 3.7 shows the log-log plot with numerically simulated time evolution of mean square displacement (MSD) with p_1 and q_1 at $\Delta\tau = 1, \varepsilon = 0.68 > \frac{2}{\pi}$, where the number of initial points is $m'_e = 2.5 \times 10^5$. The order of MSD$(n; p_1)$ and MSD$(n; q_1)$ against n is

$$\begin{aligned} \mathrm{MSD}(n;q_1) &\sim \begin{cases} n^{\nu_{q_1,S}}, & \nu_{q_1,S} \simeq 2, \quad \text{for } n \lesssim t_c, \\ n^{\nu_{q_1,L}}, & \nu_{q_1,L} \simeq 4, \quad \text{for } n \gtrsim t_c, \end{cases} \\ \mathrm{MSD}(n;p_1) &\sim n^{\nu_{p_1}}, \nu_{p_1} \simeq 2, \end{aligned}$$

where $t_c \simeq 10^{1.3}$. From Figure 3.7, we observe that

$$\nu_{q_1,S} \simeq \nu_{p_1}, \nu_{q_1,L} \simeq \nu_{p_1} + 2. \tag{3.11.14}$$

Equation (3.11.14) is consistent with that found in study by Benkadda [100]. The time t_c is considered to be a relaxation time when correlation functions decay almost completely.

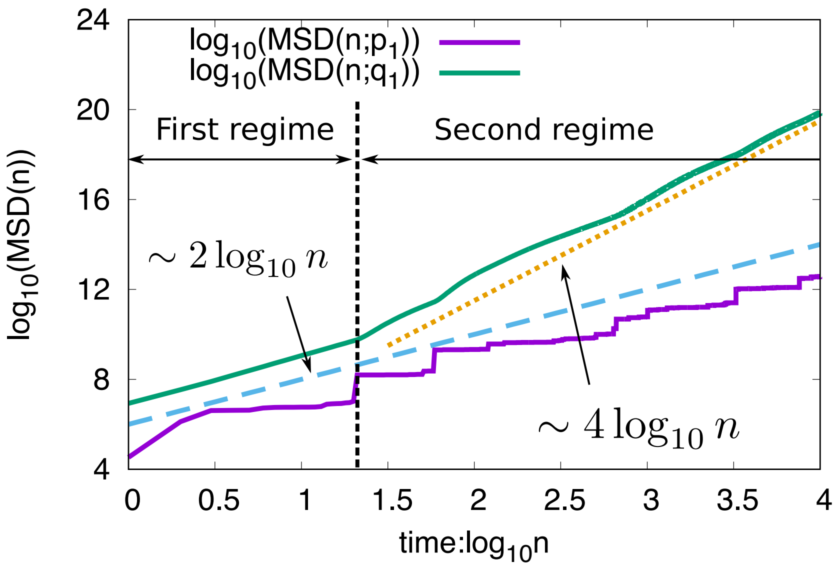

Figure 3.7: Mean square displacement (MSD) of p_1 and q_1 for the map $T_{\varepsilon,\Delta\tau}$ at $\varepsilon = 0.68$ and $m'_e = 2.5 \times 10^5$ (solid lines). The broken lines increase in the order of $\log_{10} n^2$ or $\log_{10} n^4$. One can see there occurs superdiffusion for p_1 and q_1. As initial conditions, p_1 and p_2 are distributed obeying to the Cauchy distribution whose scale parameter is 0.68 and $q_1 = q_2 = 0$. In study by Latora et. al. [121], under similar initial conditions, superdiffusion was studied.

It should be emphasized that *perfectly chaotic superdiffusion* occurs in our model, namely for almost all initial points chaotic superdiffusion occurs. According to the previous works [29, 98, 99, 122, 123], the cause of superdiffusion is considered to be the coexistence of chaotic regions and KAM tori. In particular it has been believed that normal diffusion and superdiffusion coexist in standard map. In our model however, superdiffusion occurs with probability unity, i.e. phase space is solely filled with chaotic region. Then, from our analysis we propose a new mechanism of superdiffusion.

3.12 Conclusion

In the microscopic scale, it has been proven that the map $\widehat{T}_{\varepsilon,\Delta\tau}$ which has time-reversal symmetry without scatterers, has the same ergodic properties as an Anosov diffeomorphism for $\varepsilon < 0$ or $\frac{2}{\pi(\Delta\tau)^2} < \varepsilon$, namely the dynamical system derived from the Hamiltonian without scatterers has the mixing property (ergodic).

In the macroscopic scale, in the sense of distribution functions, we also have proven that the Kolmogorov-Sinai entropy is positive for almost all initial points and the Lebesgue measure is a unique SRB measure in the parameter ranges. Then, this has indicated that a density function converges into the uniform distribution in the sense of mixing and that the time derivative of the Boltzmann entropy is positive after the system has been mixed enough. The result has assured that one can deal with the dynamical system probabilistically or statistically using the uniform distribution. In addition, we have shown that the momentum nearly obeys the Cauchy distribution if the time n is finite, which causes *perfectly chaotic superdiffusion*.

In summary, the convergence of initial density functions to the uniform distribution and positivity of entropy rate are certainly proven rigorously in our model derived from the Hamiltonian system with time-reversal symmetry for the parameter ranges $\varepsilon < 0$ or $\frac{2}{\pi(\Delta\tau)^2} < \varepsilon$. In addition, the relaxation occurs with *perfectly chaotic superdiffusion* in the whole sets of the chaotic region. From these results, it can be claimed that the convergence of initial density functions to the uniform distribution and positivity of entropy rate are compatible with microscopic time reversibility. Thus, from our analysis, “macroscopic uni-direction" can be generated by *internally chaotic mechanism* in Hamiltonian dynamical systems with time-reversal symmetry even though the systems do not have external artifacts such as the walls, collisions and scatterers.

Chapter 4

Conclusion

Let us summarize this thesis.

In Chapter 2, the universality of routes to chaos is discussed. Previous studies proposed that there is universality in the critical exponent of the Lyapunov exponent, but justified this suggestion primarily by numerical experiments. In this thesis, we have considered the generalized Boole (GB) transformations, super-generalized Boole (SGB) transformations, and extended super-generalized Boole (ESGB) transformations, and obtained the following results.

1. The GB, SGB and ESGB transformations are exact for $0 < |\alpha| < 1$.

2. Because of this exactness, any initial density function for GB, SGB and ESGB transformations converges to the unique equilibrium distribution in terms of the L^1 norm.

3. The explicit form of the Lyapunov exponent for $\alpha > 0$ corresponding to GB transformations is obtained.

4. For GB transformations, *Type* 1 intermittency occurs at $\alpha = 1$ and *Type* 3 intermittency occurs at $\alpha = 0$.

5. For GB transformations, at $\alpha = 1$, two different critical exponents are obtained: $\nu = 1$ in the limit of $\alpha = 1 + 0$, and $\nu = \frac{1}{2}$ in the limit of $\alpha \to 1 - 0$. At $\alpha = 0$, we have $\nu = \frac{1}{2}$.

6. For SGB and ESGB transformations, for a countably infinite number of maps, *Type* 1 intermittency occurs at $({}^{\forall}K, \alpha = 1)$ and $(2N + 1, \frac{1}{(2N+1)^2})$. At $|\alpha| = 1$, we have $\nu = 1$ as $|\alpha| \to 1 + 0$ and $\nu = \frac{1}{2}$ as $|\alpha| \to 1 - 0$ for all K. In the case of $K = 2N + 1$, it can be shown that $\nu = \frac{1}{2}$ as $|\alpha| \to \frac{1}{(2N+1)^2} + 0$; in the case of $K = 2N$, it can be shown that $\nu = \frac{1}{2}$ as $|\alpha| \to +0$.

7. SGB transformations preserve the Lebesgue measure for $\alpha = \pm 1$ and are ergodic in that condition. This means that we obtained countably infinite maps with infinite ergodic measure.

8. ESGB transformations preserve the following density function: $\rho_{\gamma,\beta}(x) = \frac{1}{\pi}\frac{\gamma|x|^{\beta-1}}{|x|^{2\beta}+\gamma^2}, \beta > 0$. This is a more general class than the Cauchy distribution, which corresponds to $\beta = 1$.

In Chapter 3, we treat irreversible behavior in dynamical systems with time-reversal symmetry. In the 19th century, Boltzmann proved the unidirectionality of the time evolution of his H function in rarefied gas by assuming the ergodic hypothesis. Here, we prove that, for a system with time-reversal symmetry and invariant measure (the conditions discussed by Loschmidt and Zermelo, respectively), any initial density function defined except for zero measure converges to the unique equilibrium distribution in the sense of mixing. We show this by proving the Anosov property for certain maps. In particular, we obtained the following results:

1. When the local instability condition $\varepsilon < 0, \frac{2}{\pi(\Delta\tau)^2} < \varepsilon$ is satisfied, the map $\widetilde{T}_{\varepsilon,\Delta\tau}$ is an Anosov diffeomorphism. Therefore, any initial density function defined except for zero measure converges to the uniform distribution corresponding to the SRB measure.

2. When the local instability condition $\varepsilon < 0, \frac{2}{\pi(\Delta\tau)^2} < \varepsilon$ is satisfied, the map $\widehat{T}_{\varepsilon,\Delta\tau}$ satisfies the condition *(I)*, *(II)* and *(III)* in Definition 3.8.1 where M' is not compact.

3. The map $\widetilde{T}_{\varepsilon,\Delta\tau}$ is topologically semi-conjugate to $\widehat{T}_{\varepsilon,\Delta\tau}$. Then the map $\widehat{T}_{\varepsilon,\Delta\tau}$ has the same ergodic property as the map $\widetilde{T}_{\varepsilon,\Delta\tau}$. Thus, the map $\widehat{T}_{\varepsilon,\Delta\tau}$ has the SRB measure as the Lebesgue measure. Therefore, any initial density function defined except for zero measure converges to the uniform distribution corresponding to the SRB measure.

4. When the local instability condition $\varepsilon < 0, \frac{2}{\pi(\Delta\tau)^2} < \varepsilon$ is satisfied, the variable $\{u_n = -\varepsilon\Delta\tau\tan(\pi s_n)\}_n$ follows the Cauchy distribution, the scaling parameter of which is $\varepsilon\Delta\tau$. According to the generalized central limit theorem, the mean square displacement in terms of moment obeys $\left\langle (p_n - p_0)^2 \right\rangle = \left\langle \left(\sum_{k=0}^{n-1} u_k \right)^2 \right\rangle \propto n^2$.

We will now consider some possible future extensions of the present work.

Three main avenues for further exploration of the GB, SGB, and ESGB transformations are open to us.

1. We proved that SGB transformations preserve the Lebesgue measure and that they are ergodic at $\alpha = \pm 1$. According to [79], SGB transformations are ergodic with the Lebesgue measure at $(K, \alpha) = (2, 1)$. Therefore, we plan to prove ergodicity at $\alpha = \pm 1$ for any K and β. A few examples have been proved to be ergodic with infinite measure. If we can prove this for an uncountably infinite number of maps, we will have made a major advance in ergodic theory.

2. We plan to study anomalous diffusion in GB, SGB, ESGB, or these modified maps. ESGB transformations preserve a density function in which $f(x) \sim \frac{1}{|x|^{\beta+1}}, |x| \to \infty$. It is anticipated that anomalous diffusion occurs and the exponent of the mean square displacement can be adjusted by β. That is, throughout the range $0 < \alpha < 2$, we will be able to generate any anomalous diffusion for which $\left\langle (x_n - x_0)^2 \right\rangle \propto n^{\alpha}$ holds. In addition, the map $\bar{S}_{K,\alpha}$ is defined in a bounded interval. It has been reported that anomalous diffusion occurs in maps that are generated by combining plural maps stepwise [124]. By combining plural $\bar{S}_{K,\alpha}$ maps to make a stepped form, we can observe the global diffusion in $\mathbb{R}$ and discover whether anomalous diffusion occurs.

3. We will consider multidimensional versions of the GB, SGB, and ESGB transformations. Referring to [21], we plan to make N-dimensional maps using GB, SGB, or ESGB transformations, find the conditions under which they are exact, and study their nonequilibrium steady states. If we generate maps linked in a chain and fix the density function of one side point, we expect that there will be a continuous change in the steady state density function due to the exactness of these maps.

Extending the work described in Chapter 3, we are planning to make multidimensional Anosov systems. In the two-dimensional case, there are several Anosov systems that include $\widehat{T}_{\varepsilon,\Delta\tau}$ and $\widetilde{T}_{\varepsilon,\Delta\tau}$, such as Arnold's cat map, (multi) Baker's map, Sinai billiards, and the Bunimovich stadium. We will increase the dimensionality to study such dynamical systems statistically. Usually, in multidimensional cases, the Anosov property is not proven but assumed; if we can prove that it holds for multidimensional systems, we will have advanced ergodic theory and statistical physics. In addition, we plan to study anomalous diffusion in a modified $\widehat{T}_{\varepsilon,\Delta\tau}$ map. We will generalize the tan function using a parameter $0 < \beta < 2$ as in ESGB transformations. It is expected that anomalous diffusion occurs in which the exponent of the mean square displacement can be adjusted arbitrarily.

Finally, we are considering quantizing the map $\widehat{T}_{\varepsilon,\Delta\tau}$. Studies of quantizing the standard classical symplectic map have reported that diffusion is suppressed in a quantum system, but not in a classical system [125]. In the standard map, phase space consists of chaotic regions and torus regions and both normal diffusion and superdiffusion occur. In the map $\widehat{T}_{\varepsilon,\Delta\tau}$, when the local instability condition is satisfied, phase space is covered by the chaotic region and superdiffusion occurs with probability unity. We will investigate whether superdiffusion also occurs when the map $\widehat{T}_{\varepsilon,\Delta\tau}$ is quantized.

Acknowledgement

The author, Ken-ichi Okubo, sincerely thanks Professor Ken Umeno for his guidance and valuable advice, and Professor Yoshiyuki Y. Yamaguchi for fruitful discussions.

The author is also grateful to Professor Yoshisuke Ueda, Professor Yoji Aizawa, Professor Yoshimasa Nakamura, Professor Toshio Aoyagi, Professor Hisao Hayakawa, Professor Akira Shudo, Professor Kei Inoue, Professor Kensuke Ikeda, Professor Fumiyoshi Kuwashima, Professor Kenji Wada, Professor Song-Ju Kim, Professor Takuma Akimoto, Professor Atsushi Tanaka, Dr. Hidetoshi Okutomi, Dr. Warsito Purwo Taruno, and Mr. Masaru Shintani for their kind comments.

Appendix A

New Chaos Indicators

This chapter is according to [52, 53].

A.1 Introduction

In a weakly chaotic system, we need much more computational time to obtain valid numerical results about finite Lyapunov exponents than a strongly chaotic system. Here, a weakly chaotic system is defined such that the largest Lyapunov exponent for a dynamical system is small and positive. For example, Sussmann and Wisdom [126, 127] calculated the Lyapunov time (the inverse of Lyapunov exponent) of the Solar system over 100 million years and predicted the Lyapunov time as approximately 5 million years.

According to Froeschlé, Gonczi and Lega [39], in a weakly chaotic system, it can take more than ten times longer than Lyapunov time. In order to investigate situation of the phase space, they invented Fast Lyapunov Indicator (FLI) [39, 41] for a class map

$$\boldsymbol{x}(n+1) = F(\boldsymbol{x}(n)), \quad \boldsymbol{x} \in \mathbb{R}^N. \tag{A.1.1}$$

Here, FLI is defined by

$$\mathrm{FLI}(\boldsymbol{x}(0), \boldsymbol{v}(0), n) = \sup_{0<i\leq n} \log\left(\frac{\|\boldsymbol{v}(i)\|}{\|\boldsymbol{v}(0)\|}\right), \tag{A.1.2}$$

where $\boldsymbol{x}(0)$ is an initial point, $\boldsymbol{v}(0)$ is an initial variational vector. When an initial point is in a chaotic region, the time evolution of FLI is of order $O(n)$[128]. On the other hand, when an initial point is on a torus, it holds that $\mathrm{FLI}(n) \sim O(\log n)$[128]. These relations hold if we choose a good initial variational vector.

A.1.1 Orthogonal Fast Lyapunov Indicator (OFLI)

Fouchard, Lega, Chistiane Froeschlé and Claude Froeschlé [42] improved FLI and invented Orthogonal Fast Lyapunov Indicator (OFLI) defined by

$$\mathrm{OFLI}(\boldsymbol{x}(0), \boldsymbol{v}(0), n) \equiv \sup_{0<i\leq n} \log\left(\frac{\|\boldsymbol{v}(i)^{\perp}\|}{\|\boldsymbol{v}(0)\|}\right). \tag{A.1.3}$$

Here, $\boldsymbol{v}(n)^{\perp}$ is a quadrature component of $\boldsymbol{v}(n)$ defined by

$$\left\|\boldsymbol{v}(n)^{\perp}\right\| \quad = \quad \sqrt{\|\boldsymbol{v}(n)\|^2 - \frac{\langle \boldsymbol{v}(n),\ F(\boldsymbol{x}(i))\rangle^2}{\|F(\boldsymbol{x}(i))\|^2}}. \tag{A.1.4}$$

.

A.1.2 Orthogonal Fast Lyapunov Indicator 2 (OFLI^2)

Next, Bario [43] improved OFLI and invented OFLI^2 defined by

$$\begin{aligned}
\mathrm{OFLI}^2(\boldsymbol{x}(0), \boldsymbol{v}(0), n) &\equiv \sup_{0<i<n} \log \frac{\left\|\left(\boldsymbol{v}(i) + \frac{1}{2}\boldsymbol{v}_2(i)\right)^{\perp}\right\|}{\left\|\left(\boldsymbol{v}(0) + \frac{1}{2}\boldsymbol{v}_2(0)\right)\right\|}, && \text{(A.1.5)}\\
\boldsymbol{v}(i+1) &= DF(\boldsymbol{x}(i))\boldsymbol{v}(i), && \text{(A.1.6)}\\
\boldsymbol{v}_2(i+1) &= DF(\boldsymbol{x}(i))\boldsymbol{v}_2(i) + D^2F(\boldsymbol{x}(i))\,(\boldsymbol{v}(i))^2, && \text{(A.1.7)}
\end{aligned}$$

where $DF(\boldsymbol{x}(n))$ is a Jacobian for $F(\boldsymbol{x}(n))$ and $D^2F(\boldsymbol{x}(n))\,(\boldsymbol{v}(n))^2$ is defined by

$$D^2F(x(n))\,(\boldsymbol{v}(n))^2 \equiv \sum_{i=1}^{N} {}^t\boldsymbol{v}(n)H[F_i(\boldsymbol{x}(n))]\boldsymbol{v}(n)\,\mathbf{e}_i. \tag{A.1.8}$$

Here, $F_i(\boldsymbol{x}(n))$ is a ith component of $F(\boldsymbol{x}(n))$ and $H[F_i(\boldsymbol{x}(i))]$ is a Hessian matrix and we set $\boldsymbol{v}(0) = \boldsymbol{v}_1(0), \boldsymbol{v}_2(0) = \mathbf{0}$.

A.2 Ultra Fast Lyapunov Indicator (UFLI)

In calculation of OFLI^2, the term with Hessian $(D^2F(\boldsymbol{x}(i))\,(\boldsymbol{v}(i))^2)$ uses only a linear term of $F(\boldsymbol{x}(n))$ and we need to calculate 2 terms $\boldsymbol{v}$ and $\boldsymbol{v}_2$ separately.

When iteration time n is not so large, it is possible that we cannot detect whether the orbit is of order $O(n)$ or $O(\log(n))$ as Figure A.6 and A.8. To improve this problem, we need new indicator which grows more rapidly for a chaotic orbit.

Thus, we propose an improved indicator Ultra Fast Lyapunov Indicator (UFLI) [53] defined by

$$\mathrm{UFLI}(\boldsymbol{x}(0), \boldsymbol{v}(0), n) \equiv \sup_{0<i<n} \log \frac{\left\|\boldsymbol{v}(i)^{\perp}\right\|}{\|\boldsymbol{v}(0)\|}, \tag{A.2.1}$$

$$\boldsymbol{v}(n+1) = DF(\boldsymbol{x}(n))\boldsymbol{v}(n) + \frac{1}{2}\sum_{i=1}^{N} {}^{t}\boldsymbol{v}(n)H[F_i(\boldsymbol{x}(n))]\boldsymbol{v}(n)\,\mathbf{e}_i. \tag{A.2.2}$$

Now we express $DF(\boldsymbol{x}(n))$ by DF_n. The variational vector $\boldsymbol{v}(n+1)$ can expressed by

$$\begin{aligned} \boldsymbol{v}(n+1) &= \left(\prod_{i=0}^{n} DF_i\right)\boldsymbol{v}(0) \\ &\quad + \frac{1}{2}\sum_{l=0}^{n}\left(\prod_{j=1}^{l} DF_{n-j}\right)\left(D^2F_{n-l}\right)(\boldsymbol{u}(n-l))^2 + O(\boldsymbol{v}(0)^3) \end{aligned} \tag{A.2.3}$$

where,

$$\boldsymbol{u}(n+1) = DF_n DF_{n-1}\cdots DF_0\boldsymbol{v}(0). \tag{A.2.4}$$

Then we define a term consists of second order for $\boldsymbol{v}(0)$ by $\boldsymbol{w}(n)$ as,

$$\boldsymbol{w}(n+1) \equiv \frac{1}{2}\sum_{l=0}^{n}\left(\prod_{j=1}^{l} DF_{n-j}\right)\left(D^2F_{n-l}\right)(\boldsymbol{u}(n-l))^2. \tag{A.2.5}$$

Then,

$$\boldsymbol{v}(1) = DF_0\boldsymbol{v}(0) + \frac{1}{2}D^2F_0(\boldsymbol{v}(0)^2),$$

$$\begin{aligned} \boldsymbol{v}(2) &= DF_1\boldsymbol{v}(1) + \frac{1}{2}D^2F_1(\boldsymbol{v}(1)^2), \\ &= \boldsymbol{u}(2) + \boldsymbol{w}(2) \\ &\quad + \frac{1}{4}\sum_{i=1}^{N} {}^{t}\boldsymbol{u}(1)H[F_n^i]\left[D^2F_0(\boldsymbol{v}(0))^2\right]\ \boldsymbol{e}_i + \frac{1}{4}\sum_{i=1}^{N} {}^{t}\left[D^2F_0(\boldsymbol{v}(0))^2\right]H[F_n^i]\boldsymbol{u}(1)\ \boldsymbol{e}_i \\ &\quad + \frac{1}{8}\sum_{i=1}^{N} {}^{t}\left[D^2F_0(\boldsymbol{v}(0))^2\right]H[F_n^i]\left[D^2F_0(\boldsymbol{v}(0))^2\right]\ \mathbf{e}_i \end{aligned} \tag{A.2.6}$$

The terms whose order is over two also effect UFLI while for OFL^2 only first and second order effect its value. When $\boldsymbol{u}(n)$ increase, we cannot neglect higher order. Then, UFLI increases drastically for a chaotic orbit and we researched UFLI whether it can detect chaoticity for systems with small Lyapunov exponent more rapidly and sensitively than the other three indicators.

We apply UFLI to the standard map [42, 129] (A.2.7)

$$T_S(I,\theta) = \begin{pmatrix} I + \delta \sin(I+\theta) \pmod{2\pi}, \\ I+\theta \pmod{2\pi} \end{pmatrix} \tag{A.2.7}$$

and Froeschlé map [130] (A.2.8)

$$T_F(I_1,\theta_1,I_2,\theta_2) = \begin{pmatrix} I_1 - \varepsilon \frac{\sin(I_1+\theta_1)}{\{\cos(I_1+\theta_1)+\cos(I_2+\theta_2)+4\}^2} \\ I_1+\theta_1 \pmod{2\pi} \\ I_2 - \varepsilon \frac{\sin(I_2+\theta_2)}{\{\cos(I_1+\theta_1)+\cos(I_2+\theta_2)+4\}^2} \\ I_2+\theta_2 \pmod{2\pi} \end{pmatrix}. \tag{A.2.8}$$

and the generalized Boole transformations [80] (A.2.9)

$$x_{n+1} = \alpha x_n - \frac{\beta}{x_n},\ \alpha > 0,\ \beta > 0,\ x_n \in \mathbb{R}, \tag{A.2.9}$$

In this proceeding the common logarithm is used to calculate indicators.

A.2.1 Application of UFLI for the Standard map

According to Lega and Froeschleé [129] for the standard map at $\delta = 0.9$, point A $(I,\theta) = (0.00001, 0)$ is in chaotic region, point B $(2.13, 0)$ is in KAM torus region and point C $(1.2, 1)$ is in Resonance torus region. Then, we investigated the behavior of time evolution of the indicator FLI, OFLI, OFLI^2 and UFLI. We used *exflib* to carry out multiple-precision calculations with PRECISION 50. The initial variational vector $\boldsymbol{v}(0)$ is defined by

$$\boldsymbol{v}(0) = F(\boldsymbol{x}(0)) \times d. \tag{A.2.10}$$

Figures A.1-A.8 show the comparison results for the standard map. In the case of FLI, Fouchard et. al. [42] explain it cannot work properly when initial vector is *orthogonal* to the flow. However in our numerical experiments it can distinguish the three types of orbit when the initial vector is *paralle*l to the flow. According to Bario [43], OFLI cannot distinguish the three types of orbit properly when initial variational vector is parallel to the flow for Hénon-Heils system. Figures A.5 and A.8 show OFLI cannot distinguish a chaotic orbit from a KAM torus orbit properly when initial variational vector is *parallel* to the flow. Figures A.1-A.8 show if we take the length of initial variational vector small, UFLI as well as OFLI^2 *can* distinguish three orbits even when the initial variational vector is parallel to the flow. According to Figures A.1 and A.7, around $n \sim 50$, it is difficult to determine the chaotic orbit is of order $O(n)$ for OFLI^2 while it is easy the orbit is chaotic for UFLI.

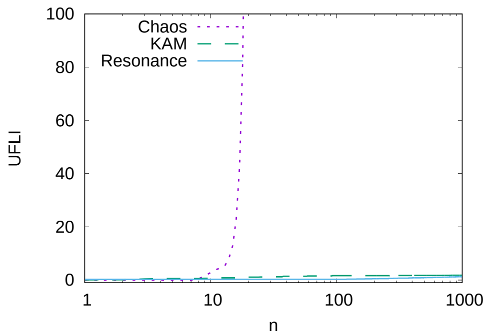

Figure A.1: Time evolution of UFLI for the standard map for $\varepsilon = 0.9$ and $d = 0.001$. Compare with the other three indicators, UFLI shows rapid growth for the chaotic orbit.

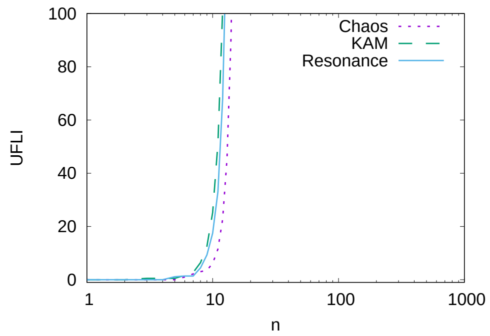

Figure A.2: Time evolution of UFLI for the standard map for $\varepsilon = 0.9$ and $d = 1.0$. In all the three cases, the time evolutions of UFLI grow exponentially. Thus, UFLI cannot distinguish the three orbits when $d = 1.0$.

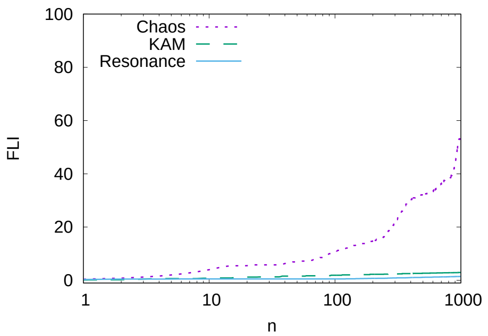

Figure A.3: Time evolution of FLI for the standard map for $\varepsilon = 0.9$ and $d = 0.001$. FLI can distinguish chaotic orbit from orbits on torus.

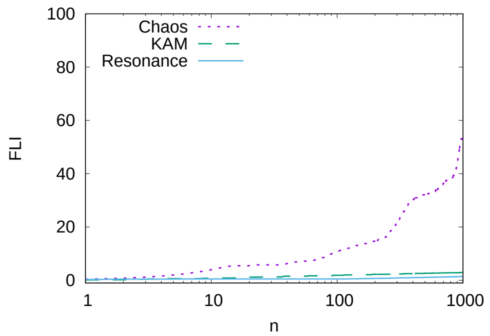

Figure A.4: Time evolution of FLI for the standard map for $\varepsilon = 0.9$ and $d = 1.0$. FLI can distinguish chaotic orbit from orbits on torus.

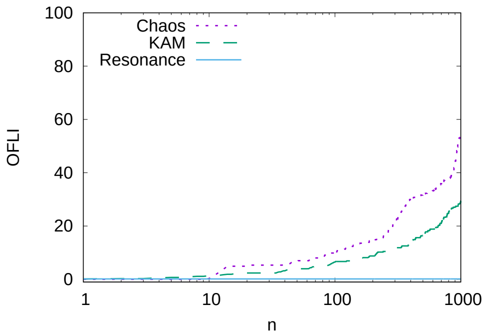

Figure A.5: Time evolution of OFLI for the standard map for $\varepsilon = 0.9$ and $d = 0.001$. OFLI cannot distinguish a chaotic orbit from orbits on torus because OFLI for the orbit on KAM torus grow exponentially.

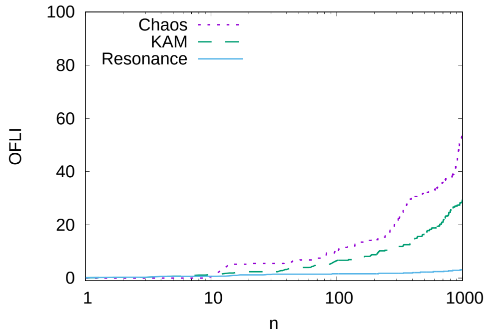

Figure A.6: Time evolution of OFLI for the standard map for $\varepsilon = 0.9$ and $d = 1.0$. OFLI cannot distinguish a chaotic orbit from orbits on torus because OFLI for the orbit on KAM torus grow exponentially.

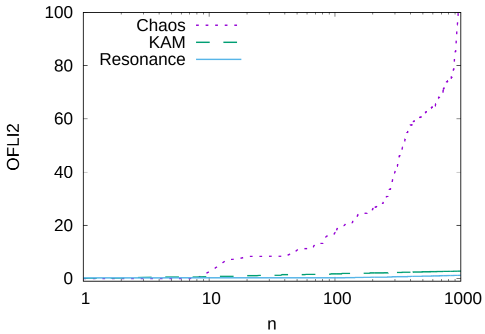

Figure A.7: Time evolution of OFLI^2 for the standard map for $\varepsilon = 0.9$ and $d = 0.001$. OFLI^2 can detect a chaotic orbit.

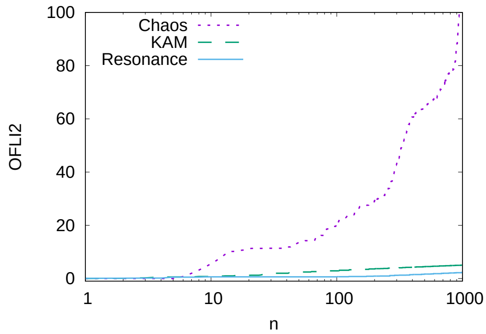

Figure A.8: Time evolution of OFLI^2 for the standard map for $\varepsilon = 0.9$ and $d = 1.0$. OFLI^2 can detect a chaotic orbit.

A.2.2 Application of UFLI for Froeschlé map

Next, we apply chaotic indicators to Froeschlé map. According to C. Froeschlé, M. Guzzo and E. Lega [131], for Froeschlé map at $\varepsilon = 0.6$ point A $(I_1, \theta_1, I_2, \theta_2) = (2.07, 0, 2.1, 0)$ is in chaotic region, point B $(1.8, 0, 1.2, 0)$ is in KAM torus region and point C $(1.67, 0, 0.91, 0)$ is in Resonance torus region. We research the behavior of FLI, OFLI, OFLI^2 and UFLI using *exflib* with PRECISION 50. The initial conditions $(I_1(0), 0, I_2(0), 0)$ is parallel to the flow as

$$\boldsymbol{v}(0) = F(\boldsymbol{x}(0)) \times 0.01, \tag{A.2.11}$$

$$\varepsilon = 0.6. \tag{A.2.12}$$

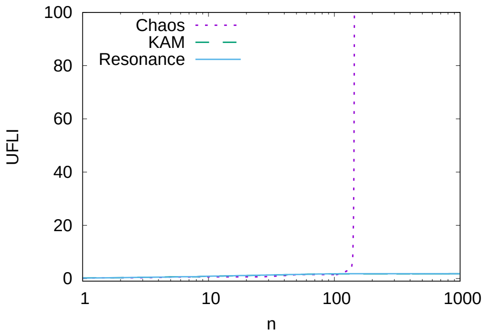

Figure A.9: Time evolution of UFLI for Froeschlé map for $\varepsilon = 0.6$ and $d = 0.01$. Compare with the other three indicators, UFLI shows rapid growth for the chaotic orbit.

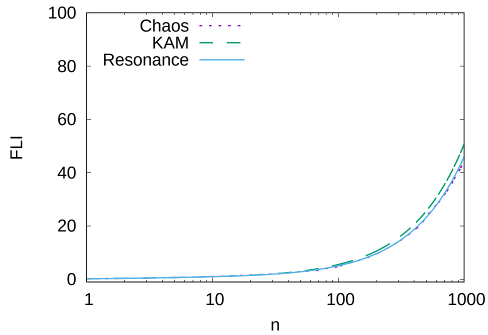

Figure A.10: Time evolution of FLI for Froeschlé map for $\varepsilon = 0.6$ and $d = 0.01$. FLI cannot distinguish the three types of orbit.

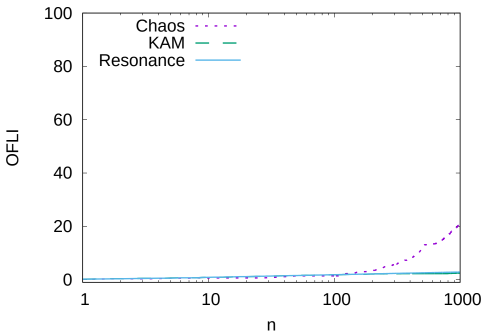

Figure A.11: Time evolution of OFLI for Froeschlé map for $\varepsilon = 0.6$ and $d = 0.01$. OFLI can distinguish chaotic orbit from the other two orbits. However around $n \sim 200$, it is difficult to determine the chaotic orbit is of order $O(n)$.

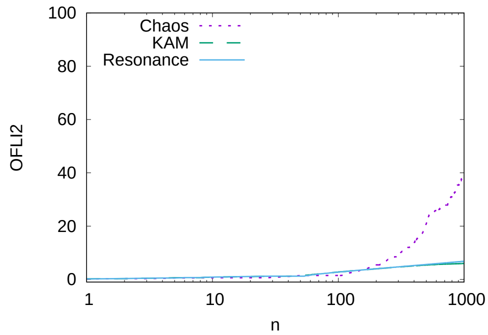

Figure A.12: Time evolution of OFLI^2 for Froeschlé map for $\varepsilon = 0.6$ and $d = 0.01$. OFLI^2 distinguish chaotic orbit from the other two orbits. However around $n \sim 200$, it is difficult to determine the chaotic orbit is of order $O(n)$.

Figures A.9-A.12 show for a chaotic orbit the time evolution of UFLI is more drastic than FLI, OFLI and OFLI^2. According to Figure A.9, the behavior of UFLI changes drastically around $100 \lesssim n \lesssim 200$. Then we researched whether these four indicators can detect chaoticity in short iterations. Figures A.13- A.20 show diagrams of chaotic indicator for Froeschlé map at $n = 200$ varying initial value of I_1 and I_2 with $\varepsilon = 0.6$. Initial values of θ_1 and θ_2 are zero.

Figures A.13, A.15, A.17 and A.19 show the values of indicators for each initial point scaled to $[1, 3] \ni \log_{10}(200)$. We can say UFLI, FLI and OFLI can detect Arnold web but OFLI^2 cannot. As explained above, for an orbit on a torus, the equation below holds.

$$\mathrm{FLI}(n) \sim O(\log(n)). \tag{A.2.13}$$

Then, if we assume the other indicators are also in accordance with $O(\log(n))$ for a orbit on torus, it can be difficult to distinguish chaotic area from torus area when we set the scale as $[1, 3] \ni \log_{10}(200)$ as Figure A.19.

Now, Figures A.14, A.16, A.18 and A.20 show the values of indicators for each initial point scaled to $[1, 200]$.

Let us focus on Figure A.14. UFLI can detect Arnold web (chaotic regions along resonance lines represented by white area) clearly. According to Figures A.14, A.16, A.18 and A.20, UFLI can represent the difference between chaotic orbits and orbits on torus more clearly than the other three indicators.

FLI (Figure A.15),OFLI (Figure A.17) and OFLI^2 (Figure A.19) cannot distinguish torus regions from chaotic regions clearly.

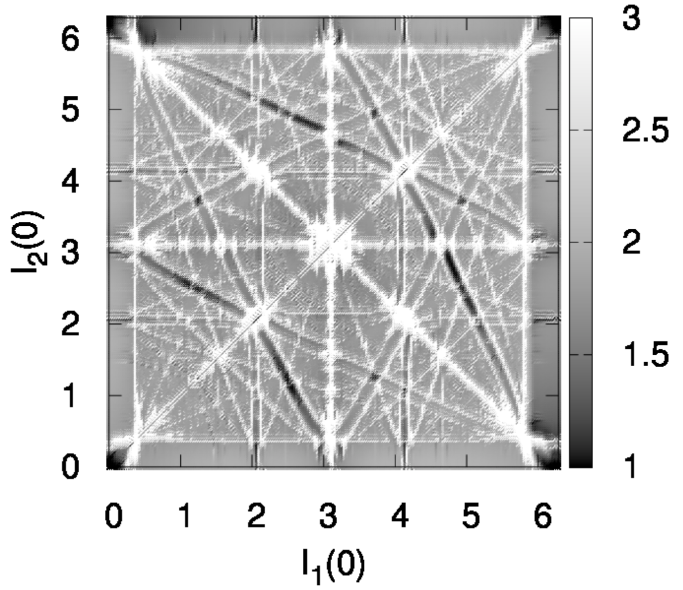

Figure A.13: Diagram of UFLI for Froeschlé map at $\varepsilon = 0.6$ at $n = 200$. UFLI can distinguish a Arnold web (chaotic regions along resonance lines represented by white area) from torus regions.

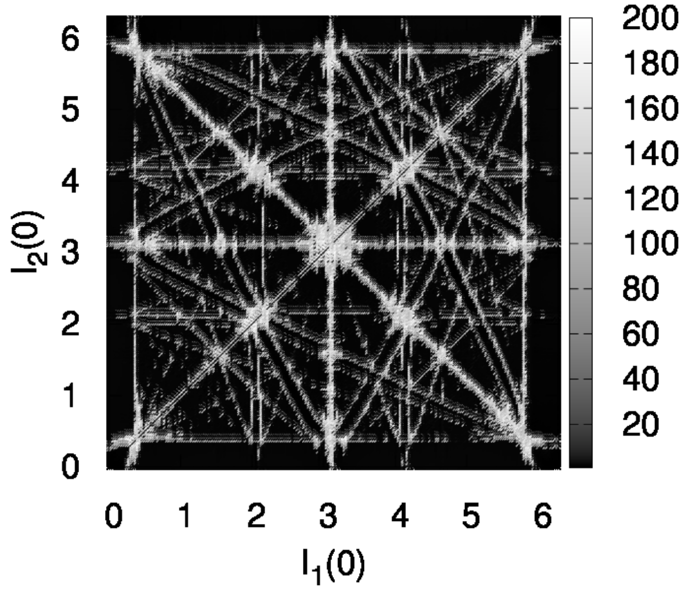

Figure A.14: Diagram of UFLI for Froeschlé map at $\varepsilon = 0.6$ at $n = 200$. The scale of value of UFLI is changed from [1, 3] to [1, 200]. The value of UFLI for a chaotic orbit is quite larger than that for an orbit on KAM torus or Resonance torus.

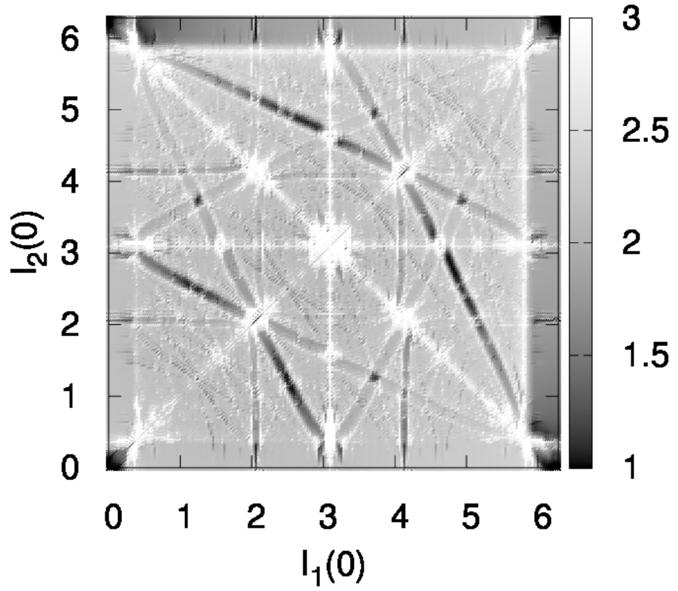

Figure A.15: Diagram of FLI for Froeschlé map at $\varepsilon = 0.6$ at $n = 200$. FLI can detect a Arnold web.

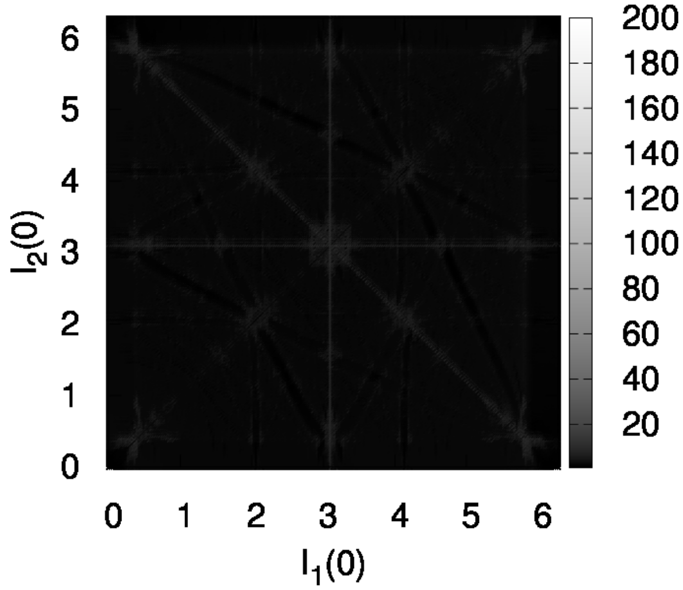

Figure A.16: The scale of value of FLI is changed from $[1, 3]$ to $[1, 200]$. The value of FLI for a chaotic orbit is not quite different from that for an orbit on KAM torus or Resonance torus. Thus, it is difficult to distinguish chaotic regions (corresponding to FLI $\sim O(200)$) from torus regions (corresponding to FLI $\sim O(\log_{10}(200))$ at $n = 200$.

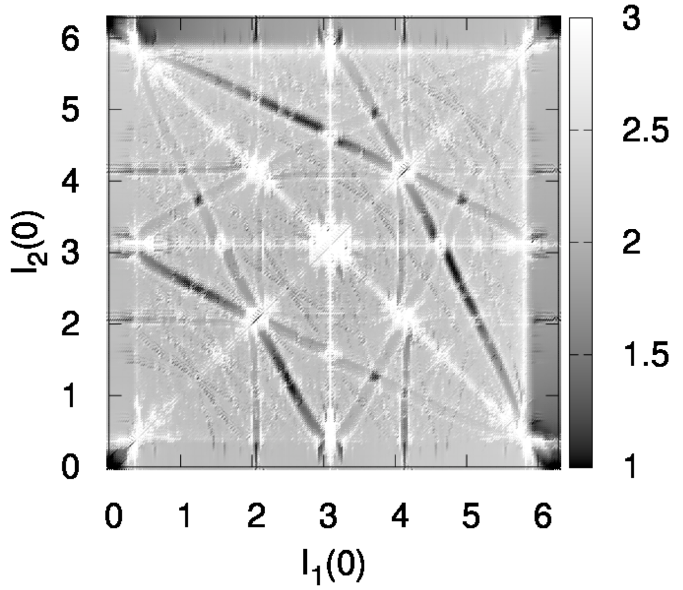

Figure A.17: Diagram of OFLI for Froeschlé map at $\varepsilon = 0.6$ at $n = 200$. OFLI can detect a Arnold web.

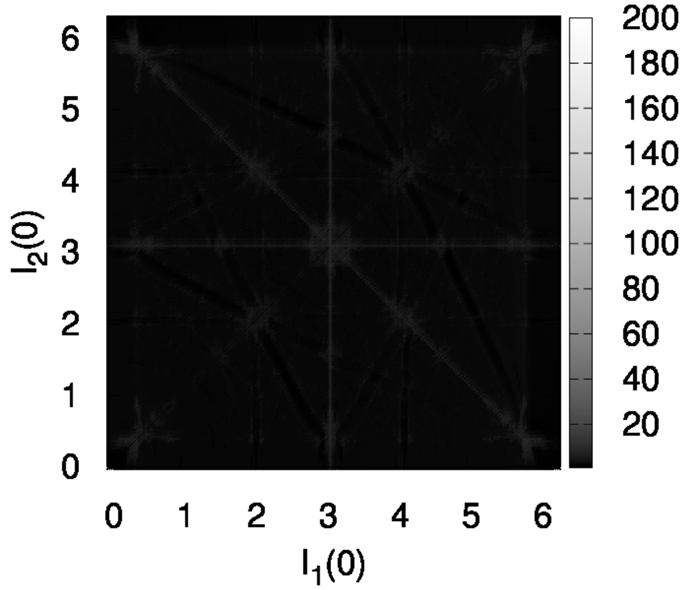

Figure A.18: Diagram of OFLI for Froeschlé map at $\varepsilon = 0.6$ at $n = 200$. The scale of value of OFLI is changed from [1, 3] to [1, 200]. The value of OFLI for a chaotic orbit is not quite different from that for an orbit on KAM torus or Resonance torus. Thus, it is difficult to distinguish chaotic regions (corresponding to OFLI $\sim O(200)$) from torus regions (corresponding to OFLI $\sim O(\log_{10}(200))$ at $n = 200$.

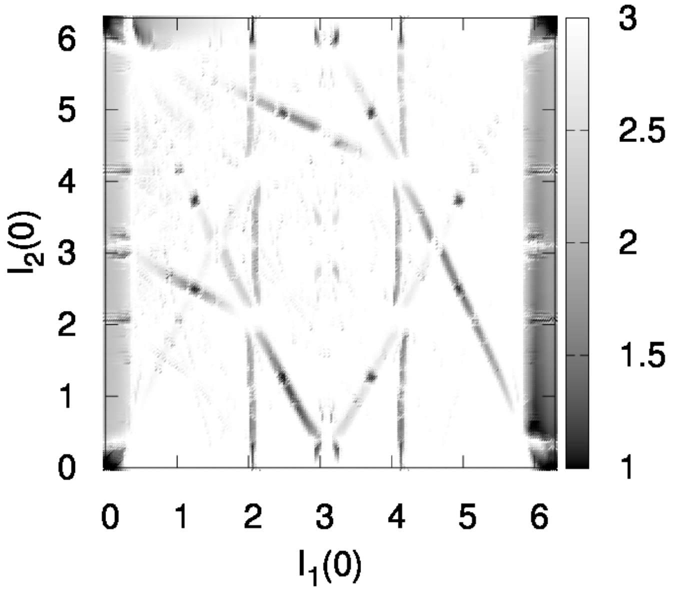

Figure A.19: Diagram of OFLI^2 for Froeschlé map at $\varepsilon = 0.6$ at $n = 200$. It is difficult to distinguish chaotic regions from torus regions.

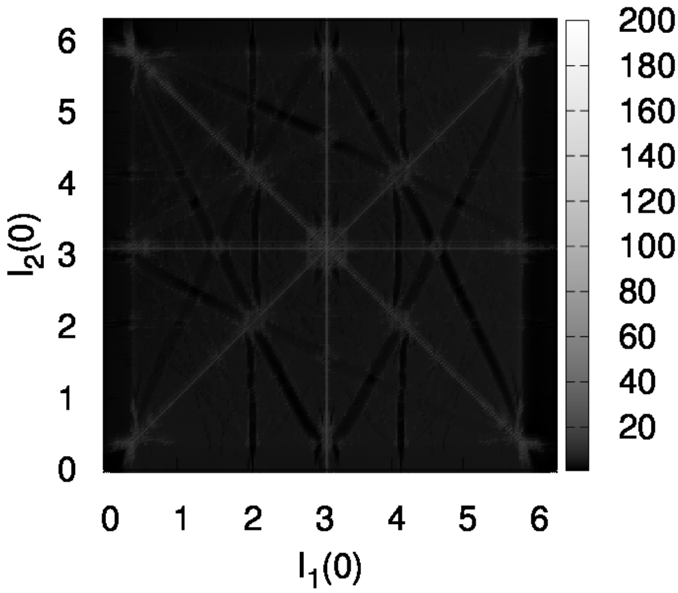

Figure A.20: Diagram of OFLI^2 for Froeschlé map at $\varepsilon = 0.6$ at $n = 200$. The scale of value of OFLI^2 is changed from [1, 3] to [1, 200]. Although some parts of Arnold web can be observed, it is less clear than that in Figure A.14.

A.2.3 Application of UFLI for the generalized Boole transformations

We investigated the sub-exponential behavior [84]. In a sub-exponential behavior, an orbital expansion rate Δ is estimated by

$$\Delta \sim \exp(n^{\tau}),\ 0 < \tau < 1. \tag{A.2.14}$$

In the Boole transformation

$$x_{n+1} = x_n - \frac{1}{x_n},\ x_n \in \mathbb{R}, \tag{A.2.15}$$

a sub-exponential behavior occurs [84] while the generalized Boole transformations (A.2.9) for $0 < \alpha < 1$, is chaotic[49] and its Lyapunov exponent λ [49] is analytically given by

$$\lambda = \log\left(1 + 2\sqrt{\alpha(1-\alpha)}\right) > 0. \tag{A.2.16}$$

The Lyapunov exponent is independent of β. Then, we compare the behavior of UFLI with FLI for both the Boole transformation and the generalized Boole transformation for $\alpha = 0.99999, 0.9999, 0.999, 0.99, 0.9$, where initial point is $x_0 = \pi$ and initial variational vector is $v(0) = 10^{-30}$. As Figures A.21 and A.22 show, both UFLI and FLI can detect chaoticity for $\alpha < 1$ in the range of $n < 10000$. However, the value of UFLI grows more rapidly than FLI except for $\alpha = 0.999$, which is the weak chaos near to the infinite ergodic point [49] while the difference in growing speed of the indicator values is relatively small compared with the standard map or the Froeschlé map.

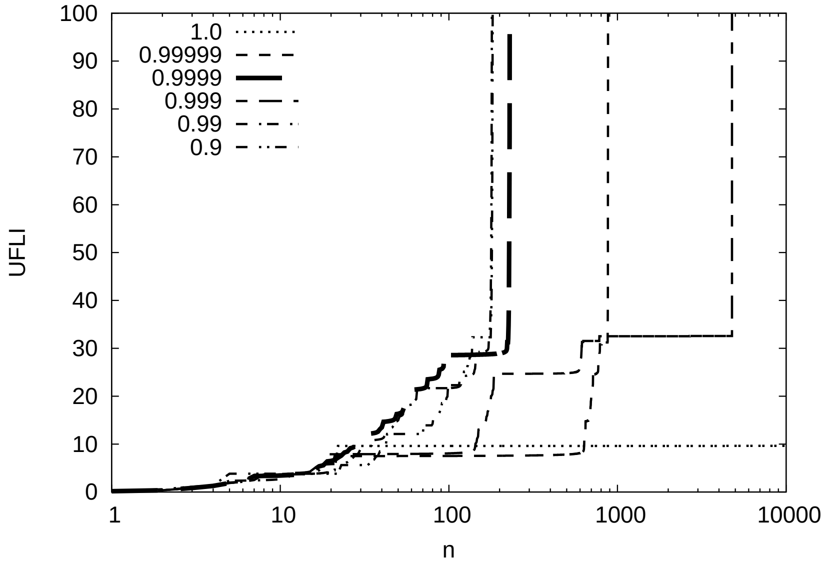

Figure A.21: Time evolutions of UFLI for the Boole transformation and the generalized Boole transforamtions for $\alpha = 0.99999, 0.9999, 0.999, 0.99, 0.9$. The initial condition is $x_0 = \pi$ and $v(0) = 10^{-30}$. At $\alpha = 0.999$, the growth rate of UFLI is smaller than that of FLI.

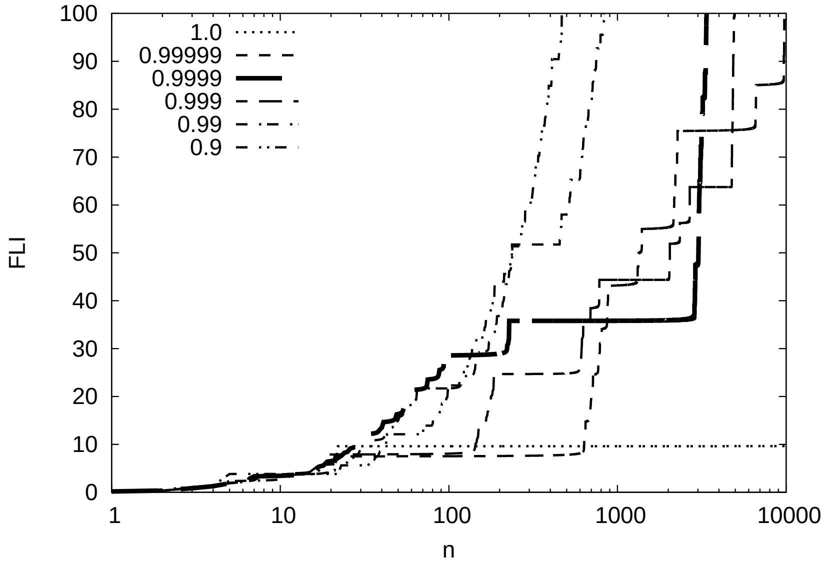

Figure A.22: Time evolutions of FLI for the Boole transformation and the generalized Boole transforamtions for $\alpha = 0.99999, 0.9999, 0.999, 0.99, 0.9$. The initial condition is $x_0 = \pi$ and $v(0) = 10^{-30}$.

A.3 Log Fast Lyapunov Indicator (LFLI)

A.3.1 Quantification of orbits with zero Lyapunov exponent

Lyapunov exponent and FLI are indicator to detect whether orbital expansion rate increases exponentially. We propose Log Fast Lyapunov Indicator (LFLI) in order to quantify orbits time evolutions of FLI of which are different although these Lyapunov exponents are zero.

A.3.2 Boole transformation and Generalized Boole transformation

It is known that Boole transformation

$$x_{n+1} = T(x_n) \stackrel{\text{def}}{=} x_n - \frac{1}{x_n} \tag{A.3.1}$$

preserves Lebesgue measure and is ergodic[79]. According to [80], for measure space $(\mathbb{R}, \mathfrak{B}, m)$ it holds that

$$\lim_{n\to\infty} \frac{1}{n} \sum_{k=1}^{n} f(T^k x) = 0, \text{ a.e.} x \in \mathbb{R}, \ {}^{\forall} f \in L^1(m) \tag{A.3.2}$$

where $\mathfrak{B}$ represents sigma-algebra for a family of subsets of $\mathbb{R}$ and m represents the Lebesgue measure. Then, by substituting $f(x_k) = \log |T'(x_k)|$, we see that the Lyapunov exponent of Boole transformation is zero. According to [84], time evolution of ensemble average of FLI obeys $O(n^{1/2})$.

On the other hand, according to [49], for generalized Boole transformation

$$x_{n+1} = T_{\alpha,\beta} \stackrel{\text{def}}{=} \alpha x_n - \frac{\beta}{x_n}, \ 0 < \alpha < 1, 0 < \beta, \tag{A.3.3}$$

its Lyapunov exponent is regardless of β and represents as

$$\lambda = \log\left(1 + 2\sqrt{\alpha(1-\alpha)}\right). \tag{A.3.4}$$

From above equation, the ensemble average of Lyapunov exponent is positive in $0 < \alpha < 1$ although it converges to zero from positive value in the limit of $\alpha \to 1$.

A.3.3 S-unimordal function

S-unimordal function whose Lyapunov exponent is zero is defined as following.

$$X_{n+1} = T_S(X_n) \stackrel{\text{def}}{=} \frac{1 - 5X_n^2}{1 + 3X_n^2}, \ X_n \in [-1, 1]. \tag{A.3.5}$$

S-unimordal function has infinite measure as invariant measure and corresponding density function is

$$\rho(X) = \frac{1}{(1+X)\sqrt{1-X^2}}. \tag{A.3.6}$$

According to [132], the orbital expansion rate for S-unimordal function is $\langle\Delta\rangle \sim \exp\left(n^{\frac{1}{2}}\right)$ and we see that its Lyapunov exponent is zero. According to infinite ergodic theorem, in finite calculation time, calculated Lyapunov exponent does not converge to zero.

A.3.4 Application of LFLI

As above discussion, generalized Boole transformation transfers to Boole transformation at $\alpha = 1$. That is, orbital expansion rate transfers from $\Delta \sim \exp(n)$ to $\Delta \sim \exp(\sqrt{n})$. In order to detect this transition, we define Log Fast Lyapunov Indicator (LFLI) as follows.

$$\mathrm{LFLI}(\boldsymbol{x}(0), \boldsymbol{v}(0), n) \stackrel{\mathrm{def}}{=} \log\left[\sup_{0<i\leq n} \log\left(\frac{\|\boldsymbol{v}(i)\|}{\|\boldsymbol{v}(0)\|}\right)\right]. \tag{A.3.7}$$

LFLI evolves with a slope of unity on a $\log n$ time scale when an initial point is on the chaotic region. When its slope is less than unity on a $\log n$ order, its Lyapunov exponent is zero. Then, Figure A.23 shows time evolution of LFLI for ensemble average for one hundred points near $x_0 = 9.3$ for Boole transformation and generalized Boole transformation at $\alpha = 0.9995$. Initial variation vector is $\boldsymbol{v}(0) = 0.00000000000000000001$ and float128 is used. The computing environment is 2.2 GHz Intel Core i7. Because the value of FLI is negative in $\log_{10} n < 3.2$, the values of LFLI do not be defined in $\log_{10} n < 3.2$. The value of LFLI do not be defined in $\log_{10} n > 5.5$ because the value of FLI is inf in that region. According to Figure A.23, the slope of LFLI is unity in $\alpha < 1$ although at $\alpha = 1$, the slope is $1/2$ because sub-exponential diffusion [84] occurs. Here, let us define

$$\begin{aligned} f(\log_{10}(n)) &= A\log_{10}(n) + B, \\ g(\log_{10}(n)) &= C\log_{10}(n) + C. \end{aligned} \tag{A.3.8}$$

and fit LFLI at $\alpha = 1$ and 0.9995 with the least squares method. Then we obtain $A \simeq 0.514$ and $C \simeq 0.917$. According to these results, we can say LFLI detects sub-exponential behavior.

In addition, Figure A.24 shows ensemble average of time evolution of LFLI for one hundred initial point near $X = \exp(-1.2)$ for S-unimordal function. The initial variation vector is $\boldsymbol{v}(0) = \exp(-5)$ and float128 is used. Because the slope of LFLI is about 0.515 which is close to 0.5, LFLI detects exponent of sub-exponential behavior.

From the above, we succeeded in detecting exponent of orbital expansion rate for maps which show sub-exponential diffusion with Lyapunov exponent zero. Exponents of orbital expansion rate is quantitative property of maps and it can be said that LFLI is an indicator which shows quantitative property of maps whose Lyapunov exponent is zero.

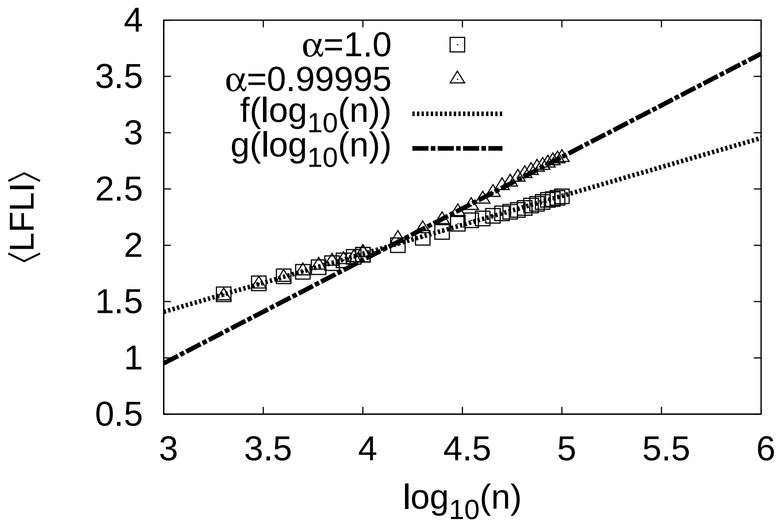

Figure A.23: The time evolution of ensemble average of LFLIs with $\alpha = 1.0$ and $\alpha = 0.99995$ and $f(\log(n))$ and $g(\log(n))$ witch are the linear approximations of the ensemble average of LFLIs. Hundred initial points are taken in the neighbourhood of the point $x = 9.3$

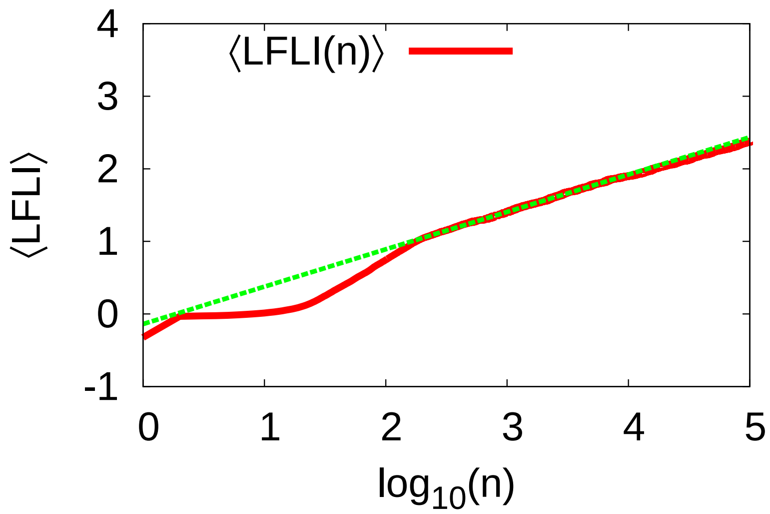

Figure A.24: The time evolution of ensemble average of LFLI of the S-unmodal function. A slape of linear approximation for LFLI is about 0.515. Hundred initial points are taken in the neighbourhood of the point $X = \exp(-1.2)$. The common logarithm is used to calculate LFLI.

A.4 Conclusion

We proposed new chaos indicators, *Ultra Fast Lyapunov Indicator* (UFLI) and *Log Fast Lyapunov Indicator* (LFLI). For the standard map for $\delta = 0.9$ and Froeschlé map for $\varepsilon = 0.6$, the value of UFLI increases more rapidly than FLI, OFLI and OFLI^2 when an initial variational vector is *parallel* to flow and the length of initial variational vector is properly chosen. That is, if an initial condition is properly chosen, the UFLI can distinguish chaos regions from torus regions in short iterations while the other three indicators cannot.

For the generalized Boole transformation, the value of UFLI grows more rapidly than FLI except for $\alpha = 0.999$, which is the weak chaos near to the infinite ergodic point while the difference in growing speed of the indicator values is relatively small compared with the standard map or the Froeschlé map.

In terms of LFLI, we checked its ability by generalized Boole transformation, Boole transformation and S- unimordal function. From results, LFLI can detect the deference between exponential behavior of orbital expansion rate and sub-exponential behavior whose Lyapunov exponent is zero.

We need an optimal condition with a length of initial variational vector. We hope to able to find a relationship between a length of initial variational vector and a threshold of iteration time in which UFLI can perform property. We also need to research whether UFLI work properly over the long range of parameters. Further researches are to be expected.

Appendix B

Super Generalized Boole transformation

B.1 Outline of this Appendix

In this Appendix it is shown that

1. the critical exponent of the Lyapunov exponent is $\nu = \frac{1}{2}$ for $K = 3, 4$ and 5.

B.2 Scaling behavior for $K = 3, 4$ and 5

The solutions of (2.3.16), which satisfied $0 < \gamma_{K,\alpha} < \infty$ in the cases of $K = 3, 4$, and 5 are determined uniquely when the parameters (K, α) are in Range A as follows.

$$
\begin{aligned}
\gamma_{3,\alpha} &= \sqrt{\frac{9\alpha - 1}{3 - 3\alpha}}, \\
\gamma_{4,\alpha} &= \sqrt{\frac{6\alpha - 1 + \sqrt{32\alpha^2 - 8\alpha + 1}}{2(1 - \alpha)}}, \\
\gamma_{5,\alpha} &= \sqrt{\frac{-5(1 - 5\alpha) + \sqrt{20(25\alpha^2 - 6\alpha + 1)}}{5(1 - \alpha)}}.
\end{aligned}
\tag{B.2.1}
$$

The analytical formulae of the Lyapunov exponent can be determined from (2.3.74) as follows.

$$
\begin{aligned}
\lambda_{3,\alpha} &= \log\left|\frac{1}{\alpha}\left(\frac{3(1-\alpha)}{8}\right)^2\left[1+\sqrt{\frac{9\alpha-1}{3-3\alpha}}\right]^4\right|, \\
\lambda_{4,\alpha} &= \log\left|\frac{\alpha(1+\gamma_4)^6}{\gamma_4^2(1+\gamma_4^2)^2}\right|, \\
\lambda_{5,\alpha} &= \log\left|\frac{25}{256\alpha}\frac{(1-\alpha)^4}{(\sqrt{125\alpha^2-30\alpha+5}+11\alpha-1)^2}|1+\gamma_5|^8\right|.
\end{aligned}
\tag{B.2.2}
$$

In the case of $K = 3$, equation (B.2.2) converges to zero in the limit of $\alpha \to \frac{1}{9}+0$ and $\alpha \to 1-0$, and the derivative of the Lyapunov exponent $\frac{\partial\lambda_{3,\alpha}}{\partial\alpha}$ diverges at $\alpha = \frac{1}{9}, 1$. When the parameter α is close to $\frac{1}{9}$, the Lyapunov exponent increases as follows.

$$
\begin{aligned}
\lambda_{3,\alpha} &= -\log\left|1+9\left(\alpha-\frac{1}{9}\right)\right| + 2\log\left|1-\frac{9}{8}\left(\alpha-\frac{1}{9}\right)\right| + 4\log\left|1+\sqrt{\frac{3\left(\alpha-\frac{1}{9}\right)}{1-\alpha}}\right|, \\
&= O\left(-9\left(\alpha-\frac{1}{9}\right)-\frac{9}{4}\left(\alpha-\frac{1}{9}\right)+4\sqrt{\frac{3\left(\alpha-\frac{1}{9}\right)}{1-\alpha}}\right), \\
&\sim 6\sqrt{\frac{3}{2}}\sqrt{\alpha-\frac{1}{9}}.
\end{aligned}
\tag{B.2.3}
$$

Then, the critical exponent ν_2 of the Lyapunov exponent at $\alpha = \frac{1}{9}$ is $\frac{1}{2}$. In the case of $\alpha \lesssim 1$, the Lyapunov exponent $\lambda_{3,\alpha}$ behaves as follows.

$$
\begin{aligned}
\lambda_{3,\alpha} &= 2\log\left|1-\frac{9}{8}(1-\alpha)\right| - \log|1-(1-\alpha)| + 4\log\left|1+\sqrt{\frac{1-\alpha}{3\left(\alpha-\frac{1}{9}\right)}}\right|, \\
&= O\left(\frac{9}{4}(1-\alpha)-(1-\alpha)+4\sqrt{\frac{1-\alpha}{3\left(\alpha-\frac{1}{9}\right)}}\right), \\
&\sim 2\sqrt{\frac{3}{2}}\sqrt{1-\alpha}.
\end{aligned}
\tag{B.2.4}
$$

Then, at $\alpha = 1$ one has $\nu_1 = \frac{1}{2}$.

For $K = 3$ and for $\frac{1}{9} < \alpha < 1$, the fixed point is only

$$x^* = 0. \tag{B.2.5}$$

In the range of $0 < \alpha < \frac{1}{9}$ and $1 < \alpha$, there are other fixed points $q_\pm(\alpha)$ denoted as $q_\pm^2(\alpha) = -\dfrac{9\alpha - 1}{3(1-\alpha)}$. Then it holds that

$$\begin{aligned} \lim_{\alpha\to\frac{1}{9}-0} q_\pm^2(\alpha) = +0, &\quad \lim_{\alpha\to\frac{1}{9}-0} S'_{3,\alpha}(q_\pm(\alpha)) = 1, \\ \lim_{\alpha\to 1+0} q_\pm^2(\alpha) = +\infty, &\quad \lim_{\alpha\to 1+0} S'_{3,\alpha}(q_\pm(\alpha)) = 1, \end{aligned} \tag{B.2.6}$$

Then, the Floquet multiplier χ at $\alpha = \frac{1}{9}$ and $\alpha = 1$ are denoted as follows.

$$\begin{aligned} \chi_{3,\frac{1}{9}} &= S'_{3,\frac{1}{9}}(0) &&= 1, \\ \chi_{3,1} &= \lim_{\alpha\to 1+0} S'_{3,\alpha}(q_\pm(\alpha)) &&= 1. \end{aligned} \tag{B.2.7}$$

On the basis of these results, we can say that only *Type 1* intermittency occurs for $K = 3$. These results represent new phenomena because, for the generalized Boole transformation (K=2), one can observe *two* different intermittency types, *Type 1* and *Type 3* [49].

In the case of $K = 4$, the Lyapunov exponent (B.2.2) is denoted as

$$\lambda_{4,\alpha} = \log\left|\frac{\alpha}{\gamma_4^2}\right| + 6\log|1+\gamma_4| - 2\log|1+\gamma_4^2|. \tag{B.2.8}$$

Let us discuss the scaling behavior of $\lambda_{4,\alpha}$ at $\alpha = 0$. Now, the first term of (B.2.8) is rewritten as

$$\begin{aligned} \left|\frac{\alpha}{\gamma_4^2}\right| &= \log\left|\frac{2\alpha(1-\alpha)}{6\alpha - 1 + \sqrt{32\alpha^2 - 8\alpha + 1}}\right|, \\ &= \left|-\frac{6\alpha - 1 - \sqrt{32\alpha^2 - 8\alpha + 1}}{2}\right|, \end{aligned} \tag{B.2.9}$$

$$\therefore \lim_{\alpha\to 0}\left|\frac{\alpha}{\gamma_4^2}\right| = 1. \tag{B.2.10}$$

Then,

$$\begin{aligned} \gamma_4 &\sim \sqrt{\alpha}, \\ \Longrightarrow \log|1+\gamma_4| &\sim \sqrt{\alpha}, \text{ and } \log\left|1+\gamma_4^2\right| \sim \alpha, \\ \therefore \lambda_{4,\alpha} &\sim 6\sqrt{\alpha} = O\left(\sqrt{\alpha}\right). \end{aligned} \tag{B.2.11}$$

Therefore, the critical exponent of the Lyapunov exponent for $K = 4, \alpha = 0$ is

$$\nu_3 = \frac{1}{2}. \tag{B.2.12}$$

Next, consider the scaling behavior of $\lambda_{4,\alpha}$ at $\alpha = 1 - 0$. From (B.2.9), it holds that, in the vicinity of $\alpha = 1$,

$$\begin{aligned} \lim_{\alpha \to 1-0} \frac{\gamma_4^2(1-\alpha)}{5} &= 1, \\ \therefore \gamma_4 &\sim \sqrt{\frac{5}{1-\alpha}} \text{ as } \alpha \to 1-0. \end{aligned} \tag{B.2.13}$$

The Lyapunov exponent of (B.2.8) are denoted as

$$\begin{aligned} \lambda_{4,\alpha} &= \log\left|\frac{\alpha}{\gamma_4^2}\right| + 6\log\gamma_4 + 6\log\left|1+\frac{1}{\gamma_4}\right| - 2\log\left|\gamma_4^2\right| - 2\log\left|1+\frac{1}{\gamma_4^2}\right|, \\ &= \log|\alpha| + 6\log\left|1+\frac{1}{\gamma_4}\right| - 2\log\left|1+\frac{1}{\gamma_4^2}\right|, \\ &= O\left(-(1-\alpha) + \frac{6}{\gamma_4} - \frac{2}{\gamma_4^2}\right), \\ \therefore \lambda_{4,\alpha} &\sim \frac{6\sqrt{5}}{5}\sqrt{1-\alpha}, \text{ as } \alpha \to 1-0. \end{aligned} \tag{B.2.14}$$

Therefore, the critical exponent of the Lyapunov exponent for $K = 4, \alpha = 1 - 0$ is

$$\nu_1 = \frac{1}{2}. \tag{B.2.15}$$

In the case of $K = 4$, the fixed points of $S_{4,\alpha}$ are as follows.

$$x_{4*} = \begin{cases} 0, & \alpha = 0, \\ \pm\sqrt{\dfrac{1-6\alpha\pm\sqrt{32\alpha^2-8\alpha+1}}{2(1-\alpha)}}, & 0 < \alpha < 1, \\ \pm\dfrac{1}{\sqrt{5}}, & \alpha = 1. \end{cases} \tag{B.2.16}$$

It also holds that

$$\begin{aligned} S_{4,\alpha}(x) - x &= \frac{4(\alpha-1)x^4 - 4(6\alpha+1)x^2 + 4\alpha}{4x^3 - 4x}, \\ \lim_{|x|\to\infty}\left(S_{4,1}(x) - x\right) &= 0. \end{aligned} \tag{B.2.17}$$

In the case of SGB transformations, at $\alpha = 0$, all points are mapped to the original point $x = 0$. As this is not interesting, other fixed points are considered as follows.

$$\begin{aligned}
\lim_{\alpha\to+0} S'_{4,\alpha}\left(\pm\sqrt{\frac{1-6\alpha+\sqrt{32\alpha^2-8\alpha+1}}{2(1-\alpha)}}\right) &= +\infty, \\
\lim_{\alpha\to+0} S'_{4,\alpha}\left(\pm\sqrt{\frac{1-6\alpha-\sqrt{32\alpha^2-8\alpha+1}}{2(1-\alpha)}}\right) &= -1, \\
S'_{4,1}\left(\pm\frac{1}{\sqrt{5}}\right) &= \frac{27}{2}, \\
\lim_{|x|\to\infty} S'_{4,1}(x) &= 1.
\end{aligned} \tag{B.2.18}$$

For $K = 4$, from (B.2.18), one obtains the Floquet multiplier at $\alpha = 1$ as

$$\chi_{4,1} = 1 \tag{B.2.19}$$

and at $\alpha = 0$ as

$$\chi_{4,0} = -1. \tag{B.2.20}$$

This result indicates that *Type 1* intermittency occurs at $\alpha = 1$ and *Type 3* intermittency occurs at $\alpha = 0$.

In the case of $K = 5$, equation (B.2.2) converges to zero in the limit of $\alpha \to \frac{1}{25} + 0$ and $\alpha \to 1 - 0$. In addition, it holds that $\left|\frac{\partial\lambda_{5,\alpha}}{\partial\alpha}\left(\frac{1}{25}\right)\right| = \left|\frac{\partial\lambda_{5,\alpha}}{\partial\alpha}(1)\right| = \infty$. The Lyapunov exponent $\lambda_{5,\alpha}$ for $\frac{1}{25} < \alpha < 1$ can be expanded as

$$\lambda_{5,\alpha} = \log\frac{25}{256} - \log|\alpha| + 4\log|1-\alpha| - 2\log\left|1 - 11\alpha - \sqrt{125\alpha^2 - 30\alpha + 5}\right| + 8\log|1+\gamma_5|. \tag{B.2.21}$$

Now, the sum from the first term to the forth term converges to zero such that

$$\lim_{\alpha\to\frac{1}{25}+0}\left[\log\frac{25}{256} - \log|\alpha| + 4\log|1-\alpha| - 2\log\left|1 - 11\alpha - \sqrt{125\alpha^2 - 30\alpha + 5}\right|\right] = 0. \tag{B.2.22}$$

When the parameter α is close to $\frac{1}{25}$, it holds that

$$\begin{aligned}
& 4\log|1-\alpha| - 2\log\left|1 - 11\alpha - \sqrt{125\alpha^2 - 30\alpha + 5}\right|, \\
= \; & 2\log\left|\frac{1}{4}\left\{1 - 11\alpha + \sqrt{125\alpha^2 - 30\alpha + 5}\right\}\right|, \\
= \; & -4\log 2 + 2\log\frac{14}{25} + 2\log\left|1 - \frac{275}{14}\left(\alpha - \frac{1}{25}\right) + \frac{25}{14}\sqrt{\frac{20}{5} - 20\left(\alpha - \frac{1}{25}\right) + 125\left(\alpha - \frac{1}{25}\right)^2}\right|.
\end{aligned} \tag{B.2.23}$$

Then, the Lyapunov exponent increases as follows

$$\begin{aligned}
\lambda_{5,\alpha} \quad = \quad & \log \tfrac{25}{256} - \log \tfrac{1}{25} - \log \left|1 + 25\left(\alpha - \tfrac{1}{25}\right)\right| \\
& -4 \log 2 + 2 \log \tfrac{14}{25} \\
& +2 \log \left|1 - \tfrac{275}{14}\left(\alpha - \tfrac{1}{25}\right) + \tfrac{25}{14}\sqrt{\tfrac{20}{5} - 20\left(\alpha - \tfrac{1}{25}\right) + 125\left(\alpha - \tfrac{1}{25}\right)^2}\right| \\
& +8 \log |1 + \gamma_5| .
\end{aligned} \tag{B.2.24}$$

From (B.2.22), the Lyapunov exponent obeys as

$$\lambda_{5,\alpha} = O\left(\left(\alpha - \frac{1}{25}\right) + 8\gamma_5\right) \sim 8\gamma_5 \sim 20\sqrt{\frac{5}{6}\left(\alpha - \frac{1}{25}\right)}. \tag{B.2.25}$$

Therefore, the critical exponent ν_2 is denoted as

$$\nu_2 = \frac{1}{2}. \tag{B.2.26}$$

For $\alpha \lesssim 1$, it holds that

$$\lim_{\alpha \to 1-0} \left\{\log \frac{25}{256} - \log|\alpha| - 2\log\left|1 - 11\alpha - \sqrt{125\alpha^2 - 30\alpha + 5}\right|\right\} = -12\log 2, \tag{B.2.27}$$

$$4\log|1-\alpha| + 8\log|1+\gamma_5| \sim 8\log\left|2\sqrt{2} + \sqrt{1-\alpha}\right| \sim 12\log 2 + 8\log\left|1 + \frac{1}{2}\sqrt{\frac{1-\alpha}{2}}\right|. \tag{B.2.28}$$

Then, the Lyapunov exponent increases as follows

$$\begin{aligned}
\lambda_{5,\alpha} \quad = \quad & \log \tfrac{25}{256} - \log|1 - (1-\alpha)| \\
& -2\log 10 - 2\log\left|1 - \tfrac{11}{10}(1-\alpha) + \sqrt{1 - 22(1-\alpha) + \tfrac{125}{100}(1-\alpha)^2}\right| \\
& +4\log|1-\alpha| + 8\log|1+\gamma_5| .
\end{aligned} \tag{B.2.29}$$

Thus, one has that in the limit of $\alpha \to 1 - 0$,

$$\lambda_{5,\alpha} = O\left((1-\alpha) + 4\sqrt{\frac{1-\alpha}{2}}\right) \sim 4\sqrt{\frac{1-\alpha}{2}}. \tag{B.2.30}$$

Therefore, the critical exponent ν_1 is denoted as

$$\nu_1 = \frac{1}{2}. \tag{B.2.31}$$

In the case of $K = 5$, the fixed points of $S_{5,\alpha}$ are as follows.

$$x_* = \begin{cases} 0, & 0 < \alpha \le 1, \\ \pm\sqrt{\dfrac{5}{3}}, & \alpha = \dfrac{1}{25}, \\ \pm\sqrt{\dfrac{5(1-5\alpha) + 2\sqrt{5(25\alpha^2 - 6\alpha + 1)}}{5(1-\alpha)}}, & \dfrac{1}{25} < \alpha < 1, \\ \pm\sqrt{\dfrac{3}{5}}, & \alpha = 1. \end{cases} \tag{B.2.32}$$

It also holds that

$$\lim_{|x|\to\infty} \left(S_{5,1}(x) - x\right) = 0. \tag{B.2.33}$$

At the fixed points $x_* = 0$, $\pm\sqrt{\dfrac{5}{3}}$, $\pm\sqrt{\dfrac{3}{5}}$ and $\pm\infty$, the derivatives $S'_{5,\alpha}(x) = \dfrac{25\alpha(1+x^2)^4}{(5x^4 - 10x^2 + 1)^2}$ are

$$\begin{aligned} S'_{5,\frac{1}{25}}(0) &= 1, \\ S'_{5,1}(0) &= 25, \\ S'_{5,\frac{1}{25}}\left(\pm\sqrt{\tfrac{5}{3}}\right) &= 16, \\ S'_{5,1}\left(\pm\sqrt{\tfrac{3}{5}}\right) &= 16, \\ \lim_{|x|\to\infty} S'_{5,1}(x) &= 1. \end{aligned} \tag{B.2.34}$$

From (B.2.34), for $K = 5$ and at $\alpha = \dfrac{1}{25}$ and $\alpha = 1$, the Floquet multipliers are obtained as

$$\begin{aligned} \chi_{5,\frac{1}{25}} &= S'_{5,\frac{1}{25}}(0) &&= 1, \\ \chi_{5,1} &= \lim_{|x|\to\infty} S'_{5,1}(x) &&= 1. \end{aligned} \tag{B.2.35}$$

Therefore, similar to the case of $K = 3$, only *Type 1* intermittency occurs, which is *different* from the case with generalized Boole transformation (K=2).

Bibliography

[1] A. E. Motter and D. K. Campbell, Chaos at fifty, *Physics Today* **66**, 27 (2013).

[2] P. S. Laplace, F. W. Truscott and F. L. Emory, trans., *A Philosophical Essay on Probabilities* (Wiley, New York 1902).

[3] H. Poincaré, F. Maitland, trans., *Science and Method*, (Nelson, New York 1914); H. Poincaré, *Les Méthodes Nouvelles de la Mécanique Céleste*, vols. 1-3, (Gauthier-Villars Paris 1899).

[4] L. Boltzmann, Weitere Studien über das Wärmegleichgewicht unter Gasmolekülen. In: F. Hasenöhrl, (ed.) *Wissenschaftliche Abhandlungen*, vol. 1, #22. (Chelsea, New York 1968).

[5] L. Boltzmann, Üder das Wärmegleichgewicht zwischen mehratomigen Gasmolekülen. In: F. Hasenöhrl. (ed.) *Wissenschaftliche Abhandlungen*, vol. 1. #18. (Chelsea, New York 1968).

[6] G. Gallavotti, *Nonequilibrium and Irreversibility*, (Springer, Switzerland, 2014).

[7] C. Cercignani, *The Boltzmann Equation and Its Applications*, (Springer-Verlag, New York, 1988).

[8] J. Loschmidt, Über den Zustand des Wärmegleichgewichtes eines Systemes von Körpern mit Rücksicht auf die Schwerkraft I-IV, *Sitzungsberichte der Akademie der Wissenschaften zu Wien* **73**, 128 (1876).

[9] E. Zermelo, Über einen Satz der Dynamik und die mechanische Wärmetheorie, *Ann. Phys.* **57**, 485 (1896). E. Zermelo, Über mechanische Erklärungen irreversibler Vorgänge *Ann. Phys.* **59**, 793 (1896).

[10] E. N. Lorentz, *The Essence of Chaos*, (U. Washington Press, Seattle (1993)). E. N. Lorentz, Deterministic nonperiodic flow, *J. Atmos. Sci.* **20**, 130 (1963).

[11] R. Abraham and Y. Ueda, *The chaos avant-garde:Memories of thr early days of chaos theory*, Vol. 39 (World scientific 2000).

[12] M. J. Feigenbaum, *J. Stat. Phys.* **19**, 25 (1978).

[13] C. Oestreicher, A history of chaos theory, *Dialogues in clinical neuroscience* **9** 279 (2007).

[14] B. A. Huberman and J. Rudnick, Scaling Behavior of Chaotic Flows, *Phys. Rev. Lett.* **45**, 154 (1980).

[15] Y. Pomeau and P. Manneville, Intermittent Transition to Turbulence in Dissipative Dynamical Systems, *Commun. Math. Phys.* **74**, 189 (1980).

[16] Y. Aizawa, C. Murakami and T. Kohyama, Statistical Mechanics of Intermittent Chaos: $f^{-\nu}$ Spectral Behaviors of the Semi-Markovian Class, *Progress of Theoretical Physics Supplement* **79**, 96 (1984).

[17] Y. Pomeau, J. C. Roux, A. Rossi, S. Bachelart and C. Vidal, Intermittent behavior in thr Belousov-Zhabotinsky reaction, *J. Physique Lett.* **42**, 271 (1981).

[18] M. Dubois, M. A. Rubio and P. Berge, Experimental Evidence of Intermittencies Associated with a Subharmonic Bifurcation, *Phys. Rev. Lett.* **51**, 1446 (1983).

[19] G. D. Birkhoff, Proof of the ergodic theorem, *Proceedings of the National Academy of Sciences* **17**, 656 (1931).

[20] S. Smale, Diffeomorphisms with many period points, *Differential and Combinatorial Topology* Princeton, 63 (1965). S. Smale, Differentiable dynamical systems, *Bulletin of the American Mathematical Society* **73**,747 (1967).

[21] S. Tasaki, T. Gilbert and J. R. Dorfman, An analytical construction of the SRB measures for Baker-type maps, *Chaos: An Interdisciplinary Journal of Nonlinear Science* **8**, 424 (1998).

[22] Y. G. Sinai, Gibbs measures in ergodic theory, *Russ. Math. Surv.* **27**, 21 (1972). D. Ruelle, A measure associated with axiom-A attractors, *Am. J. Math.* **98**, 619 (1976). R. Bowen and D. Ruelle, The ergodic theory of AxiomA flows, *Inventiones Mathematicae* **29**, 181 (1975).

[23] J. -P. Eckmann and D. Ruelle, Ergodic theory of chaos and strange attractors, *Rev. Mod. Phys.* **57**, 617 (1985).

[24] Y. G. Sinai, Dynamical systems with elastic reflections, *Russ. Math. Surv.* **25**, 137 (1970).

[25] D. I. Dolgopyat and N. I. Chernov, Anomalous current in periodic Lorentz gases with infinite horizon, *Russ. Math. Surv.* **64**, 651 (2009).

[26] L. A. Bunimovich, On the ergodic properties of nowhere dispersing billiards, *Commun. Math. Phys.* **65**, 295 (1979).

[27] M. Stenlund, A strong pair correlation bound implies the CLT for Sinai billiards, *J. Stat. Phys.* **140**, 154 (2010).

[28] M. Courbage, M. Edelman, S. M. Saberi Fathi and G. M. Zaslavsky, Problem of transport in billiards with infinite horizon, *Phys. Rev. E* **77**, 036203 (2008).

[29] G. M. Zaslavsky, *Chaos in Dynamic Systems*, (Harwood Academic Publishers, New York, 1985).

[30] S. Vaienti, Ergodic properties of the discontinuous sawtooth map, *J. Stat. Phys.* **67**, 251 (1992).

[31] V. I. Arnold and A. Avez, *Ergodic problems of classical mechanics*, (Benjamin, New York, 1968).

[32] S. Tasaki and P. Gaspard, Fick's law and fractality of nonequilibrium stationary states in a reversible multibaker map, *J. Stat. Phys.* **81**, 935 (1995).

[33] S. M. Ulam and J. von Neumann, *Bull. Am. Math. Soc.* **53**, 1120 (1947).

[34] S. Katsura and W. Fukuda, *Physica (Amsterdam) A* **130**, 597 (1985).

[35] K. Umeno, Method of constructing exactly solvable chaos, *Phy. Rev. E* **55**, 5280 (1997).

[36] K. Umeno, Superposition of chaotic processes with convergence to Lévy ’ s stable law, *Phys. Rev. E* **58**, 2644 (1998).

[37] L. S. Young, What are SRB measures, and which dynamical systems have them?, *J. Stat. Phys.* **108**, 733 (2002).

[38] K. Umeno, Chaotic Monte Carlo Computation: A Dynamical Effect of Random-Number Generations, *Japanese Journal of Applied Physics* **39**, 1442 (2000).

[39] C. Froeschlé, R. Gonczi, and E. Lega, The fast Lyapunov indicator: a simple tool to detect weak chaos. Application to the structure of the main asteroidal belt, *Planetary and space science* **45**, 881 (1997).

[40] J. Laskar, A numerical experiment on the chaotic behaviour of the solar system, *Nature* **338**, 237 (1989).

[41] C. Froeschlé, E. Lega, and R. Gonczi, Fast Lyapunov Indicators. Application to asteroidal motion, *Celestial Mechanics and Dynamical Astronomy* **67**, 41 (1997).

[42] M. Fouchard, E. Lega, Chistiane Froeschlé, and Claude Froeschlé, *On the Relationship between Fast Lyapunov Indicator and Periodic Orbits for Continuous Flows*, Modern Celestial Mechanics: From Theory to Applications, (Springer, Netherlands, 2002).

[43] R. Barrio, Sensitivity vs. Poincaré sections, *Chaos, Solitons and Fractals* **25**, 711 (2005).

[44] P. S. Linsay, Period Doubling and Chaotic Behavior in a Driven Anharmonic Oscillator, *Phys. Rev. Lett.* **47**, 1349 (1981).

[45] P. Y. Cheung and A. Y. Wong, Chaotic behavior and period doubling in plasmas, *Phys. Rev. Lett.* **59**, 551 (1987).

[46] P. Blondeaux and G. Vittori, A route to chaos in an oscillatory flow: Feigenbaum scenario, *Physics of Fluids A: Fluid Dynamics* **3**, , 2492 (1991).

[47] A. Lasota and M. C. Mackey, *Probabilistic Properties of Deterministic Systems* (Cambridge University Press, Cambridge, UK, 2008).

[48] M. C. Mackey, The dynamic origin of increasing entropy, *Rev. Mod. Phys.* **61**, 981 (1989).

[49] K. Umeno and K. Okubo, Exact Lyapunov exponents of the generalized Boole transformations, *Progress of Theoretical and Experimental Physics* **2016**, 021A01 (2016).

[50] K. Okubo and K. Umeno, Universality of the route to chaos: Exact analysis, *Progress of Theoretical and Experimental Physics* **2018**, 103A01 (2018).

[51] K. Okubo and K. Umeno, Proof of Irreversibility for Systems with Time Reversal Symmetry, arXiv 1703.10888.

[52] K. Okubo and K. Umeno, New Chaos Indicators for Systems with Extremely Small Lyapunov Exponents, *Chaos, Complexity and Transport - Proceedings of the CCT '15*, (World Scientific, USA, 2017).

[53] K. Okubo and K. Umeno, Chaos Indicators for Weak Chaos Systems, *Transactions of the Japan Society for Industrial and Applied Mathematics / Japan Society for Industrial and Applied Mathematics* **25**, 31 (2015) (In Japanese).

[54] F. T. Hioe and Z. Deng, Stability-instability transitions in Hamiltonian systems of n dimensions, *Phys. Rev. A* **35**, 847 (1987).

[55] E. Otto and J. C. Sommerer, Blowout bifurcations: the occurrence of riddled basins and on-off intermittency, *Phys. Lett. A* **188**, 39 (1994).

[56] P. Manneville and Y. Pomeau, Intermittency and the Lorenz model, *Physics Letters A* **75**, 1 (1979).

[57] M. S. Milosavljevic, J. N. Blakely, A. N. Beal, and N. J. Corron, Analytic solutions throughout a period doubling route to chaos, *Phys. Rev. E* **95**, 062223 (2017).

[58] H. Lamba and C. J. Budd, Scaling of Lyapunov exponents at nonsmooth bifurcations, *Phys. Rev. E* **50**, 84 (1994).

[59] Z. Liu, Y. C. Lai, M.A. Matias, Universal scaling of Lyapunov exponents in coupled chaotic oscillators, *Phys. Rev. E* **67**, 045203(R) (2003).

[60] H. L. Swinney, Observations of order and chaos in nonlinear systems, *Physica D* **7**, 3 (1983).

[61] J. Crutchfield, M. Nauenberg and J. Rudnick, Scaling for external noise at the onset of chaos, *Phys. Rev. Lett.* **46**, 933 (1981).

[62] L. Kabiraj and R. I. Sujith, Nonlinear self-excited thermoacoustic oscillations: intermittency and flame blowout, *J. Fluid Mech.* **73**, 376 (2012).

[63] L. Bakemeier, A. Alvermann and H. Fehske, Route to chaos in optomechanics, *Phys. Rev. Lett.* **114**, 013601 (2015).

[64] K. He and A. C.-L. Chian, Critical dynamic events at the crisis of transition to spatiotemporal chaos, *Phys. Rev. E* **69**, 026207 (2004).

[65] A. Coillet and Y. K. Chembo, Routes to spatiotemporal chaos in Kerr optical frequency combs, *Chaos: An Interdisciplinary Journal of Nonlinear Science* **24**, 013113 (2014).

[66] R. Ganapathy and A. K. Sood, Intermittency route to rheochaos in wormlike micelles with flow-concentration coupling, *Phys. Rev. Lett* **96**, 108301 (2006).

[67] Á. M. Núñez, B. Luque, L. Lacasa, J. P. Gómez, and A. Robledo, Horizontal visibility graphs generated by type-I intermittency, *Phys. Rev. E* **87**, 052801 (2013).

[68] T. Geisel and J. Nierwetberg, Intermittent diffusion: a chaotic scenario in unbounded systems, *Phys. Rev. A* **29**, 2305 (1984).

[69] M. Schell, S. Fraser and R. Kapral, Diffusive dynamics in systems with translational symmetry: A one-dimensional-map model, *Phys. Rev. A* **26**, 504 (1982).

[70] K. F. Knott, Characteristics of burst noise intermittency, *Solid-State Electoronics* **21**, 1039 (1978).

[71] D. Y. Tang, J. Pujol and C. O. Weiss, Type-III intermittency of a laser, *Phys. Rev. A* **44**, R35 (1991).

[72] M.G. Cosenza, O. A. Llamoza and G.A. Ponce, Lyapunov exponent for type-III intermittent chaos, *Commun. Nonlinear Sci. Numer. Simulat.* **15**, 2431 (2010).

[73] P. ベルジェ, Y. ポモウ and Ch. ビダル, 相澤洋二訳, カオスの中の秩序-乱流の理解へ向けて-, (産業図書 1992).

[74] G. Benettin, Power-law behavior of Lyapunov exponents in some conservative dynamical systems, *Physica D* **13**, 211 (1984).

[75] B. N. Miller and K. Ravishankar, Stochastic modeling of a billiard in a gravitational field: Power law behavior of Lyapunov exponents, *J. Stat. Phys.* **53**, 1299 (1988).

[76] Y. Ono, K. Fukushima and T. Yazaki, Critical behavior for the onset of type-III intermittency observed in an electronic circuit, *Phys. Rev. E* **52**, 4520 (1995).

[77] D. L. Feng, J. Zheng, W. Huang, C. X. Yu and W.X. Ding, Type-I-like intermittent chaos in multicomponent plasmas with negative ions, *Phys. Rev. E* **54**, 2839 (1996).

[78] G. Boole, XXXVI. On the comparison of transcendents, with certain applications to the theory of definite integrals, *Philos. Trans. Roy. Soc. London* **147**, 745 (1857).

[79] R. Adler and B. Weiss, The ergodic infinite measure preserving transformation of boole, *Israel Journal of Mathematics* **16**, 263 (1973).

[80] J. Aaronson, *An Introduction to Infinite Ergodic Theory*, (American Mathematical Society, Province 1997).

[81] J. H. B. Kemperman, The ergodic behavior of a class of real transformations, *Stochastic Processes and Related Topics I (Proc. Summer Research Inst. on Statistical Inference for Stochastic Processes, Indiana Univ., Bloomington, 1974)*, 249 (1975).

[82] G. Letac, Which functions preserve Cauchy laws?, *Proc. Amer. Math. Soc.* **67**, 277 (1977).

[83] Ya. B. Pesin, Characteristic Lyapunov exponents and smooth ergodic theory, *Russian Mathematical Surveys* **32**, 55 (1977).

[84] T. Akimoto and Y. Aizawa, Subexponential instability in one-dimensional maps implies infinite invariant measure, *Chaos: An Interdisciplinary Journal of Nonlinear Science* **20**, 033110 (2010).

[85] T. Akimoto, M. Nakagawa, S. Shinkai and Y. Aizawa, Generalized Lyapunov exponent as a unified characterization of dynamical instabilities, *Phy. Rev. E* **91**, 012926 (2015).

[86] K. Umeno, Ergodic transformations on R preserving Cauchy laws, *Nonlinear Theory and Its Applications, IEICE* **7**, 14 (2016).

[87] M. Nakagawa and Y. Aizawa, Observed Measures and Fluctuations in Dissipative Infinite Ergodic Systems: Randomization Theory for the Infinite-Modal Maps with Ant-Lion Property, *Journal of the Physical Society of Japan* **83**, 104004 (2014).

[88] M. C. Mackey, Microscopic dynamics and the second law of thermodynamics, in *Time's Arrows, Quantum Measurement and Superluminal Behavior*, (Consiglio Nazionale Delle Ricerche, Rome, 2001).

[89] H. Schwegler and M. Mackey, A simple model for the approach of entropy to thermodynamic equilibrium, *J. Phys. A.* **27**, 1939 (1994).

[90] B. V. Gnedenko and A. N. Kolmogorov, *Limit Distributions for Sums of Independent Random Variables* (Addison-Wesley, Reading, MA,1954).

[91] G. Gallavotti,*Statistical Mechanics A Short Treatise*, (Springer-Verlag, Berlin Heidelberg, 1999).

[92] M. Kac, Random walk and the theory of Brownian motion, *Am. Math. Mon.* **54**, 369 (1947).

[93] M. Kac, *Probability and Related Topics in Physical Science*, Interscience Publishers, London (1959).

[94] S. Goldstein, J. L. Lebowitz and Y. Sinai, Remark on the (non) convergence of ensemble densities in dynamical systems, *Chaos: An Interdisciplinary Journal of Nonlinear Science* **8**, 393 (1998).

[95] V. Latora and M. Baranger, Kolmogorov-Sinai entropy rate versus physical entropy, *Phys. Rev. Lett.* **82**, 520 (1999).

[96] M. Falcioni, L. Palatella, S. Pigolotti, L. Rondoni and A. Vulpiani, Initial growth of Boltzmann entropy and chaos in a large assembly of weakly interacting systems, *Physica A*, **385**, 170 (2007).

[97] R. Venegeroles and A. Saa, Non-Gaussian features of chaotic Hamiltonian transport, *J. Stat. Mech. Theor. Exp.* **2008**, P01005 (2008).

[98] G. M. Zaslavsky, Chaos, fractional kinetics, and anomalous transport, *Phys. Rep.* **371**, 461 (2002).

[99] V. Rom-Kedar and G. Zaslavsky, Islands of accelerator modes and homoclinic tangles, *Chaos: An Interdisciplinary Journal of Nonlinear Science* **9**, 697 (1999).

[100] S. Benkadda, S. Kassibrakis, R. B. White and G. M. Zaslavsky, Self-similarity and transport in the standard map, *Phys. Rev. E* **55**, 4909 (1997).

[101] J. S. W. Lamb, and J. A. G. Roberts, Time-reversal symmetry in dynamical systems: a survey, *Physica D* **112**, 1 (1998).

[102] H. Furstenberg, Poincaré recurrence and number theory, *Bull. Amer. Math. Soc.* **5**, 211 (1981).

[103] R. Mañé, *Ergodic Theorey and Differentiable Dynamics*, (Springer-Verlag, Berlin Heidelberg, 1987).

[104] J. Franks, Anosov diffeomorphisms on tori, *Trans. Amer. Math. Soc.* **145**, 117 (1969).

[105] G. Gallavotti and E. G. D. Cohen, Nonequilibrium stationary states and entropy, *Phys. Rev. E* **69**, 035104 (2004).

[106] Z. Lian, P. Liu and K. Lu, SRB measures for a class of partially hyperbolic attractors in hilbert spaces, *J. Differ. Equ.* **261**, 1532 (2016).

[107] I. A. Ibragimov, Some limit theorems for stationary processes, *Theory Probab. Appl.* **7**, 349 (1962).

[108] Y. B. Pesin, Characteristic Lyapunov exponents and smooth ergodic theory, *Usp. Mat. Nauk.* **32**, 55 (1977) [*Russ. Math. Sur.* **32**, 55 (1977)].

[109] P. Gaspard and G. Nicolis, Transport properties, Lyapunov exponents, and entropy per unit time*Phys. Rev. Lett.* **65**, 1693 (1990).

[110] B. V. Chirikov, Big entropy fluctuations in the nonequilibrium steady state: A simple model with the gauss heat bath, *J. Exp. Theor. Phys.* **92**, 179 (2001).

[111] A. von Kameke, F. Huhn, G. Fernández-García, A. P. Muñuzuri, and V. P.-Muñuzuri, Propagation of a chemical wave front in a quasi-two-dimensional superdiffusive flow, *Phys. Rev. E* **81**, 066211 (2010).

[112] A. Upadhyaya, J. P.Rieu, J. A. Glazier and Y. Sawada, Anomalous diffusion and non-Gaussian velocity distribution of Hydra cells in cellular aggregates*Physica A* **293**, 549 (2001).

[113] S. Perri and G. Zimbardo, Evidence of superdiffusive transport of electrons accelerated at interplanetary shocks, *ApJ 671*, L177 (2007).

[114] T. H. Solomon, E. R. Weeks and H. L. Swinney, Observation of anomalous diffusion and Lévy flights in a two-dimensional rotating flow, *Phys. Rev. Lett.* **71**, 3975 (1993).

[115] T. Suzuki, H. Namazue, S. Koike and H. Hayakawa, Superdiffusion of 4 T-Hydrogen in Vanadium, *Phys. Rev. Lett.* **51**, 798 (1983).

[116] C. Scalliet, A. Gnoli, A. Puglisi and A. Vulpiani, Cages and anomalous diffusion in vibrated dense granular media, *Phys. Rev. Lett.* **114**, 198001 (2015).

[117] Y. Sagi, M. Brook, I. Almog and N. Davidson, Observation of anomalous diffusion and fractional self-similarity in one dimension, *Phys. Rev. Lett.* **108**, 093002 (2012).

[118] A. M. Lacasta, J. M. Sancho, A. H. Romero, I. M. Sokolov and K. Lindenberg, From subdiffusion to superdiffusion of particles on solid surfaces*Phys. Rev. E* **70**, 051104 (2004).

[119] B. Hu, B. Li, J. Liu and Y. Gu, Quantum chaos of a kicked particle in an infinite potential well, *Phys. Rev. Lett.* **82**, 4224 (1999).

[120] D. R. Grempel, R. E. Prange and S. Fishman, Quantum dynamics of a nonintegrable system, *Phys. Rev. A* **29**, 1639 (1984).

[121] V. Latora, A. Rapisarda and S. Ruffo, Superdiffusion and out-of-equilibrium chaotic dynamics with many degrees of freedoms, *Phys. Rev. Lett.* **83**, 2104 (1999).

[122] S. C. Venkataramani, T. M. Antonsen Jr and E. Ott, Lévy flights in fluid flows with no Kolmogorov-Arnold-Moser surfaces,*Phys. Rev. Lett.* **78**, 3864 (1997).

[123] R. Venegeroles, Calculation of superdiffusion for the Chirikov-Taylor model*Phys. Rev. Lett.* **101**, 054102 (2008).

[124] T. Akimoto, Distributional Response to Biases in Deterministic Superdiffusion, *Phys. Rev. Lett.* **108**, 164101 (2012).

[125] S. Adachi, M. Toda and K. Ikeda, Potential for Mixing in Quantum Chaos, *Phys. Rev. Lett.* **61**, 655 (1988). S. Adachi, M. Toda and K. Ikeda, Quantum-Classical Correspondence in Many-Dimensional Quantum Chaos, *Phys. Rev. Lett.* **61**, 659 (1988).

[126] G. J. Sussman and J. Wisdom, Chaotic evolution of the solar system, *Science* **257**, 56 (1992).

[127] J. Lasker, *Is the solar system stable?*, Chaos, (Springer, Basel, 2013).

[128] M. Guzzo, E. Lega, and C. Froeschlé, On the numerical detection of the effective stability of chaotic motions in quasi-integrable systems, *Physica D* **163**, 1 (2002).

[129] E. Lega and C. Froeschlé, On the Relationship Between Fast LyapunovIndicator and Periodic Orbits for Symplectic Mappings, *Celestial Mechanics and Dynamical Astronomy* **81**, 129 (2001).

[130] C. Froeschlé, M. Guzzo, and E. Lega, Graphical Evolution of the Arnold Web: From Order to Chaos, *Science* **289**, 2108 (2000).

[131] C. Froeschlé, M. Guzzo and E. Lega, *Local and global diffusion along resonant lines in discrete quasi-integrable dynamical systems*, A Comparison of the Dynamical Evolution of Planetary Systems, (Springer, Netherlands, 2005).

[132] M. Thaler, Transformations on [0, 1] with Infinite Invariant Measures, *Israel Journal of Mathematics* **46**, 67 (1983).

List of author's papers related to this thesis

1. Ken Umeno and Ken-ichi Okubo, Exact Lyapunov exponents of the generalized Boole transformations, *Progress of Theoretical and Experimental Physics* **2016**, 021A01 (2016).

2. Ken-ichi Okubo and Ken Umeno, Universality of the route to chaos: Exact analysis, *Progress of Theoretical and Experimental Physics* **2018**, 103A01 (2018).

3. Ken-ichi Okubo and Ken Umeno, Proof of Irreversibility for Systems with Time Reversal Symmetry, arXiv:1703.10888.

4. 大久保健一, 梅野健, 弱カオス系のカオス性判定について, 日本応用数理学会論文誌 **25**, pp.31-56 (2015).

5. Ken-ichi Okubo and Ken Umeno, New chaos indicators for systems with extremely small Lyapunov exponent, *Chaos, Complexity and Transport: Proceedings of the CCT '15 : Conference on Chaos, Complexity and Transport 2015, Marseilles, France, 1-5 June 2015*, pp.185-203, World Scientific (2016).

- Chapter 2 and Appendix B are based on papers 1 and 2.
- Chapter 3 is based on paper 3.
- Appendix A is based on papers 4 and 5.

Figures and Tables

Source of figures

Figure 2.1 K. Umeno and K. Okubo, *Progr. Theor. Exp. Phys.* **2016**, 021A01 (2016).
Figure 2.2 K. Umeno and K. Okubo, *Progr. Theor. Exp. Phys.* **2016**, 021A01 (2016).
Figure 2.3 K. Umeno and K. Okubo, *Progr. Theor. Exp. Phys.* **2016**, 021A01 (2016).
Figure 2.4 K. Umeno and K. Okubo, *Progr. Theor. Exp. Phys.* **2016**, 021A01 (2016).
Figure 2.5 K. Umeno and K. Okubo, *Progr. Theor. Exp. Phys.* **2016**, 021A01 (2016).
Figure 2.6 K. Umeno and K. Okubo, *Progr. Theor. Exp. Phys.* **2016**, 021A01 (2016).
Figure 2.7 K. Okubo and K. Umeno, *Progr. Theor. Exp. Phys.* **2018**, 103A01 (2018).
Figure 2.8 K. Okubo and K. Umeno, *Progr. Theor. Exp. Phys.* **2018**, 103A01 (2018).
Figure 2.9 K. Okubo and K. Umeno, *Progr. Theor. Exp. Phys.* **2018**, 103A01 (2018).
Figure 2.10 Original.
Figure 3.1 K. Okubo and K. Umeno, arXiv:1703.10888.
Figure 3.2 K. Okubo and K. Umeno, arXiv:1703.10888.
Figure 3.3 Original.
Figure 3.4 Original.
Figure 3.5 Original.
Figure 3.6 Original.
Figure 3.7 K. Okubo and K. Umeno, arXiv:1703.10888.
Figure A.1 K. Okubo and K. Umeno, *New Chaos Indicators for Systems with Extremely Small Lyapunov Exponents*, Chaos, Complexity and Transport - Proceedings of the Cct '15, World Scientific USA (2017).
Figure A.2 K. Okubo and K. Umeno, *New Chaos Indicators for Systems with Extremely Small Lyapunov Exponents*, Chaos, Complexity and Transport - Proceedings of the Cct '15, World Scientific USA (2017).
Figure A.3 K. Okubo and K. Umeno, *New Chaos Indicators for Systems with Extremely Small Lyapunov Exponents*, Chaos, Complexity and Transport - Proceedings of the Cct '15, World Scientific USA (2017).
Figure A.4 K. Okubo and K. Umeno, *New Chaos Indicators for Systems with*

Extremely Small Lyapunov Exponents, Chaos, Complexity and Transport - Proceedings of the Cct '15, World Scientific USA (2017).
Figure A.5 K. Okubo and K. Umeno, *New Chaos Indicators for Systems with Extremely Small Lyapunov Exponents*, Chaos, Complexity and Transport - Proceedings of the Cct '15, World Scientific USA (2017).
Figure A.6 K. Okubo and K. Umeno, *New Chaos Indicators for Systems with Extremely Small Lyapunov Exponents*, Chaos, Complexity and Transport - Proceedings of the Cct '15, World Scientific USA (2017).
Figure A.7 K. Okubo and K. Umeno, *New Chaos Indicators for Systems with Extremely Small Lyapunov Exponents*, Chaos, Complexity and Transport - Proceedings of the Cct '15, World Scientific USA (2017).
Figure A.8 K. Okubo and K. Umeno, *New Chaos Indicators for Systems with Extremely Small Lyapunov Exponents*, Chaos, Complexity and Transport - Proceedings of the Cct '15, World Scientific USA (2017).
Figure A.9 K. Okubo and K. Umeno, *New Chaos Indicators for Systems with Extremely Small Lyapunov Exponents*, Chaos, Complexity and Transport - Proceedings of the Cct '15, World Scientific USA (2017).
Figure A.10 K. Okubo and K. Umeno, *New Chaos Indicators for Systems with Extremely Small Lyapunov Exponents*, Chaos, Complexity and Transport - Proceedings of the Cct '15, World Scientific USA (2017).
Figure A.11 K. Okubo and K. Umeno, *New Chaos Indicators for Systems with Extremely Small Lyapunov Exponents*, Chaos, Complexity and Transport - Proceedings of the Cct '15, World Scientific USA (2017).
Figure A.12 K. Okubo and K. Umeno, *New Chaos Indicators for Systems with Extremely Small Lyapunov Exponents*, Chaos, Complexity and Transport - Proceedings of the Cct '15, World Scientific USA (2017).
Figure A.13 K. Okubo and K. Umeno, *New Chaos Indicators for Systems with Extremely Small Lyapunov Exponents*, Chaos, Complexity and Transport - Proceedings of the Cct '15, World Scientific USA (2017).
Figure A.14 K. Okubo and K. Umeno, *New Chaos Indicators for Systems with Extremely Small Lyapunov Exponents*, Chaos, Complexity and Transport - Proceedings of the Cct '15, World Scientific USA (2017).
Figure A.15 K. Okubo and K. Umeno, *New Chaos Indicators for Systems with Extremely Small Lyapunov Exponents*, Chaos, Complexity and Transport - Proceedings of the Cct '15, World Scientific USA (2017).
Figure A.16 K. Okubo and K. Umeno, *New Chaos Indicators for Systems with Extremely Small Lyapunov Exponents*, Chaos, Complexity and Transport - Proceedings of the Cct '15, World Scientific USA (2017).
Figure A.17 K. Okubo and K. Umeno, *New Chaos Indicators for Systems with Extremely Small Lyapunov Exponents*, Chaos, Complexity and Transport - Proceedings of the Cct '15, World Scientific USA (2017).

Figure A.18 K. Okubo and K. Umeno, *New Chaos Indicators for Systems with Extremely Small Lyapunov Exponents*, Chaos, Complexity and Transport - Proceedings of the Cct '15, World Scientific USA (2017).
Figure A.19 K. Okubo and K. Umeno, *New Chaos Indicators for Systems with Extremely Small Lyapunov Exponents*, Chaos, Complexity and Transport - Proceedings of the Cct '15, World Scientific USA (2017).
Figure A.20 K. Okubo and K. Umeno, *New Chaos Indicators for Systems with Extremely Small Lyapunov Exponents*, Chaos, Complexity and Transport - Proceedings of the Cct '15, World Scientific USA (2017).
Figure A.21 K. Okubo and K. Umeno, *New Chaos Indicators for Systems with Extremely Small Lyapunov Exponents*, Chaos, Complexity and Transport - Proceedings of the Cct '15, World Scientific USA (2017).
Figure A.22 K. Okubo and K. Umeno, *New Chaos Indicators for Systems with Extremely Small Lyapunov Exponents*, Chaos, Complexity and Transport - Proceedings of the Cct '15, World Scientific USA (2017).
Figure A.23 大久保健一, 梅野健, 弱カオス系のカオス性判定について, 日本応用数理学会論文誌 **25**, 31 (2015).
Figure A.24 大久保健一, 梅野健, 弱カオス系のカオス性判定について, 日本応用数理学会論文誌 **25**, 31 (2015).

Source of tables

Table 2.1 K. Umeno and K. Okubo, *Progr. Theor. Exp. Phys.* **2016**, 021A01 (2016).
Table 2.2 K. Umeno and K. Okubo, *Progr. Theor. Exp. Phys.* **2016**, 021A01 (2016).
Table 3.1 Original